

ELECTROKINETIC ION TRANSPORT THROUGH UNSATURATED SOILS:

THEORY AND APPLICATION

By

Earl Douglas Mattson

Submitted in partial fulfillment of the requirements for
the degree of Doctor of Philosophy in Hydrology

Department of Earth and Environmental Science
New Mexico Institute of Mining and Technology
Socorro, New Mexico

August 1999

ABSTRACT

Previous studies of electrokinetic ion and water transport have generally disregarded its application to remediation of unsaturated soils due to a lack of theoretical understanding, numerical predictive capabilities, and suitable electrodes. The research focus of this dissertation is on the electromigration of ions in unsaturated soils. Electrokinetic transport theory, three-dimensional numerical model development, comparison of model predictions to experimental results, and a surfactant-coating procedure for the anode electrode casings are all described in this dissertation.

An electromigration transport model was developed based on a modified Nernst-Planck equation describing the electromigration and diffusive flux of ions in a porous medium and on the equation of continuity. A steady-state electric potential field was assumed, an assumption valid for highly buffered soils or when the electrode electrolysis reactions are neutralized. The model also assumed advective water movement through the soil due to either electric or hydraulic potentials was negligible. The transport and continuity equations were implemented in the model using public domain ground-water flow (MODFLOW) and transport (MT3D) numerical codes that were modified to allow prediction of ion transport due to an electric potential field.

Effective ionic mobility and diffusion parameters for porous media were calculated using a tortuosity function based on a closed-form solution of an equation describing electrical conductivity dependence on moisture content. The effect of ionic strength on ionic mobility was estimated using the activity coefficient calculated by the Davies equation.

One-dimensional laboratory experiments that measured anionic dye electromigration rates as a function of moisture content were used to verify the model. Laboratory experiments were conducted using a 10-mA, constant-current condition. Predicted red dye No. 40 migration rates matched the experimental data very well. Both the numerical simulations and the experimental

results showed a maximum electromigration velocity at moisture contents less than saturation. This maximum is believed to be due to competing effects between current density and tortuosity.

A six-month field demonstration was conducted to examine ion electromigration through heterogeneous unsaturated sandy soils. Acetate electromigration transport in the field demonstration indicated preferential transport through soil layers exhibiting higher moisture content and electrical conductivity.

Modeling was used to assess the effects of spatial heterogeneities on electromigration transport at the field-scale. The measured soil properties of the field demonstration were conceptualized as a layered system or as a homogeneous system. The layered model had three layers where each layer was assigned a moisture content and electrical conductivity value. The homogeneous model represented a single homogeneous profile with average properties of the layered model. Numerical results from these models suggest that spatial heterogeneities in soil properties must be accounted for in order to predict electromigration transport in a heterogeneous soil profile. The numerical predictions of the layered model qualitatively matched observations from the field experiments.

A surfactant-coating procedure for ceramic electrode casings was developed that eliminates excess electroosmotic flow from the anode into unsaturated soils. Anode porous ceramic casings were treated with hexadecyltrimethylammonium at concentrations above the critical micelle concentration. Laboratory experimental results suggested the surfactant coating formed a bilayer on the ceramic surface, reversed the zeta potential and hence the electroosmotic flow direction within the treated-ceramic pores. A six-month field demonstration confirmed the stability and effectiveness of the surfactant treatment on the porous ceramic.

The results of this dissertation illustrate the importance of moisture content and its relationship to electrical conductivity on electromigration transport, and the importance of including spatial heterogeneity in electrokinetic transport models. The steady-state electric

potential field assumption allowed soil spatial variability effects on electromigration to be incorporated in a three-dimensional transport model. Electrokinetic transport models assuming homogeneous soil parameters will not adequately predict ion transport pathways at the field-scale in heterogeneous soil profiles.

ACKNOWLEDGMENTS

To all the people who helped me complete this dissertation, a great thank you. Rob Bowman, my advisor, provided encouragement and introduced me to the interesting world of surface chemistry. Eric Lindgren provided me the opportunity to perform electrokinetic research with Sandia National Laboratories. Pat Duda was always ready to assist in field and laboratory experiment and kept the project within ES&H protocol. The Sandia technicians, Bruce Reavis, Jim Swanson, and Bob Helgesen, and a student worker, Chris Sears, spent many hours building and installing laboratory and field equipment needed for the experiments.

Special thanks go to my wife, Alva, and my three children, Eli, Anna, and Erika, for their support and sacrifice of family-time together to allow me to complete this dissertation.

The field and laboratory experimentation was performed at Sandia National Laboratories, which is operated for the U.S. Department of Energy under Contract No. DE-AC04-94AL85000. Funding was provided by the Department of Energy's Office of Science and Technology through the Subsurface Contaminant Focus Area and by the New Mexico Waste-management Education & Research Consortium (WERC).

TABLE OF CONTENTS

| | |
|--|------|
| Abstract | ii |
| Acknowledgements | v |
| Table of Contents | vi |
| List of Tables | x |
| List of Figures | xi |
| Chapter 1 – INTRODUCTION | 1-1 |
| 1-1. Electrokinetic Phenomena | 1-1 |
| 1-2. Motivation for Investigating Electrokinetic Transport in Unsaturated Soils..... | 1-3 |
| 1-3. Organization of this Dissertation | 1-6 |
| 1-4. References | 1-7 |
| Chapter 2 – ELECTROKINETIC ION TRANSPORT THROUGH UNSATURATED SOIL: 1. THEORY, MODEL DEVELOPMENT AND TESTING | 2-1 |
| Abstract | 2-1 |
| 2-1. Introduction | 2-2 |
| 2-2. Theory | 2-6 |
| 2-3. Numerical Development | 2-10 |
| 2-4. Laboratory Experiments | 2-12 |
| 2-4.1 Materials and Methods | 2-12 |
| 2-4.2 Results | 2-15 |
| 2-5. Electromigration Transport Model Testing | 2-16 |
| 2-5.1 Input Parameters | 2-17 |

| | |
|---|------|
| 2-5.2 Electromigration Transport Model Simulations | 2-18 |
| 2-6. Conclusions | 2-19 |
| Appendix 2-A: Ionic Mobility Dependence on Concentration | 2-21 |
| Appendix 2-B Tortuosity..... | 2-23 |
| 2-7. References | 2-26 |
| Chapter 3 – ELECTROKINETIC ION TRANSPORT THROUGH UNSATURATED | |
| SOIL: 2. APPLICATION TO A HETEROGENEOUS FIELD SITE | |
| Abstract | 3-1 |
| 3-1. Introduction..... | 3-2 |
| 3-2. Field Methods..... | 3-4 |
| 3-2.1 Site Characterization | 3-4 |
| 3-2.2 Experimental Equipment | 3-5 |
| 3-2.3 Experimental Methodology | 3-8 |
| 3-3. Field Results | 3-9 |
| 3-4. Numerical Methods..... | 3-10 |
| 3-5. Numerical Results | 3-12 |
| 3-6. Discussion..... | 3-13 |
| 3-7. Summary..... | 3-16 |
| 3-8. References | 3-17 |
| Chapter 4 –ELECTROKINETIC REMEDIATION IN UNSATURATED SOILS | |
| USING SURFACTANT-COATED CERAMIC CASINGS | |
| Abstract | 4-1 |
| 4-1. Introduction..... | 4-2 |

| | |
|---|------------|
| 4-2. Theory | 4-5 |
| 4-3. Material and Methods | 4-8 |
| 4-3.1. Ceramic | 4-8 |
| 4-3.2. Surfactant | 4-8 |
| 4-3.3. Ceramic Surfactant Treatment | 4-8 |
| 4-3.4. Laboratory Experiments | 4-9 |
| 4-3.5. Field Experiments | 4-11 |
| 4-4. Results and Discussion | 4-14 |
| 4-4.1. Laboratory Experiments | 4-14 |
| 4-4.2. Field Experiments | 4-16 |
| 4-5. Summary and Conclusions | 4-18 |
| 4-6. References | 4-19 |
| 4-7. Notation | 4-22 |
| Chapter 5 – SUMMARY | 5-1 |
| 5-1. Introduction | 5-1 |
| 5-2. Summary of this Dissertation | 5-1 |
| 5-3. Where to Go from Here | 5-4 |
| 5-4. References | 5-9 |
| Appendix A MODFLOW and LKMT Code Modifications | A-1 |
| Appendix B MODFLOW Input File Example: One-Dimensional Laboratory Dye Experiment | B-1 |
| Appendix C MT3D Input File Example: One-Dimensional Laboratory Dye Experiment | C-1 |
| Appendix D MODFLOW Output File Example: One-Dimensional Laboratory | |

| | |
|---|-----|
| Dye Experiment | D-1 |
| Appendix E MT3D Output File Example: One-Dimensional Laboratory Dye Experiment | E-1 |
| Appendix F Experimental Electrode Control System..... | F-1 |
| Appendix G MODFLOW Input File Example: Three-Dimensional Field Demonstration | G-1 |
| Appendix H MT3D Input File Example: Three-Dimensional Field Demonstration | H-1 |
| Appendix I MODFLOW Output File Example: Three -Dimensional Field Demonstration | I-1 |
| Appendix J MT3D Output File Example: Three -Dimensional Field Demonstration | J-1 |

LIST OF TABLES

| Table | | Page |
|-------|--|------|
| 1-1 | Description of appendices | 1-9 |
| 2-1 | Electromigration transport model parameters substituted for conventional MODFLOW groundwater flow parameters | 2-29 |
| 2-2 | Parameters required for the electromigration transport model added to MODFLOW input blocks..... | 2-30 |
| 2-3 | Mean red dye no. 40 velocity as a function of water content. Numbers in parentheses are the 95% confidence limits..... | 2-31 |
| 3-1 | Ion, soil/water, and regression parameters used in the 3D model. | 3-20 |
| 3-2 | Voltage and concentration boundary conditions used in the 3D model..... | 3-21 |
| 3-3 | One dimensional predicted electromigration velocity predicted by Eq. (3-5) for the soil layers in the layered and homogeneous models. Input parameters were from Table 3-1 and the electric potential gradient was 55 V m^{-1} | 3-22 |
| 4-1 | Electrode operation equipment used in the 1994 and 1996 field experiments ... | 4-23 |

LIST OF FIGURES

| Figure | Page |
|---|------|
| 1-1 Electrokinetic phenomena in a soil pore..... | 1-10 |
| 1-2 Electrical conductivity of Hanford dune sand as a function of moisture content | 1-11 |
| 2-1 Laboratory test cell apparatus used to determine red dye No. 40 electromigration transport velocities..... | 2-32 |
| 2-2 Laboratory observations of the leading-edge dye location from the spiked dye strip as a function of time. Line represents the linear regression of the data set | 2-33 |
| 2-3 Laboratory analysis of moisture content (diamonds) and pH of 1:2 soil-water extracts (squares) from post-test soil samples take from the 9.5% moisture experiment after 24 hours of applied electricity..... | 2-34 |
| 2-4 Electrical conductivity of the bulk pore water as a function of volumetric moisture content. Laboratory data represented by crosses. Solid line represents fitted Mualem and Freidman (1991) continuous function. | 2-35 |
| 2-5 Initial location of red dye no. 40 in test cell, and model predictions of dye concentrations after 1, 3, and 5 hours of simulation time | 2-36 |
| 2-6 Observed and predicted transport velocities of red dye No. 40. Points represent observed electromigration velocities with 95% confidence intervals as determined from dye location versus time regression analysis. The solid line represents velocities predicted by the numerical model..... | 2-37 |
| 2-7 Tortuosity as a function of moisture content as calculated by Eq. (2-9) for the laboratory experiments..... | 2-38 |
| 2-A-1 Normalized equivalent electrical conductivity of CuSO_4 as a function of ionic strength. Diamonds represent data obtained from the CRC (1970, Table 3-36), solid line represents chemical activity coefficient adjustment to the equivalent electrical conductivity at infinite dilution. | 2-39 |
| 3-1 Plan view illustrating the electrode positions and numerical model domain for the southern half of the field demonstration. Open circles indicate ceramic-cased electrodes while closed circles indicate pipe electrodes with no electrolysis reaction neutralization. | 3-23 |
| 3-2 Electrode construction and installation method. (a) Anode and Phase 1 cathode ceramic-cased electrode, (b) Phase 2 cathode pipe electrode. | 3-24 |

| Figure | Page |
|--------|---|
| 3-3 | Schematic of the water circulation system and pH control system for the ceramic-cased field electrodes 3-25 |
| 3-4 | Representative cross-section of soil properties prior to electrokinetic experiments. Numbers are sample values. Contour lines are hand-drawn. Box illustrates model simulation area. (a) Apparent electrical conductivity (EC_a) ($S\ m^{-1}$), (b) volumetric moisture content (%) by soil sampling. 3-26 |
| 3-5 | Cross-section illustrating acetate concentrations (mg acetate per Kg soil) at the completion of the field demonstration (end of Phase 2). The solid contour line represents the zero concentration level. Gray contours lines represent apparent electrical conductivity values as shown in Figure 3-4(a). 3-27 |
| 3-6 | Three-dimensional view of the numerical model domain indicating cells size and electrode locations used during Phase 1 and Phase 2. Shading represents cells containing the ceramic portion of the electrode casing 3-28 |
| 3-7 | Tortuosity as a function of moisture content. Line represents best fit of Equation 2-9 of Mattson et al. (1999a) to field measured data. 3-29 |
| 3-8 | Predicted acetate concentrations (relative to input) after 1246 hrs (Phase 1) of electrokinetic transport. Anode and cathode electrodes used during this phase are shaded. (a) layered model – gray shading indicates electrically conductive/wetter layer, (b) homogeneous model. 3-30 |
| 3-9 | Predicted acetate concentrations (relative to the input) after an additional 837 hrs (Phase 2) of electrokinetic transport. Anode and cathode electrodes used during this phase are shaded. (a) layered model – gray shading indicates electrically conductive/wetter layer, (b) homogeneous model 3-31 |
| 3-10 | Model predicted acetate ion velocity as a function of moisture content in a 1-dimensional $55\ V\ m^{-1}$ electric potential gradient. 3-32 |
| 4-1 | Cross-section of the laboratory apparatus 4-24 |
| 4-2 | Schematic cross-section of the operational systems, internal components, and installation characteristics of a field electrode 4-25 |
| 4-3 | Electroosmotic permeability of HDTMA-treated and untreated ceramic measured in the laboratory as a function of pore volumes electroosmotically flushed through the ceramic 4-26 |
| 4-4 | Schematic of electroosmotic, hydraulic, and the net velocity profile resulting from superpositioning in a HDTMA-treated ceramic pore. 4-27 |

CHAPTER 1. INTRODUCTION

Inorganic contamination in unsaturated soil is a widespread problem at Environmental Protection Agency Superfund sites, Department of Energy sites, and privately-owned facilities throughout the nation. Viable methods for remediating unsaturated soils that contain dissolved ionic contaminants such as heavy metals are limited. Recently, there has been a focus on developing and assessing innovative in-situ technologies to treat contaminated soil. One such innovative technology is electrokinetic remediation, the use of a direct electrical current potential field to induce ion and pore water transport.

1-1. ELECTROKINETIC PHENOMENA

The application of a direct electrical current imposed between electrodes implanted in soil leads to a number of effects collectively known as electrokinetic phenomena. The transport of ions dissolved in the soil pore water under the influence of an electric potential field is known as electromigration. Similarly, charged particle transport towards the oppositely charged electrode is known as electrophoresis. Finally, electroosmosis describes movement of soil water in response to the electric potential field (Hunter, 1981).

Soil water is typically transported towards the cathode due to the excess net positive charges in the double layer associated with the negative surface charge of the soil. Under the influence of an electric potential field, these positive charges migrate toward the cathode and create a viscous drag effect on the bulk pore water. Non-charged contaminants will be transported with the electroosmotic water flux. Charged contaminants dissolved in the pore water, and charged particles such as colloids, will migrate to the oppositely charged electrode. The combination of these phenomena, electroosmosis, electromigration, and electrophoresis, leads to contaminant transport toward the electrodes (Figure 1-1).

The electromigration velocity of an ion transported in a porous medium is a function of the ionic mobility and the voltage gradient:

$$v_{em} = \mu_i^* \frac{dV}{dx} \quad (1-1)$$

where v_{em} is the electromigration velocity (m s^{-1}), μ_i^* is the effective ionic mobility ($\text{m}^2 \text{V}^{-1} \text{s}^{-1}$), and dV/dx is the voltage gradient (V m^{-1}). The ionic mobility in a solution can be calculated from the Nernst-Einstein equation describing the ionic mobility as a function of the diffusion coefficient or can be found in published references. Previous researchers (Shapiro et al., 1989; Yeung, 1990; Alshawabkeh and Acar, 1996) have provided corrections for μ_i^* to account for tortuosity in a porous medium.

Similarly, the Helmholtz-Smoluchowski equation (Hunter, 1981) describing water transport due to electroosmotic flow in a capillary tube has also been corrected for tortuosity to extend the description of electroosmosis to porous media:

$$v_{eo} = \frac{\varepsilon \zeta}{\eta \tau_f} \frac{dV}{dx} \quad (1-2)$$

where v_{eo} is the electroosmosis velocity (m s^{-1}), ε is the fluid permittivity ($\text{C V}^{-1} \text{m}^{-1} [\text{N V}^{-2}]$), ζ is the zeta potential (V), τ_f is a tortuosity factor (-) describing the ratio of the ion pathway to the straight-line pathway, and η is the fluid viscosity ($\text{Pa s} [\text{N m}^{-2} \text{s}]$).

1-2. MOTIVATION FOR INVESTIGATING ELECTROKINETIC TRANSPORT IN UNSATURATED SOILS

Previous electrokinetic research has focused on saturated, fine-grained soils and clays that are difficult to remediate using typical pump-and-treat methods. The predominance of these environments in electrokinetics work has led to a common misconception that electrokinetics is not applicable to unsaturated, sandy soils even though limited experimental electrokinetics work in such media has been documented (Runnells and Larson, 1986; Dahab et al., 1992; Lindgren et al., 1992; Mattson and Lindgren, 1995).

Further support that electrokinetic transport would be applicable in unsaturated soil comes from understanding the transfer of electrical current through a soil-water medium. Assuming the soil minerals are non-conducting, then the fluxes of individual ionic species through the bulk pore water (electromigration) and through the double layer (electroosmosis) are the two mechanisms that transfer electrical current (Figure 1-1). Therefore, if an electrical current is passed through an unsaturated non-conducting soil, then ionic species must be transported through the pore water.

The electrical conductivity of an unsaturated soil does not immediately drop to a negligible value as soon as the soil begins to desaturate. Rather, the draining of pores reduces the cross-sectional area for electrical current transport and increases the length of the electrical pathway, producing a smooth continuum of electrical conductivity reduction as a soil desaturates. For example, Figure 1-2 illustrates the electrical conductivity of Hanford dune sand as a function of volumetric moisture content. The electrical conductivity is at a maximum when the soil is fully saturated and decreases with decreasing moisture content. Throughout this entire range of moisture content, ion transport through the bulk pore water and through the double layer are responsible for the resulting electrical conductivity.

This is not to say that because an electrical current can be passed through an unsaturated soil it can be easily remediated. The decrease of electrical conductivity is nonlinear with respect

to soil moisture. At soil moisture values near the residual value, the electrical conductivity decreases rapidly, implying a much larger voltage gradient is needed to transfer an equivalent amount of electrical current as the soil dries. In addition, engineering a remediation system becomes more complex in drier soil.

The work presented in this dissertation is an extension of research conducted for Sandia National Laboratories (SNL), Albuquerque, New Mexico. SNL was interested in evaluating whether the electrokinetic remediation process could remediate a chromate plume emanating from an unlined chromic acid pit (UCAP) at their chemical waste landfill.

The SNL chemical waste landfill was the chemical disposal site for SNL from 1962 to 1985. During this time, chemicals were separated by type and disposed of in unlined trenches. It is estimated that over 16 m^3 (4290 gallons) of chromic/sulfuric acid solution was disposed in the chromic acid pits (SNL, 1991). The chromium was disposed of in the hexavalent form, and the very low organic fraction present in the native soil suggests the chromium should stay in the anionic hexavalent form adsorbing weakly to soil beneath the chemical waste landfill (Persaud and Wierenga, 1982). Chemical analysis of soil samples collected from boreholes drilled in 1987 indicated chromium transport to a depth of at least 25 m (75 ft) below the land surface. Soil moisture content in the chromium-contaminated soil was in the range of 2 to 12% by weight.

Prior to this dissertation, a detailed study of moisture content effects on electrokinetic transport of ions through unsaturated soil had not been performed. For this dissertation, an experimental data set illustrating the electromigration transport velocity of red dye #40 as a function of moisture content was developed from a series of laboratory experiments. Red dye #40 was used as a surrogate contaminant for chromate since both are anions with a valance of -2 . In addition, red dye #40 had the advantage of being non-hazardous and allowing visual observation of transport phenomena during an experiment. Chapter 2 details the laboratory experiments and results of the red dye #40 electromigration rate as a function of moisture content.

In addition to lack of experimental data sets, the theoretical relationships describing electromigration transport in unsaturated soils had not been developed. Although the laboratory experiments performed by Runnells and Larson (1986) and Dahab et al. (1992) demonstrated electrokinetic transport of copper ions in a sandy soil, these experiments lacked a theoretical description of electrokinetic transport phenomena in an unsaturated soil. Chapter 2 addresses this issue by describing the effects of varying cross-sectional area of the pore water and the tortuosity as a function of moisture content on the electrokinetic transport processes.

Electrokinetic transport models have generally been confined to a single dimension due to the complexity of coupling the electrokinetic flux equation and the electric current equation (Shapiro et al., 1989; Yeung, 1990, Alshawabkeh and Acar, 1996). While one-dimensional simulations are useful to examine physicochemical effects on electrokinetic phenomena, such models can not predict changes in the electric potential field due to electrode geometry or spatial variability of the soil/water properties. These one-dimensional models have limited application for predicting electrokinetic transport at the field scale.

This dissertation describes a three-dimensional ion transport model through unsaturated soils. The model assumes a constant moisture content and electrical potential field with respect to time but allows both variables to vary in space. This model is described in Chapter 2 of this dissertation and is tested against electrokinetic field demonstration results in Chapter 3.

Previous models also assumed ionic mobility was equal to the values at infinite dilution, thereby overestimating an ion's velocity at a constant voltage potential. Kohlrausch demonstrated through a series of laboratory measurements (Bockris and Reedy, 1973) that the equivalent conductivity of a free solution decreases with the square root of concentration. Numerical models must account for this reduction of ionic mobility as the concentration of the pore water increases. For this dissertation, the reduction in mobility was estimated using the activity coefficient calculated by the Davies Equation (see Chapter 2, Appendix A).

Finally, a method was developed to control the rate of water entering the soil at the anode electrode. A continuous water pathway is required to maintain an applied electrical potential, but excess water could saturate the soil causing the contaminants to be transported deeper into the soil profile. Chapter 4 describes a surfactant coating procedure of the porous ceramic anode casing necessary for the successful application of electrokinetics to unsaturated soils.

The research focus of this dissertation is on the electromigration of ions in unsaturated soils. Electrokinetic transport theory, three-dimensional numerical model development, comparison of model predictions to experimental results, and a surfactant-coating procedure for anode electrode casings are all described here.

1-3. ORGANIZATION OF THIS DISSERTATION

Each chapter of this dissertation discusses a particular topic related to the electrokinetic transport or removal of ions in unsaturated soil. Chapter 1 (this chapter) introduces the fundamental phenomena of ion transport in porous media due to an electric potential field and describes the organization of this dissertation.

Chapter 2 is the first of two companion papers to be submitted to the journal *Water Resources Research*. Chapter 2 describes the history of electrokinetic numerical modeling, the theory of electromigration of ions in soils, and simplifying assumptions used in this dissertation for numerical model development. Implementation of the transport and continuity equations by modifying a ground-water flow code (MODFLOW) and a transport code (MT3D) to allow predictions of electromigration transport through unsaturated soils is described. The model was verified by comparing numerical predictions to laboratory experimental electromigration results.

Chapter 3 is the second of the companion papers and describes an electrokinetic field demonstration in unsaturated soil conducted at SNL in Albuquerque, NM. The effects of spatial heterogeneities on the transport of acetate at the field-scale are discussed based on the results of both numerical model predictions and field measurements.

Chapter 4 describes a surfactant-coating procedure for anode ceramic casings that reverses the electroosmotic flow direction within the treated-ceramic pores. This paper was submitted to the *Journal of Environmental Engineering* for publication. Laboratory experiments and a field demonstration results compare electroosmotic flow rates from untreated- and treated-ceramic electrode casings to evaluate the effectiveness of the treatment procedure.

Chapter 5 concludes the dissertation and presents suggestions for future research.

Finally, the appendices provide additional details about some aspects of the dissertation project. Table 1-1 lists each appendix, provides a brief description of its content, and indicates the chapter to which the appendix is related.

1-4. REFERENCES

- Alshawabkeh, A. N., and Y. B. Acar, Electrokinetic remediation. II: Theoretical model, *J. Geotech. Eng.*, 122, 186-196, 1996.
- Bockris, J. O'M., and A. K. N. Reddy, *Modern Electrochemistry, Volume 1*, 622 pp., Plenum, New York, 1973.
- Dahab, M. F., W. E. Kelly, and F. R. Goderya, Removal of metallic contaminants in unsaturated soils using electrokinetics, *Proc. U.S. Department of Energy Electrokinetic Workshop*, Atlanta, GA, 1992.
- Hunter, R. J., *Zeta Potential in Colloid Science*, Academic Press Ltd, London, 386 pp., 1981.
- Lindgren E. R., E. D. Mattson, and M. W. Kozak, Electrokinetic remediation of contaminated soils: An update, in *Waste Management '92*, Tucson, AZ, 1309 - , 1992.
- Mattson, E. D., and E.R. Lindgren, Electrokinetic extraction of chromate from unsaturated soils, *Emerging Technologies in Hazardous Waste Management*, edited by D.W. Tedder and F.G. Pohland, ACS Series 607, Washington, DC, 10-20, 1995.
- Persaud, N. and Wierenga, "Solute Interactions and Transport in Soils from Waste Disposal Sites at Sandia Laboratories." Report submitted to Sandia National Laboratories by Dept. of Agronomy, New Mexico State University, June, 1982.
- Runnells, D.D., Larson, J.L. "A laboratory study of electromigration as a possible field technique for the removal of contaminants from ground water." *Ground Water Monitoring Review*, 6(3), 85-91, 1986.

SNL (Sandia National Laboratories), "Chemical Waste Landfill Final Closure Plan and Post-Closure Permit Application." Prepared by SNL Environmental Impact and Restoration Division 7723, December, 1991.

Shapiro, A. P., P. C. Renauld, and R. E. Probstein, Preliminary studies on the removal of chemical species from saturated porous media by electroosmosis, *PhysicoChem. Hydrodyn.*, 11, 785-802, 1989.

Yeung, A. T., Coupled flow equations for water, electricity, and ionic contaminants through clayey soils under hydraulic, electrical and chemical gradients, *J. Non-Equil. Thermodyn.*, 15, 247-267, 1990.

Table 1-1. Description of Appendices

| Appendix | Name | Description | Related Chapter |
|----------|--|--|-----------------|
| A | MODFLOW and LKMT Code Modifications | Fortran listing of changes to the MODFLOW code modules. | 2 |
| B | MODFLOW Input File Example: One-Dimensional Laboratory Dye Experiment | Example of *.dat files used to determine the electric potential field for anionic dye simulations. | 2 |
| C | MT3D Input File Example: One-Dimensional Laboratory Dye Experiment | Example of *.inp files used to determine the anionic dye concentrations | 2 |
| D | MODFLOW Output File Example: One-Dimensional Laboratory Dye Experiment | Example of electric potential field output. | 2 |
| E | MT3D Output File Example: One-Dimensional Laboratory Dye Experiment | Example of anionic dye concentration output. | 2 |
| F | Experimental Electrode Control System | Provides additional detail of the construction and installation of the field electrodes. | 3 |
| G | MODFLOW Input File Example: Three-Dimensional Field Demonstration | Example of *.dat files used to determine the electric potential field for acetate simulations | 3 |
| H | MT3D Input File Example: Three-Dimensional Field Demonstration | Example of *.inp files used to determine the acetate concentrations | 3 |
| I | MODFLOW Output File Example: Three-Dimensional Field Demonstration | Example of electric potential field output. | 3 |
| J | MT3D Output File Example: Three-Dimensional Field Demonstration | Example of acetate concentration output. | 3 |

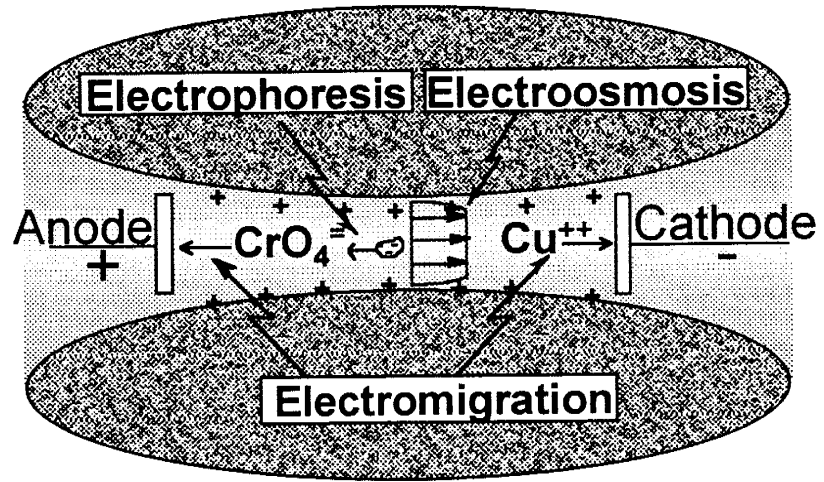


Figure 1-1. Electrokinetic phenomena in a soil pore.

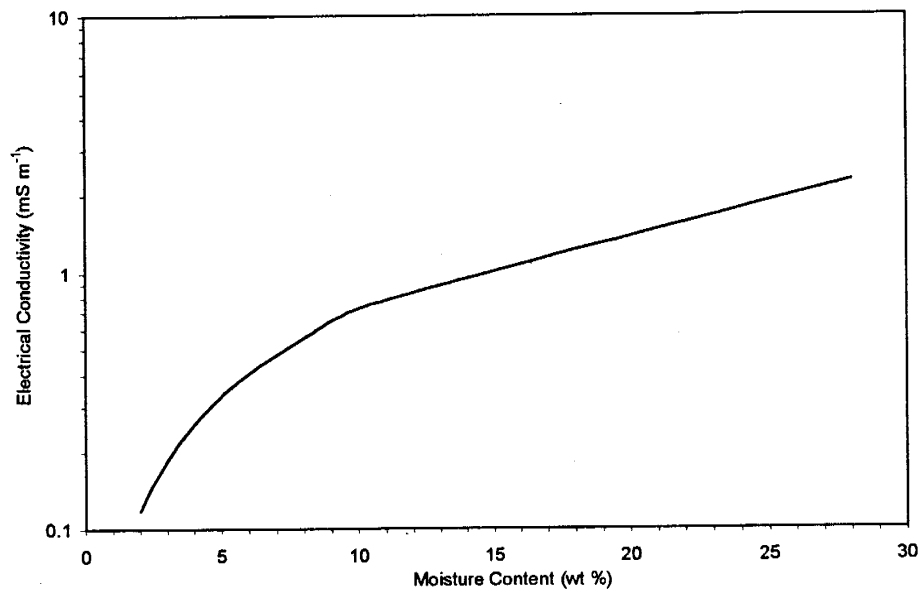


Figure 1-2. Electrical conductivity of Hanford dune sand as a function of moisture content.

CHAPTER 2. ELECTROKINETIC ION TRANSPORT THROUGH UNSATURATED SOIL: 1. THEORY, MODEL DEVELOPMENT, AND TESTING

Earl D. Mattson^{1,2}, Robert S. Bowman¹, and Eric R. Lindgren³

¹Department of Earth and Environmental Science, New Mexico Institute of Mining and Technology, 801 Leroy Place, Socorro, NM 87801

²Now at the Department Integrated Earth Science, LMITCO, INEEL, PO Box 1625, Idaho Falls, ID, 83415-2107

³Sandia National Laboratories, PO Box 5800, Albuquerque, NM 87185-0719

(to be submitted to *Water Resources Research*)

ABSTRACT

A three-dimensional electromigration transport model for ion transport in unsaturated soil was developed and tested against laboratory experiments. This model assumed the electric potential field was constant with respect to time, an assumption valid for highly buffered soil, or when the electrode electrolysis reactions are neutralized. The model also assumed constant moisture contents with respect to time, and that electroosmotic and hydraulic transport of water through the soil was negligible. A functional relationship between ionic mobility and the electrolyte concentration was estimated using the chemical activity coefficient. Tortuosity was calculated from a mathematical relationship fitted to the electrical conductivity of the bulk pore water and soil moisture data. The functional relationship between ionic mobility, pore-water concentration, and tortuosity as a function of moisture content allowed the model to predict ion transport in heterogeneous unsaturated soils. The model was tested against laboratory measurements assessing anionic electromigration as a function of moisture content. In the test cell, a strip of soil was spiked with red dye No. 40 and monitored for a 24-h period while a 10-mA current was maintained between the electrodes. Electromigration velocities predicted by the electromigration transport model

were in agreement with laboratory experimental results. Both laboratory-measured and model-predicted dye migration results indicated a maximum transport velocity at moisture contents less than saturation due to competing effects between current density and tortuosity as moisture content decreases.

2-1. INTRODUCTION

Electrokinetic remediation describes a transport process intended to extract dissolved ions and organic compounds from porous media. To initiate electrokinetic transport, a DC electric potential field is applied to the porous medium. The applied current transports dissolved charged ions due to electromigration towards the oppositely charged electrode. Concurrently, electroosmosis moves the pore water in response to the electric field, typically towards the cathode because of the negative surface charge of the soil. The magnitude of the transport velocity due to electromigration and electroosmosis is directly related to the electric potential gradient.

In recent years, there has been an interest in using electrokinetics as an in-situ remediation technology to extract heavy metals, radionuclides, and organic compounds from saturated and unsaturated soils, sediments, and groundwater. Considerable effort has been devoted to the development of mathematical and numerical models describing the remediation process.

Modeling electrokinetic transport through porous media is complex due to use of the current equation to determine the electric potential gradient, the driving potential for electromigration and electroosmotic transport. This method calculates the fluxes of all the ions in the fluid system to determine the current density, then iteratively solves the current equation until the calculated electric potential across the computational system matches the boundary conditions (Shapiro et al., 1989; Alshawabkeh and Acar, 1996). Although theoretically correct, the solution scheme is numerically intensive due to the small time steps required, the number of ion fluxes to

be calculated, and the iterative approach required to solve the current equation. The change in the electric potential appears to be due to chemical reactions within the pore water. When electrode electrolysis reactions change the pore-water pH and hence the electric potential gradient, then the iterative solution scheme is required.

However, in many situations, the electric potential gradient does not significantly change with time. Electrolysis reactions can be neutralized at the electrodes, minimizing pH effects. In addition, many soils have large buffering capacities that neutralize electrokinetically introduced pH effects in the soil. For example, due to such a large buffer capacity, Jacobs and Probst (1996) found the closest agreement between model simulation results and observed effluent phenol concentrations in laboratory experiments when electromigration of hydrogen ions was ignored. In situations where the pH is constant, a model that either calculates a steady state electric potential field from soil electrical conductivity or assumes an electric potential field can be used.

The first electrokinetic modeling efforts were initiated from an engineering desire to use electrokinetics for enhancement of soil slope stability, with a focus on electroosmotic water movement rather than ion transport. Erisman (1968) and Lewis and Humpheson (1973) developed models to study electroosmotic de-watering of clay soils. These early models simulated soil consolidation and de-watering, both of which affect the apparent soil electrical conductivity, yet they assumed a constant electric potential gradient.

Shapiro et al. (1989) extended an electrophoresis model by Saville and Palusinski (1986) to a saturated porous medium by introducing electroosmosis processes, porosity, and tortuosity. Advective hydraulic transport was neglected, although dissociation reactions, electrochemical reactions, and local pH effects on surface charge were all included in the Shapiro et al. (1989) model. Laboratory results for phenol removal from a saturated kaolin clay soil were compared to numerical simulation results (Shapiro et al., 1989).

The Shapiro et al. (1989) model has been modified to include additional complex chemical effects on transport. Shapiro and Probstein (1993) added linear adsorption and compared the numerical results to laboratory experiments with phenol and acetic acid. Adsorption, complexation, dissolution, and precipitation reactions were added by Jacobs et al. (1994) to simulate zinc removal from kaolin clays in laboratory experiments. In a parallel effort, Shapiro modified the Shapiro and Probstein (1993) model to include ion transport in the double layer, pH buffering by the soil, and the dependence of zeta potential on pH and ionic strength (Monsanto, 1996). Alshawabkeh and Acar (1996) also developed a one-dimensional model similar to that of Jacobs et al. (1994) and simulated lead removal from clay.

During this same time period, Acar et al. (1991) developed a one-dimensional analytical model to predict the migration of pH fronts in kaolin clay media. Their model superimposed hydraulic and electrical gradients that were all assumed constant in time and space. Mitchell and Yeung (1990) developed a one-dimensional model based on the non-equilibrium thermodynamics on the coupled flow. Later Yeung and Datla (1995) presented an electrokinetics model assuming electric neutrality was maintained by the formation of hydrogen and hydroxyl ion. Yeung and Datla performed a numerical analysis to calculate pH distributions in kaolin clay, and compared their modeling simulations to laboratory pH results published by Acar et al. (1991).

Much less effort has been directed toward the development of multi-dimensional electrokinetic models. A few two-dimensional electroosmosis models have been developed for aquifer de-watering applications. Lewis and Gardner (1972) simulated water flow beneath sheet pilings by coupling electroosmosis and advective hydraulic flow. Renaud and Probstein (1987) examined steady-state coupling between electroosmotic and hydraulic flow to evaluate the effectiveness of electroosmosis to divert groundwater around hazardous waste sites. They evaluated different site geometries, electrode configurations, and values of physicochemical parameters.

To date, only one multi-dimensional electrokinetic model has been developed to predict electromigration ion transport in a saturated porous medium. Jacobs and Probstein (1996) developed a two-dimensional model that included hydraulic advection, electroosmosis, electromigration, and diffusion based transport processes as well as chemical processes including complexation, dissolution, precipitation reactions, surface complexation and sorption, and electrochemical reactions. An artificial diffusivity was necessary to facilitate numerical stability and convergence, in the simulation of phenol removal from homogeneous kaolin clay in a small-scale (12-cm electrode spacing) laboratory experiment.

Applications of electrokinetic models to large-scale experiments are limited. Most models have been applied to laboratory-scale experiments where the distance between electrodes varied from 10 cm (Acar et al., 1991) to 50 cm (Shapiro and Probstein, 1993). Shapiro (Monsanto, 1996) applied his one-dimensional model to a larger-scale experiment, a pilot-scale field test where the electrodes were 3 m apart.

There is a need for electrokinetic transport models suitable for field applications. Such models must address spatial heterogeneities in soil properties and in pore water solution chemistry. Existing electrokinetic models typically assume homogeneous soil parameters, saturated moisture content and hence a constant tortuosity term throughout the entire model domain. Tortuosity is a strongly nonlinear function of moisture content. Furthermore, these models do not adjust the ionic mobility for electrolyte concentration effects, instead using ion electric mobilities determined at infinite dilution for their simulations. In reality, as the electrolyte solution becomes more concentrated, individual ion mobilities are reduced due to ion interactions.

We developed a three-dimensional saturated/unsaturated electromigration transport model to address the limitations of previous models. A direct analogy between groundwater flow and ion flow prompted the application of the three-dimensional groundwater flow model MODFLOW (McDonald and Harbaugh, 1988), and the three-dimensional transport model MT3D

(Zheng, 1990), to predict ion transport due to an electric field. The numerical implementation of ion transport by an electric field was based on the assumption that the flow lines of current under an electric gradient through soil are the same as the flow lines of water molecules under a hydraulic gradient. The electromigration transport model was implemented by calculating the electric potential field by MODFLOW. Using this electric potential field, ion migration velocities were determined in the linking program module and transferred to MT3D. The transport model then solved the electromigration transport equation with no further modifications.

In this paper we describe the model development and compare model predictions to results of laboratory experiments in unsaturated soils. In a companion paper, we compare model predictions to ion transport in a heterogeneous field soil.

2-2. THEORY

The equation of continuity describing the transport of a species through a unit volume of porous medium is:

$$\frac{\partial c_i}{\partial t} = -\nabla \cdot j_i + R_i \quad (2-1)$$

where $\partial c_i / \partial t$ is the change in concentration of component i in the unit volume with respect to time ($\text{mol m}^{-3} \text{s}^{-1}$), j_i is the molar flux of component i ($\text{mol m}^{-2} \text{s}^{-1}$), and R_i is the molar source/sink of component i ($\text{mol m}^{-3} \text{s}^{-1}$).

The molar flux of an ion due to an electric potential gradient is governed by the Nernst-Planck equation that describes the diffusive flux, electromigration flux, and the convective bulk water flux (all with units of $\text{mol m}^{-2} \text{s}^{-1}$) in a capillary tube. The Nernst-Planck equation has been extended by numerous researchers (Shapiro et al., 1989; Yeung, 1990; Alshawabkeh and Acar, 1996; Jacobs and Probstein, 1996) to a porous medium by modifying the transport coefficients to include the effects of tortuosity:

$$j_i = -D_i^* \nabla c_i + \mu_i^* c_i \nabla \phi + v c_i \quad (2-2)$$

where D_i^* is the effective molecular diffusion coefficient of ion i in a porous medium ($\text{m}^2 \text{s}^{-1}$), μ_i^* is ion i 's effective ionic mobility in a porous medium ($\text{m}^2 \text{V}^{-1} \text{s}^{-1}$), ϕ is the electrostatic potential (V), and v is the linear pore water velocity including the effects of both electroosmotic and hydraulic flow (m s^{-1}).

The effective diffusion coefficient in a porous medium is related to that in free-water by:

$$D_i^* = D_i \theta \tau(\theta) \quad (2-3)$$

where D_i is the molecular diffusion coefficient in water ($\text{m}^2 \text{s}^{-1}$), θ is the volumetric moisture content ($\text{m}^3 \text{m}^{-3}$), and τ is the tortuosity (L/L_e)², where L_e is the average length of the streamlines in a porous medium and L is the straight-line length.

Similarly, the effective ionic mobility is calculated as:

$$\mu_i^* = \mu_i \theta \tau(\theta) \quad (2-4)$$

where μ_i is the ionic mobility of ion i in water ($\text{m}^2 \text{V}^{-1} \text{s}^{-1}$). Previous models have assumed that μ_i is the same as the ionic mobility at infinite dilution. However, appropriate use of the ionic mobility involves adjusting for the presence of other ions in the pore water solution. The method proposed in this paper (detailed in Appendix 2-A) calculates the effective ionic mobility by multiplying the ionic mobility of ion i at infinite dilution in water, μ_i^0 , ($\text{m}^2 \text{V}^{-1} \text{s}^{-1}$), by the activity coefficient as calculated by the Davies Equation:

$$\mu_i = \mu_i^0 10^{\left(-0.5085z^2 \left(\frac{\sqrt{I}}{1+\sqrt{I}} - 0.3I\right)\right)} \quad (2-5)$$

where z is the valence of ion i , and I is the ionic strength (mol kg^{-1}).

Wolt (1994) summarized several published empirical relationships for the ionic strength of an electrolyte solution as a function of the solution electrical conductivity. Based on Wolt's summary, the equation of Griffin and Jurinak (1973) appears to be the most appropriate for the

study presented in this paper. Griffin and Jurinak modified an earlier linear relationship developed by Ponnampetuna et. al. (1966) by: 1) including ion-pair formation in the calculation of the actual ionic strength and, 2) extending the validity of the empirical relationship to solutions of higher salt contents representative of semi-arid ecosystems. They fitted a linear relationship between the ionic strength and the electrical conductivity from a data set including 124 river water samples and 27 pore-water extracts with electrical conductivities up to 3.24 S m^{-1} :

$$I = 0.127EC_w - 0.003 \quad (2-6)$$

where EC_w is the electrical conductivity of a free solution (S m^{-1}).

Mualem and Friedman (1991) presented a functional relationship between EC_w and the electrical conductivity of the bulk soil solution, EC_b (S m^{-1}). EC_b is the effective electrical conductivity of liquid phase within a porous medium including the effects of tortuosity, and cross sectional area of the liquid phase. See Appendix 2-B for details of the Mualem and Friedman model. Solving Mualem and Friedman's Eq. 27 (1991, p. 2773) for EC_w provides:

$$EC_w = \frac{EC_b}{\left[\frac{F(\lambda)(\Theta)^{n+2}}{(\Theta)_{sat}} \right]} \quad (2-7)$$

where the effective moisture content, Θ , is represented by:

$$\Theta = \theta - \theta_o \quad (2-8)$$

$F(\lambda)$ and n are fitting parameters derived from the EC_b versus Θ data, and θ_o ($\text{m}^3 \text{ m}^{-3}$) is the immobile water content along the soil solid surface at which there is no ion flow through the bulk water. θ_o has been assumed to be equal to the residual moisture content (Mualem and Friedman, 1991) or zero (Kelly and Kalinski, 1993).

Tortuosity as a function of moisture content was also calculated from the conceptual model proposed by Mualem and Friedman (1991). Appendix 2-B contains a detailed explanation of the tortuosity function:

$$\tau(\theta) = \frac{F(\lambda)(\Theta)^{n+1}}{(\Theta)_{sat}} \quad (2-9)$$

Most researchers (Mattson and Lindgren, 1994; Jacobs and Probst, 1996; Alshwabkeh and Acar, 1996) agree that electromigration is the dominant transport mechanism of ionic species under the influence of an electric potential gradient. The sandy soil used in this study exhibits little electroosmosis flow, even when saturated. Furthermore, the hydraulic conductivity decreases rapidly as the water content of a coarse-grained soil decreases. Therefore, the advective term on the right hand side of Eq. (2-2) is neglected for this study, simplifying the transport equation for porous media to:

$$j_i = -D_i^* \nabla c_i + \mu_i^* c_i \nabla \phi \quad (2-10)$$

Finally, substituting Eq. (2-10) into Eq. (2-1) results in the governing electrokinetic transport equation:

$$\frac{\partial c_i}{\partial t} = -\nabla \cdot (-D_i^* \nabla c_i + \mu_i^* c_i \nabla \phi) + R_i \quad (2-11)$$

Equation 2-11 is numerically difficult to solve because it is written in terms of both concentration and electric potential gradients. Previous researchers (eg., Shapiro, 1989; Lindgren et al., 1995; Alshwabkeh and Acar, 1996) used a relationship called the current equation where the current within a soil pore is defined as the sum of the individual ion fluxes multiplied by their valance and Faraday's constant. The difficulty with this numerical approach lies in determining the potential field due to each ion's flux in the system. The solution requires very small time steps to reach numerical stability [e.g., the Shapiro et al. (1989) model], resulting in a numerically intensive solution.

Our approach assumed the electric potential field was constant with respect to time. This approach de-couples the electric potential gradient and the ion concentrations allowing a much simpler solution scheme. The electric potential gradient was solved from a macroscopic viewpoint by incorporating the relationships of Ohm's Law in an existing groundwater flow code.

2-3. NUMERICAL DEVELOPMENT

The numerical description of ion transport by an electric potential gradient begins with the assumption that the flow lines of ions under an electric potential gradient in soil are the same as the flow lines of water molecules due to a hydraulic potential. The governing equation for water flow is:

$$\nabla \cdot (K_{ii} \nabla h) - W = S_s \frac{\partial h}{\partial t} \quad (2-12)$$

where K_{ii} is the hydraulic conductivity in the principle directions of flow (m s^{-1}), h is the hydraulic head (m), W is the volumetric flux rate per volume (s^{-1}) representing sources and sinks, and S_s is the specific storage (m^{-1}). The form of Eq. (2-12) is similar to that for current flow:

$$\nabla \cdot (EC_{a\ ii} \nabla \phi) - J_T = 0 \quad (2-13)$$

where $EC_{a\ ii}$ is the apparent electrical conductivity of the soil in the principle directions (S m^{-1}), and J_T is the applied current at an electrode. The apparent electrical conductivity is that measured through a soil medium and is equal to the summation of the electrical conductivity through the pore water and the electrical conductivity along the soil.

This direct analogy between groundwater flow and ion flow prompted the application of an existing USGS three-dimensional groundwater flow model, MODFLOW (McDonald and Harbaugh, 1988), to solve for the electric potential gradient (Eq. 2-13) and an existing solute transport model, MT3D (Zheng, 1990) to solve the continuity equation (Eq. 2-1).

The original MODFLOW simulates groundwater flow using a block-centered finite difference approach. The flow model interface module, LKMT (Zheng, 1990), links output from MODFLOW and transfers it as input to MT3D. Specifically, Zheng's LKMT module sends the hydraulic heads, flux of groundwater across each cell face, and the locations and flow rates of the sources and sinks to MT3D. MT3D was then used to solve the continuity equation (Eq. 2-1).

MT3D simulates advection, dispersion, and chemical reactions of dissolved constituents in ground-water systems (Zheng, 1990), using the upstream finite difference method.

The electromigration transport model used the existing USGS models to calculate the electric potential and ion transport due to a electric potential field. Electrical parameters of the soil properties replaced the analogous groundwater flow parameters to obtain the electric potential field. Table 2-1 shows the electromigration transport model parameters that were used as input for the MODFLOW code to calculate the electric potential field.

Several modifications were required before MODFLOW and LKMT code modules could be used to simulate ion transport under the influence of an electric potential gradient. LKMT was modified such that the electric potential gradient, the equivalent Darcy ion flux across each cell face, and the location and current flow rate of the electrical source and sinks were generated by MODFLOW to be used as input to the MT3D calculations. MODFLOW was modified by adding additional input and output blocks to module BCF1.FOR. The additional blocks included transport properties of the ion of interest and soil electrical properties (Table 2-2). In addition, the X-array size was increased in module BAS1.FOR to allow the new electromigration transport model input parameters to be stored. Finally, LKMT.INC was changed to read the additional electromigration transport model input parameters from the BCF.dat input file. Appendix A contains a list of the FORTRAN code modifications made to the above MODFLOW modules. No code modifications were required for the MT3D transport model.

To conduct an electromigration model run, first Eq. (2-13) was solved to calculate the electric potential field throughout the model domain. Next, the effective ionic mobility was calculated using Eqs. (2-4) through (2-9), adjusting the ionic mobility for concentration and tortuosity effects. The advective ion velocity (v_{iA} , $m\ s^{-1}$) through each cell face was calculated using the electric potential gradient as calculated by:

$$v_{iA} = \mu_i^* \frac{d\phi}{dx_{ii}} \quad (2-14)$$

where v_{iA} is the velocity of ion i across a cell face (m s^{-1}), and $d\phi/dx_{ii}$ is the electric potential gradient (V m^{-1}) across the cell face. The equivalent Darcy ion velocity was calculated by multiplying Eq. (2-14) by the cross-sectional area of the cell face. Finally, in MT3D the equivalent Darcy velocity was multiplied by the cell concentration to determine the electromigration flux (the second term on the right-hand-side of Eq. (2-10)). The diffusional flux was calculated in MT3D as described by Zheng (1990).

2-4. LABORATORY EXPERIMENTS

One-dimensional laboratory experiments were conducted to examine electromigration anion transport as a function of moisture content. The soil was chemically equilibrated with a 0.005 M CaCl_2 solution in an attempt to have a known pore water electrical conductivity value. Laboratory experiments were conducted in test cells under uniform moisture content conditions ranging from 9.5 to 37.5% ($\text{m}^3 \text{m}^{-3}$) (approximately 25 to 100% saturation). Each experiment was operated for a period of approximately 24 hours at a constant applied current of 10 mA.

2-4.1 Materials and Methods

Soil for the experiments was obtained from alluvial surface sediments collected at Sandia National Laboratories in Albuquerque, New Mexico. The soil was composed of Quaternary granitic alluvium contained pedogenic calcite and clasts of limestone. Primary mineralogic constituents included quartz, potassium-feldspar, gypsum, and calcium carbonate; the calcareous components comprised approximately 10 weight percent of the soil (Persaud and Wierenga, 1982).

In preparation for the laboratory experiments, the soil was wet-sieved to retain the 150 to 300 μm diameter fraction, then soaked in successive aliquots of a 0.005 M CaCl_2 solution until the electrical conductivity of the supernatant stabilized to approximately 0.12 S m^{-1} . At this time it was assumed that the soil sorption sites were in equilibrium with the CaCl_2 solution. To

prevent CaCl_2 precipitation that would have occurred by oven drying the sample, the soil was then dewatered in a pressure plate apparatus at approximately 6 bars, reducing the moisture content to approximately 4 wt %. Prior to packing the test cell, additional 0.005 M CaCl_2 solution was added to the dewatered soil until the desired moisture content was obtained. Moisture content of the soil was determined by microwave-drying a representative subsample following ASTM Method 4643 (ASTM, 1993). This preparation method provided a soil at a known moisture content and pore-water electrical conductivity for the laboratory experiments.

Independent measurements of the physical and electrical properties of the soil and pore water were used to approximate θ_0 , EC_s , θ_s , and EC_w . θ_0 was assumed to be the moisture content at which there was no electrical conduction through the bulk pore water. θ_0 had a value of 0.01 in laboratory experiments (described below). Alternatively, θ_0 could have been estimated from moisture retention data (i.e., θ at 15 bars) as suggested by others (Mualem and Friedman, 1991; Kelly and Kalinski, 1993).

EC_s , the electrical conductivity of the matrix surface (S m^{-1}), was calculated following the procedure outlined by Rhoades et al. (1976). Different values of EC_a were measured on laboratory soil samples using pore waters of varying EC_w at a moisture content of 10 weight percent. The EC_a EC_w data set was regressed to find the intercept. The intercept, where EC_w equals zero, was assumed to represent the soil surface electrical conductivity (Rhoades et al., 1976). Using this method, the surface conductivity was estimated to be $2.8 \times 10^{-3} \text{ S m}^{-1}$.

The measured θ_s for the alluvial sand was $0.375 \text{ m}^3 \text{ m}^{-3}$. The EC_w in the dye experiment (described below) was assumed to be equal to that of the synthetic ground water used to prepare the soil (0.12 S m^{-1}).

The experiment test cell was constructed of clear acrylic with internal dimensions of 15.2 cm \times 25.2 cm \times 1.9-cm. Graphite rods (Ultra Carbon, Inc.), 1.9 \times 1.9-cm² by 15.2-cm long, were placed at each end of the test cell to act as electrodes (Figure 2-1).

The test cells were packed with the prepared soil using a 1.2×10^4 -kg (12-ton) hydraulic press. A single lift of soil was spread evenly along the bottom of the test cell and covered with a 1.2-cm thick by 15.2-cm x 21.4-cm steel plate. The steel plate was used to distribute the force of the hydraulic piston evenly across the soil. The soil was compacted using the maximum force of the hydraulic press. The resulting dry bulk densities ranged from 1.45 to 1.6 g cm⁻³, depending on the moisture content during packing.

Next, a strip of soil spiked with 0.02 M FD&C red dye No. 40 (Warner Jenkinson Company) was placed midway between the electrodes. Chemically, the red dye No. 40 is a disodium salt of 6-hydroxy-5[(2-methy-4-sulfohenyl) azo-]-2-naphthalenesulfonic acid with a molecular weight of 450. Lindgren et al. (1992) suggest that sodium ions will completely dissociate from the sulfate groups even at low pH creating a red anionic tracer with a valance of -2. The red dye No. 40 soil was placed in the test cell by excavating a 0.6-cm x 1.9-cm x 15.2-cm channel midway between the electrodes. The channel was filled with spiked soil matching the desired moisture content of the experiment. Prior to attaching the cover plate of the cell, a sheet of plastic wrap was placed over the soil to provide a moisture barrier, followed by a 3-mm thick closed-cell styrofoam sheet to prevent the soil from shifting. The test cell was orientated horizontally as illustrated in Figure 2-1 to allow clear visual access to the soil and spiked dye strip and to minimize pore water redistribution due to gravity.

An experiment was conducted by applying an electric potential to the electrodes located at each end of the cell. A 10-mA current was applied for up to 24 h across the graphite electrodes, which were connected to a programmable power supply (Fisher Scientific, Model FB701). The applied voltage and current were recorded hourly with a Fluke Model 45 multimeter. Photographs were taken at 1-h intervals to record the location of the red dye No. 40 within the test cell. When the electric potential application was stopped, a strip of soil through the middle portion of the test cell extending from the anode to the cathode was removed, sub-sampled at 1- to 2-cm increments, and analyzed for moisture content and pH (2 to 1 soil water

extract). The average moisture content of the soil samples was used to define the moisture content of that experiment.

2-4.2 Results

The velocity of the leading edge of the red dye over time was determined by analyzing photographs of the test cell for each laboratory experiment. The leading edge of the red dye No. 40 was visually located in each photograph to determine the migration distance the dye had traveled. An example of leading edge dye position as a function of time for the 9.5% moisture content experiment is presented in Figure 2-2. The dye position showed a nearly linear progression across the test cell throughout the experiment. For each experiment, the measured dye velocity was calculated from the linear regression of the dye location versus time. The dye transport velocity was quite constant throughout the experiment duration, as indicated by the high R^2 values (Table 2-3).

Ion transport is proportional to the electric potential gradient (Eq. 2-14). The linear progression of the leading edge of the red dye No. 40 across the cell suggests that the electric potential field was constant with respect to time. Electrolysis reactions that produce H^+ ions at the anode and OH^- ions at the cathodes would be expected to alter the electric potential gradient. The buffering capacity of the soil resulting from the high carbonate content likely retarded hydrogen transport from the anode to the dye transport region, resulting in a constant voltage field. This assertion is supported by uniform pH of the soil samples measured across the test cell in post-test pore-water extracts.

Electrode reactions had little effect on moisture content and pH in the dye transport region. Figure 2-3 shows a post-test analysis of soil for the 9.5% moisture content experiment. Moisture content and pH were generally constant except for the soil immediately adjacent to the electrodes. The high moisture content in the middle of the experiment likely represents a deviation due to the addition of the dye spike. Hydrogen ion production is indicated by the lower

pH values adjacent to the anode while hydroxyl ion production is indicated by higher pH values at the cathode. The low moisture content at the anode suggests limited electroosmosis transport of water towards the cathode. However, within the dye transport region, analysis of post-test soil samples indicated moisture contents within $\pm 1\%$ ($\text{m}^3 \text{m}^{-3}$) and pH values within 0.3 units of the initial values.

The anionic dye was transported by electromigration in the direction opposite to the electroosmotic flow, an indication that electromigration of charged ions was the dominant transport process in this unsaturated sandy soil. This behavior supports the theoretical prediction of Mattson and Lindgren (1994).

2-5. ELECTROMIGRATION TRANSPORT MODEL TESTING

To test the electromigration transport model, one-dimensional numerical simulations of the laboratory experiments were performed to predict the red dye No. 40 electromigration transport rate. The laboratory test set-up was discretized into 2100 cells, each 1×10^{-4} -m long. The first and last cells of the model domain were designated to be the anode and cathode, respectively. For the MODFLOW simulations, the electrodes were assumed to be a constant flux source or sink. The anode “injected” a constant 10 mA while the cathode was “pumped” 10 mA. In addition, the cathode voltage was assumed equal to zero volts. During MT3D transport simulations, both electrodes were assumed to be zero concentration boundaries. A 20 mol m^{-3} dye concentration was assigned to the dye strip (cells 951 to 1050) matching the experimental initial conditions. The remaining cells were assigned an initial dye concentration of zero.

Initial conditions were assigned for the EC_a and θ for the simulations. EC_a was assumed to be constant in the non-dyed soil. Within the dye region (cells 951 to 1050), EC_a was assigned a value four times that of the non-dyed soil due to the presence of both red dye No. 40 and sodium ions.

2-5.1 Input Parameters

Measurements of the bulk electrical conductivity of the pore water, EC_b , versus Θ measurements were fitted to a power curve to obtain regression parameters, $F(\lambda)$ and n . The $EC_b(\Theta)$ data set was determined using Eq. (2-B-2) where EC_a was calculated from the initial electric potential gradient and current density for each laboratory test, and a surface electrical conductivity value equal to $3.5 \times 10^{-3} \text{ S m}^{-1}$. The EC_s used in this regression analysis was slightly higher than the $2.8 \times 10^{-3} \text{ S m}^{-3}$ estimated using the Rhoades et al., (1976) method on core samples. This higher EC_s was found to produce a better fit of the power curve to the experimental dye data set due to denser soil packing in the dye experiments as compared to the soil packing in core samples measured by the Rhoades et al., (1976) method. The EC_b - Θ data set was fitted to a power curve regression:

$$EC_b(\Theta) = D(\Theta)^x \quad (2-15)$$

where D and x are the fitted parameters.

Parameters $F(\lambda)$ and n can be calculated by noting the relationship between the power fit regression parameters (Eq. 2-15) and the Mualem and Friedman (1991) functional relationship as illustrated in Appendix 2-B (Eq. 2-B-7). Parameter $F(\lambda)$ can be calculated as:

$$F(\lambda) = \frac{D \Theta_{sat}}{EC_w} \quad (2-16)$$

where the parameter n (in Eq. 2-B-7) is directly related to the exponent x from Eq. (2-15) by the power fit:

$$n = x - 2 \quad (2-17)$$

The measured EC_b and θ data and the regressed function (Eq. 2-15) are shown in Figure 2-4. The EC_b power curve regression had an R^2 of 0.98. Values for $F(\lambda)$ and n were calculated to

be 1.58 and 0.71 respectively. These values are close to the empirical values of 1.0 and 0.5 suggested by Mualem and Friedman (1991) for coarse-grained soils.

The ionic mobility of red dye No. 40 at infinite dilution has not been measured. Therefore, the red dye No. 40 ionic mobility at infinite dilution was adjusted until the predicted and observed dye velocities matched at the saturated moisture content. This dye ionic mobility value equaled $4.41 \times 10^{-8} \text{ m}^2 \text{ v}^{-1} \text{ s}^{-1}$ and is in the range of those for other aromatic disulfonic acids listed by Friedl et al. (1995).

2-5.2 Electromigration Transport Model Simulations

To test the electromigration transport model, one-dimensional modeling simulations were performed to predict the dye velocity over a series of moisture contents. Figure 2-5 illustrates an example of model results showing the dye concentration as a function of position. Initially the dye (20 mol m^{-3}) was located between the electrodes in a 1-cm wide channel. After electricity was applied, the dye was transported by electromigration toward the anode. The dye migration front velocity was approximately four times faster than the velocity in the dye-spiked region. This velocity difference was due to the four times higher voltage gradient in the dye-free soil as compared to the higher conductivity dye-spiked soil. The location of the first moment of the dye migration front after 5 h of simulated time was used to determine the migration velocity.

Predicted dye velocities matched the experimental data very well (Figure 2-6). The electromigration transport model predictions illustrate a maximum dye migration velocity at moisture contents less than saturation, in agreement with the measured dye velocities. The model agrees with the measured dye transport velocities at the higher moisture contents but overpredicts the observed dye velocities at moisture contents approaching the residual value. The overprediction is likely due to deviations between the fitted and measured bulk electrical conductivity at low moisture contents, or possible significant electroosmosis effects. It is not believed that resistive heating is responsible for the modeling prediction deviations. Significant temperature

increases were not noted during the lower moisture content experiments. Furthermore, an increase in temperature would result in underprediction of the dye migration rate.

The observed dye migration velocity for the laboratory experiments and the electromigration transport model simulation results show a maximum velocity when θ is approximately equal to 0.2 (Figure 2-6). This set of laboratory experiments was conducted using constant current conditions. We hypothesize that the dye velocity profile is due to two competing effects; initially, as the moisture content decreases from saturation, the velocity increases due to a decrease in the cross-sectional area available for current transport, thus increasing the current density within the pore water. After the moisture content decreases below 0.2, the observed dye velocities begin to decrease due to tortuosity of the pore water pathways increasing faster than the cross-sectional area decrease.

The electromigration transport model calculated tortuosity to adjust the ionic mobility for the more tortuous pathway of the soil medium. Tortuosity was calculated as a function of θ , $F(\lambda)$, n , and θ_0 , according to Eqs. (2-8) and (2-9). The relationship of tortuosity to moisture content is shown in Figure 2-7. At saturation ($0.375 \text{ m}^3 \text{ m}^{-3}$), tortuosity was calculated to be 0.77. As the moisture content decreases, the ion migration pathways through the pore water become much longer.

2-6. Conclusions

A three-dimensional electromigration transport model for ion transport in unsaturated soil was developed and tested against laboratory experiments. This model assumed the electric potential field was constant with respect to time, an assumption that is valid for highly buffered soil, or when the electrode electrolysis reactions are neutralized. The model also assumed that advective water movement through the soil due to either electric or hydraulic potentials was negligible. The linking code between two public domain ground water flow (MODFLOW) and

transport (MT3D) numerical codes was modified to allow these codes to predict ion transport due to an electric potential gradient.

The effects of pore-water ionic strength on ionic mobility were included in the electromigration transport model. Ionic mobility is a function of the concentration of ions in the electrolyte solution (i.e., ionic strength). Previous electrokinetic models neglected the reduction in ionic mobility as the concentration of the pore water increases. Our electromigration transport model estimated ionic strength from electrical conductivity data using an empirical equation proposed by Griffin and Jurinak (1973). Ionic mobility reduction (approximately 64% of μ^0 at an EC_w equal to 0.12 S m^{-1}) was estimated using the chemical activity coefficient as calculated by the Davies equation. Although chemical activity does not exactly represent the processes that reduce ionic mobility, it does provide an initial estimate of ionic mobility as a function of ionic strength. More studies are needed to better predict ionic mobility in multi-component solutions.

Tortuosity and apparent electrical conductivity functions required as input to the electromigration transport model were developed from the model of Mualum and Friedman (1991). Their model assumes that the electrical conductivity of the bulk solution can be calculated using Mualem's (1976) closed form solution. Bulk electrical conductivity of the pore water versus effective moisture content measurements were fitted to a power function to obtain the regression parameters necessary to calculate the apparent electrical conductivity and tortuosity functionality relationships to moisture content.

Anionic dye migration velocities were measured at various moisture contents in laboratory experiments under constant electrical current conditions. The velocities predicted by the electromigration transport model were in agreement with laboratory experimental results. Both the laboratory-measured and the model-predicted dye results indicated a maximum transport velocity at a moisture content less than saturation due to competing effects between current density and tortuosity.

This electromigration transport model is believed to be the first to describe electrically induced ion transport through variably saturated soil. Although anions were used in this study, the model could also be used to predict the transport of cations and colloids in the bulk pore water due to an electric potential gradient. However, the model does not account for electromigration transport of cations located in the double layer. For soils exhibiting a low zeta potential such as the Sandia soil, neglecting electromigration transport of cations in the double layer is acceptable. Additional experimental data sets are required to test the applicability of this model to other soil types, different electrode geometries, and other ions or colloids.

APPENDIX 2-A: IONIC MOBILITY DEPENDENCE ON CONCENTRATION

There is currently a need to obtain effective ionic mobilities for multi-component solutions in porous media (Alshawabkeh and Acar, 1996; Yeung and Menon, 1997). Previous electrokinetic models neglected ionic mobility reduction as a function of increasing ionic strength. Using ion mobilities derived at infinite dilution will over-predict the electromigration transport rate.

Kohlrausch was the first to recognize that the equivalent conductivity, Λ ($\text{S m}^2 \text{eq}^{-1}$) decreases as the solution concentration increases. The equivalent conductivity is the electrical conductivity of the solution, EC_w (S m^{-1}) normalized by the solution concentration in equivalents, c_{eq} (eq m^{-3}): Kohlrausch developed an empirical relationship between the equivalent conductivity and the square root of the concentration in equivalents, c_{eq} , (eq m^{-3}) that became known as Kohlrausch's Law (Bockris and Reddy, 1973), a relationship that is valid for solutions with concentrations up to about 0.01 N:

$$\Lambda = \Lambda^\circ - E c_{eq}^{1/2} \quad (2-A-1)$$

where Λ° is the equivalent conductivity at infinite dilution and E is an empirical constant.

Furthermore, the equivalent conductivity is related to Faraday's constant, F (96,500 C mol) and the sum of the ion mobilities:

$$\Lambda = F \sum (\mu_j) \quad (2-A-2)$$

where subscript j represents all of the ions in the solution. It follows that an individual ion's ionic mobility also follows the relationship described by Eq. (2-A-1):

$$\mu = \mu^\circ - E' c_{eq,i}^{1/2} \quad (2-A-3)$$

where E' is an empirical constant.

The rate of electromigration of cations and anions decreases as the ions interact with each other. Although Kohlrausch documented a linear relationship between equivalent electrical conductivity and the square root of the equivalent solution concentration, the slope of the relationship [E in Eq. (2-A-1)] depended on the particular set of anions and cations. This species dependence is described by the Debye-Huckel-Onsager (DHO) Equation (Bockris and Reddy's Equation 4.294, [1973]):

$$\Lambda = \Lambda^\circ - (A + B\Lambda^\circ)c^{1/2} \quad (2-A-4)$$

where A and B are constants dependent on the valences of the ion pair. However, the DHO Equation is only valid for dilute electrolyte solutions (<0.001 N) derived from a single salt. In contrast, soil pore water is composed of multiple ions and is typically at higher concentrations than described by for the DHO Equation.

Due to the limitations of using the DHO Equation to describe the ionic mobility for the presence of other ions in solution, the approach taken in this study adjusted the ionic mobility using the chemical activity coefficient calculated from the ionic strength, using the Davies equation :

$$\mu = \mu_i^0 10^{\left(-.5085 z^2 \left(\frac{\sqrt{I}}{1 + \sqrt{I}} - .3I\right)\right)} \quad (2-A-5)$$

where μ_i^0 is the ionic mobility at infinite dilution ($\text{m}^2 \text{v}^{-1} \text{s}^{-1}$), z is the ion's valance (-), and I is the ionic strength of the solution (mol kg^{-1}). This approach stems from the fact that an ion's mobility depends on the Debye-Huckel reciprocal length, χ , Bockris and Reddy, 1973. Furthermore, χ is a function of the square root of the ionic strength. Using the ionic strength rather than individual ions to adjust the ionic mobility has the advantage of examining electrolyte solutions composed of multiple ions rather than a single salt species as examined by the DHO Equation. The contaminant ionic mobility can be estimated by multiplying the ionic mobility at infinite dilution by its activity coefficient.

An example of the concentration effects for a copper sulfate solution is illustrated in Figure 2-A-1. At ionic strengths of 0.10 mol l^{-1} the effective equivalent electrical conductivity is reduced by over 50% due to the greater interaction of ions in the solution. Equivalent electrical conductivity calculated by Eq. (2-A-5), although not exact, follows the copper sulfate data set well. Eq. (2-A-5) slightly under predicts the normalized equivalent electrical conductivity data set but captures the general nature of the reduction of the equivalent electrical conductivity as a function of ionic strength.

APPENDIX 2-B: TORTUOSITY

Transforming the governing transport equation (2-11) from a pure liquid solution to a porous medium requires accounting for the tortuous path through the porous medium and a reduced cross-sectional area available for ion transport. The approach taken in this study assumed that electrical current flows through a soil along two parallel conductors; one conductor is the bulk pore water while the second conductor is along the soil surface. The sum of these two conductivities equals the apparent electrical conductivity (EC_a), which is the electrical conductivity of the soil measured by resistivity techniques. Several researchers (Dutt and Anderson, 1964; Rhoades et al., 1976; Mualem and Friedman, 1991) have related the apparent

soil electrical conductivity to the pore water electrical conductivity and the surface electrical conductivity using the relationship:

$$EC_a = f(\theta)EC_w + EC_s \quad (2-B-1)$$

where EC_a is the apparent electrical conductivity ($S\ m^{-1}$), $f(\theta)$ is a geometric factor that accounts for the reduced cross-sectional area for current flow as well as the more tortuous pathway the ions follow in a porous medium, and EC_s is the electrical conductivity of the matrix surface ($S\ m^{-1}$). In order to be able to evaluate tortuosity, it is useful to define the electrical conductivity of the bulk soil solution EC_b , as the measured electrical conductivity minus that portion carried by the soil surface:

$$EC_b = EC_a - EC_s \quad (2-B-2)$$

Furthermore, EC_b is related to the electrical conductivity of the pore water as a free solution, EC_w , adjusted by the effects of the reduced cross-sectional area and increased tortuosity due to the presence of the soil. Substituting Eq. (2-B-1) into Eq. (2-B-2) relates EC_b to EC_w :

$$EC_b = f(\theta)EC_w \quad (2-B-3)$$

Numerous researchers (Archie, 1942; Rhoades et al., 1976; 1989) have developed relationships to represent $f(\theta)$ for both saturated and unsaturated media. We used the method of Mualem and Friedman (1991) which assumes the area immediately adjacent to the solid surface is not available for ion migration and therefore an effective cross-sectional moisture content, Θ ($m^3\ m^{-3}$), Eq. (2-8) must be used to calculate the $f(\theta)$ of Eq. (2-B-1). Using the effective moisture content approach, Eq. (2-B-3) becomes Mualem and Friedman's Equation 16, (1991, p. 2772):

$$EC_b(\Theta) = F_G(\Theta) \Theta EC_w \quad (2-B-4)$$

where $F_G(\Theta)$ is the geometry factor that accounts for the variable cross-sectional area of the pore water and the longer travel path through the soil.

Mualem (1976) used an analogous approach to solve Eq. (2-B-4) in order to develop a relationship between hydraulic conductivity and moisture content. Assuming that the moisture

retention curve can be approximated by a power function relationship, EC_b is related to EC_w as in Mualem and Friedman's Equation 27 (1991, p. 2773):

$$EC_b(\Theta) = F(\lambda) \frac{\Theta^{n+2}}{\Theta_{sat}} EC_w \quad (2-B-5)$$

where $F(\lambda)$ and n are functions of the soil moisture retention curve power fit.

Equation 2-B-4 is similar in form to Eq. (2-B-3) in as much as the geometry factors are related. The geometry factor, $f(\theta)$, of Eq. (2-B-3), accounts for both tortuosity and reduced cross-section area. The geometry factor, F_G , from Eq. (2-B-4) accounts solely for the long travel pathways through the soil since Θ , (Eq. 2-B-4) accounts for the reduced cross-sectional area for current flow. Therefore, F_G describes the tortuosity, τ , (Eqs. 2-3 and 2-4) for an ion migrating through a porous media:

$$\tau(\theta) = F_G(\Theta) \quad (2-B-6)$$

To calculate the tortuosity as a function of moisture content, we made use of the parameters relating EC_b , to EC_w , in Eqs. (2-B-3) and (2-B-5) and solved for τ using Eq. (2-B-6):

$$\tau(\theta) = \frac{F(\lambda) \Theta^{n+1}}{\Theta_{sat}} \quad (2-B-7)$$

Acknowledgments. This work was funded in part by Sandia National Laboratories for the United States Department of Energy under contract DE-AC04-94AL85000 and by the New Mexico Waste-management Education and Research Consortium (WERC).

2-7. REFERENCES

- Acar Y. B., R. J. Gale, J. Hamed, and G. Putnam, Acid/base distribution in electrokinetic soil processing, *Transportation Research Record 1288*, 23-33, 1991.
- Alshawabkeh, A. N. and Y. B. Acar, Electrokinetic remediation. II: Theoretical model, *J. Geotech. Eng.*, 122, 186-196, 1996.
- Archie, G. E., The electrical resistivity log as an aid in determining some reservoir characteristics, *Trans. Am. Inst. Min. Metall, Pet. Eng.*, 146-154, 1942.
- ASTM, Standard test method for determination of water (moisture) content of soil by the microwave oven method, *1993 Annual Book of ASTM Standards, Section 4, Vol. 04.08 Soil and Rock (I)*, Designation 4643-93, 1993.
- Bockris, J. O'M., and A. K. N. Reddy, *Modern Electrochemistry, Volume 1*, 622 pp., Plenum, New York, 1973.
- CRC (The Chemical Rubber Company), *Handbook of Chemistry and Physics*. Section 4, p. D82, 1970-1971.
- Dutt. G. R., and W. D. Anderson, Effect of Ca-saturated soils on the conductance and activity of Cl^- , SO_4^{2-} , and Ca^{2+} , *Soil Sci.*, 98, 377-382, 1964.
- Ersig, M. I., Pore pressures, consolidation, and electro-kinetics, *Jour. Soil. Mech. Fdns. Div. Am. Soc. Civ. Engrs*, 94, 899-921, 1968.
- Friedl, W, J. C. Reijenga, and E. Kenndler, Ionic strength and charge number correction for mobilities of multivalent organic anions in capillary electrophoresis, *Jour. of Chromatography A*, 709, 163-170, 1995.
- Griffin, R. A., and J. J. Jurinak, Estimation of activity coefficients from the electrical conductivity of natural aquatic systems and soil extracts, *Soil Science*, 116, 26-30, 1973.
- Jacobs, R. A., M. Z. Sengun, Jr., E. Hicks, and R. F. Probstein, Model and experiments on soil remediations by electric fields," *J. Environ. Sci. Health, Part A*, A29, 1933-1955, 1994.
- Jacobs R. A., and R. F. Probstein, Two-dimensional modeling of electroremediation, *Am. Inst. Ch. Eng. J Jour.*, 42, 1685-1696, 1996.
- Kelly, W. E., and R. Kalinski, Comment on "Theoretical Predication of Electrical Conductivity in Saturated and Unsaturated Soil" by Y. Mualem and S. P. Friedman, *Water Resour. Res.*, 29, 3835-3836, 1993.
- Lewis R. W., and C. Humpheson, Numerical analysis of electro-osmotic flow in soils, *J. of the Soil Mech. and Fnd. Div., Proc. of the ASCE*, 99, 603-616, 1973.
- Lewis R. W., and R. W. Gardner, A finite element solution of coupled electrokinetic and hydrodynamic flow in porous media, *Intl. J. for Num. Meth. in Eng.*, 5, 41-55, 1972.

- Lindgren E. R., E. D. Mattson, and M. W. Kozak, Electrokinetic remediation of contaminated soils: An update, in *Waste Management '92*, Tucson, AZ, 1309 - , 1992.
- Lindgren, E. R., R. R. Rao, and B. A. Finlayson, Numerical simulation of electrokinetic phenomena, in *Emerging Technologies in Hazardous Waste Management V*, edited by D.W. Tedder and F. G. Pohland, ACS Symposium Series 607, 48-62, 1995.
- Mattson, E. D., and E. R. Lindgren, 1994. Electrokinetics: An innovative technology for in-situ remediation of heavy metals, in *Proceedings of the Eighth National Outdoor Action Conference and Exposition*, Minneapolis, Minnesota, 235-245, 1994.
- McDonald M. C., and A. W. Harbaugh, A modular three-dimensional finite-difference groundwater flow model, USGS Open-File Report 83-875, 1988.
- Mitchell J. K., and T. C. Yeung, Electro-kinetic flow barriers in compacted clay, in *Geotechnical Engineering 1990*, Transportation Research Board, National Research Council, Washington, D.C., Transportation Research Record No. 1288. 1-10, 1991.
- Monsanto Company, Development of an integrated, in-situ remediation technology - Task 2-4 - Electrokinetic modeling, *Topical Report # DOE/METC/31185-5391,DE97002135*, 1996.
- Mualem, Y., A new model for predicting the hydraulic conductivity of unsaturated porous media, *Water Resour. Research*, 12, 513-522, 1976.
- Mualem, Y., and S. P. Friedman, Theoretical predication of electrical conductivity in saturated and unsaturated soil, *Water Resour. Res.*, 27, 2771-2777, 1991.
- Persaud, N., and P. J. Wierenga, Solute interactions and transport in soils from waste disposal sites at Sandia Laboratories, *Report prepared for Sandia National Laboratories*, contract numbers 07-3196 and 46-3243, 1982.
- Ponnamperuna, F. N., E. M., Tianco, and T. A. Loy, Ionic strengths of soil solutions composition variation with water content for desaturated soils, *Soil Sci. Soc. Proc.*, 35, 436-442, 1966.
- Rhoades, J. D., P. A. C. Ratts, and R. J. Prather, Effects of liquid-phase electrical conductivity, water content, and surface conductivity on bulk soil electrical conductivity, *Soil Sci. Soc. Am. J.*, 40, 651-655, 1976.
- Rhoades, J. D., N. A. Manteghi, P. J. Shouse, and W. J. Alves, Soil electrical conductivity and soil salinity: New formulation and calibrations, *Sol Sci. Soc. Am. J.*, 53, 433-439, 1989.
- Renaud, P. C, and R. F. Probstein, Electroosmotic control of hazardous wastes, *PhysicoChem. Hydrodyn.*, 9, 345-360, 1987.
- Saville, D. A. and O. A. Palusinski, Theory of electrophoretic separations part I: Formulation of a mathematical model, *Am. Inst. Ch. Eng. J.*, 32, 207-214, 1986.
- Shapiro, A. P., Renaud P. C., and R. E. Probstein, Preliminary studies on the removal of chemical species from saturated porous media by electroosmosis, *PhysicoChem. Hydrodyn.*, 11, 785-802, 1989.

- Shapiro A. P., and R. E. Probstein, Removal of contaminants from saturated clay by electroosmosis, *Environ. Sci. and Technol.*, 27, 283-291, 1993.
- Wolt, J. D., *Soil Solution Chemistry: Application to Environmental Science and Agriculture*, John Wiley & Sons, New York, 1994.
- Yeung, A. T., Coupled flow equations for water, electricity, and ionic contaminants through clayey soils under hydraulic, electrical and chemical gradients, *J. Non-Equil. Thermodyn.*, 15, 247-267, 1990.
- Yeung A. T., and S. Datla, Fundamental formulation of electrokinetic extraction of contaminants from soil, *Can. Geotech. J.*, 32, 569-583, 1995.
- Yeung A. T., and R. M. Menon, Discussion on "Electrokinetic remediation. II: Theoretical model", *Jour. of Geotech. Eng.*, 123, 1078-1080, 1997.
- Zheng C., *MT3D: A Modular Three-Dimensional Transport Model for Simulation of Advection, Dispersion and Chemical Reactions of Contaminants in Groundwater Systems*, a report prepared for the U.S. EPA, Robert S. Kerr Environmental Research Laboratory, Ada, OK., October, 1990.

Table 2-1. Electromigration Transport Model Parameters Substituted for Conventional MODFLOW Groundwater Flow Parameters

| Electromigration Transport Parameter | Hydraulic Parameter |
|--|---|
| <i>Input</i> | |
| Apparent Electrical Conductivity, EC_a ($S\ m^{-1}$) | Saturated Hydraulic Conductivity, K ($m\ s^{-1}$) |
| Current at Electrode, Q ($C\ s^{-1}$) | Pumping Rate, W ($m^3\ s^{-1}$) |
| <i>Output</i> | |
| Voltage, V (V) | Hydraulic Head, h (m) |

Table 2-2. Parameters Required for the Electromigration Transport Model added to MODFLOW Input Blocks

| Additional MODFLOW Input Parameters |
|---|
| Ionic Mobility at Infinite Dilution, μ_o ($\text{m}^2 \text{v}^{-1} \text{s}^{-1}$) |
| Ion Valance, z (-) |
| Electrical Conductivity of Soil Surface, EC_s (S m^{-1}) |
| Constants to Calculate Ionic Strength, [Eq. (2-6): 0.127 and -0.003] |
| Moisture Content, θ ($\text{m}^3 \text{m}^{-3}$) |
| Saturated Moisture Content, θ_s ($\text{m}^3 \text{m}^{-3}$) |
| Moisture Content where $EC_a = EC_s$, θ_o ($\text{m}^3 \text{m}^{-3}$) |
| Fitting Parameters to $EC_b(\Theta)$ Function, [$F(\lambda)$ and n of Eqs. (2-7) and (2-8)]. |

Table 2-3. Mean Red Dye No. 40 Velocity as a Function of Water Content. Numbers in Parentheses are the 95% Confidence Limits

| θ ($\text{m}^3 \text{ m}^{-3} \%$) | Mean Dye Velocity (cm hr^{-1}) | R^2 |
|--|--|-------|
| 9.5 | 0.46 (± 0.08) | 0.97 |
| 13.5 | 0.62 (± 0.11) | 0.96 |
| 24.5 | 0.91 (± 0.14) | 0.97 |
| 29.0 | 0.89 (± 0.08) | 1.00 |
| 37.5 | 0.75 (± 0.03) | 1.00 |

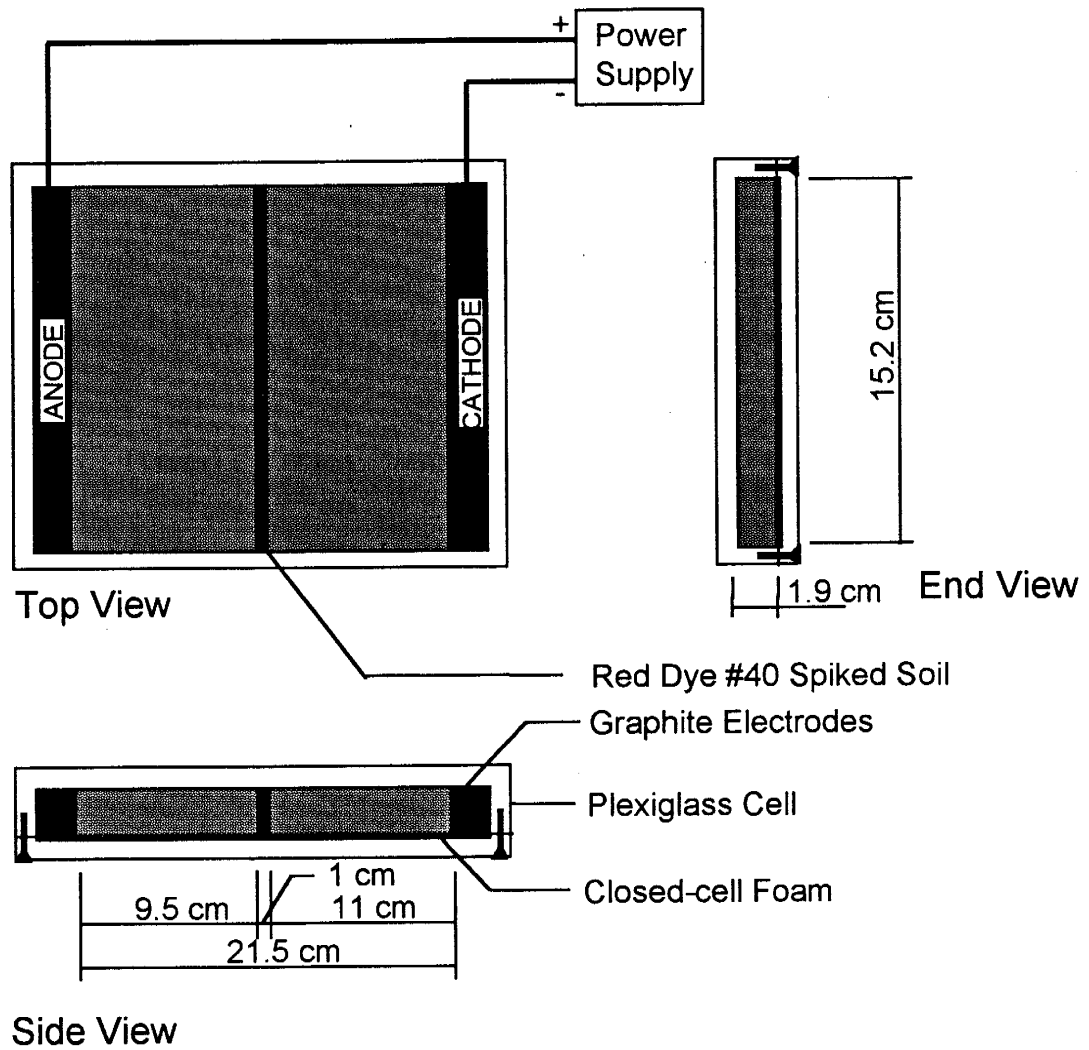


Figure 2-1. Laboratory test cell apparatus used to determine red dye No. 40 electromigration transport velocities.

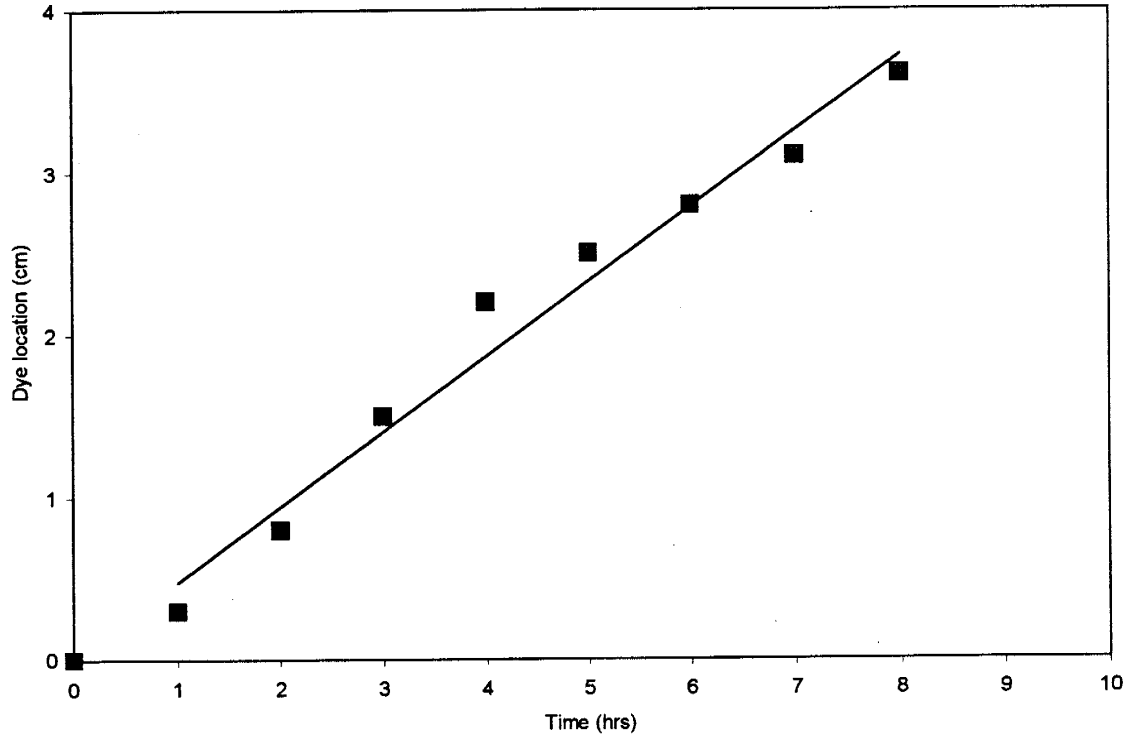


Figure 2-2. Laboratory observations of the leading-edge dye location from the spiked dye strip as a function of time. Line represents the linear regression of the data set.

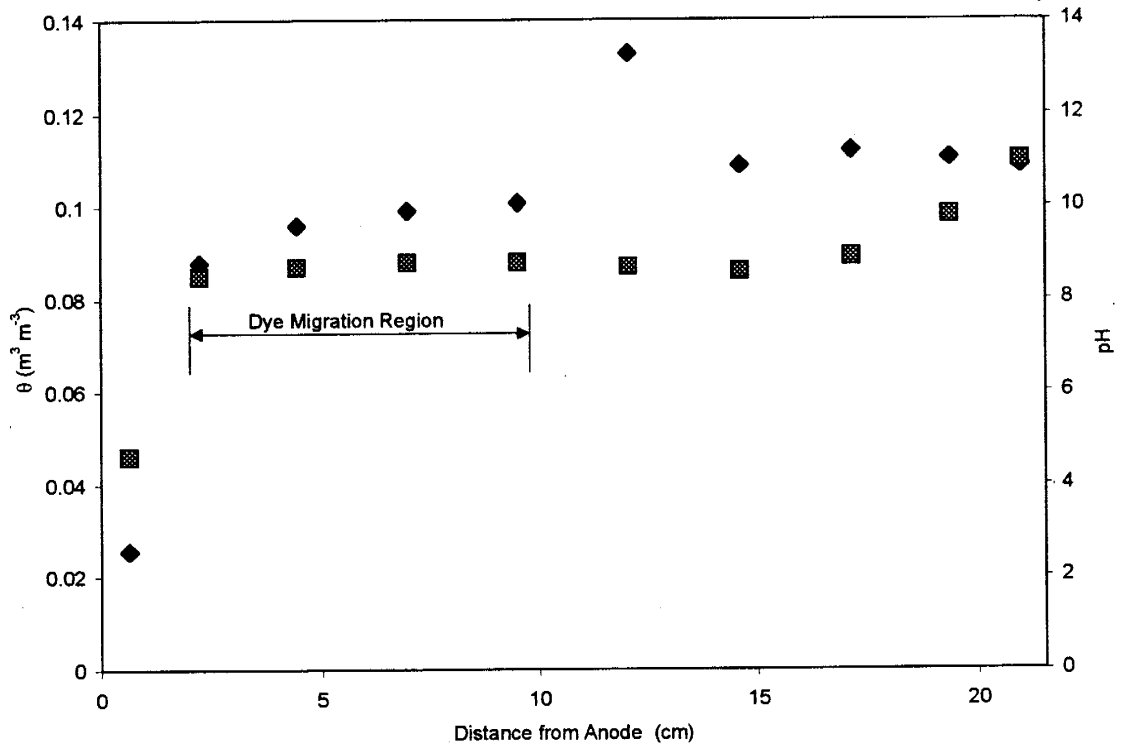


Figure 2-3. Laboratory analysis of moisture content (diamonds) and pH of 1:2 soil-water extracts (squares) from post-test soil samples take from the 9.5% moisture experiment after 24 hours of applied electricity.

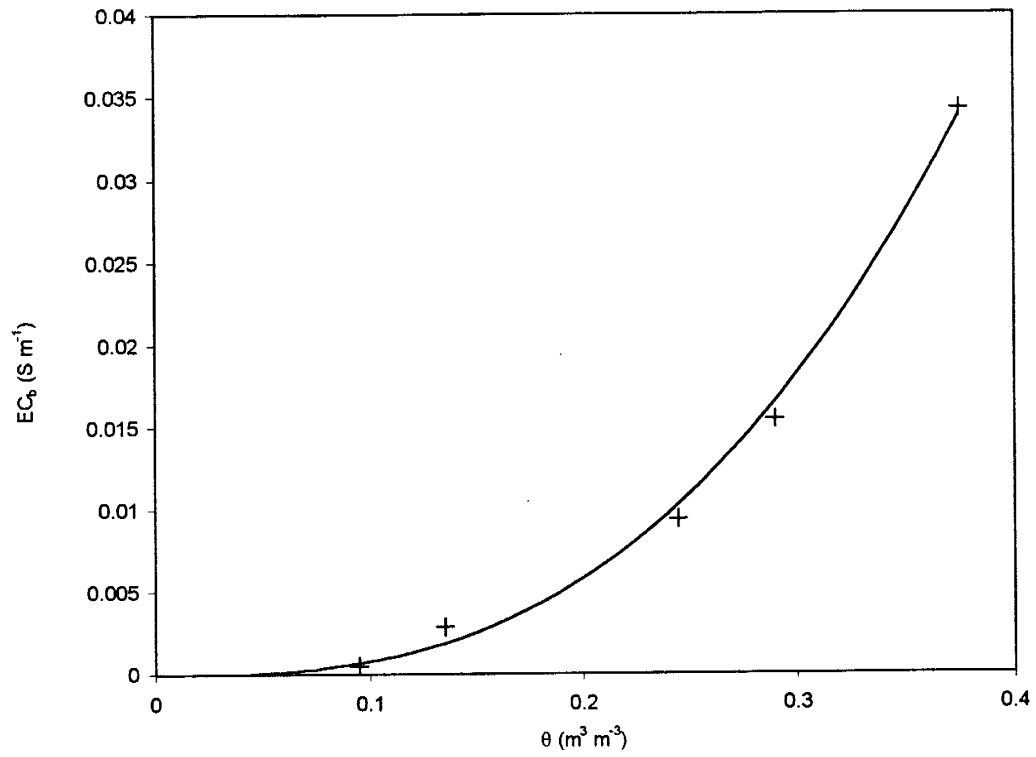


Figure 2-4. Electrical conductivity of the bulk pore water as a function of volumetric moisture content. Laboratory data represented by crosses. Solid line represents fitted Mualem and Friedman (1991) continuous function.

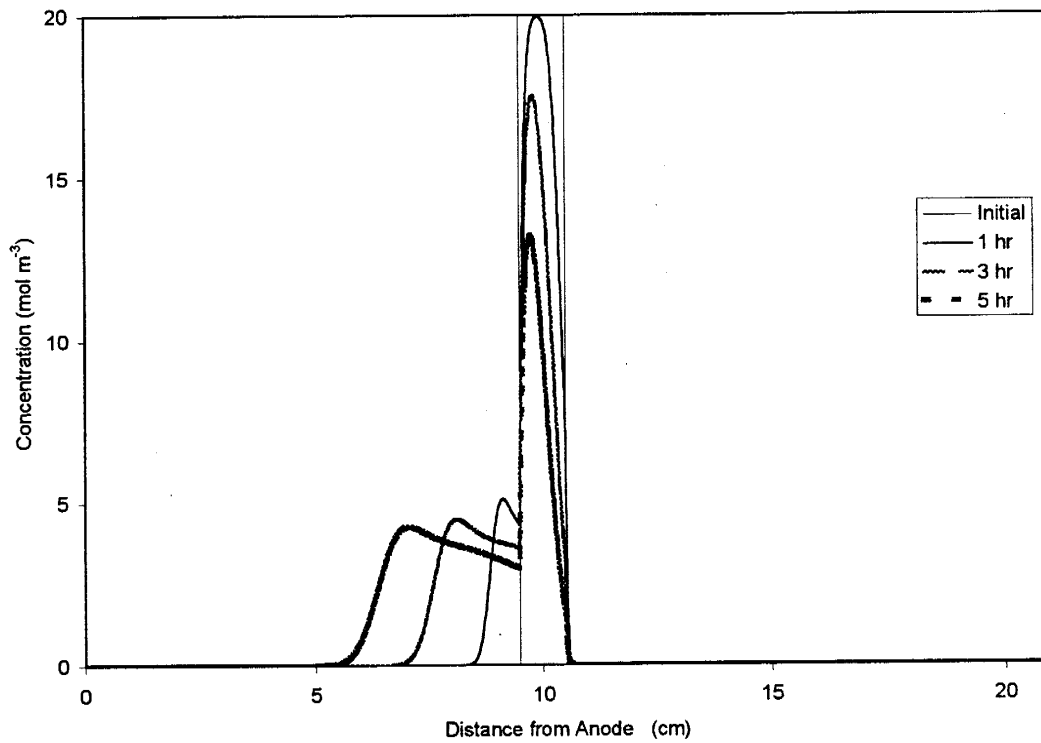


Figure 2-5. Initial location of red dye No. 40 in test cell, and model predictions of dye concentrations after 1, 3, and 5 hours of simulation time.

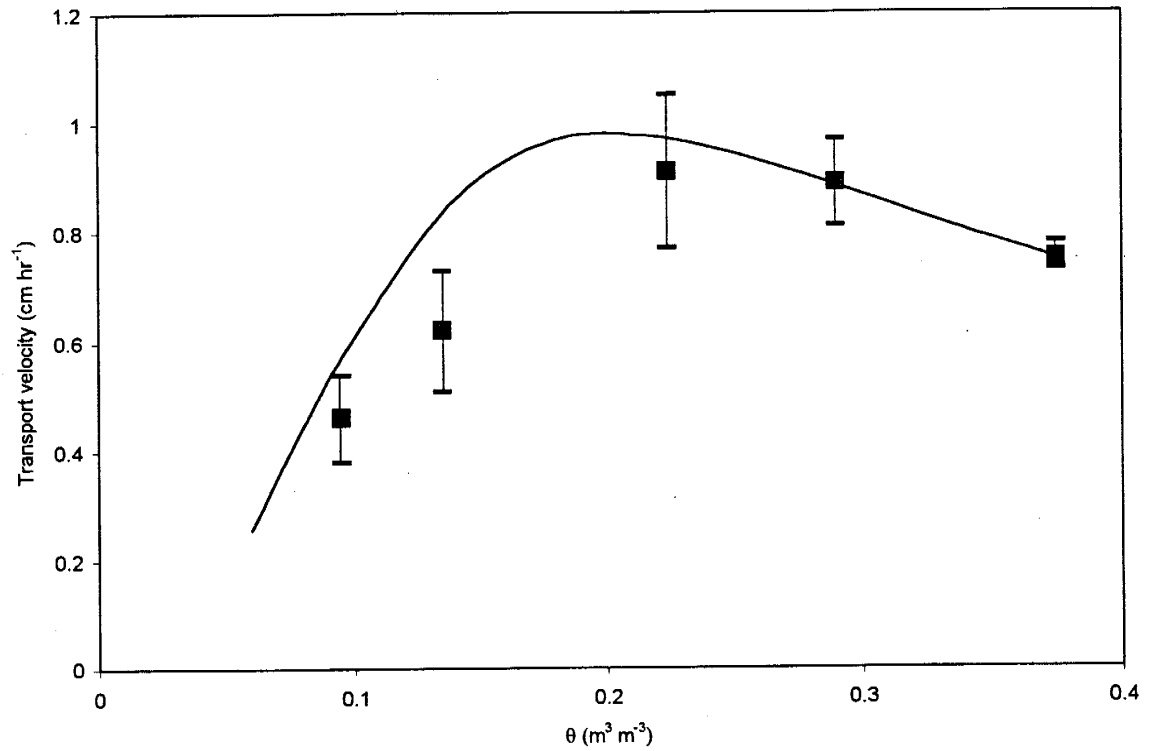


Figure 2-6. Observed and predicted transport velocities of red dye No. 40. Points represent observed electromigration velocities with 95% confidence intervals as determined from dye location versus time regression analysis. The solid line represents velocities predicted by the numerical model.

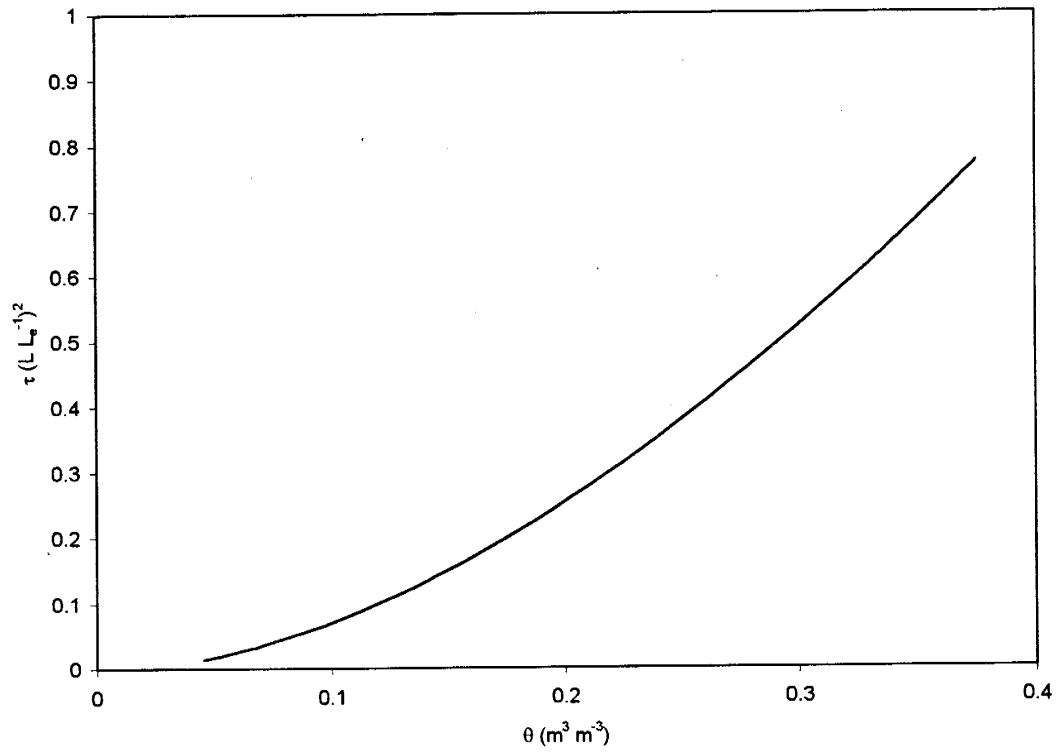


Figure 2-7. Tortuosity as a function of moisture content as calculated by Eq. (2-9) for the laboratory experiments.

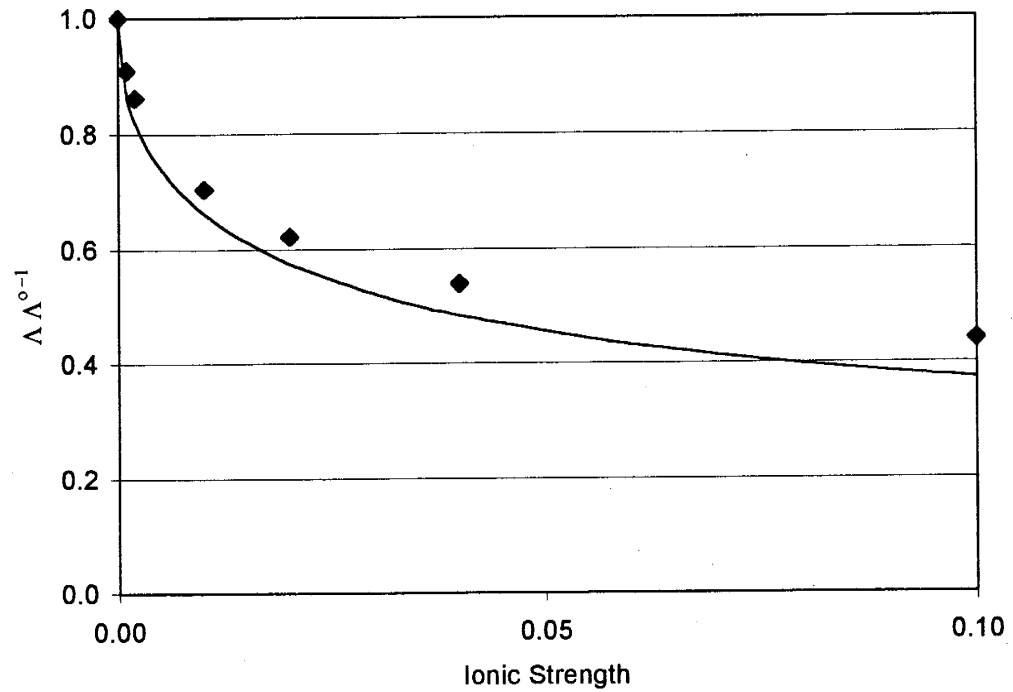


Figure 2-A-1. Normalized equivalent electrical conductivity of CuSO_4 as a function of ionic strength. Diamonds represent data obtained from the CRC (1970, Table 3-36), solid line represents chemical activity coefficient adjustment to the equivalent electrical conductivity at infinite dilution.

CHAPTER 3. ELECTROKINETIC ION TRANSPORT THROUGH UNSATURATED SOIL: 2. APPLICATION TO A HETEROGENEOUS FIELD SITE

Earl D. Mattson^{1,2}, Robert S. Bowman¹, and Eric R. Lindgren³

¹Department of Earth and Environmental Science, New Mexico Institute of Mining and
Technology, 801 Leroy Place, Socorro, NM 87801

²Now at the Department Integrated Earth Science, LMITCO, INEEL, PO Box 1625, Idaho Falls,
ID, 83415-2107

³Sandia National Laboratories, PO Box 5800, Albuquerque, NM 87185-0719

(to be submitted to *Water Resources Research*)

ABSTRACT

Results of a field demonstration of electrokinetic transport of acetate through an unsaturated heterogeneous soil are compared to numerical modeling predictions. The numerical model was based on the groundwater flow and transport codes MODFLOW and MT3D modified to account for electrically induced ion transport. The six-month field demonstration was conducted in an unsaturated layered soil profile where the soil moisture content ranged from 4 to 28 % ($\text{m}^3 \text{m}^{-3}$). Specially designed ceramic-cased electrodes maintained a steady-state moisture content and electric potential field between the electrodes during the field demonstration. Acetate, a byproduct of acetic acid neutralization of the cathode electrolysis reaction, was transported from the cathode to the anode by electromigration. Field demonstration results indicated preferential transport of acetate through soil layers exhibiting higher moisture content/electrical conductivity. These field transport results agree with theoretical predictions that electromigration velocity is proportional to a power function of the effective moisture content. A numerical model using a homogeneous moisture content/electrical conductivity domain did not adequately predict the acetate field results. Numerical model predictions using a three-layer electrical conductivity/moisture content profile agreed qualitatively with the observed

acetate distribution. These results suggest that field heterogeneities must be incorporated into electrokinetic models to predict ion transport at the field-scale.

3-1. INTRODUCTION

Multi-dimensional electrokinetic transport models have not been applied to large-scale field experiments. The application problem appears to lie with the numerical intensity of solving the electrokinetic transport equation coupled with the current equation (Mattson et al., 1999a). For example, the two-dimensional finite element electrokinetic transport model described by Jacobs and Probst (1996) was used to simulate phenol removal in a laboratory experiment in which the electrodes were 12 cm apart. This numerical model required 1172 elements (Jacobs, 1995). It is not practical to apply a model requiring this density of elements to field-scale situations where the electrodes are meters apart.

Monsanto (1996) applied a one-dimensional transport model to predict trichloroethylene removal at a field demonstration where the electrodes were 3 m apart. Homogeneous soil parameters were assumed. Modeling results indicated that although the electrolysis reactions at the electrodes produced hydrogen and hydroxyl ions, the buffering capacity of the soil and electric current transport in the double layer resulted in a very uniform electric field with time. These modeling results were confirmed by field observations that measured the electric field at the Lasagna demonstration. Nonuniformities of the observed electric field were attributed to soil heterogeneity rather than the redistribution of ions by electromigration (Monsanto, 1996).

To incorporate multi-dimensionality and spatial variability of soil properties in an electrokinetic transport model, Mattson et al. (1999a) modified the linking program between MODFLOW (McDonald and Harbaugh, 1988) and MT3D (Zheng, 1990) to account for the electromigration of ions in heterogeneous soil. This model is applicable to saturated/unsaturated soils if the electric potential field is constant with respect to time. The constant electric potential field assumption greatly simplifies the numerical solution, and therefore allows multi-

dimensional models of large-scale problems that account for variable moisture content effects on electromigration transport.

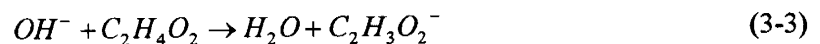
Transfer of electric current from an electrode to an electrolytic fluid involves the oxidation or reduction of the fluid or an ion within the fluid. For water, the reduction reaction at the cathode is:



Similarly, the oxidation reaction at the anode is:



Researchers (e.g., Acar et al., 1991) who have not neutralized these electrode reactions have reported pH values adjacent to anodes and cathodes of 1-4 and 10-13, respectively. Changes in the pH of the pore water can geochemically alter the electrokinetic transport processes (Probstein and Hicks, 1993; Yeung and Datla, 1995; Alshawabkeh and Acar, 1996; Monsanto, 1996). By neutralizing the electrode reactions, the processes that hinder electromigration can be minimized. Acetic acid may be used to neutralize hydroxyl generated at the cathode, resulting in the production of acetate ions:



An electrokinetic field demonstration was conducted beneath an unlined chromic acid disposal trench in the southwest corner of the Chemical Waste Landfill at Sandia National Laboratories, Albuquerque, New Mexico. The size of the demonstration was approximately 4-m \times 4-m \times 5-m deep. The purpose of this demonstration was to extract chromate from unsaturated soil by electromigration. Lindgren et al. (1998) described the chromate removal portion of the field demonstration in detail. This paper focuses on the southern portion of the field demonstration that included two phases of electrokinetic tests. Each phase tested a different electrode configuration. The southern portion of the field demonstration was chosen because acetic acid was used as a hydroxyl-neutralizing agent at the cathodes during Phase 1. The acetate

anions transported by electromigration from the cathodes to the anodes were used to trace electromigration pathways through this heterogeneous soil. Acetate concentrations measured at the end of the field demonstration were compared to numerical model predictions for a layered and a homogeneous system using the Mattson et al. (1999a) electromigration transport model.

3-2. FIELD METHODS

3-2.1 Site Characterization

The near-surface geology at the field demonstration site is heterogeneous in nature, consisting of alluvial fan deposits interspersed with eolian deposits. The deposits consist of intercalated fine- to coarse-grained, well- to poorly-sorted sands, gravels, and cobbles that are typically composed of unconsolidated to poorly cemented, sub-rounded to sub-angular fragments of granite, limestone, and quartzite. Caliche cement and grain coatings act as the primary means of formation induration when present. Little organic matter (0 to 0.2%) was measured in soil samples taken from the site (Persaud and Wierenga, 1982). This soil was the same as used by Mattson et al. (1999a) except that the less than 200 mesh particles were discarded during laboratory experimentation of dye migration.

Surface geophysical surveys were conducted over the field demonstration site to evaluate its suitability for electrokinetic treatment. A survey for metallic debris was made using a GeoMetric G-858 cesium vapor magnetometer and a Geonics EM-61 high-precision metal locator. Metallic objects are detrimental to electrokinetics due to their conductive nature that allows short-circuiting of electric current through the soil. The average soil conductivity was measured by an electromagnetic (inductive) technique using a Geonics EM-31.

Soil electrical conductivity depth profiling was accomplished using a Geoprobe electrical conductivity probe. This probe has the advantage of measuring the soil conductivity at discrete points whereas the Geonics EM-31 measures an average soil conductivity from the surface to a depth of 6 m. The electrical conductivity probe consists of a slightly tapered tip that contains four

electrically isolated stainless steel rings. A 150-Hz AC sine wave was applied to the two outer electrodes using a Tektronix FG 502 Function Generator. Both the current applied to the outer rings and the resulting electric potential between the two inner rings were measured by dual Fluke 25 multimeters. The ratio of the applied current to the measured electric potential is proportional to the soil electrical conductivity.

Soil samples were collected using a Geoprobe large-bore soil sampler before and after the field demonstration to measure the moisture content, pH, and electrical conductivity. Post-test soil sample analysis also included acetate concentration. The large-bore sampler is approximately 60-cm long and contains a 2.5-cm ID plastic sampling sleeve. Following sample retrieval, soil samples were homogenized in a stainless steel bowl, then split into two fractions. The first fraction of the soil was oven-dried 105° for 24 h to determine moisture content. These gravimetric moisture contents were converted to volumetric moisture content with an assumed soil bulk density of 1.8-g cm⁻³.

Soil-water extracts (1:2) were obtained from the second fraction by following a method similar to that described by Rhoades (1982). Moist soil samples (approximately 10 g) were placed in centrifuge tubes with enough deionized water to provide a 1:2 ratio of soil to water as determined by the first fraction moisture content. After shaking for two hours and settling overnight (approximately 15-20 h), the aqueous extracts were separated from the soil by centrifuging. Electrical conductivities of the extracts were measured prior to acetate chemical analyses. Acetate concentrations were measured by ion chromatography (Dionex model 4000) with an AS-11 column. Acetate detection limits were 1 mg L⁻¹ by weight in soil (Lindgren et al., 1998).

3-2.2 Experimental Equipment

The portion of the field demonstration discussed in this paper contained three rows of five electrodes spaced in a grid at approximately 0.91-m intervals (Figure 3-1). There were two

rows of cathodes (one for each phase of the southern portion of the field demonstration) plus a single row of anodes that were used during both phases of the demonstration.

The anodes and cathodes used during Phase 1 of testing were contained in porous ceramic casings and had a more sophisticated operating system than the cathodes used during Phase 2. The ceramic casing provided a method to add/remove soil water, buffer the electrolysis reactions, and remove ions transported into the casings through electromigration (Lindgren and Mattson, 1995). These electrode casings were constructed from two 0.91-m-long ceramic tube sections (Coors[®] ceramic PC3 material) topped with a 2.4-m-long section of schedule 40 PVC pipe and fittings (Figure 3-2a). A metallic electrode (copper at the cathode or iridium-coated titanium at the anode) was placed inside the electrode casing and water was added to a level above the ceramic/PVC interface. A 47-KPa vacuum was applied to the headspace above the water to control the hydraulic flux leaving the electrode casing.

The ceramic used in the anode casing was treated with hexadecyltrimethylammonium (HDTMA) to prevent electroosmotic water transport of water out of the casing. The treatment process formed a HDTMA bilayer on the ceramic surface, reversing the zeta potential. Thus, the electroosmotic flow through the HDTMA-treated ceramic at the anode was from the soil into the casing, as discussed in detail by Mattson et al. (1999b). Cathode ceramic casings were not treated with HDTMA.

The ceramic-cased anodes and Phase 1 cathodes were installed using a method similar to that used to install suction lysimeters (Rhoades and Oster, 1986). First, uncased boreholes were drilled with a 15-cm diameter hollow-stem auger rig. The electrode casings were placed in the boreholes and backfilled with a native soil slurry mixture as illustrated in Figure 3-2a. The ceramic portions of the electrode casings were located 2.4 to 4.3 m below land surface (BLS).

A circulation system was employed to monitor the liquid pH condition in the electrode, to cool the liquid in the electrode, and to sample and remove liquid from the electrode (Figure 3-3). A QED[®] P1101S bladder pump contained in the ceramic electrode casing powered the water-

circulation system. This system resulted in recycle flow rates of approximately 4 L min^{-1} .

Lindgren et al. (1998) describes the electrode equipment and operation in detail.

Due to resistive heating of the water in the electrode and the surrounding soil, the water in the electrode casing was cooled by an ITT Bell & Gossett BP Honeycomb™ heat exchanger (Model 410-30 for cathodes and Model 410-40 for anodes). Remcor® (Model CH-3002-A) chillers circulated deionized water at approximately $6 \text{ }^\circ\text{C}$ at a rate of 6 L min^{-1} to each heat exchanger to remove the excess heat. This cooling system maintained the water temperature in the electrode casings at approximately 8 to $10 \text{ }^\circ\text{C}$.

The water level in the electrode casings was maintained above the ceramic/PVC interface with a set of reed-type water-level float switches (Flowline® Model LV10 series). The switches were spaced approximately 15 cm apart. A dual-float switch controller (Levelite® Model GLL 100000) opened and closed an influent solenoid valve to allow water to enter the electrode. Separate 1000-L storage tanks (one for the anodes and one for the cathodes) contained the influent water source; these tanks were monitored for water use.

Water was removed from the electrode casings by effluent batch controllers (Signet® 9020 Intelek-Pro® Batch Controller). These controllers redirected user-specified volumes of the circulating water (0.1 to 0.5 L) at 30-min intervals to effluent barrels.

A series of pH sensors, transmitters, controllers, and chemical feed pumps monitored and controlled the pH of the fluid in the electrode casings (Figure 3-3). A Cole-Parmer® (Model 27001-97) pH electrode monitored the pH of the circulation water and emitted a signal that was converted to a milliamp signal by a Jenco® (Model 695PH) current transmitter. A Signet® 9030 pH controller converted this signal and emitted a pulse signal controlling the pumping rate of a ProMinent® (Model G/4a) chemical feed pump. These pumps were fed either $10 \text{ wt}\%$ NaOH to control the pH in the anodes or $20 \text{ wt}\%$ acetic acid to control the Phase 1 cathode pH. A 207-kPa

stainless steel pressure relief valve provided adequate backpressure of the neutralization solution to prevent siphoning of the solution into the electrode.

Phase 2 cathodes, located between the Phase 1 cathodes and the anodes (Figure 3-1), were constructed of copper pipes placed directly in the ground. One and a half-meter by 1.9-cm OD copper pipes were installed between 2.4 and 4.2 m BLS in 3.8-cm diameter hydraulically punched holes. The holes were backfilled in the same manner as the holes for the porous ceramic casings (Figure 3-2b). Water addition/removal, electrolysis reaction neutralization, and ion removal systems were not included in the Phase 2 cathodes.

Pairs of anode and cathode electrodes were energized by 10-kW power supplies (Sorensen[®] Model DTR-600-16T). Each power supply was capable of outputting 16 A at 600 V DC. The power supplies were operated under constant voltage conditions.

3-2.3 Experimental Methodology

During Phase 1 of the field demonstration a 109-V electric potential was applied between the anode and Phase 1 cathode electrodes for 1246 hours. Acetic acid (at the cathode) or sodium hydroxide (at the anode) was added to the ceramic casings to neutralize the products of electrolysis reactions Eqs. (3-1 and 3-2). The pH of the electrode solution was maintained at 8.8 for the anodes and 5.5 for the cathodes

Phase 2 of the field demonstration used the same anodes but activated the inner row of copper cathode electrodes (Figure 3-1). The Phase 1 cathodes were emptied of fluid and disconnected from the electrical system. During Phase 2 an electric potential of 68 V was applied between the Phase 2 cathodes and the anodes for 837 hours. Electrolysis reactions at the Phase 2 cathode electrode copper pipe surfaces were not neutralized, although the same pH control system used in Phase 1 was applied to the ceramic-cased anode electrodes.

Acetate produced during Phase 1 at the cathode electrodes was transported through the soil towards the anodes by electromigration. The amount of acetate produced at each cathode

electrode is proportional to the amount of electrical current transmitted Eqs. (3-1 and 3-3).

Subsequent post-demonstration soil samples analyzed for acetate illustrated the soil zones of major electromigration transport.

3-3. FIELD RESULTS

Both surface and depth-profiling geophysical surveys indicated that the site was amenable to the application of electrokinetics. The surface surveys indicated an absence of metal objects buried in the area of interest (Lindgren et al., 1998). An apparent average soil conductivity of 23 to 30 mS m^{-1} in the 0-6 m depth interval was measured by the Geonics EM-31 survey. Depth profiling of the field site by the Geoprobe electrical conductivity probe, however, indicated a layered electrical conductivity profile. Soil exhibiting electrical conductivities greater than 30 mS m^{-1} were recorded between 1- and 3-m BLS, surrounded by soil exhibiting electrical conductivities less than 10 mS m^{-1} (Figure 3-4a). Electrical conductivity as high as 111 mS m^{-1} was measured in the 2- to 3-m layer.

The measured soil moisture contents also exhibited a layered soil profile (Figure 3-4b) similar to the depth-profiling electrical conductivity measurements. Moisture contents greater than 15% ($\text{m}^3 \text{m}^{-3}$) were located between 2 and 3 m BLS. These high moisture contents are in the same soil profile as the high electrical conductivity measured with the Geoprobe electrical conductivity survey. The soil zone at the lower portion of the electrodes generally exhibited moisture contents of less than 10% ($\text{m}^3 \text{m}^{-3}$).

Cross-sections developed for electrical conductivity and moisture content represent the general profile across the southern portion of the field demonstration and not any particular electrode pair. The depth profiling numbers illustrated in Figures 3-4(a and b) are generally within 1 m of an electrode pair plane. Both cross-sections indicate laterally continuous soil layers are present between the anode and cathode electrodes. Lindgren et al. (1998) also noted laterally

continuous soil properties on cross-sections developed perpendicular to those presented in Figures 3-4(a and b).

Electromigration transport resulted in an acetate tracer plume between the Phase 1 cathode and anode electrodes. According to the post-demonstration sampling results at the end of Phase 2, acetate was located between the upper portion of the electrodes, while no acetate was detected at the lower portion of the electrodes (Figure 3-5). Sampling for acetate was not conducted between Phase 1 and Phase 2.

3-4. NUMERICAL METHODS

The acetate concentration distribution at the end of the field demonstration was predicted using the three-dimensional electromigration model for ion transport in unsaturated soil developed by Mattson et al. (1999a). This model assumed a constant electric potential field with respect to time and that the water transported through the soil by either electric or hydraulic potentials was negligible. The steady-state electric potential field assumption is valid for highly buffered soils, when the electrode electrolysis reactions are neutralized, and/or when the zeta potential of the soil is low. Mattson et al. (1999a) used an existing USGS three-dimensional groundwater flow model, MODFLOW (McDonald and Harbaugh, 1988), and a solute transport model, MT3D (Zheng, 1990), as a base to implement the electromigration transport model. MODFLOW and the linking module between MODFLOW and MT3D were modified to describe the electromigration transport of ions. Analogous electrical parameters were used as input in place of the conventional groundwater flow and transport parameters required by MODFLOW and MT3D. Functional relationships that account for concentration effects on ionic mobility and tortuosity were calculated for various moisture contents to allow model application to heterogeneous unsaturated soil systems.

A representative three-dimensional model domain was established to simulate the acetate ion transport from the cathode to the anode through a representative portion of the field

demonstration (Figure 3-1). Due to symmetry of the electrode locations only a single pair of anode and cathode electrodes were simulated. The overall model dimensions were 0.91-m × 2.13-m × 3.66-m deep (Figure 3-6) and consisted of a grid of 5 rows, 14 columns, and 12 layers (840 cells). The cell faces on the exterior of the model domain were assumed to be no-flow boundaries.

Two different models of the field demonstration site were developed to examine the importance of spatial variability on ion transport. The first model assumed the apparent electrical conductivity (EC_a) ($S\ m^{-1}$) of the soil profile could be represented as a simple three-layer system (Table 3-1). The layers were assumed to be laterally continuous with the middle layer (1.83 to 2.74 m BLS) exhibiting an EC_a value approximately twelve times greater than the adjacent two layers. It was also assumed that the higher EC_a of the middle layer was solely due to higher moisture content in the soil profile (Figure 3-4b). The second model assumed the soil profile could be represented by an equivalent homogenous soil (Table 3-1). The homogeneous model assumed one EC_a value for the entire model domain based upon the weighted arithmetic mean of the layered EC_a model. Acetate distribution for both the layered and the homogeneous soil domains were simulated using two phases of electricity application that matched the field demonstration electrode configuration and operation.

To predict the Phase 1 acetate distribution, cells representing the Phase 1 ceramic-cased cathode were set at a constant voltage of zero with an acetate concentration of $1\ mol\ m^{-3}$ (Table 3-2). Cells representing the anode were assumed to have an electric potential of 109 V and an acetate concentration equal to zero. It was assumed that no acetate was initially present in the system. For the remainder of the model domain, the electric potential was calculated a single time in MODFLOW while acetate concentrations were calculated through time in MT3D.

To simulate Phase 2, cells representing the Phase 2 cathode were set to zero volts while cells representing the anode electrode were set to 68 volts. No new acetate sources were included

in the Phase 2 simulation. The final acetate distribution predicted for Phase 1 was used as the initial acetate distribution for Phase 2.

A continuous function relating tortuosity to moisture content was developed using the relationships described by Mattson et al. (1999a, Eq. 2-9). Five pairs of EC_a and θ data (Figures 3-4a and 3-4b) were used to develop the function. Soil zones of stable electrical conductivity (i.e., not varying by more than 50% from measurements 0.3-m above and below) were used to minimize spatial variability effects between the data pairs. Residual moisture content (θ_r) and surface electrical conductivity (EC_s) ($S\ m^{-1}$) were both assumed to be equivalent to the minimum values measured at the field demonstration site and water electrical conductivity (EC_w) ($S\ m^{-1}$) was assumed to be equal to that of the 1:2 extract solution measured in the laboratory. Figure 3-7 illustrates the resulting relationship between tortuosity and moisture content. Table 3-1 lists the regressed values of the five data pairs.

Input values for EC_a were based upon measured moisture contents. Analysis of soil samples taken during the installation of the electrodes indicated moisture contents of approximately 11% by weight ($19.8\%\ m^3\ m^{-3}$) in the 2.4-m deep soil samples. Equation 2-9 from Mattson et al. (1999a) and the parameters listed in Table 3-1 were used to calculate the corresponding value of EC_a . The weighted arithmetic mean of the EC_a of the layered model was used to calculate an effective EC_a for the homogeneous model (Table 3-1). The remaining ion, soil/water, and regression input parameters were assumed constant over the domain for both models (Table 3-1).

3-5. NUMERICAL RESULTS

Acetate concentration distributions were predicted for both phases of the field demonstration using the layered and the homogeneous models. Figures 3-8a and 3-8b illustrate the predicted acetate concentrations relative to the input concentration for both models at the

completion of Phase 1 (the first 1246 hours). In the layered model, acetate was transported from the Phase 1 cathode to the anode through the high EC_a middle layer (Figure 3-8a). The acetate front, as defined by the 0.25 contour, was transported approximately half way between the cathode and anode in the layers with lower electrical conductivity. In comparison, acetate in the homogeneous model (Figure 3-8b) was transported as a much smoother, uniform front from the cathode to the anode. The acetate front progressed much closer to the anode in the homogeneous model than in the layered model.

For Phase 2 predictions, no additional acetate was added and the Phase 2 cathodes were used instead of the Phase 1 cathodes. Figures 3-9a and 3-9b illustrate the predicted acetate concentration distribution after the completion of the field demonstration at the end of Phase 2 after 837 additional hours of applied electrical current. Both model results indicated that low acetate concentrations were present between the Phase 2 cathode and the anode with higher acetate concentrations in the zone above the electrodes (Figures 3-9a, and 3-9b). The largest difference of the predicted acetate transport between the layered and homogenous models was in the zone beneath the electrodes. The homogeneous model indicated acetate transport beneath the electrodes (see 0.25 contour, Figure 3-9b) while the layered model showed very low acetate concentrations at that location (Figure 3-9a).

3-6. DISCUSSION

The assumption of a constant electric potential field with respect to time appears to be valid for this field site. Lindgren et al. (1998) concluded the soil electrical conductivity did not change significantly based on pre- and post-test EC_a measurements. The buffering capacity of the soil, pH conditioning at the ceramic cased electrodes, as well as the steady moisture contents contributed to the stable electrical conductivity profile. The constant electric potential field in buffered soils is consistent with Lasagna field demonstration results (Monsanto, 1996).

Numerical modeling results of the acetate distributions suggest enhanced ion transport in high electrically conductive/moist layers compared to less conductive/dryer layers. The tortuous pathway of the ion is inversely correlated to moisture content. Therefore, examination of an ion's velocity dependence on moisture content can partially explain the numerical modeling results.

The velocity of an ion in one-dimension can be calculated from its effective ionic mobility, tortuosity, and the electric potential gradient (Shapiro et al. 1989):

$$v(\theta) = \mu(c) \tau(\theta) \frac{d\phi}{dx} \quad (3-4)$$

where $v(\theta)$ is the electromigration velocity (m s^{-1}), $\mu(c)$ is the ionic mobility ($\text{m}^2 \text{V}^{-1} \text{s}^{-1}$) adjusted for concentration effects, $\tau(\theta)$ is the tortuosity factor (-) as a function of moisture content, and $d\phi/dx$ is the electric potential gradient (V m^{-1}). Substituting relationships for concentration effects on ionic mobility and tortuosity ((Eqs. 2-5, 2-6, and 2-9) of Mattson et al., 1999a) into (3-4) results in the electromigration ion transport velocity through porous media as a function of some easily measured/regressed input variables:

$$v(\theta) = \mu_o 10^{\left(-0.5085z^2 \left(\frac{\sqrt{1.127RC_o - 0.003}}{1 + \sqrt{1.127RC_o - 0.003}} - 3(1.127RC_o - 0.003) \right) \right)} \frac{F(\lambda) (\theta - \theta_o)^{n+1}}{(\theta_s - \theta_o)} \frac{d\phi}{dx} \quad (3-5)$$

where μ_o is ionic mobility at infinite dilution ($\text{m}^2 \text{V}^{-1} \text{S}^{-1}$), z is the ion valance, $F(\lambda)$ and n are fitting parameters in the Mualem and Friedman (1991) electrical conductivity/moisture content model, θ is the volumetric moisture content ($\text{m}^3 \text{m}^{-3}$), θ_o is the residual volumetric moisture content ($\text{m}^3 \text{m}^{-3}$), and θ_s is the saturated volumetric moisture content ($\text{m}^3 \text{m}^{-3}$). Equation (3-6) indicates that ion velocity is directly related to the effective moisture content ($\theta - \theta_o$) to the $n+1$ power.

For the data presented in this paper, n is close to zero (Table 3-1), so that the ion velocity is approximately proportional to effective volumetric moisture content. Figure 3-10 illustrates acetate electromigration velocity using the data in Table 3-1 and assuming the average electric

potential gradient of Phase 1 (55 V m^{-1}). Results from applying this one-dimensional analysis to the field data indicate the higher conductive wet layer transports acetate ions approximately six times faster than the layers with lower electrical conductivity (Table 3-3). This phenomenon is best illustrated in Figure (3-8a) by the accelerated acetate front in the wetter/more electrical conductive middle layer.

Phase 2 numerical results for the layered and homogeneous models were qualitatively similar in the upper portion of the model domain but exhibited a greater deviation in the lower portion of the domain near the anode (Figures 3-9a and 3-9b). The layered model predicted no acetate present near the base of the anode electrode at the end of the demonstration. During Phase 1, only a small amount of acetate was transported to the area past the Phase 2 cathode with the bulk of the acetate located near the Phase 1 cathode (Figure 3-8a). Therefore, at the initiation of Phase 2, there was little acetate between the Phase 2 cathode and the anode to be transported to the anode electrode. In contrast, the homogeneous model results indicate a fairly symmetric acetate distribution that exhibited high acetate concentrations between the Phase 2 cathode and the anode electrode at the end of Phase 1 (Figure 3-8b). This acetate distribution resulted in a significant acetate source between the anode and Phase 2 cathode for subsequent transport during Phase 2.

Quantitative comparison between the measured acetate concentrations and the model predictions is not possible. Acetate concentration in the Phase 1 cathodes was not measured during the field demonstration. The numerical models assumed an acetate concentration equal to 1 mol m^{-3} in the Phase 1 cathode. In addition, acetate was assumed to behave as a conservative tracer for the model predictions, however it likely underwent some biodegradation during the experiment. Field sampling for acetate was not conducted at the end of Phase 1, precluding a comparison of the Phase 1 model predictions with field results.

Qualitatively, the acetate concentration distribution measured in the field appears to agree with the layered model predictions. Both the layered and homogeneous models (Figures 3-9a and

3-9b) explained the acetate distribution in the upper portions of the field demonstration site (Figure 3-5). However, the homogeneous model also predicted significant acetate concentrations beneath the electrodes. The layered model predicted very low acetate concentrations in this region and no acetate was detected during field sampling in this area.

Acetate concentrations measured in field samples were correlated with the high electrical conductivity layer (Figure 3-5). In contrast, no acetate was detected in the lower portion of the field demonstration in areas with low electrical conductivity. Moisture content is positively correlated with EC_a . At residual moisture content, electrical current is carried solely by the cations in the soil double layer. Acetate, an anion, would not be transported by electromigration at the residual moisture content (see Figure 3-10).

The acetate concentrations measured in the field suggest most of the electric current was confined to the electrically conductive/wetter soil layer. Soil layers exhibiting high acetate concentrations indicate areas where the ions initially present were replaced by other ions. If the initial ions were chromate, then these areas would have been remediated. Conversely, the soil zones with low acetate concentrations measured in post-test soil samples indicate zones of low ion flux and hence soil zones which would not have been remediated. The correlation between acetate tracer detection and areas of chromate remediation was supported by chromate concentration field results. Field results indicated reduced chromate concentration in the upper soil zone while chromate concentrations near the base of the anodes were not reduced (Lindgren et al., 1998).

3-7. SUMMARY

An electrokinetic field demonstration of ion transport by an electric field in unsaturated soil was performed at Sandia National Laboratories. The field site was heterogeneous with respect to moisture content and apparent electrical conductivity. Acetate, a byproduct of the neutralization reactions at the ceramic-cased cathodes, was used to trace electrical current

pathways through the soil. Acetate detection in soil samples appeared to be correlated to soil zones exhibiting high moisture content/electrical conductivity, suggesting the moisture content distribution is an important parameter controlling the electromigration transport of ions. The Mattson et al. (1999a) electromigration model indicates that the velocity of an ion in an electric field is proportional to the effective moisture content raised to the $n+1$ power.

Predictions from layered and homogeneous electrical conductivity models were qualitatively compared to the field results. The layered model correctly predicted higher acetate concentrations in the more moist/electrically conductive layer while the homogeneous model predicted a symmetric acetate concentration above and below the electrodes. Numerical model results suggest that both soil spatial heterogeneity and multi-dimensional potential fields must be considered to correctly predict electromigration transport at the field scale.

ACKNOWLEDGEMENTS

This work was performed at Sandia National Laboratories, which is operated for the U.S. Department of Energy under Contract No. DE-AC04-94AL85000. Funding was provided in part by Department of Energy's Office of Science and Technology through the Subsurface Contaminant Focus Area, and by the New Mexico Waste-management Education & Research Consortium (WERC).

3-8 REFERENCES

- Acar, Y.B., R.J. Gale, J. Hamed, and G. Putnam, Acid/base distributions in electrokinetic soil processing, *Transportation Research Record* 1288, 23-38, 1991.
- Alshawabkeh, A. N., and Y. B. Acar, Electrokinetic remediation. II: Theoretical model, *J. Geotech. Eng.*, 122, 186-196, 1996.
- Jacobs, R. A., *Two-dimensional modeling of the removal of contaminants from soils by electric fields*, Ph.D. Diss., Dept. of Mechanical Engineering, MIT, 1995.
- Jacobs, R. A., and R. F. Probstein, Two-dimensional modeling of electroremediation, *Am. Inst. Ch. Eng. J Jour.*, 42, 1685-1696, 1996.

- Kelly, W. E., and R. Kalinski, Comment on "Theoretical Predication of Electrical Conductivity in Saturated and Unsaturated Soil" by Y. Mualem and S. P. Friedman, *Water Resour. Res.*, 29, 3835-3836, 1993
- Lindgren, E. R., and E. D. Mattson, Electrokinetic system for extraction of soil contaminants from unsaturated soils, *United States patent # 5,435, 895*, 1995.
- Lindgren, E. R., M. G. Hankins, E. D. Mattson, and P. M. Duda, *Electrokinetic Demonstration at the Unlined Chromic Acid Pit*, SAND97-2592, Sandia National Laboratories, Albuquerque, NM. 1998.
- Mattson, E. D., R. B. Bowman, and E. R. Lindgren, 1999a, Electrokinetic ion transport through unsaturated soils: 1. Theory, model development, and testing, (this issue)
- Mattson, E. D., R. B. Bowman, and E. R. Lindgren, 1999b, Sustained electrokinetic remediation in unsaturated soils using surfactant coated electrodes, (submitted to *Jour. of Envir. Engr*)
- McDonald, M. C., and A. W. Harbaugh, A Modular Three-Dimensional Finite-Difference Ground-Water Flow Model, *USGS Open-File Report 83-875*, 1988.
- Monsanto Company, Development of an integrated, in-situ remediation technology – Task 2-4 electrokinetic modeling, *Topical Report # DOE/METC/31185-5391, DE97002135*, 1996.
- Mualem, Y., and S. P. Friedman, Theoretical prediction of electrical conductivity in saturated and unsaturated soil, *Water Resour. Res.*, 27, 2771-2777, 1991.
- Persaud, N. and Wierenga, Solute interactions and transport in soils from waste disposal sites at Sandia Laboratories, *Report prepared for Sandia National Laboratories, Dept. of Agronomy, NM State Univ.*, 1982.
- Probstein, R. F., and R. E. Hicks, Removal of contaminants from soils by electric fields, *Science*, 260, 498, 1993.
- Rhoades J. D., Soluble salts, in *Methods of Soil Analysis, Part 2 – Chemical and Microbiological Properties, second edition*, American Society of Agronomy, Inc., Soil Sci. Soc. of Am., Inc., Madison, WI, 1982.
- Rhoades J. D., and J. D. Oster, Solute content, in *Methods of Soil Analysis, Part 1 – Physical and Mineralogical Methods, second edition*, American Society of Agronomy, Inc., Soil Sci. Soc. of Am., Inc., Madison, WI, 1986.
- Shapiro, A. P., Renauld P. C., and R. E. Probstein, Preliminary studies on the removal of chemical species from saturated porous media by electroosmosis, *PhysicoChem. Hydrodyn.*, 11, 785-802, 1989.
- Yeung, A. T., and S. Datla, Fundamental formulation of electrokinetic extraction of contaminants from soils, *Can. Geotech. J.*, 32, 569-583, 1995.

Zheng C., *MT3D: A Modular Three-Dimensional Transport Model for Simulation of Advection, Dispersion and Chemical Reactions of Contaminants in Groundwater Systems*, a report prepared for the U.S. EPA, 1990.

Table 3-1. Ion, soil/water, and regression parameters used in the 3D model.

| Cell Layer # | Depth Interval BGS (m) | Layered Model | | Homogeneous Model | |
|--------------|---------------------------|--------------------------------------|-------------------------------------|--------------------------------------|-------------------------------------|
| | | EC _a (S m ⁻¹) | θ (m ³ m ⁻³) | EC _a (S m ⁻¹) | θ (m ³ m ⁻³) |
| 1 - 2 | 1.22 - 1.83 | 4.461e ⁻³ | 0.072 | 1.722e ⁻² | 0.126 |
| 3 - 5 | 1.83 - 2.74 | 5.55e ⁻² | 0.198 | 1.722e ⁻² | 0.126 |
| 6 - 12 | 2.74 - 4.88 | 4.461e ⁻³ | 0.072 | 1.722e ⁻² | 0.126 |

Input Parameters used in cells for both models

Ion parameters: $\mu_o = 4.24e-8$ (m² v⁻¹ s⁻¹), $z = -1$

Soil/water parameters: EC_s = 0.003 (S m⁻¹), $\theta_s = 0.375$ (m³ m⁻³), $\theta_o = 0.045$ (m³ m⁻³)

Regression parameters: $F(\lambda) = 1.394$, $n = 0.0651$ (Eq. 2-9 of Mattson et al., 1999a)

Table 3-2. Voltage and concentration boundary conditions used in the 3D model.

| | Electrode | Row # | Col. # | Cell Layer # | Voltage (V) | Acetate Concentration (mol m ⁻³) |
|-----------|-----------|----------|-----------|--------------------|----------------|--|
| Phase 1 | Cathode | 3 | 1 | 5 - 10 | 0 | 1 |
| 1246 hrs | Anode | 3 | 14 | 5 - 10 | 109 | 0 |
| Phase 2 | Cathode | 3 | 7 | 6 - 10 | 0 | - |
| 837 hours | Anode | 3 | 14 | 5 - 10 | 68 | 0 |

Table 3-3. One dimensional predicted electromigration velocity predicted by Eq. (3-5) for the soil layers in the layered and homogeneous models. Input parameters were from Table 3-1 and the electric potential gradient was 55 V m^{-1} .

| Model Type | Moisture Content ($\text{m}^3 \text{ m}^{-3}$) | Effective Moisture Content ($\text{m}^3 \text{ m}^{-3}$) | Electromigration Velocity (m s^{-1}) |
|--------------------|---|---|--|
| Layered | Low EC_a | .072 | $1.67\text{e-}7$ |
| | High EC_a | .198 | $1.06\text{e-}6$ |
| Homogeneous EC_a | .126 | .081 | $5.37\text{e-}7$ |

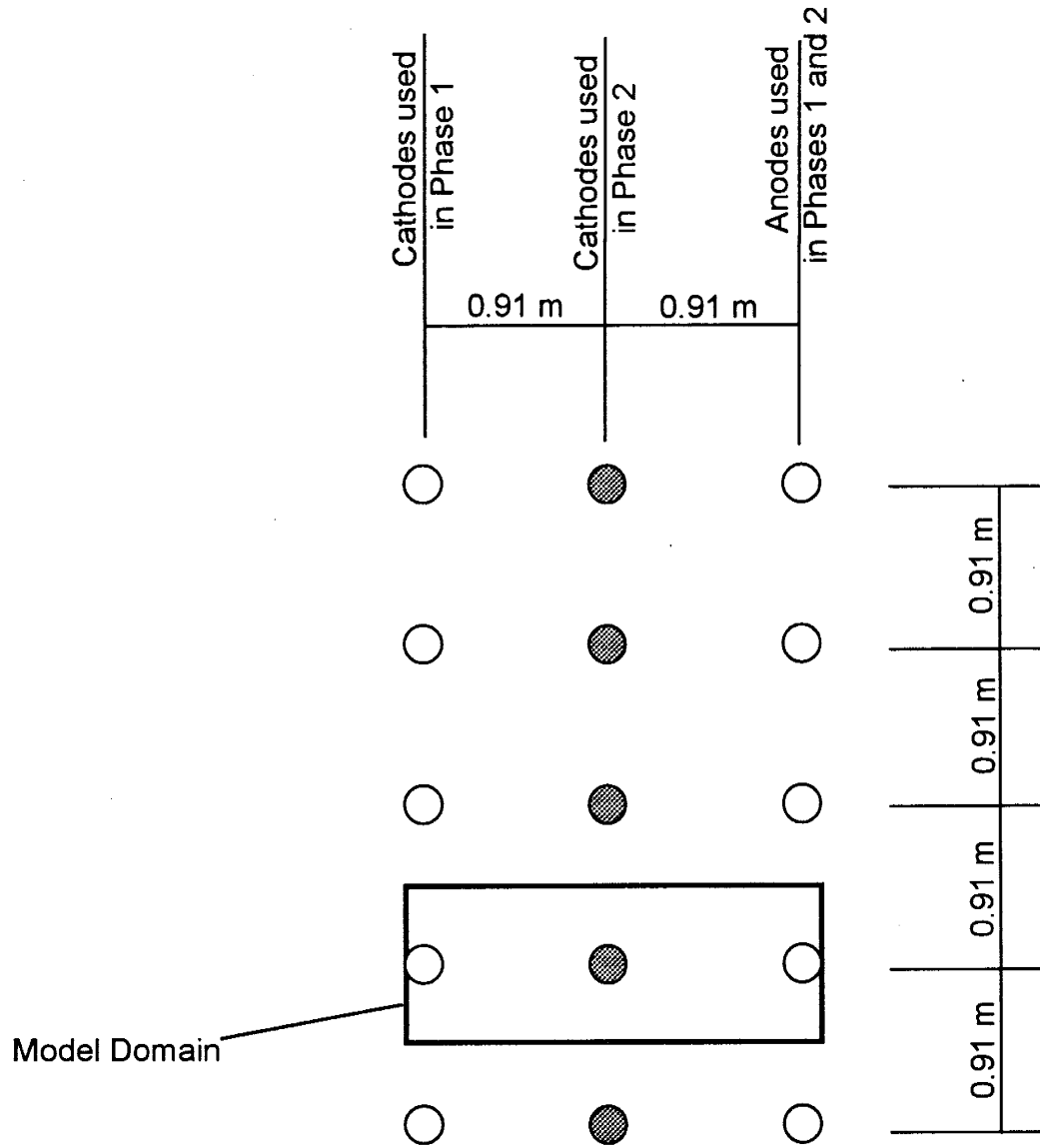


Figure 3-1. Plan view illustrating the electrode positions and numerical model domain for the southern half of the field demonstration. Open circles indicate ceramic-cased electrodes while closed circles indicate pipe electrodes with no electrolysis reaction neutralization.

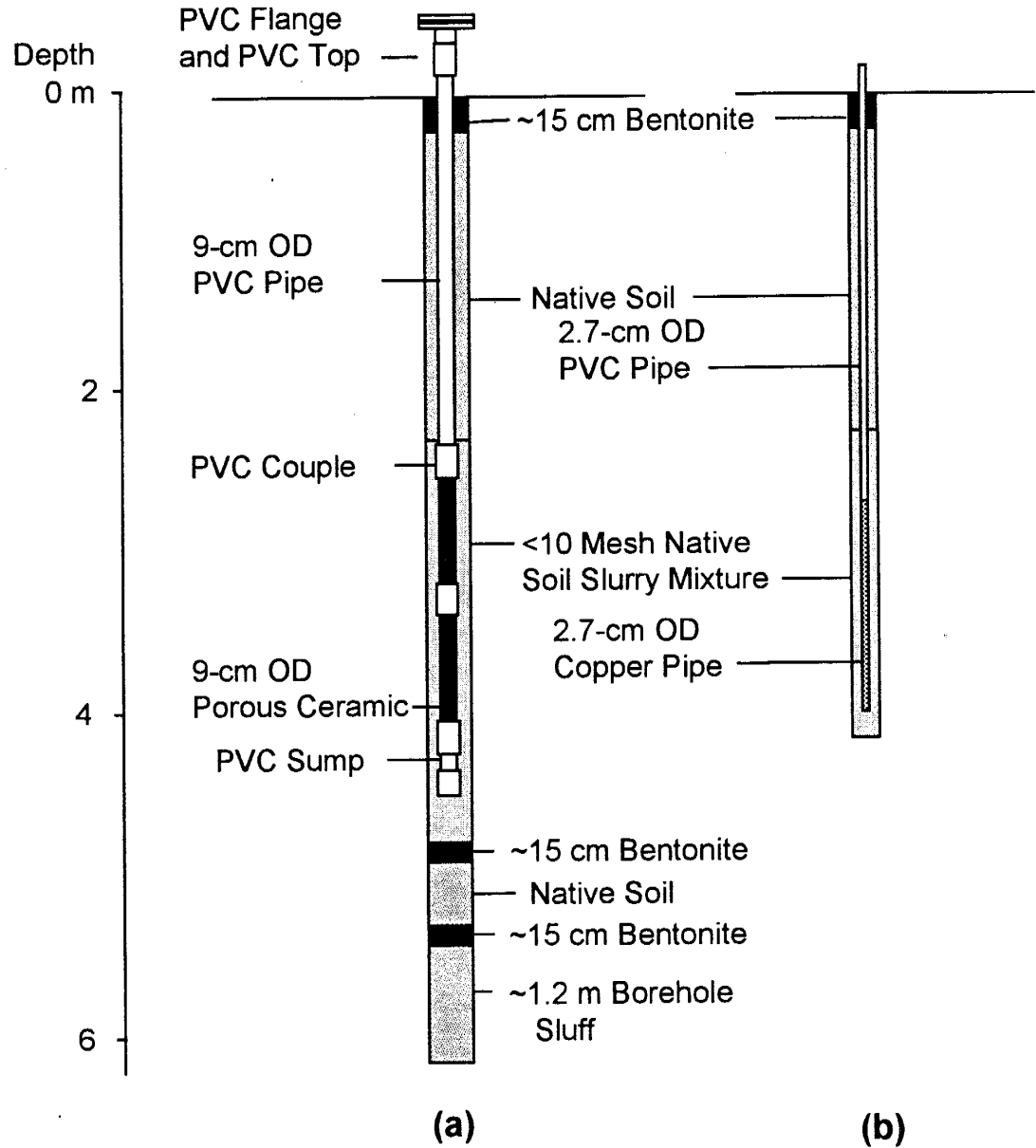


Figure 3-2. Electrode construction and installation method. (a) Anode and Phase 1 cathode ceramic-cased electrode, (b) Phase 2 cathode pipe electrode.

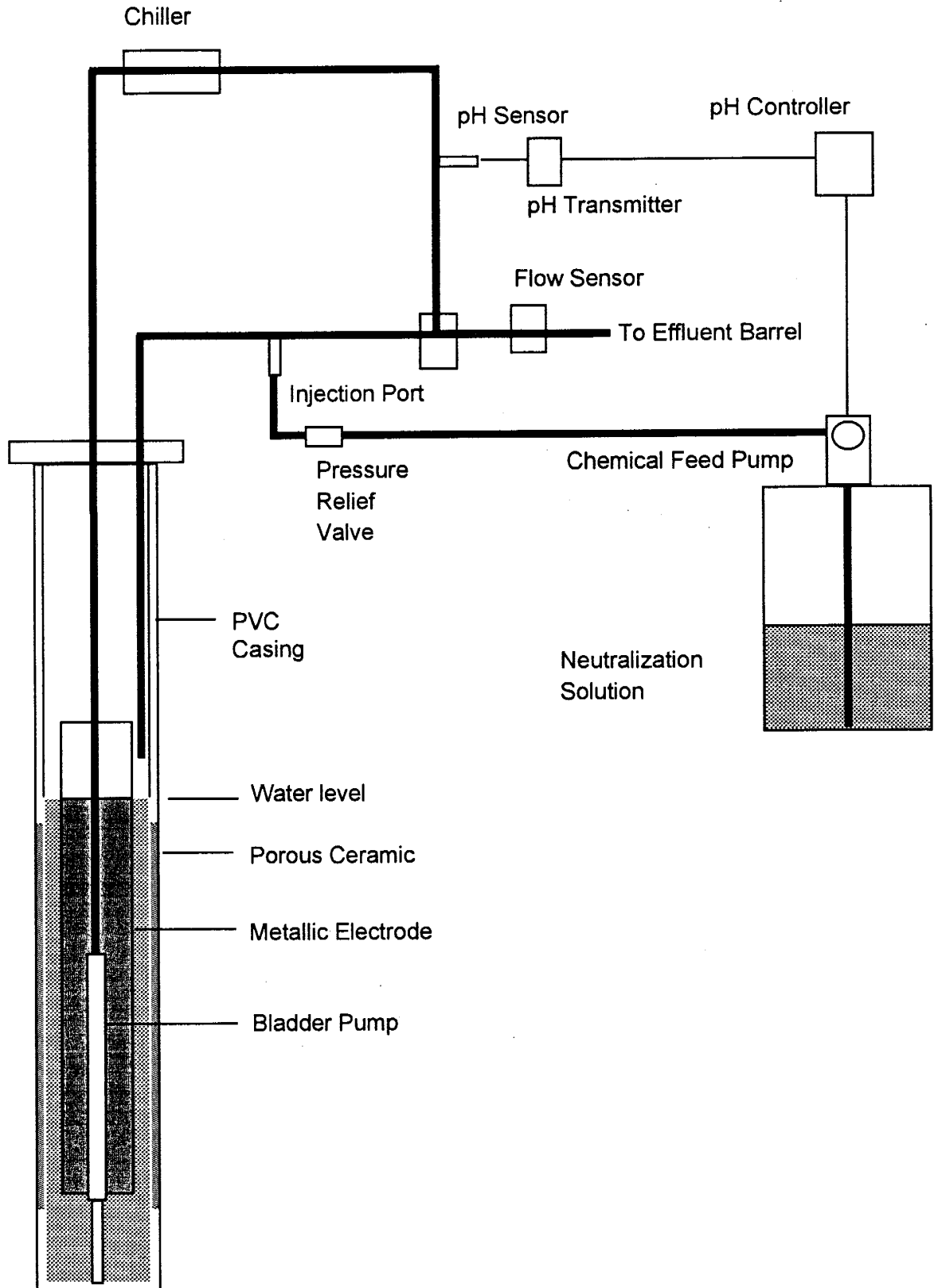


Figure 3-3. Schematic of the water circulation system and pH control system for the ceramic-cased field electrodes.

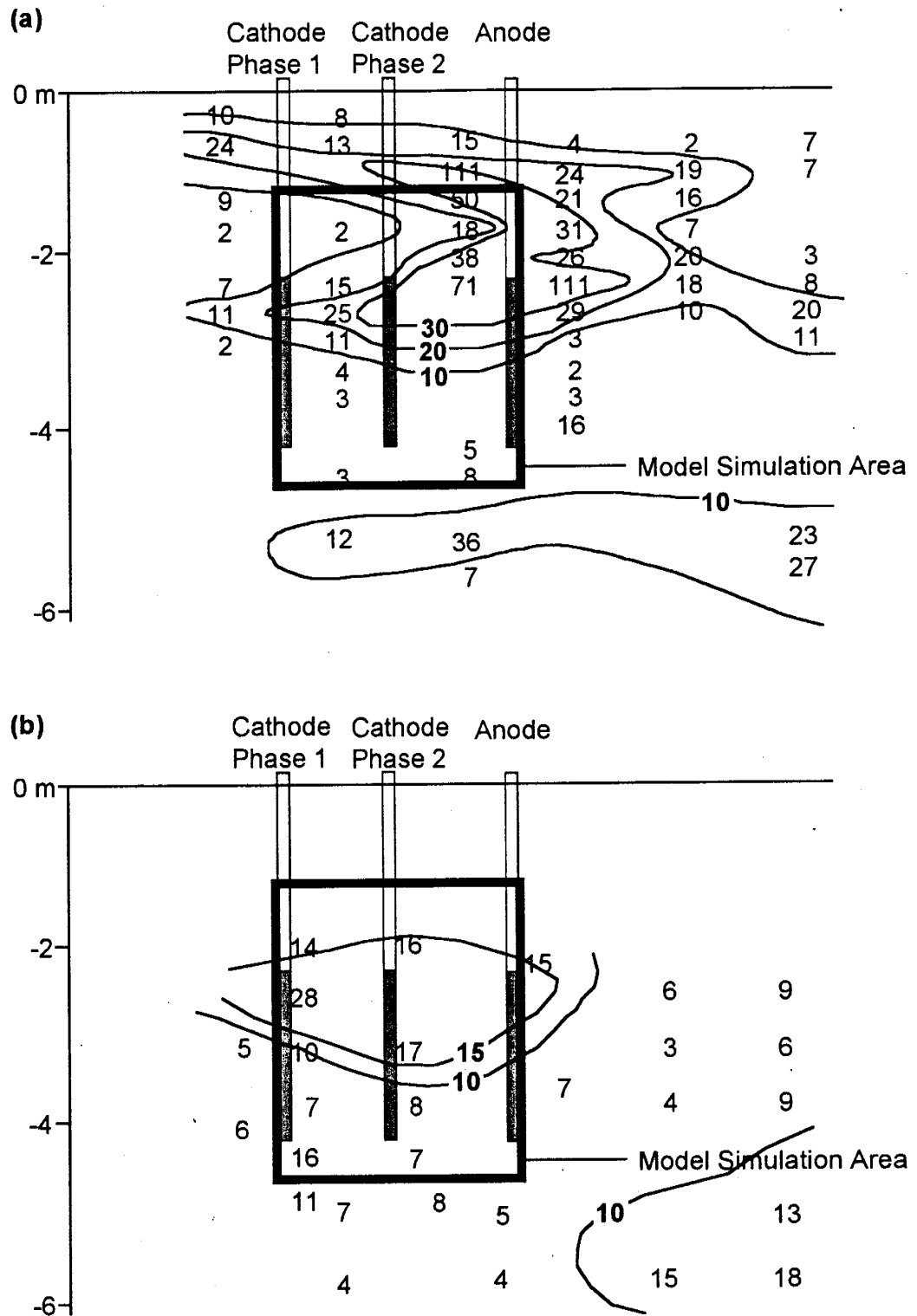


Figure 3-4. Representative cross-section of soil properties prior to electrokinetic experiments. Numbers are sample values. Contour lines are hand-drawn. Box illustrates model simulation area. (a) Apparent electrical conductivity (EC_a) (S m⁻¹), (b) volumetric moisture content (%) by soil sampling.

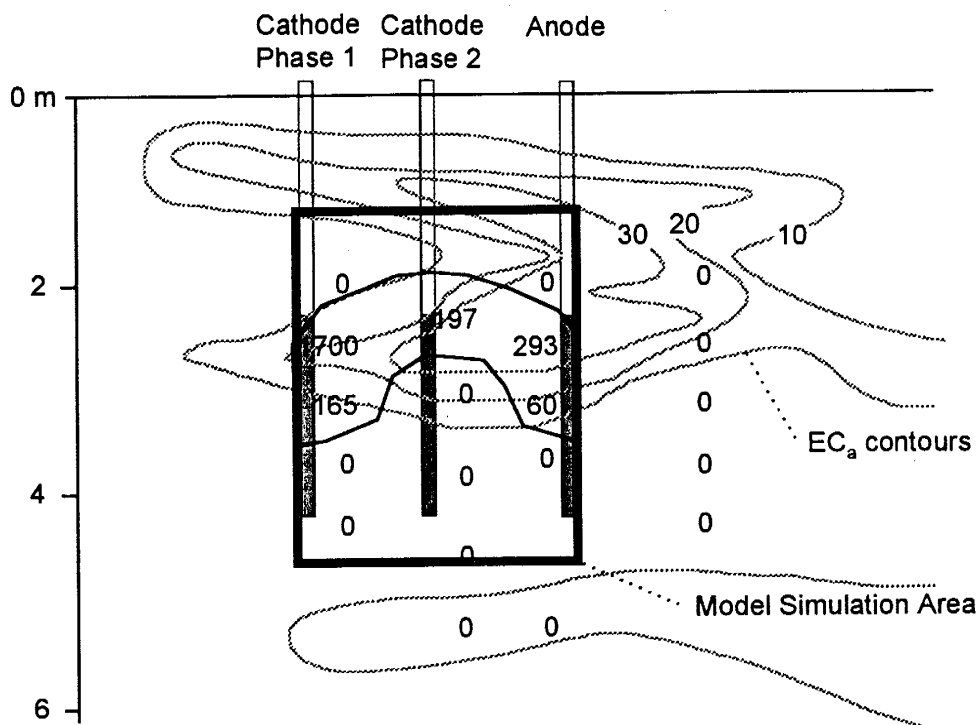


Figure 3-5. Cross-section illustrating acetate concentrations (mg acetate per kg soil) at the completion of the field demonstration (end of Phase 2). The solid contour line represents the zero concentration level. Gray contour lines represent apparent electrical conductivity values as shown in Figure 3-4(a).

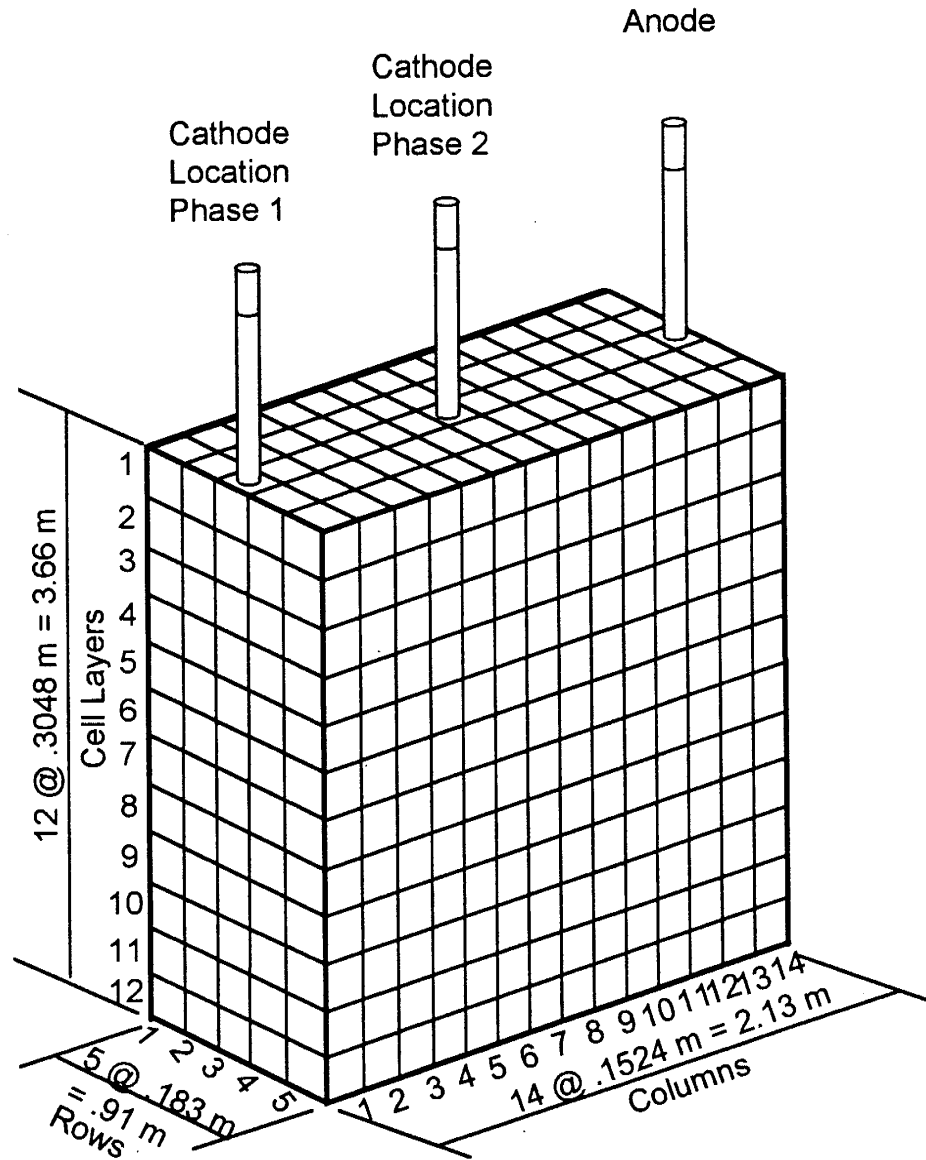


Figure 3-6. Three-dimensional view of the numerical model domain indicating cells size and electrode locations used during Phase 1 and Phase 2. Shading represents cells containing the ceramic portion of the electrode casing.

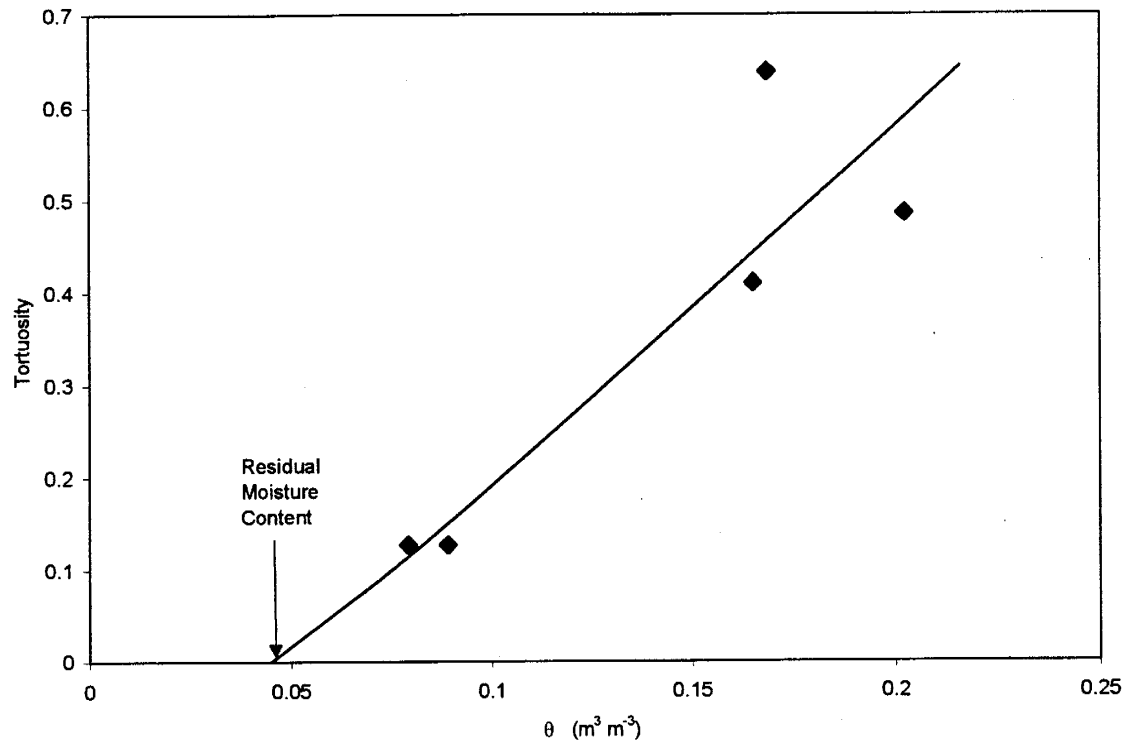


Figure 3-7. Tortuosity as a function of moisture content. Line represents best fit of Equation 2-9 of Mattson et al. (1999a) to field measured data.

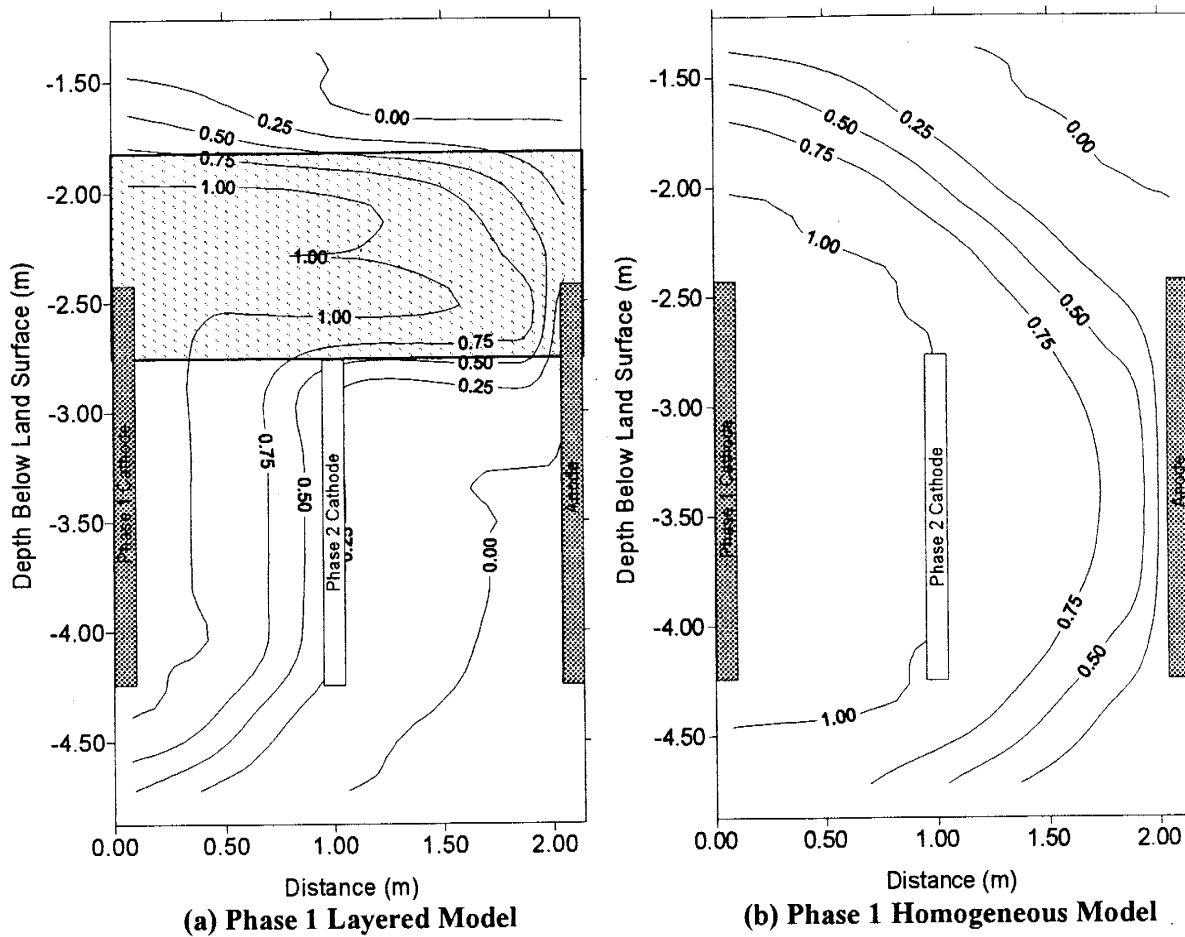


Figure 3-8. Predicted acetate concentrations (relative to input) after 1246 hrs (Phase 1) of electrokinetic transport. Anode and cathode electrodes used during this phase are shaded. (a) layered model – light gray shading indicates electrically conductive/wetter layer, (b) homogeneous model.

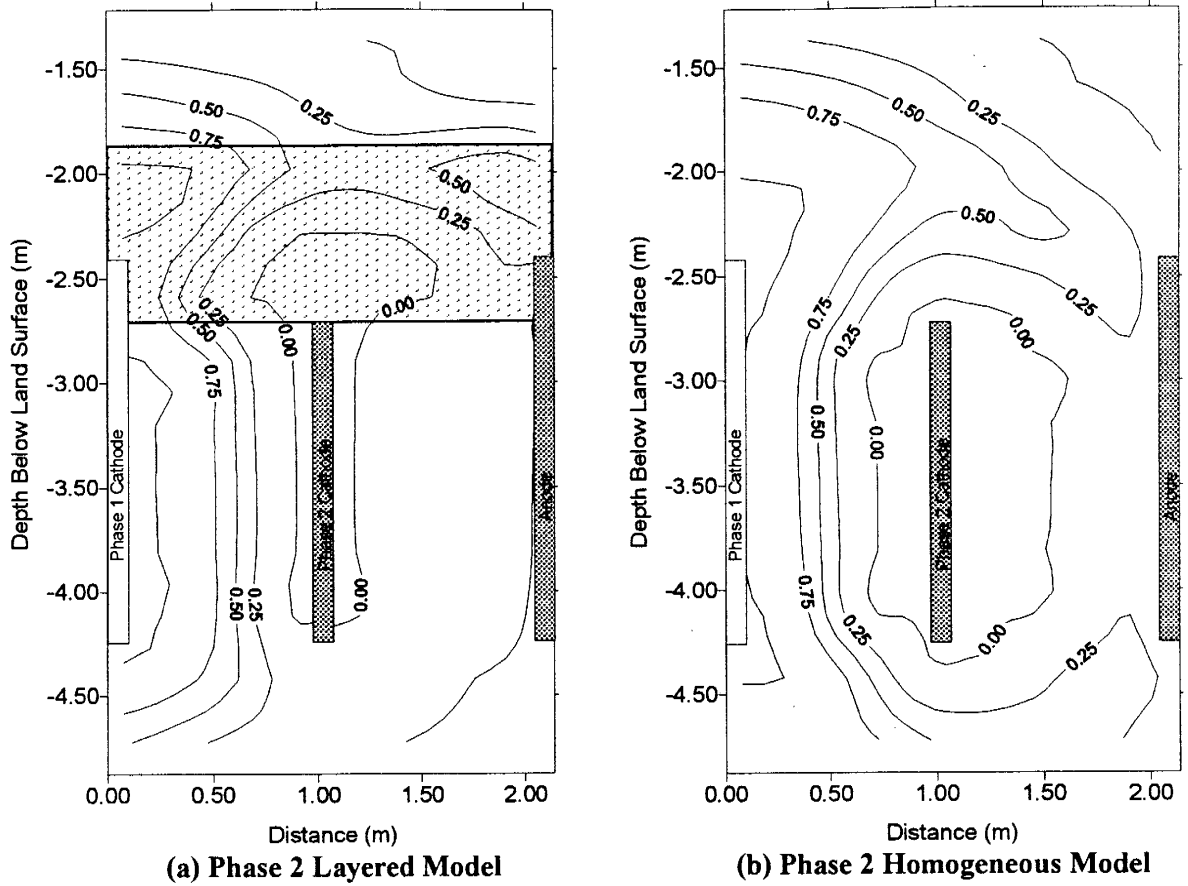


Figure 3-9. Predicted acetate concentrations (relative to the input) after an additional 837 hrs (Phase 2) of electrokinetic transport. Anode and cathode electrodes used during this phase are shaded. (a) layered model – light gray shading indicates electrically conductive/wetter layer, (b) homogeneous model.

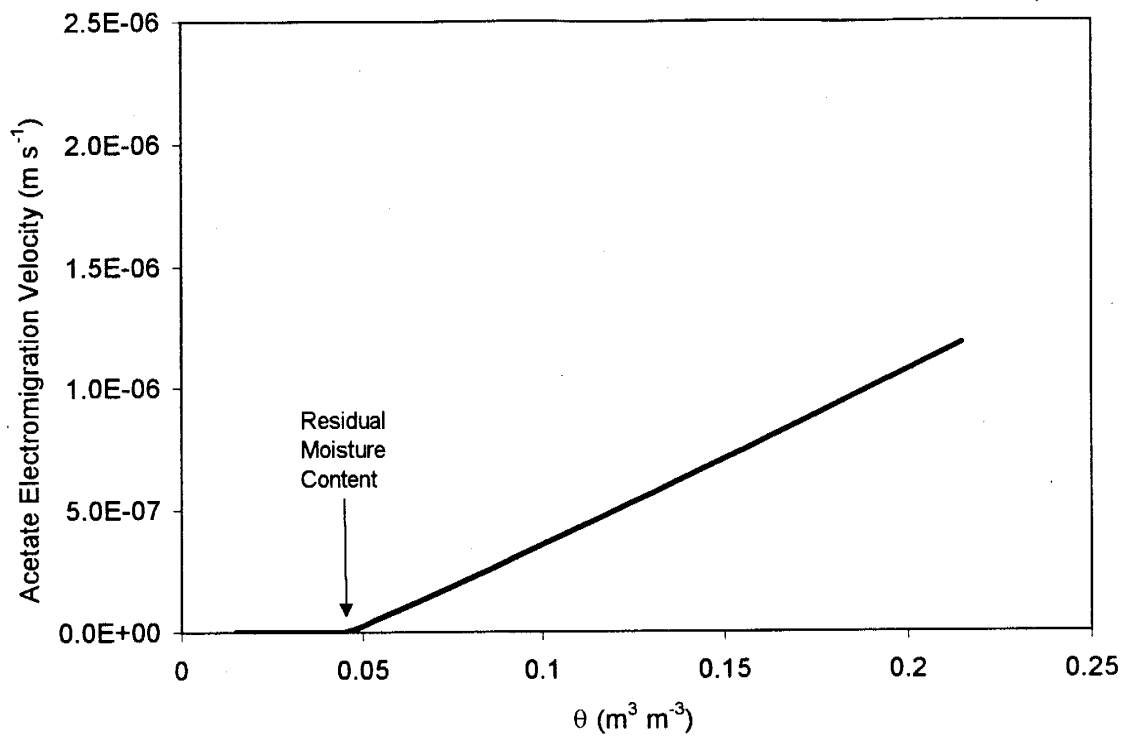


Figure 3-10. Model predicted acetate ion velocity as a function of moisture content in a 1-dimensional 55 V m⁻¹ electric potential gradient.

CHAPTER 4. ELECTROKINETIC REMEDIATION IN UNSATURATED SOILS USING SURFACTANT-COATED CERAMIC CASINGS

Earl D. Mattson¹, Associate Member, ASCE, Robert S. Bowman², and Eric R. Lindgren³

(Submitted to *ASCE Journal of Environmental Engineering*, May 4, 1999)

ABSTRACT

Electrokinetic remediation is an emerging technique that can be used to remove metals from saturated or unsaturated soils and sediments. In unsaturated systems, control of the medium's water content is essential. Previously used electrode designs have caused detrimental soil wetting due to excess electroosmotic flow out of ceramic-encased anodes. We tested a method to reverse the electroosmotic flow at the anode by treating the ceramic casing with the cationic surfactant hexadecyltrimethylammonium (HDTMA). Laboratory tests showed the untreated ceramic had an electroosmotic permeability of $2.4 \times 10^{-5} \text{ cm}^2 \text{ V}^{-1} \text{ s}^{-1}$. Ceramic treated with HDTMA had an electroosmotic permeability of $-1.3 \times 10^{-5} \text{ cm}^2 \text{ V}^{-1} \text{ s}^{-1}$. Under an applied electric potential, electroosmotic flow was reversed in the HDTMA-treated ceramic, indicating a reversed zeta potential due to formation of an HDTMA bilayer on the ceramic surface. Field tests conducted over a 6-mo period with 2700 h of applied voltage showed negligible water loss from HDTMA-treated ceramic (0.03 L h^{-1}) compared to untreated ceramics (up to 6 L h^{-1}). The results indicated that a surfactant treatment to the anode ceramic casing material can greatly improve the application of electrokinetics in unsaturated environments.

¹ Research Assistant, New Mexico Institute of Mining and Technology, Department of Earth and Environmental Science, 801 Leroy Place, Socorro, NM 87801. (505) 856-3311

² Professor, New Mexico Institute of Mining and Technology, Department of Earth and Environmental Science, 801 Leroy Place, Socorro, NM 87801.

³ Principal Member of Technical Staff, Sandia National Laboratories, P.O. Box 5800, Albuquerque, NM 87185-0719.

4-1. INTRODUCTION

Electrokinetics offers an in-situ remediation solution to remove heavy-metal contamination from unsaturated soils. To conduct electrokinetic remediation, anode and cathode electrodes are placed in the soil and direct current is applied between the two electrodes. The applied current transports dissolved ions due to electromigration towards the oppositely charged electrode. Concurrently, electroosmosis moves the soil water in response to the electric potential. Soil water is typically transported towards the cathode due to the excess net positive charges in the double layer associated with the negative surface charge of the soil. Under the influence of an electric potential, these positive charges migrate toward the cathode and create a viscous transport effect on the bulk pore water. Once heavy metal ions reach an electrode they can be extracted to the soil surface for further treatment and/or disposal.

The first electrokinetic investigations in the United States focussed on the role of electroosmosis rather than electromigration. Casagrande (1949) described the use of electroosmosis to dewater clays for engineering applications. Other researchers reported the use of electroosmosis to dewater mine tailings (Sprute and Kelsh 1974; Sprute and Kelsh 1976), kaolinite clay (Lockhart 1983a), and a variety of materials in settling ponds (Lockhart 1983b). Early electrokinetic remediation studies in the United States were conducted in groundwater systems where contaminants were found in low permeability media where the typical pump-and-treat technology was not effective (Mitchell 1986; Renaud and Probststein 1987). Shapiro et al. (1989) performed saturated column experiments to confirm the electroosmotic transport processes to remove organics from clay. Electroosmosis was also used to remove heavy metals from saturated clays in bench-scale experiments (Acar et al. 1990; Hamed et al. 1991).

The importance of the role of electromigration appears to have been recognized with a metal prospecting study in the Soviet Union (Shmakin 1985). Shmakin described the transport process in terms of electromigration rather than electroosmosis, but still within saturated, fine-

grained material. Lageman (1989) described a field-scale application of electrokinetics designed to transport and remove lead, copper, arsenic, and zinc using electromigration in saturated or nearly saturated fine-grained soil in the Netherlands. The EPA recently summarized all electrokinetic studies (patented processes, conceptual studies, as well as bench- and field-scale experiments) performed between 1992 to 1997 (EPA 1997). Most work described in this report was focussed on saturated fine-grained soil, clay, or low permeability soils with the exception of studies at Sandia National Laboratories where work in unsaturated, sandy soil was documented.

The previous emphasis on saturated, fine-grained soils and clays led to a common misconception that electrokinetics was not applicable to unsaturated, sandy soils, even though limited experimental work in these conditions has been documented. Runnells and Larson (1986) and Dahab et al. (1992) both demonstrated electrokinetic transport of copper to the cathode electrode in unsaturated sands but did not remove the copper from the soil. Lindgren et al. (1994) demonstrated electromigration of anionic food dye and chromate through unsaturated fine-grained sand to the anode electrode in laboratory experiments. Mattson and Lindgren (1995) later published experimental results of chromate migration and its removal from unsaturated sandy soil at the laboratory-scale.

Slotted well casings typically used in the saturated zone are not suitable to use as anode casings in unsaturated, sandy soils. Hydraulic flow from the slotted electrode casings to the soil can cause the formation of a saturated wetted bulb surrounding the bottom of the casing. The steady-state outflow rate is dependent on soil texture, well diameter, and height of water in the casing (Amoozegar and Warrick 1986). Water outflow rate may be significant enough to eliminate the use of slotted well casings as anodes for electrokinetic remediation in sandy, unsaturated soils.

On the other hand, anode metallic electrodes installed in unsaturated soil have the opposite problem. Electroosmotic water transport through the soil causes a depletion of water in the vicinity of the anode (Mattson and Lindgren 1995). Soil electrical conductivity is related to moisture

content. As the moisture content decreases to its residual value, the soil electrical conductivity becomes too low for the practical application of electrokinetic remediation.

Porous ceramic casings may be used to control the hydraulic flux of water to the soil. However, the direction of electroosmotic flow within the ceramic pores has a strong influence on the net amount of water being added to the soil from the ceramic casing. For example, infiltration rates from anode ceramic casings increased greatly after an electric potential was applied in a field experiment conducted at Sandia National Laboratories (Mattson 1995). Four 0.9-m long suction lysimeter ceramic casings were installed in dry (2 to 4% by weight) alluvial deposits. A constant vacuum was applied to the headspace above the ceramic portion of the electrode casing (10-cm Hg vacuum). Steady state infiltration prior to the application of electricity was approximately 3 L d^{-1} from both the anode and cathode casings. When an electric potential was applied between the anode and cathode, the infiltration rate out of the anode increased to about 40 L d^{-1} while water loss from the cathode ceramic electrode casings decreased to less than 1 L d^{-1} . During this time a 30-V differential was measured across the ceramic casings. The only operational difference between the anode and cathode electrodes was the direction of electroosmotic flow relative to the ceramic casing. Electroosmotic flow occurred from the interior of the anode electrode casing into the soil whereas at the cathode, the electroosmotic flow was from the soil to the interior of the electrode casing. The anode ceramic casing would have been suitable for long-term electrokinetic remediation if the electroosmotic flow direction was from the surrounding soil toward the interior of the anode casing.

Control over the rate of water addition at the anode is critical for the success of electrokinetic remediation in unsaturated soils. A continuous water pathway is required to maintain an applied electric potential, but excess water could cause saturated conditions that could transport contaminants deeper into the soil profile. This paper describes a surface coating procedure for the anode ceramic casing that allows the electrokinetic remediation process to be

applied to unsaturated, sandy soils. The electroosmotic flow direction can be reversed within the ceramic anode casing by coating the casing with a cationic surfactant such as hexadecyltrimethylammonium (HDTMA). The effective surface charge of the ceramic casing is reversed from a net negative charge to a net positive charge if the surfactant coats the ceramic as a bilayer. In this case, under the influence of an applied electric potential the excess negative ions in the double layer move towards the anode, inducing electroosmotic flow towards the anode.

4-2. THEORY

For this study, water transport was assumed to occur by electroosmotic and hydraulic mechanisms. The net water discharge (i.e., the volumetric water flow rate divided by the cross-sectional flow area) in one-dimension is defined as:

$$q_n = q_{eo} + q_h \quad (4-1)$$

where q_n is the net discharge (m s^{-1}), q_{eo} is the electroosmotic discharge (m s^{-1}), and q_h equals the hydraulic specific discharge (m s^{-1}). Depending on the gradients of the driving forces and whether the zeta potential is positive or negative, the electroosmotic and hydraulic water transport phenomenon may occur in the same or opposite directions.

From a macroscopic viewpoint, q_{eo} is proportional to the electroosmotic permeability and the applied voltage:

$$q_{eo} = -K_{eo} \frac{dV}{dx} \quad (4-2)$$

where K_{eo} is the electroosmotic permeability ($\text{m}^2 \text{V}^{-1} \text{s}^{-1}$) and dV/dx equals the electric potential (V m^{-1}). K_{eo} is usually determined experimentally using soil samples by measuring the volumetric discharge per unit electric potential in the laboratory.

The direction of the electroosmotic discharge (q_{eo}) with respect to the electric potential is determined by the sign (positive or negative) of the K_{eo} . Assuming that the soil/ceramic pores can be treated as a bundle of capillary tubes, the Helmholtz-Smoluchowski equation can be used to describe K_{eo} (Hunter 1981) if the equation is modified to account for moisture content:

$$K_{eo} = -\frac{\varepsilon \zeta \theta}{\eta} \quad (4-3)$$

where ε is the fluid permittivity ($\text{C}^2 \text{N}^{-1} \text{m}^{-2}$), ζ equals the zeta potential (V), θ is the fraction of the cross-sectional area available for flow (-), and η is the fluid viscosity (N s m^{-2}). The zeta potential is the only variable in Eq. (4-3) that can change sign and therefore, the direction of electroosmotic flow. The direction of electroosmotic flow, relative to the electric potential, is solely determined by whether the zeta potential is positive or negative. Most soils and porous ceramics exhibit a negative zeta potential causing the direction of the electroosmotic flux to be from the anode and towards the cathode. Adsorbing a cationic surfactant bilayer to a negatively charged surface can change the zeta potential from negative to positive (Li and Bowman, 1998), and hence the direction of the electroosmotic flux.

The second important potential moving water through saturated porous medium is the hydraulic head gradient. In this case, the equation to describe hydraulic specific discharge (Darcy's Law) is:

$$q_h = -K_h \frac{dH}{dx} \quad (4-4)$$

where K_h is the hydraulic conductivity ($m\ s^{-1}$), and dH/dx describes the hydraulic head gradient (-).

The K_h is not only a function of the fluid but also of the porous medium (Hubbert, 1940), as illustrated by the relationship:

$$K_h = -\frac{k\rho g}{\eta} \quad (4-5)$$

where k is the intrinsic permeability (m^2), ρ is the fluid density ($kg\ m^{-3}$), and g is the gravitational constant ($m^2\ s^{-1}$). Intrinsic permeability is a function of the size, shape and distribution of the pore spaces.

Although the forms of Eqs. (4-2) and (4-4) are similar there are distinct differences between K_{eo} and K_h . K_h is always a positive number and, therefore, the hydraulic gradient always determines the direction of hydraulic flow. In contrast, the K_{eo} can be either positive or negative resulting in flow with or against the electric potential. Secondly, the magnitude of K_h is dependent on the pore size distribution and configuration through the intrinsic permeability factor in Eq. (4-5). However, K_{eo} in Eq. (4-3) is independent of pore size as long as the sizes of the pores are large compared to thickness of the double layer and if surface conduction can be ignored (Hunter 1981). Finally, the hydraulic flow velocity profile is parabolic, with the fastest velocities located in the center of the soil pore while the electroosmotic flow velocity exhibits a flat profile across the pore because the region of varying velocity extends only through the double layer (Hunter 1981).

4-3. METHODS AND MATERIALS

4-3.1. Ceramic

The ceramic casings used for the laboratory and field experiments were constructed of type P3C porous ceramic tubing (Coors Ceramic, Inc.). P3C ceramic is 98% Al_2SiO_5 with the remaining 2% composed of calcium, magnesium, iron, titanium, potassium, and sodium oxides. None of the minor components are greater than 0.5% by weight. The P3C material has a porosity of 42% with a pore diameter of approximately 1.5 to 2.2 μm (Coors Ceramic, Inc. 1998). The K_h of the P3C was determined to be $6 \times 10^{-8} \text{ m s}^{-1}$ following constant head test procedures described by Klute and Dirksen (1986).

4-3.2. Surfactant

The porous ceramic was treated with a cationic surfactant, HDTMA, in the hydroxyl form (HDTMA-OH). A 0.010 M HDTMA-OH surfactant solution was prepared by pumping a 0.010 M HDTMA-Br (Aldrich Chemical) solution through a 30-cm anion ion exchange column packed with Ionac ASB-1 resin (Culligan, Inc.) in the hydroxyl form. The final pH of the HDTMA-OH solution was 10.97.

The 0.010 M HDTMA-OH used in this study had a concentration approximately 5 to 10 times greater than critical micelle concentration (CMC). Bunton et al. (1981) lists a CMC of $0.86 \times 10^{-3} \text{ M}$ whereas Sepulveda and Cortes (1985) list a CMC of $1.9 \times 10^{-3} \text{ M}$.

4-3.3. Ceramic Surfactant Treatment

There were several steps in the process developed to coat the porous ceramic tubing with the surfactant. First, eight pore volumes of 0.10 M HCl were flushed through the ceramic to protonate the available exchange sites. Two pore volumes of deionized water flushed the excess HCl from the pore space. Next, the 0.010 M HDTMA-OH solution was hydraulically flushed through the ceramic until the effluent pH stabilized at 10.9. It was assumed that all available

exchange sites were occupied by the HDTMA surfactant and at least a partial HDTMA bilayer was formed. Previous work supports the assumption that addition of excess HDTMA to aluminosilicate surfaces results in formation of a surfactant bilayer or partial bilayer (Xu and Boyd 1995; Li and Bowman 1997). The laboratory experiment ceramics had additional treatment steps consisting of a deionized water rinse followed by a 0.010 M phosphate buffer (50/50 mixture of $\text{KH}_2\text{PO}_4/\text{Na}_2\text{HPO}_4$) rinse. The phosphate buffer rinse was necessary to equilibrate the fluid in the ceramic pores to that used in the laboratory experiments. The alkali cations in the buffer are not expected to displace the HDTMA from surfaces (Li et al., 1998).

4-3.4. Laboratory Experiments

Laboratory experiments were performed on porous ceramic test samples: 1) to calculate K_{eo} with and without cationic surfactant coatings, and 2) to observe whether the surfactant coating was stable under controlled conditions.

The test samples for the laboratory experiments were constructed from a 7.6-cm long piece of P3C ceramic tubing (8.9 cm OD with 6.4 mm wall thickness). A sheet of PVC plastic was glued onto the bottom and a 7.6-cm piece of PVC pipe was glued to the top of the ceramic test sample as illustrated in Fig. 4-1. Electrodes to measure the voltage differential across the ceramic were constructed from 1-cm wide strip of #50-mesh stainless steel placed on the inner and outer surfaces of the ceramic.

The K_{eo} experiments were set up in a cylindrical outer plastic test cell that allowed radial symmetry to be maintained. The anode (6.4-mm graphite rod [Ultra Pure Graphite Inc.]) was placed in the center of the ceramic tubing and the cathode (6.4-mm woven wire fabric) was located along the outer test cell wall (Fig. 4-1). Both electrodes were connected to a constant current power supply (Fisher Scientific, Model FB 701). A voltmeter (Fluke, Model 45) measured the voltage differential across the ceramic.

To begin a laboratory experiment, a test sample of either HDTMA-treated or untreated ceramic was placed in the test cell. The 0.010 M phosphate buffer solution was added to equal heights in the anode and cathode reservoirs covering the ceramic portion of the test sample. The buffer solution maintained a pH of approximately 6 within the reservoirs during the experiments. An electric potential was imposed across the ceramic by energizing the center graphite anode and outer wire fabric cathode electrodes. The electrical current was held constant at 200 mA by the power supply. To minimize hydraulic counter-flow through the ceramic, a test was conducted only until the fluid level difference between the inner and outer reservoirs became greater than 1 cm. At this point the experiment was stopped, the anode and cathode buffer solutions were chemically equilibrated by mixing them together, the buffer solutions were added back the reservoirs, and the test was repeated. Test measurements were recorded at one to two hour intervals to document: 1) the buffer levels within the anode and cathode reservoirs, 2) applied voltage and current, 3) voltage differential through the ceramic tubing, and 4) experimental time.

Even though the head differential was minimized between the inner and outer cathode reservoirs, the calculated electroosmotic flux was corrected for hydraulic flux effects to obtain better accuracy. The hydraulic flux was calculated using the laboratory-derived K_h values and the average head differential between the anode and cathode reservoirs. The K_{eo} through the ceramic was calculated using:

$$K_{eo} = \frac{-\left(q_n + K_h \frac{dH}{dx}\right)}{\frac{dV}{dx}} \quad (4-6)$$

Pore volumes of fluid electroosmotically flushed through the ceramic were cumulatively calculated for each successive test. The cumulative number of pore volumes for each test was calculated from the net volume of water change in the anode reservoir divided by the pore volume of the ceramic test sample.

4-3.5. Field Experiments

Two field experiments were conducted in dry (< 10% soil moisture by weight) sandy soil at Sandia National Laboratories, Albuquerque, New Mexico, during the summers of 1994 and 1996. The 1994 experiment investigated the effects of excess water flow from untreated ceramic anode casings. The 1996 experiment examined the long-term stability of the surfactant treatment as well as water loss from a HDTMA-treated ceramic anode casing. Both experiment sites were located within 100 m of one another in the same hydrogeologic environment. The porous ceramic anode casings and the HDTMA-OH treatment processes were identical to those used in the laboratory experiments except for the phosphate buffer rinse.

The ceramic casings for the field experiments were designed to account for conditions in unsaturated soils rather than the liquid baths open to the atmosphere used in the laboratory. The lower portion of the electrode casing was constructed from the porous ceramic tubing and is permeable to water as well as electricity. The upper portion of the electrode casing was constructed of 3.5-in OD PVC pipe capped with a plastic flange and lid to facilitate tubing and wiring egress (see Fig. 4-2).

The ceramic-PVC assembly constituted a modified suction lysimeter (Fig. 4-2) and was installed using a similar to a method described by Rhoades and Oster (1986). First an uncased borehole was drilled with a 15-cm hollow stem auger rig. The electrode casing was placed in the borehole and backfilled with a native soil slurry mixture to a depth above the ceramic portion of

the casing. The rest of the borehole was backfilled with soil cuttings to the surface and capped with a bentonite seal to prevent surface infiltration.

The electrodes were operated nearly identically in both field experiments although there were differences in the specific monitoring and control equipment, as listed in Table 4-1. The system that controlled the field electrodes was comprised of three separate components: 1) the fluid control system, 2) the vacuum control system, and 3) the electrode power system.

The fluid control system maintained a constant water level, monitored the water addition and extraction, circulated the water, and conditioned the pH of the fluid in the electrode casing (Fig. 4-2). The water level was maintained at a set level above the ceramic portion of the electrode casing by either an optical-level-control probe or a float switch. The water level control probe operated a solenoid valve connected to a water inlet tank that contained tap water. When the water level in the electrode casing fell to levels below the water level sensor, the solenoid valve was opened to allow water to enter the electrode casing. A circulation pump mixed the electrode solution within the electrode casing, and provided sufficient pressure to allow for fluid extraction from the electrode casing to an effluent tank. Approximately 0.5 to 1 L of effluent per hour were removed by a batch controller system at one-hour intervals. A pH probe located within the circulation system monitored the pH of the solution. The pH probe was connected to a pH controller that allowed either 20-wt% acetic acid at the cathode or a 10-wt% NaOH solution at the anode to enter the electrode casing. Except for brief periods, the pH of the electrode fluid was maintained between 6 and 8 during the experiments.

The vacuum control system maintained a constant vacuum in the casing headspace, limiting the hydraulic movement of water into the soil. Table 4-1 lists the applied vacuum used for both field experiments.

Finally, the electrode power system supplied electricity to the electrodes. Electrodes (iridium-coated titanium anodes, copper cathodes) were placed within the porous ceramic casings

and connected to a constant voltage power supply. The electric potential through the ceramic casing was measured between the anode and a stainless steel wire mesh attached to the outside of the casing.

The 1994 experiment used untreated ceramic casings for the anodes and cathodes at the corners of a 1.2 m × 2.4 m rectangle with the anode and cathode electrodes spaced 1.2 m apart. The ceramic portion of the electrode casing was 0.9-m long and located between 2.7 and 3.6 m below the ground surface. The influent and effluent reservoirs for each electrode casing as well as the acid or base reservoirs were located on Mettler 30-kg balances. An automatic data collection program recorded the balance readings hourly.

The 1994 experiment lasted 188 days. For the first 76 days, water was added to the electrode casing and allowed to infiltrate into the surrounding soil while a 10-cm Hg vacuum was applied to the casing headspace. No electricity was applied to the electrodes during this time and therefore the water loss was solely due to the hydraulic gradient between the electrode fluid and the soil. After 76 days a electric potential was applied between the cathodes and anodes. This water loss from the electrode casings, and the voltage differentials across the porous ceramic casing were recorded hourly to determine the K_{eo} .

The 1996 experiment used HDTMA-treated ceramic casings for the anodes and untreated casings for the cathodes. This experiment was conducted beneath an abandoned, unlined, chromate acid disposal pit. The electrodes were arranged in three rows spaced 1.8-m apart. Each row contained five electrodes 0.9-m apart. The middle row of electrodes was anodes and the outer two rows were cathodes. Each electrode casing had a 1.8-m porous ceramic portion and was placed 2.4 to 4.3 m below the land surface. In general, the operation of the anode electrodes was identical to that of the 1994 experiment although the electrode solution in the 1996 experiment was maintained at approximately 8 to 10° C by circulating the electrode solution through heat exchangers connected to chillers.

Electricity was applied to the system for 2700 h over a six-month period during the 1996 experiment. Mass balance analyses were used to examine fluid loss/gain at each set of electrode casings. For this experiment all of the cathodes and all of the anode casings were each connected to 950-L water tanks precluding a determination of K_{eo} for individual electrodes. Effluents from the electrode casings were directed to individual 200-L plastic drums. The volume of water loss/gained by each type of electrode was calculated by: 1) adding the volume of water added to each type of electrode plus the amount of neutralizing solution added to maintain the desired pH, and 2) subtracting the amount of effluent removed. K_{eo} of the electrode casings was calculated using the calculated water loss/gain, the area of the ceramic portion of the electrode casing, and the average electric potential across the ceramic casing using Eq. (4-2).

4-4. RESULTS AND DISCUSSION

4-4.1. Laboratory Experiments

The calculated electroosmotic permeabilities for the laboratory experiments are illustrated in Fig. 4-3. The average head differential and electric potentials were used to calculate the K_{eo} of both the untreated and HDTMA-treated porous ceramics using Eq. (4-6). The untreated ceramic had a positive K_{eo} , suggesting water flowed from the anode reservoir through the ceramic and into the cathode reservoir. This flow direction indicates a negative zeta potential Eq. (4-3) and hence a negative surface charge on the ceramic. Ceramic treated with HDTMA exhibited electroosmotic flow in the opposite direction. The net flux of water was from the cathode towards the anode, suggesting the zeta potential and surface charge of the ceramic were both positive. Experimental error bars were calculated by assuming a 0.05-cm measurement error while reading the height of the fluid in the anode reservoir at the end of a test.

For both the untreated and HDTMA-treated ceramics, approximately two pore volumes were electroosmotically flushed through the ceramic before K_{eo} reached a steady state value. The

untreated ceramic K_{eo} was $3.0 \times 10^{-5} \text{ cm}^2 \text{ V}^{-1} \text{ s}^{-1}$ after one pore volume was flushed, however, after two pore volumes, K_{eo} was reduced by 20% and appeared to reach a steady state value of $2.4 \times 10^{-5} \text{ cm}^2 \text{ V}^{-1} \text{ s}^{-1}$ (Fig. 4-3). This reduction of electroosmotic flow possibly indicates a change in the pore water chemical composition within the ceramic pores due to electroosmotic flushing. It has been well documented that K_{eo} increases as the ionic strength of the conducting fluid decreases (Grossman and Colburn 1992; Guzman 1993). Although the ceramic was hydraulically flushed with phosphate buffer solution prior to conducting an experiment, the data suggests that chemical equilibrium between the 0.01M phosphate buffer and the ceramic surface prior to the steady-state K_{eo} was not completely obtained. The ionic strength of the fluid in the anode reservoir was likely higher than that initially contained in the ceramic pores at the onset of the experiment. As the fluid from the anode reservoir replaced that in the ceramic during the experiment, the K_{eo} would be expected to decrease.

The HDTMA-treated ceramic exhibited a similar reduction in electroosmotic flow with time. After one pore volume of electroosmotic flushing, the K_{eo} was calculated to be $-3.6 \times 10^{-5} \text{ cm}^2 \text{ V}^{-1} \text{ s}^{-1}$. After two pore volumes, K_{eo} decreased by a factor of three to a steady state value of $-1.3 \times 10^{-5} \text{ cm}^2 \text{ V}^{-1} \text{ s}^{-1}$ (Fig. 4-3). In addition to a possible ionic strength effect as discussed for the untreated ceramic experiments, the magnitude of this decrease in K_{eo} implies an additional mechanism involved in the K_{eo} reduction. Possibly a portion of the surfactant may have leached off the ceramic surface resulting in patchy bilayer coverage on the ceramic surface rather than complete coverage. If patchy bilayer coverage occurred, then the net zeta potential would be reduced, resulting in a steady state electroosmotic flow rate less (in the absolute sense) than that initially observed in the untreated ceramic.

4-4.2. Field Experiments

The K_{eo} s from the 1994 field test for the untreated ceramic anodes were calculated by assuming a constant hydraulic flux occurred from the anode casing. Prior to applying an electric voltage each untreated ceramic casing lost approximately 0.12 L hr^{-1} of water to the soil. When voltage was applied to the field electrodes, the water loss from the untreated ceramic anode casing increased by over 40 times (up to 6 L h^{-1}). The calculated K_{eo} using Eqs. (4-1) and (4-2), was $6 \times 10^{-5} \text{ cm}^2 \text{ V}^{-1} \text{ s}^{-1}$. Although the hydraulic flux was considered constant, in actuality the hydraulic flux would decrease with the superimposed electroosmotic flux due to a reduction in the matrix potential outside of the electrode casings. Therefore, the calculated electroosmotic flux underestimated the actual K_{eo} . Still, the calculated K_{eo} of the untreated field ceramic casing was approximately twice as high as the value obtained from laboratory testing, possibly because the ionic strength of the solution within the field electrode casing was less than of the laboratory buffer solutions. Water loss at the anodes caused soil moisture contents adjacent to the untreated ceramic anode electrode casings to increase from 2-5% to over 11% by weight. In contrast, water loss through the untreated ceramic cathode casings decreased to less than 0.05 L h^{-1} .

The K_{eo} of the HDTMA-treated ceramic field casings could not be quantitatively calculated for the 1996 field experimental setup because there was not an initial infiltration period prior to applying electricity to the soil and no hydraulic gradient measurement through the ceramic. The HDTMA-treated ceramic anode casing lost very little water (82 L per electrode) to the soil over 2700 hours of operation (0.03 L h^{-1}). Over the same time period, the untreated ceramic cathode casings gained nearly the same amount (62 L per electrode) of water (0.02 L h^{-1}). Water loss at the anodes and water gain at the cathodes suggests water transport between the electrodes due to electroosmotic flow through the soil. Even with this electroosmotic flux, the net rate of

water loss from the HDTMA-treated ceramic anode casings to the surrounding soil was over 100 times less than that of the 1994 experiment.

Probable water circulation within the HDTMA-treated ceramic pores maintained saturated conditions in the anode electrode casings of the 1996 test. In the ceramic, the electroosmotic flow was toward the interior of the electrode casing due to the HDTMA double layer. However, the hydraulic flow component was towards the exterior of the casing, resulting in two competing velocity profiles within the ceramic pores. The electroosmotic velocity profile rises from a value of zero at the plane of shear to a uniform velocity across the pore as a result of ion transport in the double layer (Hunter 1981). Meanwhile, the hydraulic flow profile had the greatest velocity at the center of the pore (Fig. 4-4), and flowed in the opposite direction. Superimposing these two profiles upon one another results in a net velocity profile that flows in one direction along the walls of the pore but in the opposite direction in the center portion of the pore. The result is net water circulation within the pores of the ceramic casing. Dukhin and Derjaguin (1974) have discussed this mode of water circulation in capillary tubes.

The head differential required to counteract the electroosmotic flux through the ceramic can be calculated using Eqs. (4-2) and (4-4), the laboratory derived K_{eo} and K_h values, and the electric potential measured across the ceramic from field data. Assuming the calculated ceramic K_{eo} from the laboratory experiment was equal to the actual (but unknown) field value, the calculated head differential across the ceramic was approximately 50-cm of water, a value much lower than the published bubbling pressure (1200-cm H₂O) of the P3C ceramic. This matrix potential was not sufficient to desaturate the ceramic.

The hydraulic flux of water leaving the HDTMA-treated anode ceramic casings in the 1996 field experiment was sufficient to replenish electroosmotic transported water in the soil immediately adjacent to the casing. A depletion of soil water would occur at the soil/ceramic interface stopping the electrokinetic process if water was not supplied to the soil through the

electrode casing. Electroosmotic water flux in the unsaturated soil adjacent to the anode casing was likely hydraulically replenished through the ceramic in sufficient amounts to maintain electrical continuity through the ceramic pore water. These results were confirmed by a statistical comparison between pre- and post-test soil samples. The statistical test results indicated that measured moisture content adjacent to the anode electrode casings did not significantly change.

4-5. SUMMARY AND CONCLUSIONS

A treatment process was developed which allows porous ceramic to be used as an electrokinetic anode casing material in unsaturated soils. The sorption of HDTMA to the ceramic resulted in a strongly sorbed surfactant bilayer or at least a partial bilayer on the ceramic surface. Laboratory testing illustrated surface charge reversal occurred when the ceramic was coated with HDTMA resulting in a reversal in the direction of the electroosmotic flow.

The field experiment results indicated the surfactant coating was maintained on the ceramic surface over a 6-mo period during which 2700 h of electricity was applied. It is hypothesized that hydraulic flow occurred through the center of the HDTMA-treated ceramic pores. This hydraulic flux kept the HDTMA-treated porous ceramic casing saturated and supplied a sufficient water flux to the soil to replenish the water that was electroosmotically transported away from the electrode in the soil. The results indicated that a surfactant treatment to the anode ceramic casing material can greatly improve the application of electrokinetics in unsaturated environments.

ACKNOWLEDGEMENTS

This work was performed at Sandia National Laboratories, which is operated for the U.S. Department of Energy under Contract No. DE-AC04-94AL85000. Funding was provided by the Department of Energy's Office of Science and Technology through the Subsurface Contaminant

Focus Area, and by the New Mexico Waste-management Education & Research Consortium (WERC). The authors would like to recognize the contribution of Dr. Mathew Hankins (Sandia National Laboratories) for his assistance with coating the porous ceramic casings.

4-6. REFERENCES

- Acar, Y., Gale, R., Putnam, G., Hamed, J, and Wong, R. (1989). "Electrochemical processing of soils: Theory of pH gradient development by diffusion, migration and linear convection." *J. Envir. Sci. and Health Part (a), Envir. Sci. and Engrg.*, 25(6), 687-714.
- Amoozegar, A., Warrick, A.W. (1986). "Hydraulic conductivity of saturated soils: Field methods." *Methods of soil analysis, Part 1 – Physical and mineralogical methods, second edition, A.Klute, ed., American Society of Agronomy, Inc., Soil Science Society of America, Inc., Madison, WI., 735-770.*
- Bunton, C.A., Gan, L., Moffatt, J. R., Romsted, L. S., and Savelli, G. (1981). "Reactions in micelles of cetyltrimethylammonium hydroxide: Test of the pseudophase model for kinetics." *J. Phys. Chem.*, 85(26), 4118-4125.
- Casagrande, L. (1949). "Electro-osmosis in soils." *Geotechnique*, 1(3), 159.
- Dahab, M.F., Kelly, W.E., and Goderya, F. (1992). "Removal of metallic contaminants in unsaturated soils using electrokinetics." *Proc., U.S. Department of Energy Electrokinetic Workshop, Atlanta, GA.*
- Dukhin, S. S., and Derjaguin, B.V. (1974). *Surface and colloid science, Vol. 7, E. Matejevic, ed., Wiley and Sons, New York, NY.*
- Grossman, P.D., and Colburn, J.C. (1992). *Capillary electrophoresis: Theory and practice, Academic Press, San Diego, CA.*
- Guzman, N. (1993). *Capillary electrophoresis technology, Marcel Dekker, New York, NY.*
- Hamed, J., Acar, Y.B., and Gale, R.J. (1991). "Pb(II) removal from kaolinite by electrokinetics." *J. Geotech. Engrg. Div., ASCE*, 117(2), 241-271.
- Hubbert M.K. (1940). "The theory of groundwater motion." *J. Geol.*, 48, 785-944.
- Hunter, R. J. (1981). *Zeta potential in colloid science, Academic Press Ltd, London, 386.*
- Klute, A., and Dirksen, C. (1986). "Hydraulic conductivity and diffusivity: Laboratory methods." *Methods of soil analysis, Part 1 – Physical and mineralogical methods, second edition, A. Klute, ed., American Society of Agronomy, Inc., Soil Science Society of America, Inc., Madison, WI, 687-734.*

- Lageman R. (1989). "Electro-reclamation in theory and practice." Forum on Innovative Hazardous Waste Treatment Technologies for Contaminated Land and Ground Water, NATO/CCMS, Copenhagen, Denmark, 57-76.
- Li, Z.H., and Bowman, R.S. (1997). "Counterion effects on the sorption of cationic surfactants and chromate on natural clinoptilolite." *Environ. Sci. Technol.*, 31(8), 2407-2412.
- Li, Z.H., and Bowman, R.S. (1998). "Sorption of perchloroethylene by surfactant-modified zeolite as controlled by surfactant loading." *Environ. Sci. Technol.*, 32(15), 2278-2282.
- Li, Z.H., Roy, S.J., Zou, Y.Q., and Bowman, R.S. (1998). "Long term chemical and biological stability of surfactant-modified zeolite." *Environ. Sci. Technol.*, 32(17), 2628-2632.
- Lindgren, E. R., Mattson, E.D., and Kozak, M.W. (1994) "Electrokinetic remediation of unsaturated soils." *Emerging Technologies in Hazardous Waste Management IV*, D.W. Tedder and F.G. Pohland, eds., ACS Symposium Series 554, Washington, DC, 33-50.
- Lockhart, N.C. (1983a) "Electroosmotic dewatering of clays. I. Influence of voltage." *Colloids and Surfaces*, 6, 229-238.
- Lockhart, N.C. (1983b). "Electro-osmotic dewatering of fine tailings from mineral processing." *International Journal of Mineral Processing*, 10, 131-140.
- Mattson, E. D. (1995). "Borehole effects on unsaturated electrokinetic remediation." *Proc. of the 5th Annual WERC Technology Development Conference*, Las Cruces, NM.
- Mattson, E. D., and Lindgren, E.R. (1995). "Electrokinetic extraction of chromate from unsaturated soils." *Emerging Technologies in Hazardous Waste Management*, ACS Symposium Series, D.W. Tedder and F.G. Pohland, eds., ACS Series 607, Washington, DC, 10-20.
- Mitchell, J.K. (1986). "Potential uses of electrokinetics for hazardous waste site remediation." *Workshop on Electrokinetic Treatment and its Application in Environmental Geotechnical Engineering for Hazardous Waste Site Remediation*, Seattle, WA, 1-20.
- Renaud, P.C., and Probst, R.F. (1987). "Electroosmotic control of hazardous wastes." *PhysicoChemical Hydrodynamics*, 9(1/2), 345-360.
- Rhoades J. D., and Oster, J.D. (1986). "Solute content." *Methods of soil analysis, Part 1 - Physical and mineralogical methods*, second edition, A.Klute, ed., American Society of Agronomy, Inc., Soil Science Society of America, Inc., Madison, WI, 985-1006.
- Runnells, D.D., Larson, J.L. (1986). "A laboratory study of electromigration as a possible field technique for the removal of contaminants from ground water." *Ground Water Monitoring Review*, 6(3), 85-91.
- Shapiro, A.P., Renaud, P.C., and Probst, R.F. (1989). "Preliminary studies on the removal of chemical species from saturated porous media by electroosmosis." *PhysicoChemical Hydrodynamics*, 11(5/6), 785-802.

- Sepuelveda, L., and Cortes, J. (1985). "Ionization degrees and critical micelle concentrations of hexadecyltrimethylammonium and tetradecyltrimethylammonium micelles with different counterions." *J. Phys. Chem.*, 89(24), 5322-5324.
- Shmakin, B.M. (1985). "The method of partial extraction of metals in a constant current electrical field for geochemical exploration.", *J. of Geochemical Exploration*, 23, 27-33.
- Sprute, R.H., and Kelsh, D.J. (1974). "Laboratory experiments in electrokinetic densification of mill tailings. (in two parts). 2. Application to various types and classifications of tailings." U.S. Bureau of Mines, Report of Investigations 7900.
- Sprute, R.H., Kelsh, D.J. (1976). "Electrokinetic consolidation of slimes in an underground mine." U.S. Bureau of Mines, Report of Investigations 8190.
- U.S. Environmental Protection Agency (EPA). (1997). "Electrokinetic laboratory and field processes applicable to radioactive and hazardous mixed waste in soil and groundwater." EPA 402-R-97-006, 77.
- Xu, S., and Boyd, S.A. (1995). "Cationic surfactant sorption to a vermiculitic subsoil via hydrophobic bonding." *Environ. Sci. Technol.*, 29(2), 312-320.

4-7. NOTATION

The following symbols are used in this paper:

| | | |
|---------------|---|--|
| dH/dx | = | hydraulic head gradient (-); |
| dV/dx | = | electric potential ($V\ m^{-1}$); |
| g | = | gravitational constant ($m^2\ s^{-1}$); |
| K_{eo} | = | electroosmotic permeability ($m^2\ V^{-1}\ s^{-1}$); |
| K_h | = | hydraulic conductivity ($m\ s^{-1}$); |
| k | = | intrinsic permeability (m^2); |
| q_{eo} | = | electroosmotic discharge ($m\ s^{-1}$); |
| q_h | = | hydraulic specific discharge ($m\ s^{-1}$); |
| q_n | = | net discharge ($m\ s^{-1}$); |
| ε | = | fluid permittivity ($C^2\ N^{-1}\ m^{-2}$); |
| η | = | fluid viscosity ($N\ s\ m^{-2}$); |
| θ | = | fraction of the cross-sectional area available for flow (-); |
| ρ | = | fluid density ($kg\ m^{-3}$); and |
| ξ | = | zeta potential (V). |

Table 4-1. Electrode Operation Equipment Used in the 1994 and 1996 Field Experiments

| | 1994 Field Experiment | 1996 Field Experiment |
|-------------------------------|--|---|
| FLUID CONTROL SYSTEM | | |
| Water Level Control | Levelite Optical Probe | Flowline LV-10 |
| pH Probe | Cole-Parmer E-27001-80 | Cole-Parmer 27001-97 |
| pH Controller | Omega pHCN-37 | Signet 9030 |
| Circulation Pump | Bennett sampling pump | QED P1101S bladder pump |
| Chiller | None | ITT Bell & Gossett BP honeycomb 410-40 |
| Batch Controller | Omega DPF402 | Signet 9020 Intelek-Pro |
| Circulation Rate | 0.5 l/h | 0.2 to 1.0 l/h |
| VACUUM SYSTEM | | |
| Vacuum Generator | PIAB LX5 | PIAB LX10 |
| Vacuum Regulator | Moore 44-20 | Moore 44-20 |
| Applied Vacuum | 10-cm Hg | 35 cm Hg |
| ELECTRODE POWER SYSTEM | | |
| Anode material | 0.64-cm diameter iridium-coated titanium rod | 5.08-cm diameter iridium-coated titanium tube |
| Cathode Material | 0.64-cm diameter copper rod | 6.4-cm copper pipe |
| Power Supply | Sorensen DTR-600-4.5 | Sorensen DTR-600-16T |

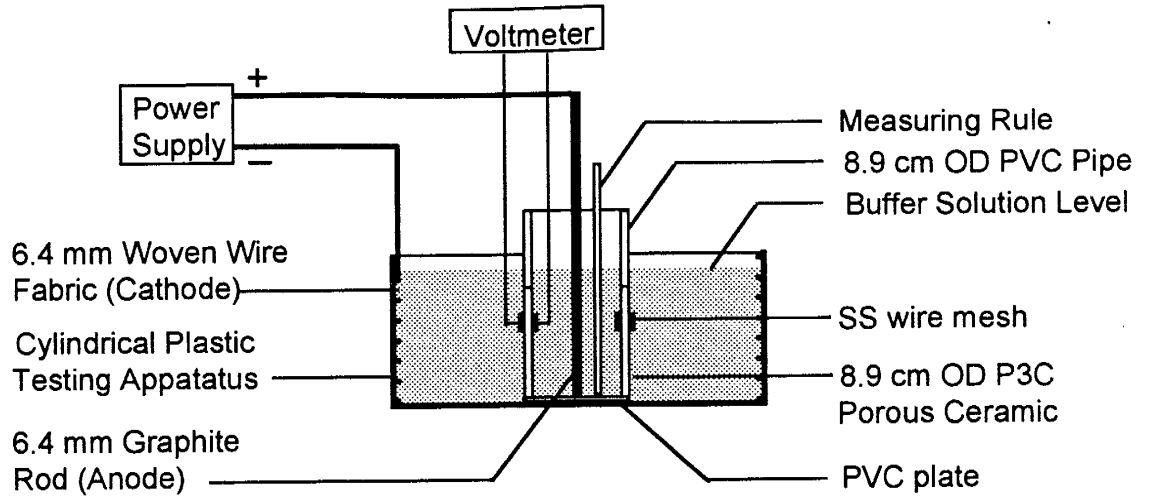


Figure. 4-1. Cross-section of the laboratory apparatus

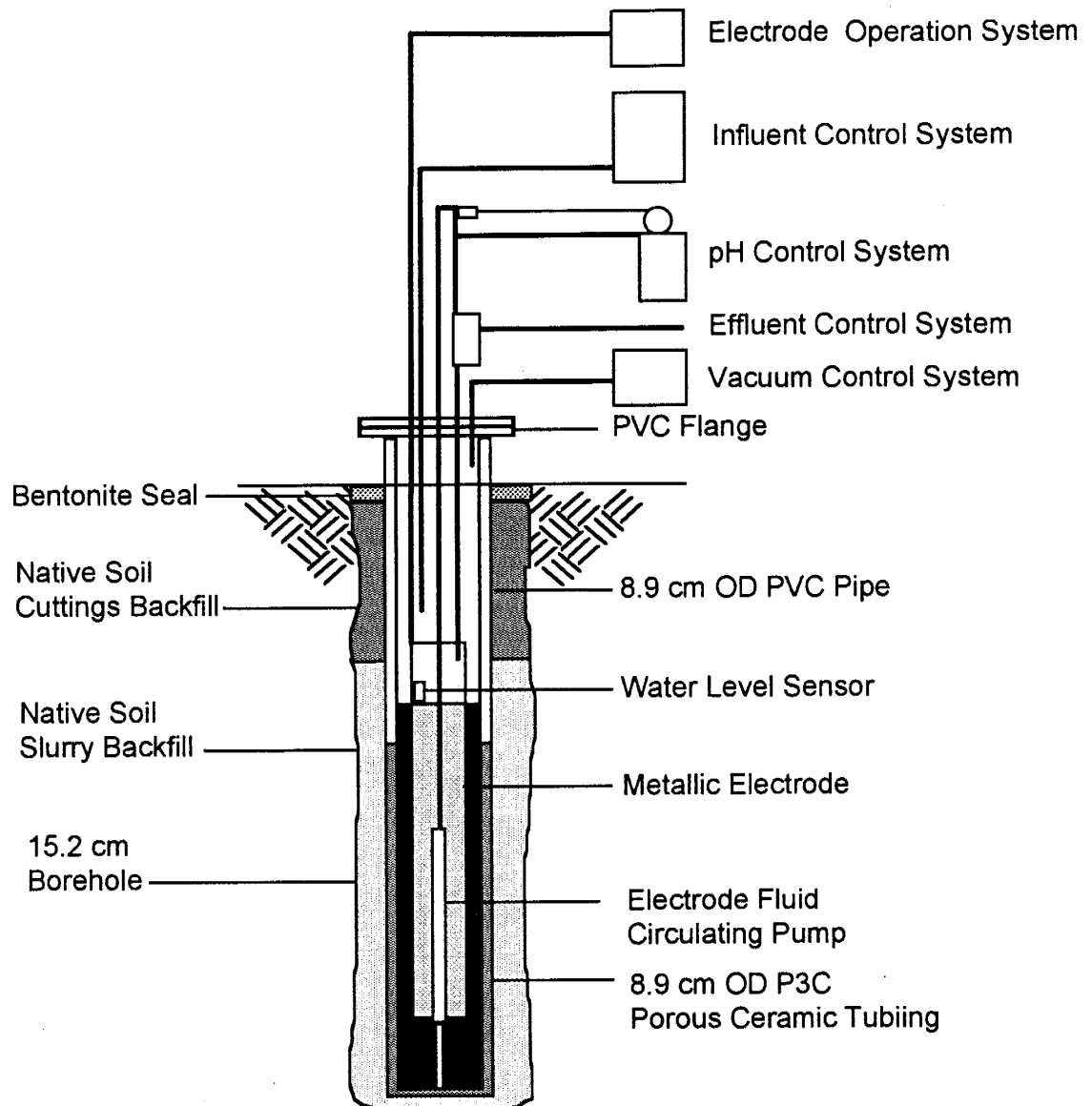


Figure. 4-2. Schematic cross-section of the operational systems, internal components, and installation characteristics of a field electrode

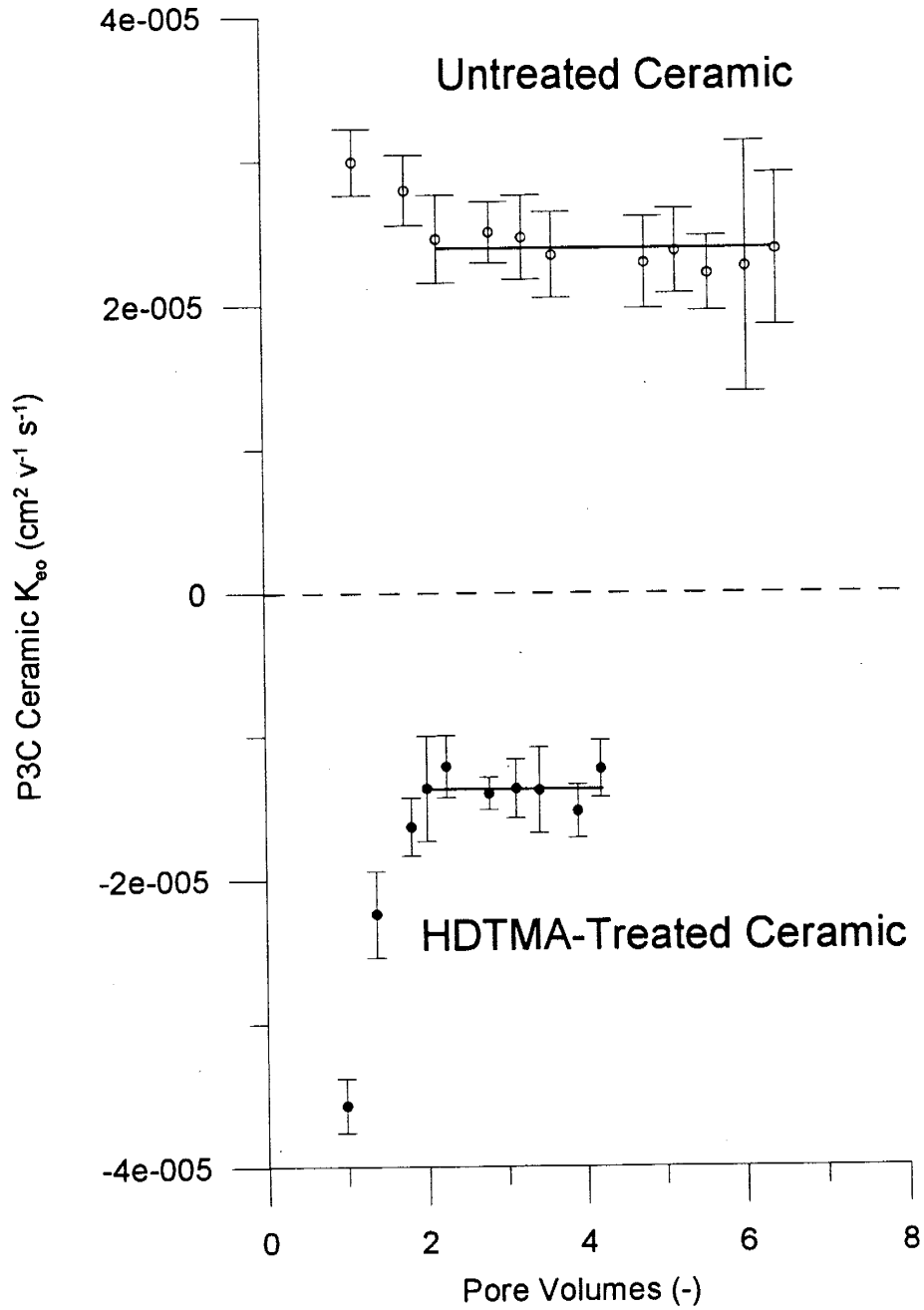


Figure 4-3. Electroosmotic permeability of HDTMA-treated and untreated ceramic measured in the laboratory as a function of pore volumes electroosmotically flushed through the ceramic

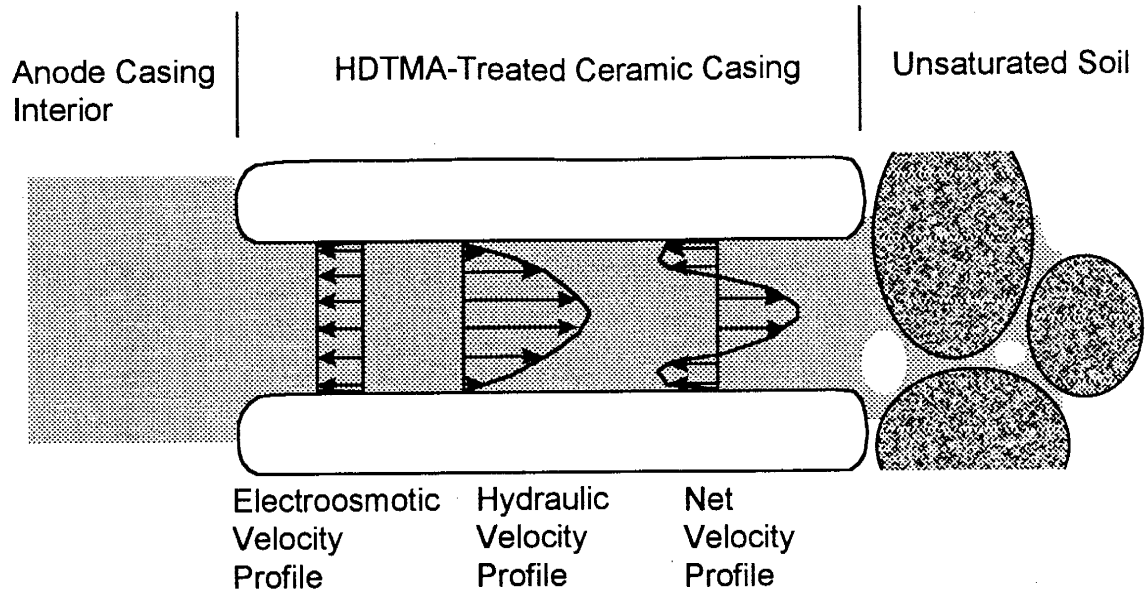


Figure 4-4. Schematic of electroosmotic, hydraulic, and the net velocity profile resulting from superposition in a HDTMA-treated ceramic pore

CHAPTER 5. SUMMARY

5-1. INTRODUCTION

Electrokinetic remediation offers an alternative method to remove contaminants from saturated and unsaturated soils. Contaminants are transported by electromigration if they exhibit a net charge or by electroosmosis if they are uncharged. Unsaturated soil is more difficult to remediate than saturated soil due to the lower electrical conductivity and the electrode engineering difficulties that need to be overcome; however this remediation process is applicable down to near a soil's residual moisture content. A sound theoretical understanding of the governing processes is necessary to successfully implement and predict results of electrokinetic remediation in unsaturated soils.

5-2. SUMMARY OF THIS DISSERTATION

A three-dimensional electromigration model for ion transport in unsaturated soil was developed. This model assumed the electric potential field was constant with respect to time, an assumption that is valid for highly buffered soils or when the electrode electrolysis reactions are neutralized. The model also assumed that advective water movement through the soil due to either electric or hydraulic potentials was negligible. The linking code between two public domain ground water flow (MODFLOW) and transport (MT3D) numerical codes was modified to allow these codes to predict ion transport due to an electric potential field.

The effects of pore water ion concentration on ionic mobility were included in the electromigration transport model. Ionic mobility is a function of the total concentration of ions in the electrolyte solution (i.e., of the ionic strength). Previous electrokinetic models neglected the reduction in ionic mobility as the concentration of the pore water increased. The electromigration transport model estimated ionic strength from electrical conductivity data using an empirical equation proposed by Griffin and Jurinak (1973). Ionic mobility reduction was estimated using

the chemical activity coefficient as calculated by the Davies equation. Although chemical activity does not exactly represent the processes that reduce ionic mobility, it does provide an initial estimate of ionic mobility as a function of concentration. More studies are needed to predict ionic mobility in multi-component solutions.

Tortuosity and apparent electrical conductivity functions required as input to the electromigration transport model were developed from the model of Mualum and Friedman (1991). Their model assumed that the electrical conductivity of the bulk solution could be calculated using Mualem's (1976) closed-form solution. Bulk electrical conductivity of the pore water versus effective moisture content measurements were fitted to a power function to obtain the regression parameters necessary to calculate the apparent electrical conductivity and tortuosity as functions of moisture content.

Anionic dye migration velocities were measured at various moisture contents in laboratory experiments under constant electrical current conditions. The velocities predicted by the electromigration transport model were in agreement with the laboratory experimental results. Both the laboratory-measured and the model-predicted red dye No. 40 results indicated a maximum transport velocity at moisture contents less than saturation due to competing effects between current density and tortuosity as moisture content decreases.

A treatment process was developed that allows porous ceramic to be used as electrokinetic anode casings in unsaturated soils. The sorption of HDTMA to the ceramic resulted in a strongly sorbed surfactant bilayer or at least a partial bilayer. Laboratory testing illustrated surface charge reversal occurred when the ceramic was coated with HDTMA, resulting in a reversal of the direction in the electroosmotic flow.

A field demonstration of electromigration ion transport through unsaturated soil was performed at Sandia National Laboratories using HDTMA-treated ceramic anode casings. The field demonstration results indicated the HDTMA coating was maintained on the ceramic surface over a six-month period during which 2700 hours of electricity was applied. It appeared that a

hydraulic flux, counter to the electroosmotic flux, occurred through the center of the treated ceramic pores that kept the treated-ceramic pores saturated and supplied a sufficient water flux to the soil to replenish soil water that was electroosmotically transported away from the anode. Laboratory and field results indicated that the HDTMA-treated ceramic casings greatly improved the application of electrokinetics to unsaturated soil.

Field demonstration results also indicated preferential electromigration pathways were present between the cathode and anode electrodes. Moisture content and apparent electrical conductivity measurements in the field showed that the soil profile was heterogeneous with respect to moisture content and apparent electrical conductivity. A wetter, more electrically conductive soil layer was measured at the upper portions of the electrodes. Acetate, a byproduct of the neutralization reactions at the ceramic-cased cathodes, was used to trace electromigration pathways through the soil. Acetate concentrations in soil samples were correlated to soil zones exhibiting high moisture content/electrical conductivity, suggesting moisture content and its corresponding electrical conductivity greatly affect the electromigration transport pathways. The theory developed in this dissertation shows that the electromigration velocity is proportional to the effective moisture content raised to the $n+1$ power. This result indicates that field sites being considered for electrokinetic remediation must be adequately characterized in terms of the lateral and vertical distribution of moisture content and electrical conductivity.

Predicted acetate concentrations from layered and homogeneous models were qualitatively compared to the field demonstration results. The layered model agreed well with the field measurements where the highest acetate concentrations were observed in layers that had the greatest electrical conductivities and moisture contents. The homogeneous model predicted a symmetric acetate concentration distribution between the electrodes that was not consistent with field observations. These numerical model results suggest that accounting for soil spatial heterogeneity is required to correctly predict electromigration transport at the field scale.

Although the numerical models presented in this dissertation assumed a zero-concentration boundary condition, a flux-based boundary condition would better describe the actual field demonstration electrodes. Acetate was removed at the anode boundary during numerical simulations of the field demonstration. If the purpose of the numerical simulation is to quantitatively predict removal rates, then there would be a need for more accurate boundary conditions at the anode. An approach implementing a flux boundary would be to use the electrical transference number for the ion of interest. The transference number describes the ratio of the current that is transported by a specific ion species to the total applied electrical current. This method can accurately describe the molar removal rate of an ion species at the electrode. Numerical results of ion removal rates at the electrode using a flux boundary condition could be compared to break-through curves from laboratory and field results.

5-3. WHERE TO GO FROM HERE

Electrokinetic remediation as described in this dissertation is not the “golden bullet” to remediate ionic contaminants in unsaturated soil. This method is limited by inadequate predictive numerical capabilities, and insufficient technological development of the electrode systems. Like all remediation techniques, electrokinetics will fail if applied in an inappropriate situation with unrealistic expectations. However, electrokinetic remediation can be successful either by itself or with in conjunction with other complimentary technologies provided that transport theory and secondary effects of applying DC current through soils are understood.

The electromigration transport model developed in this dissertation is believed to be the first to describe electrically induced ion transport through unsaturated soil. Although the focus of the research presented herein was anion transport, the model could also be used to predict the electromigration of cations and colloids in the bulk pore water due to an electric potential field. However, the model does not account for electromigration transport of cations located in the double layer. For soils exhibiting a low negative zeta potential such as the SNL field

demonstration site, neglecting electromigration transport of cations in the double layer is acceptable. Additional experimental data sets are required to verify the applicability of this model to other soil types, different electrode geometries, and other ions or colloids.

The patented electrode system developed with SNL allows ion transfer from the unsaturated soil to a free liquid inside the electrode for subsequent extraction. However, this system is not developed sufficiently for commercial applications. The need for liquid control, pH conditioning and vacuum systems make the extraction system cumbersome and prone to breaking down. Developing simpler electrode systems that incorporate contaminant-sorbing media are necessary to commercialize electrokinetic remediation.

Limited research has been performed on the secondary effects of soil heating in conjunction with electrokinetic remediation. Some soil heating can be beneficial from the standpoint of reduced soil electrical conductivity and enhanced bioremediation. However, too much soil heating would be detrimental by focusing electrical current pathways, killing indigenous bacteria, and transporting VOC contamination out of the electrokinetic remediation zone.

The generation of heat via passing an electrical current through unsaturated soil will likely limit electrokinetic remediation from becoming a robust remediation technique. The transport of ions due to the application of current will cause an increase in the soil temperature. The greater the rate of current application (i.e., the faster the transport of ions), the greater the rate of heat generation. Generated heat can be expressed as kilowatt-hours per cubic meter. In an adiabatic system, the amount of heat generated in the soil will be proportional to the amount of energy input into the system.

However, soil generally is not considered to be adiabatic, and heat is dissipated from the soil by conduction. In this case, comparison of the rate of energy input (i.e., power) to the rate of heat dissipation will determine the rate of soil temperature change. Heat conduction generally takes place in the soil particles and pore water phase with little heat transfer through the air phase.

Heat transport by radiation, convection, and distillation are of secondary importance (Hillel, 1980).

In soils much of the heat transport takes place through the soil particles; however, soil pore water also plays an important role in the transport phenomena. Although the thermal conductivity of quartz is approximately twenty times higher than that of water, the overall thermal conductivity of a soil is a function of the ratio of the two phases as well as the internal geometry of the soil particles. Soil particles, as thermally conductive as they are, are not well connected to one another physically. For heat to be transferred from one soil particle to the next, it will be transferred mainly from the first particle through the soil water and then to the next particle. As a saturated sandy soil dries, the thermal conductivity basically decreases proportionally to the decrease in volumetric water content. In this case, heat is being transferred through both the solid and liquid phases, and the decrease in thermal conductivity is due chiefly to the decrease in the water in the soil pores available to transmit the heat. However, as the soil dries further, the amount of water diminishes to the point where the water between the soil grains is affected, and the soil particles are not completely connected thermally. Soil thermal conductivity per volumetric water reduction will decrease as the water connecting the individual soil particles dries up.

The application of current to soil during electrokinetic remediation increases the temperature of the soil in the remediation zone. Heat generated by the application of electrical energy is dissipated by thermal conduction out of the zone of remediation. The increase in soil temperature is a function of the rate of energy applied per unit volume of soil (i.e., kilowatts per cubic meter), the volumetric heat capacity, the thermal conductivity of the soil, as well as the location, geometry, and type of heat sinks. Needless to say, calculating the actual soil temperature increase is not a trivial matter. In general, however, applying more electrical power to the soil generally results in a corresponding increase in soil temperature.

The effects of spatial variability are a possible complication to electrical heating during electrokinetic remediation. Electrical current pathways are concentrated in soil horizons that exhibit greater electrical conductivity. These soil horizons are likely to have the greatest power density in the remediation zone and therefore the greatest heat generation. As the temperature of this soil horizon increases above that of the surrounding soil, the soil water viscosity decreases and, hence, the electrical conductivity of this soil horizon increases. As the electrokinetic process continues, this cascading effect due to the interrelationship between power density, temperature, and electrical conductivity will likely result in certain soil horizons transmitting a disproportionately high amount of the current. The increasing soil temperature will induce movement of the soil water out of the soil zone (i.e., by thermally induced flow or evaporation and vapor transport). At some point, the soil moisture content will then decrease which in turn will significantly decrease the soil electrical conductivity. Thus the electrical current pathways change over time. The interaction of heat generation in soil and its effect on electrokinetic transport, bioremediation, and volatilization could make an interesting extension of this dissertation.

The process of bioremediation is also affected by soil heating. Bioremediation, either actively managed or by natural attenuation, therefore could be either enhanced or inhibited by electrokinetic remediation. Most bacteria are sensitive to temperature fluctuation. Bioremediation appears most promising in soil temperatures from 0 to 25 °C. In cold climates electrokinetic remediation could be utilized to maintain the soil temperature within temperature ranges that support many of the bioremediation organisms. Care must be taken not to overheat the soil, as soil temperatures exceeding 40 °C can severely limit most soil bacteria's metabolic rates (Stanier et al., 1986). In addition, soil drying due to electrokinetic heating effects would also limit bacterial activity.

Enhanced vaporization of VOCs through soil heating could be accomplished in conjunction with electrokinetic remediation. Vapor pressures of VOCs increase with increasing

temperature. If an electrokinetic remediation zone contains VOCs, the increase in soil temperature would result in higher VOC concentrations in the soil pores. This enhanced vapor phase could be extracted from the electrokinetic remediation zone with soil-venting techniques, making electrokinetic and soil venting complimentary technologies. On the negative side the bacteria present in the soil would probably be killed with large temperature increases.

The effects of soil spatial variability on electrokinetic transport have received no attention despite its inherent presence at the field scale. As illustrated in this dissertation, the efficiency of electrokinetic remediation will generally be reduced by spatial variability of electrical conductivity in unsaturated soil. Electrical current will be focussed through high electrical conductivity layers in a fashion that may be advantageous in certain situations. For example, if electrical conductivity is strongly correlated with moisture content and the contaminant of interest is also correlated with moisture content, this correlation could be beneficial. More studies are needed to develop a deeper understanding of the effects of spatial variability on the electrokinetic transport processes.

One method to evaluate the effectiveness of electrokinetic remediation and that has received surprisingly little attention is to normalize the contaminant transport flux to the applied electrical charge. In other words, relate the amount of contaminant transported to the amount of applied electrical current. The relationship is quantified by the transference number (Bard and Faulkner, 1980). A transference number is a dimensionless number that describes the amount of current carried by species *i* compared to the total current. A transference number can be determined with either currents or conductivities (Mattson et al. 1997; Lindgren and Mattson, 1998). The current-based transference number relates the amount of contaminant transported across a plane (in terms of electrical charge) to the amount of current applied over some period of time (i.e., the total applied charge in coulombs or amp-hours).

To evaluate a potential remediation site for electrokinetic remediation, a prediction of the current-based transference number could be determined by looking at conductivity-based

transference numbers of soil water-extraction samples. For example, conductivity-based transference numbers can be calculated by multiplying the molar conductivity of chromate in the soil water by the concentration of the contaminant and dividing this product by the measured electrical conductivity of the solution. Mattson and Lindgren (1997) and Lindgren and Mattson (1998) have obtained good quantitative agreement in predicting chromate removal at the SNL field demonstration using the transference number approach.

Overall, the work presented in this dissertation advanced the application of electrokinetic transport of ions through unsaturated soils as a remediation technique. We developed a three-dimensional electromigration transport model and tested it against laboratory results. We conducted a field demonstration of the electrokinetic remediation process in unsaturated soils. In addition, we developed a surfactant treatment for porous ceramic casings that controlled water addition at the anode. However, additional research is needed to better understand the effects of ionic mobility as a function of concentration, soil heating, spatial variability, coupling with other remediation technologies on the electrokinetic transport process. As previously discussed, additional studies could examine using electrokinetic transport with complimentary remediation technologies, such as bioremediation or soil venting, in an attempt to create more robust remediation techniques.

5-4. REFERENCES

- Bard, A.J., and Faulkner, L.R., 1980. *Electrochemical Methods Fundamentals and Applications*. John Wiley and Sons, New York.
- Griffin, R. A., and J. J. Jurinak, Estimation of activity coefficients from the electrical conductivity of natural aquatic systems and soil extracts, *Soil Science*, 116, 26-30, 1973.
- Hillel, D., 1980. *Fundamentals of Soil Physics*. Academic Press, New York, NY.
- Lindgren, E. R., and E. D. Mattson, Electrokinetic Demonstration at Sandia National Laboratories: Use of Transference Numbers for Site Characterization and Process Evaluation, Waste-Management 98, Tucson AZ

Mattson, E. D., and E. R. Lindgren, Chromate Removal From Unsaturated Contaminated Soils Using Electrical Currents. Abstract presented at fall AGU meeting 1997

Mualem, Y., A new model for predicting the hydraulic conductivity of unsaturated porous media, *Water Resour. Res.*, 12, 513-522, 1976.

Mualem, Y., and S. P. Friedman, Theoretical predication of electrical conductivity in saturated and unsaturated soil, *Water Resour. Res.*, 27, 2771-2777, 1991.

Stanier, R.Y., Ingraham, J.L., Wheelis, M.L., and Painter, P.R., *The Microbial World*. Prentice Hall, New Jersey, 1986.

APPENDIX A. MODFLOW and LKMT Code Modifications

The electromigration transport model required several modifications to the MODFLOW and LKMT code modules before it could simulate ion transport under the influence of an electric field. Appendix A includes listings of MODFLOW modules and LKMT modules that were modified to implement the model. Portions of the code that were deleted are shown with a line striking out the text. Additions to code are shown as underlined text.

The major portion of the code modifications were made to LKMT.FOR. This module was changed such that electric potential, the equivalent Darcy ion flux across each cell face, and the location and current flow rate of the electrical source and sinks were sent from MODFLOW output to be used as input to the MT3D calculation.

The remainder of the MODFLOW modules only required small changes. Additional input and output blocks were added to module BCF1.FOR. The additional blocks included transport properties of the ion of interest and soil electrical properties. MAIN.FOR transferred these data back to the appropriate MODFLOW module. The X-array size was increased in module BAS1.FOR to allow the new electromigration transport model input parameters to be stored. Finally, LKMT.INC was changed to read the additional electromigration transport model input parameters from the BCF.dat (see Appendix B) input file.

A-2
MAIN.FOR Modifications

```
C Last change: E 11 Jul 98 4:56 pm
C
C *****
C MAIN CODE FOR MODULAR MODEL -- 9/1/87
C BY MICHAEL G. MCDONALD AND ARLEN W. HARBAUGH
C-----VERSION 1638 24JUL1987 MAIN1
C WITH PCG1 PACKAGE BY L.K. Kuiper, 1987 (USGS)
C STR1 PACKAGE BY D.E. Prudic, 1989 (USGS)
C LKMT PACKAGE BY C. Zheng, 1990 (SSP&A)
C
C Note: PCG1 implemented on IUNIT (13)
C STR1 implemented on IUNIT (14)
C LKMT implemented on IUNIT (22)
C Code modification by C. Zheng, 1987-90
C
C Modified again by E Mattson for electric and ion flow
C June 1998
C *****
C
C SPECIFICATIONS:
C-----
C PARAMETER (LENX=750000)
C DIMENSION X(LENX)
C COMMON X
C COMMON /FLWCOM/LAYCON(80)
C CHARACTER*4 HEADNG,VBNM,FLNAME*30
C DIMENSION HEADNG(32),VBNM(4,20),VBVL(4,20),IUNIT(24)
C DOUBLE PRECISION DUMMY
C EQUIVALENCE (DUMMY,X(1))
C
C C--WRITE AN IDENTIFIER
C WRITE(*,101)
C 101 FORMAT(1X,'MODFLOWFORMAT(1X,'MionFLOW for MT3D, V1.10. ',
C & 'S.C. Papadopoulos & Associates,'Sat-Unsat, Inc. '/')
C
C C2-----ASSIGN BASIC INPUT UNIT AND PRINTER UNIT.
C INBAS=1
C IOUT=6
C
C C--OPEN MAIN INPUT & OUTPUT FILES
C FLNAME='Standard Output File: '
C CALL UOPFIL(IOUT,0,FLNAME)
C FLNAME='BAS Package Input File: '
C CALL UOPFIL(INBAS,1,FLNAME)
C
C C3-----DEFINE PROBLEM ROWS,COLUMNS,LAYERS,STRESS PERIODS,PACKAGES
C CALL BASIDF(ISUM,HEADNG,NPER,ITMUNI,TOTIM,NCOL,NROW,NLAY,
C 1 NODES,INBAS,IOUT,IUNIT)
C
C C--OPEN INPUT FILES FOR VARIOUS PACKAGES
C IF (IUNIT(1).GT.0) THEN
C FLNAME='BCF Package Input File: '
C CALL UOPFIL(IUNIT(1),1,FLNAME)
C ENDIF
C IF (IUNIT(2).GT.0) THEN
C FLNAME='WEL Package Input File: '
C CALL UOPFIL(IUNIT(2),1,FLNAME)
C ENDIF
C IF (IUNIT(3).GT.0) THEN
C FLNAME='DRN Package Input File: '
C CALL UOPFIL(IUNIT(3),1,FLNAME)
C ENDIF
C IF (IUNIT(4).GT.0) THEN
C FLNAME='RIV Package Input File: '
C CALL UOPFIL(IUNIT(4),1,FLNAME)
C ENDIF
C IF (IUNIT(14).GT.0) THEN
C FLNAME='STR Package Input File: '
C CALL UOPFIL(IUNIT(14),1,FLNAME)
C ENDIF
C IF (IUNIT(5).GT.0) THEN
C FLNAME='EVT Package Input File: '
C CALL UOPFIL(IUNIT(5),1,FLNAME)
C ENDIF
C IF (IUNIT(7).GT.0) THEN
C FLNAME='GHB Package Input File: '
C CALL UOPFIL(IUNIT(7),1,FLNAME)
C ENDIF
C IF (IUNIT(8).GT.0) THEN
C FLNAME='RCH Package Input File: '
C CALL UOPFIL(IUNIT(8),1,FLNAME)
C ENDIF
C IF (IUNIT(9).GT.0) THEN
C FLNAME='SIP Package Input File: '
C CALL UOPFIL(IUNIT(9),1,FLNAME)
C ENDIF
C IF (IUNIT(11).GT.0) THEN
C FLNAME='SOR Package Input File: '
C CALL UOPFIL(IUNIT(11),1,FLNAME)
C ENDIF
C IF (IUNIT(13).GT.0) THEN
C FLNAME='PCG Package Input File: '
C CALL UOPFIL(IUNIT(13),1,FLNAME)
C ENDIF
C IF (IUNIT(12).GT.0) THEN
```

A-3
MAIN.FOR Modifications

```

        FLNAME='OpC Options Input File: '
        CALL UOPFIL(IUNIT(12),1,FLNAME)
    ENDIF

C
C4-----ALLOCATE SPACE IN "X" ARRAY.
    CALL BASIAL(ISUM, LENX, LCHNEW, LCHOLD, LCIBOU, LCCR, LCCC, LCCV,
1      LCHCOF, LCRHS, LCDELRL, LCDELCL, LCSTRT, LCBUFF, LCIOFL,
2      INBAS, ISTRT, NCOL, NROW, NLAY, IOUT, lecond, ltheta,
3      lthetas, lthetao, lexpn, lthk, LFY)
    IF (IUNIT(1).GT.0) CALL BCFIAL(ISUM, LENX, LCSC1, LCHY,
1      LCBOT, LCTOP, LCSC2, LCTRPY, IUNIT(1), ISS,
2      NCOL, NROW, NLAY, IOUT, IBCFCB)
    IF (IUNIT(2).GT.0) CALL WELIAL(ISUM, LENX, LCWELL, MXWELL, NWELLS,
1      IUNIT(2), IOUT, IWELCB)
    IF (IUNIT(3).GT.0) CALL DRNIAL(ISUM, LENX, LCDRAI, NDRAIN, MXDRN,
1      IUNIT(3), IOUT, IDRNCB)
    IF (IUNIT(8).GT.0) CALL RCHIAL(ISUM, LENX, LCIRCH, LCRECH, NRCHOP,
1      NCOL, NROW, IUNIT(8), IOUT, IRCHCB)
    IF (IUNIT(5).GT.0) CALL EVTIAL(ISUM, LENX, LCIEVT, LCEVTR, LCEXDP,
1      LCSURF, NCOL, NROW, NEVTOP, IUNIT(5), IOUT, IEVTCB)
    IF (IUNIT(4).GT.0) CALL RIVIAL(ISUM, LENX, LCRIVR, MXRIVR, NRIVER,
1      IUNIT(4), IOUT, IRIVCB)
    IF (IUNIT(14).GT.0) CALL STRIAL(ISUM, LENX, LCSTRM, ICSTRM, MXSTRM,
1      NSTREM, IUNIT(14), IOUT, ISTRCB1, ISTRCB2, NSS, NTRIB,
2      NDIV, ICALC, CONST, LCTBAR, LCTRIB, LCIVAR, LCFGAR)
    IF (IUNIT(7).GT.0) CALL GHBIAL(ISUM, LENX, LCBNDS, NBOUND, MXBND,
1      IUNIT(7), IOUT, IGHBCB)
    IF (IUNIT(9).GT.0) CALL SIPIAL(ISUM, LENX, LCEL, LCFL, LGL, LCV,
1      LCHDCG, LCLRCH, LCW, MXITER, NPARM, NCOL, NROW, NLAY,
2      IUNIT(9), IOUT)
    IF (IUNIT(11).GT.0) CALL SORIAL(ISUM, LENX, LCA, LCRES, LCHDCG, LCLRCH,
1      LCIEQP, MXITER, NCOL, NLAY, NSLICE, MBW, IUNIT(11), IOUT)
    IF (IUNIT(13).GT.0) CALL PCGIAL(ISUM, LENX, LCXXV, LCXXS, LCDT, LCE2,
1      LCF2, LCG2, LCVV, LCE22, LCD2S, LCNUI, MXITER, NPCOND, ITYP, NCOL,
2      NROW, NLAY, IUNIT(13), IOUT, NOD)

C
C5-----IF THE "X" ARRAY IS NOT BIG ENOUGH THEN STOP.
    IF (ISUM-1.GT.LENX) STOP

C
C6-----READ AND PREPARE INFORMATION FOR ENTIRE SIMULATION.
    CALL BASIRP(X(LCIBOU), X(LCHNEW), X(LCSTRT), X(LCHOLD),
1      ISTRT, INBAS, HEADNG, NCOL, NROW, NLAY, NODES, VBVL, X(LCIOFL),
2      IUNIT(12), IHEDFM, IDDNFM, IHEDUN, IDDNUN, IOUT)
C ** electrokinetic information read here**
    IF (IUNIT(1).GT.0) CALL BCFIRP(X(LCIBOU), X(LCHNEW), X(LCSC1),
1      X(LCHY), X(LCCR), X(LCCC), X(LCCV), X(LCDELRL),
2      X(LCDELCL), X(LCBOT), X(LCTOP), X(LCSC2), X(LCTRPY),
3      IUNIT(1), ISS, NCOL, NROW, NLAY, NODES, IOUT,
4      X(lecond), X(ltheta), X(lthetas), X(lthetao),
5      X(lexpn), X(ekmob), X(alance), X(eqcond), X(LTHK), X(ecsoil),
6      X(LFY), AIS, BIS)
    IF (IUNIT(9).GT.0) CALL SIPIRP(NPARM, MXITER, ACCL, HCLOSE, X(LCW),
1      IUNIT(9), IPCALC, IPRSIP, IOUT)
    IF (IUNIT(11).GT.0) CALL SORIRP(MXITER, ACCL, HCLOSE, IUNIT(11),
1      IPRSOR, IOUT)
    IF (IUNIT(13).GT.0) CALL PCGIRP(MXITER, HCLOSE, RESERR, X(LCNUI),
1      IUNIT(13), IOUT, IWRT)

C
C--OPEN UNFORMATTED FILES
    IF (IHEDUN.GT.0) THEN
        FLNAME='Unformatted Head File: '
        ITMP=IHEDUN
        CALL UOPFIL(ITMP,0,FLNAME)
    ENDIF
    IF (IDDNUN.GT.0) THEN
        FLNAME='Unformatted Drawdown File: '
        ITMP=IDDNUN
        CALL UOPFIL(ITMP,0,FLNAME)
    ENDIF
    IF (IBCFCB.GT.0) THEN
        FLNAME='Unformatted Flow File: '
        ITMP=IBCFCB
        CALL UOPFIL(ITMP,0,FLNAME)
    ENDIF
    IF (IUNIT(22).GT.0) THEN
        FLNAME='Unformatted [MT3D] File: '
        ITMP=IUNIT(22)
        CALL UOPFIL(ITMP,0,FLNAME)
    ENDIF

C
C7-----SIMULATE EACH STRESS PERIOD.
    DO 300 KPER=1, NPER
        KKPER=KPER
        WRITE(*,*) 'STRESS PERIOD NO.', KKPER

C
C7A-----READ STRESS PERIOD TIMING INFORMATION.
        CALL BASIST(NSTP, DELT, TSMULT, PERTIM, KKPER, INBAS, IOUT)

C
C7B-----READ AND PREPARE INFORMATION FOR STRESS PERIOD.
        IF (IUNIT(2).GT.0) CALL WELIRP(X(LCWELL), NWELLS, MXWELL, IUNIT(2),
1      IOUT)
        IF (IUNIT(3).GT.0) CALL DRNIRP(X(LCDRAI), NDRAIN, MXDRN, IUNIT(3),
1      IOUT)
        IF (IUNIT(8).GT.0) CALL RCHIRP(NRCHOP, X(LCIRCH), X(LCRECH),
1      X(LCDELRL), X(LCDELCL), NROW, NCOL, IUNIT(8), IOUT)

```

A-4
MAIN.FOR Modifications

```

IF (IUNIT(5).GT.0) CALL EVT1RP (NEVTOP,X (LCIEVT), X (LCEVTR),
1 X (LCEXDP), X (LCSURF), X (LCDELR), X (LCDELC), NCOL, NROW,
1 IUNIT(5), IOUT)
IF (IUNIT(4).GT.0) CALL RIV1RP (X (LCRIVR), NRIVER, MXRIVR, IUNIT(4),
1 IOUT)
IF (IUNIT(14).GT.0) CALL STR1RP (X (LCSTRM), X (ICSTRM), NSTREM,
1 MXSTRM, IUNIT(14), IOUT, X (LCTBAR), NDIV, NSS,
1 NTRIB, X (LCIVAR), ICALC, IPTFLG)
IF (IUNIT(7).GT.0) CALL GH11RP (X (LCBND), NBOUND, MXBND, IUNIT(7),
1 IOUT)
C
C7C-----SIMULATE EACH TIME STEP.
DO 200 KSTP=1, NSTP
KKSTP=KSTP
WRITE (*, *) 'TIME STEP NO.', KKSTP
C
C7C1----CALCULATE TIME STEP LENGTH. SET HOLD=HNEW..
CALL BAS1AD (DELT, TSMULT, TOTIM, PERTIM, X (LCHNEW), X (LCHOLD), KKSTP,
1 NCOL, NROW, NLAY)
C
C7C2----ITERATIVELY FORMULATE AND SOLVE THE EQUATIONS.
IFLAG=0
DO 100 KITER=1, MXITER
KKITER=KITER
C
C7C2A---FORMULATE THE FINITE DIFFERENCE EQUATIONS.
CALL BAS1FM (X (LCHCOF), X (LCRHS), NODES)
IF (IUNIT(1).GT.0) CALL BCF1FM (X (LCHCOF), X (LCRHS), X (LCHOLD),
1 X (LCSC1), X (LCHNEW), X (LCIBOU), X (LCCR), X (LCCC), X (LCCV),
2 X (LCHV), X (LCTRPY), X (LCBOT), X (LCTOP), X (LCSC2),
3 X (LCDELR), X (LCDELC), DELT, ISS, KKITER, KKSTP, KKPER, NCOL,
4 NROW, NLAY, IOUT)
IF (IUNIT(2).GT.0) CALL WEL1FM (NWELLS, MXWELL, X (LCRHS), X (LCWELL),
1 X (LCIBOU), NCOL, NROW, NLAY)
IF (IUNIT(3).GT.0) CALL DRN1FM (NDRAIN, MXDRN, X (LCDRAI), X (LCHNEW),
1 X (LCHCOF), X (LCRHS), X (LCIBOU), NCOL, NROW, NLAY)
IF (IUNIT(8).GT.0) CALL RCH1FM (NRCHOP, X (LCIRCH), X (LCRECH),
1 X (LCRHS), X (LCIBOU), NCOL, NROW, NLAY)
IF (IUNIT(5).GT.0) CALL EVT1FM (NEVTOP, X (LCIEVT), X (LCEVTR),
1 X (LCEXDP), X (LCSURF), X (LCRHS), X (LCHCOF), X (LCIBOU),
1 X (LCHNEW), NCOL, NROW, NLAY)
IF (IUNIT(4).GT.0) CALL RIV1FM (NRIVER, MXRIVR, X (LCRIVR), X (LCHNEW),
1 X (LCHCOF), X (LCRHS), X (LCIBOU), NCOL, NROW, NLAY)
IF (IUNIT(14).GT.0) CALL STR1FM (NSTREM, X (LCSTRM), X (ICSTRM),
1 X (LCHNEW), X (LCHCOF), X (LCRHS), X (LCIBOU),
2 MXSTRM, NCOL, NROW, NLAY, IOUT, NSS, X (LCTBAR),
3 NTRIB, X (LCTTRIB), X (LCIVAR), X (LCFGAR), ICALC, CONST)
IF (IUNIT(7).GT.0) CALL GH11FM (NBOUND, MXBND, X (LCBND), X (LCHCOF),
1 X (LCRHS), X (LCIBOU), NCOL, NROW, NLAY)
C
C7C2B---MAKE ONE CUT AT AN APPROXIMATE SOLUTION.
IF (IUNIT(9).GT.0) CALL SIP1AP (X (LCHNEW), X (LCIBOU), X (LCCR), X (LCCC),
1 X (LCCV), X (LCHCOF), X (LCRHS), X (LCEL), X (LCFL), X (LCGL), X (LCV),
2 X (LCW), X (LCHDCG), X (LCLRCH), NPARM, KKITER, HCLOSE, ACCL, ICNVG,
3 KKSTP, KKPER, IPCALC, IPRSTP, MXITER, NSTP, NCOL, NROW, NLAY, NODES,
4 IOUT)
IF (IUNIT(11).GT.0) CALL SOR1AP (X (LCHNEW), X (LCIBOU), X (LCCR),
1 X (LCCC), X (LCCV), X (LCHCOF), X (LCRHS), X (LCA), X (LCRES), X (LCIEQP),
2 X (LCHDCG), X (LCLRCH), KKITER, HCLOSE, ACCL, ICNVG, KKSTP, KKPER,
3 IPRSOR, MXITER, NSTP, NCOL, NROW, NLAY, NSLICE, MBW, IOUT)
IF (IUNIT(13).GT.0) CALL PCG1AP (X (LCHNEW), X (LCIBOU), X (LCCR),
1 X (LCCC), X (LCCV), X (LCHCOF), X (LCRHS), X (LCXXV), X (LCXXS),
2 X (LCDT), X (LCE2), X (LCF2), X (LGG2), X (LCVV), X (LCD22), X (LCD2S),
3 X (LCNU1), NPCOND, ITYP, KITER, HCLOSE, RESERR, ICNVG, MXITER,
4 NCOL, NROW, NLAY, IOUT, IWRT, NODES, NOD, KSTP, KPER, MCNT, KSTPS, KPERS,
5 IFLAG)
C
C7C2C---IF CONVERGENCE CRITERION HAS BEEN MET STOP ITERATING.
IF (IFLAG.EQ.1) GO TO 110
IF (ICNVG.EQ.1) GO TO 110
100 CONTINUE
KITER=MXITER
110 CONTINUE
C
C7C3----DETERMINE WHICH OUTPUT IS NEEDED.
CALL BAS1OC (NSTP, KKSTP, ICNVG, X (LCIOFL), NLAY,
1 IBUDFL, ICBCFL, IHDDFL, IUNIT(12), IOUT)
C
C7C4----CALCULATE BUDGET TERMS. SAVE CELL-BY-CELL FLOW TERMS.
MSUM=1
IF (IUNIT(1).GT.0) CALL BCF1BD (VBNM, VBVL, MSUM, X (LCHNEW),
1 X (LCIBOU), X (LCHOLD), X (LCSC1), X (LCCR), X (LCCC), X (LCCV),
2 X (LCTOP), X (LCSC2), DELT, ISS, NCOL, NROW, NLAY, KKSTP, KKPER,
3 IBCFCB, ICBCFL, X (LCBUFF), IOUT)
IF (IUNIT(2).GT.0) CALL WEL1BD (NWELLS, MXWELL, VBNM, VBVL, MSUM,
1 X (LCWELL), X (LCIBOU), DELT, NCOL, NROW, NLAY, KKSTP, KKPER, IWELCB,
1 ICBCFL, X (LCBUFF), IOUT)
IF (IUNIT(3).GT.0) CALL DRN1BD (NDRAIN, MXDRN, VBNM, VBVL, MSUM,
1 X (LCDRAI), DELT, X (LCHNEW), NCOL, NROW, NLAY, X (LCIBOU), KKSTP,
2 KKPER, IDRNCB, ICBCFL, X (LCBUFF), IOUT)
IF (IUNIT(8).GT.0) CALL RCH1BD (NRCHOP, X (LCIRCH), X (LCRECH),
1 X (LCIBOU), NROW, NCOL, NLAY, DELT, VBVL, VBNM, MSUM, KKSTP, KKPER,
2 IRCHCB, ICBCFL, X (LCBUFF), IOUT)
IF (IUNIT(5).GT.0) CALL EVT1BD (NEVTOP, X (LCIEVT), X (LCEVTR),
1 X (LCEXDP), X (LCSURF), X (LCIBOU), X (LCHNEW), NCOL, NROW, NLAY,

```

A-5
MAIN.FOR Modifications

```
2   DELT,VBVL,VBNM,MSUM,KKSTP,KKPER,IEVTGB,ICBCEL,X(LCBUFF),IOUT)
  IF(IUNIT(4).GT.0) CALL RIVIBD(NRIVER,MXRIVR,X(LCRIVR),X(LCIBOU),
1   X(LCHNEW),NCOL,NROW,NLAY,DELT,VBVL,VBNM,MSUM,
2   KKSTP,KKPER,IRIVCB,ICBCEL,X(LCBUFF),IOUT)
  IF(IUNIT(14).GT.0) CALL STRIBD(NSTREM,X(LCSTRM),X(ICSTRM),
1   X(LCIBOU),MXSTRM,X(LCHNEW),NCOL,NROW,NLAY,DELT,VBVL,VBNM,MSUM,
2   KKSTP,KKPER,ISTCB1,ISTCB2,ICBCEL,X(LCBUFF),IOUT,NTRIB,NSS,
3   X(LCTRIB),X(LCTBAR),X(LCIVAR),X(LCFGAR),ICALC,CONST,IPTFLG)
  IF(IUNIT(7).GT.0) CALL GHB1BD(NBOUND,MXBND,VBNM,VBVL,MSUM,
1   X(LCBNDS),DELT,X(LCHNEW),NCOL,NROW,NLAY,X(LCIBOU),KKSTP,
2   KKPER,IGHBCB,ICBCEL,X(LCBUFF),IOUT)
C
C-----SAVE CELL-BY-CELL FLOW TERMS FOR USE IN MT3D
  INCLUDE 'LKMT.INC'
C
C7C5---PRINT AND OR SAVE HEADS AND DRAWDOWNS. PRINT OVERALL BUDGET.
  CALL BAS1OT(X(LCHNEW),X(LCSTRT),ISTRM,X(LCBUFF),X(LCIOFL),
1   MSUM,X(LCIBOU),VBNM,VBVL,KKSTP,KKPER,DELT,
2   PERTIM,TOTIM,ITMUNI,NCOL,NROW,NLAY,ICNVG,
3   IHDDFL,IBUDFL,IHEDFM,IHEDUN,IDDNFM,IDDNUN,IOUT)
C
C7C6---IF ITERATION FAILED TO CONVERGE THEN STOP.
  IF(ICNVG.EQ.0) STOP
  200 CONTINUE
  300 CONTINUE
C
C8-----END PROGRAM
  STOP
C
  END
```

A-6
BAS1.FOR Modifications

```

C      Last change: E      11 Jul 98      4:47 pm
SUBROUTINE BAS1DF (ISUM, HEADNG, NPER, ITMUNI, TOTIM, NCOL, NROW,
1      NLAY, NODES, INBAS, IOUT, IUNIT)

C
C-----VERSION 1513 12MAY1987 BAS1DF
C      *****
C      DEFINE KEY MODEL PARAMETERS
C      *****
C
C      SPECIFICATIONS:
C      -----
C      CHARACTER*4 HEADNG
C      DIMENSION HEADNG(32), IUNIT(24)
C      -----
C
C1-----PRINT THE NAME OF THE PROGRAM.
      WRITE(IOUT,1)
      1 FORMAT(1H1,20X,'U.S. GEOLOGICAL SURVEY MODULAR',
1          ' FINITE-DIFFERENCE GROUND-WATER MODEL')
C
C2-----READ AND PRINT A HEADING.
      READ(INBAS,2) HEADNG
      2 FORMAT(20A4)
      WRITE(IOUT,3) HEADNG
      3 FORMAT(1H0,32A4)
C
C3-----READ NUMBER OF LAYERS, ROWS, COLUMNS, STRESS PERIODS AND
C3-----UNITS OF TIME CODE.
      READ(INBAS,4) NLAY, NROW, NCOL, NPER, ITMUNI
      4 FORMAT(8I10)
C
C4-----PRINT # OF LAYERS, ROWS, COLUMNS AND STRESS PERIODS.
      WRITE(IOUT,5) NLAY, NROW, NCOL
      5 FORMAT(1X, I4, ' LAYERS', I10, ' ROWS', I10, ' COLUMNS')
      WRITE(IOUT,6) NPER
      6 FORMAT(1X, I3, ' STRESS PERIOD(S) IN SIMULATION')
C
C5-----SELECT AND PRINT A MESSAGE SHOWING TIME UNITS.
      IF(ITMUNI.LT.0 .OR. ITMUNI.GT.5) ITMUNI=0
      GO TO (10,20,30,40,50), ITMUNI
      WRITE(IOUT,9)
      9 FORMAT(1X, 'MODEL TIME UNITS ARE UNDEFINED')
      GO TO 100
      10 WRITE(IOUT,11)
      11 FORMAT(1X, 'MODEL TIME UNIT IS SECONDS')
      GO TO 100
      20 WRITE(IOUT,21)
      21 FORMAT(1X, 'MODEL TIME UNIT IS MINUTES')
      GO TO 100
      30 WRITE(IOUT,31)
      31 FORMAT(1X, 'MODEL TIME UNIT IS HOURS')
      GO TO 100
      40 WRITE(IOUT,41)
      41 FORMAT(1X, 'MODEL TIME UNIT IS DAYS')
      GO TO 100
      50 WRITE(IOUT,51)
      51 FORMAT(1X, 'MODEL TIME UNIT IS YEARS')
C
C6-----READ & PRINT INPUT UNIT NUMBERS (IUNIT) FOR MAJOR OPTIONS.
      100 READ(INBAS,101) IUNIT
      101 FORMAT(24I3)
      WRITE(IOUT,102) (I,I=1,24), IUNIT
      102 FORMAT(1H0, 'I/O UNITS: '/1X, 'ELEMENT OF IUNIT:', 24I3,
1          '/1X, ' I/O UNIT:', 24I3)
C
C7-----INITIALIZE TOAL ELAPSED TIME COUNTER STORAGE ARRAY COUNTER
C7-----AND CALCULATE NUMBER OF CELLS.
      TOTIM=0.
      ISUM=1
      NODES=NCOL*NROW*NLAY
C
C8-----RETURN
      RETURN
      END
      SUBROUTINE BAS1AL (ISUM, LENX, LCHNEW, LCHOLD, LCIBOU, LCCR, LCCC, LCCV,
1          LCHCOF, LCRHS, LCDELRL, LCDELCL, LCSTRT, LCBUFF, LCIOFL, INBAS,
1          ISTRT, NCOL, NROW, NLAY, IOUT, lecond, ltheta, lthetaa,
1          lthetao, lexpn, lthk, LFY)
C-----VERSION 1515 12MAY1987 BAS1AL
C      *****
C      ALLOCATE SPACE FOR BASIC MODEL ARRAYS
C      *****
C
C      SPECIFICATIONS:
C      -----
C
C1-----PRINT A MESSAGE IDENTIFYING THE PACKAGE.
      WRITE(IOUT,1) INBAS
      1 FORMAT(1H0, 'BAS1 -- BASIC MODEL PACKAGE, VERSION 1, 9/1/87',
2          ' INPUT READ FROM UNIT', I3)
C
C2-----READ & PRINT FLAG IAPART (RHS & BUFFER SHARE SPACE?) AND
C2-----FLAG ISTRT (SHOULD STARTING HEADS BE SAVED FOR DRAWDOWN?)
      READ(INBAS,2) IAPART, ISTRT

```

A-7
BAS1.FOR Modifications

```

2 FORMAT(2I10)
IF (IAPART.EQ.0) WRITE(IOUT,3)
3 FORMAT(1X,'ARRAYS RHS AND BUFF WILL SHARE MEMORY.')
IF (ISTRN.NE.0) WRITE(IOUT,4)
4 FORMAT(1X,'START HEAD WILL BE SAVED')
IF (ISTRN.EQ.0) WRITE(IOUT,5)
5 FORMAT(1X,'START HEAD WILL NOT BE SAVED',
1 ' -- DRAWDOWN CANNOT BE CALCULATED')
C
C3-----STORE, IN ISOLD, LOCATION OF FIRST UNALLOCATED SPACE IN X.
ISOLD=ISUM
NRCL=NROW*NCOL*NLAY
C
C4-----ALLOCATE SPACE FOR ARRAYS.
LCHNEW=ISUM
ISUM=ISUM+2*NRCL
LCHOLD=ISUM
ISUM=ISUM+NRCL
LCIBOU=ISUM
ISUM=ISUM+NRCL
LCCR=ISUM
ISUM=ISUM+NRCL
LCCC=ISUM
ISUM=ISUM+NRCL
LCCV=ISUM
ISUM=ISUM+NROW*NCOL*(NLAY-1)
LCHCOF=ISUM
ISUM=ISUM+NRCL
LCRHS=ISUM
ISUM=ISUM+NRCL
LCDELR=ISUM
ISUM=ISUM+NCOL
LCDELC=ISUM
ISUM=ISUM+NROW
LCIOFL=ISUM
ISUM=ISUM+NLAY*4
C6 **added electrokinetic additional terms**
.....ISUM=ISUM+NRCL
.....lexpn=ISUM
.....ISUM=ISUM+NRCL
.....ltheta=ISUM
.....ISUM=ISUM+NRCL
.....ltheta=ISUM
.....ISUM=ISUM+NRCL
.....ltheta=ISUM
.....ISUM=ISUM+NRCL
.....lexpn=ISUM
.....ISUM=ISUM+NRCL
.....lthk=ISUM
.....ISUM=ISUM+NRCL
.....LFY=ISUM
.....ISUM=ISUM+NRCL
C **end of added terms**
C
C5-----IF BUFFER AND RHS SHARE SPACE THEN LCBUFF=LCRHS.
LCBUFF=LCRHS
IF (IAPART.EQ.0) GO TO 50
LCBUFF=ISUM
ISUM=ISUM+NRCL
C
C6-----IF STRT WILL BE SAVED THEN ALLOCATE SPACE.
50 LCSTRT=ISUM
IF (ISTRN.NE.0) ISUM=ISUM+NRCL
ISP=ISUM-ISOLD
C
C7-----PRINT AMOUNT OF SPACE USED.
WRITE(IOUT,6) ISP
6 FORMAT(1X,I8,' ELEMENTS IN X ARRAY ARE USED BY BAS')
ISUM1=ISUM-1
WRITE(IOUT,7) ISUM1,LENX
7 FORMAT(1X,I8,' ELEMENTS OF X ARRAY USED OUT OF',I8)
IF (ISUM1.GT.LENX) WRITE(IOUT,8)
8 FORMAT(1X,' ***X ARRAY MUST BE DIMENSIONED LARGER***')
C
C
C8-----RETURN
RETURN
C
END
SUBROUTINE BAS1AD(DELTA,TSMULT,TOTIM,PERTIM,HNEW,HOLD,KSTP,
1 NCOL,NROW,NLAY)
C
C-----VERSION 1412 22FEB1982 BAS1AD
C
C *****
C ADVANCE TO NEXT TIME STEP
C *****
C
C SPECIFICATIONS:
C -----
C DOUBLE PRECISION HNEW
C
C DIMENSION HNEW(NCOL,NROW,NLAY), HOLD(NCOL,NROW,NLAY)
C -----
C

```

A-8
BAS1.FOR Modifications

```

C1-----IF NOT FIRST TIME STEP THEN CALCULATE TIME STEP LENGTH.
      IF (KSTP.NE.1) DELT=TSMULT*DELT
C
C2-----ACCUMULATE ELAPSED TIME IN SIMULATION(TOTIM) AND IN THIS
C2-----STRESS PERIOD(PERTIM).
      TOTIM=TOTIM+DELT
      PERTIM=PERTIM+DELT
C
C3-----COPY HNEW TO HOLD.
      DO 10 K=1,NLAY
      DO 10 I=1,NROW
      DO 10 J=1,NCOL
      10 HOLD(J,I,K)=HNEW(J,I,K)
C
C4-----RETURN
      RETURN
      END
      SUBROUTINE BAS1FM(HCOF,RHS,NODES)
C
C
C-----VERSION 1632 24JUL1987 BAS1FM
C *****
C      SET HCOF=RHS=0.
C *****
C
C      SPECIFICATIONS:
C -----
C      DIMENSION HCOF(NODES),RHS(NODES)
C -----
C
C1-----FOR EACH CELL INITIALIZE HCOF AND RHS ACCUMULATORS.
      DO 100 I=1,NODES
      HCOF(I)=0.
      RHS(I)=0.
      100 CONTINUE
C
C2-----RETURN
      RETURN
      END
      SUBROUTINE BAS1OC(NSTP,KSTP,ICNVG,IOFLG,NLAY,
      1      IBUDFL,ICBCFL,IHDDFL,INOC,IOUT)
C
C-----VERSION 1632 24JUL1987 BAS1OC
C *****
C      OUTPUT CONTROLLER FOR HEAD, DRAWDOWN, AND BUDGET
C *****
C
C      SPECIFICATIONS:
C -----
C      DIMENSION IOFLG(NLAY,4)
C -----
C
C1-----TEST UNIT NUMBER (INOC (INOC=IUNIT(12))) TO SEE IF
C1-----OUTPUT CONTROL IS ACTIVE.
      IF (INOC.NE.0) GO TO 500
C
C2-----IF OUTPUT CONTROL IS INACTIVE THEN SET DEFAULTS AND RETURN.
      IHDDFL=0
      IF (ICNVG.EQ.0 .OR. KSTP.EQ.NSTP) IHDDFL=1
      IBUDFL=0
      IF (ICNVG.EQ.0 .OR. KSTP.EQ.NSTP) IBUDFL=1
      ICBCFL=0
      GO TO 1000
C
C3-----READ AND PRINT OUTPUT FLAGS AND CODE FOR DEFINING IOFLG.
      500 READ(INOC,1) INCODE,IHDDFL,IBUDFL,ICBCFL
      1  FORMAT(4I10)
      WRITE(IOUT,3) IHDDFL,IBUDFL,ICBCFL
      3  FORMAT(1H0,'HEAD/DRAWDOWN PRINTOUT FLAG =',I2,
      1    5X,'TOTAL BUDGET PRINTOUT FLAG =',I2,
      2    5X,'CELL-BY-CELL FLOW TERM FLAG =',I2)
C
C4-----DECODE INCODE TO DETERMINE HOW TO SET FLAGS IN IOFLG.
      IF (INCODE) 100,200,300
C
C5-----USE IOFLG FROM LAST TIME STEP.
      100 WRITE(IOUT,101)
      101 FORMAT(1H , 'REUSING PREVIOUS VALUES OF IOFLG')
      GO TO 600
C
C6-----READ IOFLG FOR LAYER 1 AND ASSIGN SAME TO ALL LAYERS
      200 READ(INOC,201) (IOFLG(1,M),M=1,4)
      201 FORMAT(4I10)
      DO 210 K=1,NLAY
      IOFLG(K,1)=IOFLG(1,1)
      IOFLG(K,2)=IOFLG(1,2)
      IOFLG(K,3)=IOFLG(1,3)
      IOFLG(K,4)=IOFLG(1,4)
      210 CONTINUE
      WRITE(IOUT,211) (IOFLG(1,M),M=1,4)
      211 FORMAT(1H0,'OUTPUT FLAGS FOR ALL LAYERS ARE THE SAME: '/
      1  1X,' HEAD DRAWDOWN HEAD DRAWDOWN'/
      2  1X,'PRINTOUT PRINTOUT SAVE SAVE'/
      3  1X,34('-')/1X,15,I10,I8,I8)

```

A-9
BAS1.FOR Modifications

```

GO TO 600
C
C7-----READ IOFIG IN ENTIRETY
300 READ(INOC,301) ((IOFLG(K,I),I=1,4),K=1,NLAY)
301 FORMAT(4I10)
WRITE(IOUT,302)
302 FORMAT(1H0,'OUTPUT FLAGS FOR EACH LAYER: '/
1 1X,' HEAD DRAWDOWN HEAD DRAWDOWN'/
2 1X,'LAYER PRINTOUT PRINTOUT SAVE SAVE'/
3 1X,41('-'))
WRITE(IOUT,303) (K, (IOFLG(K,I),I=1,4),K=1,NLAY)
303 FORMAT(1X,I4,I8,I10,I8,I8)
C
C8-----THE LAST STEP IN A STRESS PERIOD AND STEPS WHERE ITERATIVE
C8-----PROCEDURE FAILED TO CONVERGE GET A VOLUMETRIC BUDGET.
600 IF(ICNVG.EQ.0 .OR. KSTP.EQ.NSTP) IBUDFL=1
C
C9-----RETURN
1000 RETURN
END
SUBROUTINE BAS1OT(HNEW,STRT,ISTR,IBUFF,IOFLG,MSUM,IBOUND,VBNM,
1 VBVL,KSTP,KPER,DELT,PERTIM,TOTIM,ITMUNI,NCOL,NROW,NLAY,ICNVG,
2 IHDDFL,IBUDFL,IHEDFM,IHEDUN,IDDNFM,IDDNUN,IOUT)
C-----VERSION 1522 12MAY1987 BAS1OT
C *****
C OUTPUT TIME, VOLUMETRIC BUDGET, HEAD, AND DRAWDOWN
C *****
C
C SPECIFICATIONS:
C-----
C CHARACTER*4 VBNM
DOUBLE PRECISION HNEW
C
C DIMENSION HNEW(NCOL,NROW,NLAY),STRT(NCOL,NROW,NLAY),
1 VBVM(4,20),VBVL(4,20),IOFLG(NLAY,4),
2 IBOUND(NCOL,NROW,NLAY),IBUFF(NCOL,NROW,NLAY)
C-----
C
C1-----CLEAR PRINTOUT FLAG (IPFLG)
IPFLG=0
C
C2-----IF ITERATIVE PROCEDURE FAILED TO CONVERGE PRINT MESSAGE
IF(ICNVG.EQ.0) WRITE(IOUT,1) KSTP,KPER
1 FORMAT(1H0,10X,'****FAILED TO CONVERGE IN TIME STEP',I3,
1 ' OF STRESS PERIOD',I3,'****')
C
C3-----IF HEAD AND DRAWDOWN FLAG (IHDDFL) IS SET WRITE HEAD AND
C3-----DRAWDOWN IN ACCORDANCE WITH FLAGS IN IOFLG.
IF(IHDDFL.EQ.0) GO TO 100
C
CALL SBAS1H(HNEW,IBUFF,IOFLG,KSTP,KPER,NCOL,NROW,
1 NLAY,IOUT,IHEDFM,IHEDUN,IPFLG,PERTIM,TOTIM)
CALL SBAS1D(HNEW,IBUFF,IOFLG,KSTP,KPER,NCOL,NROW,NLAY,IOUT,
1 IDDNFM,IDDNUN,STRT,ISTR,IBOUND,IPFLG,PERTIM,TOTIM)
C
C4-----PRINT TOTAL BUDGET IF REQUESTED
100 IF(IBUDFL.EQ.0) GO TO 120
CALL SBAS1V(MSUM,VBVM,VBVL,KSTP,KPER,IOUT)
IPFLG=1
C
C5-----END PRINTOUT WITH TIME SUMMARY AND FORM FEED IF ANY PRINTOUT
C5-----WILL BE PRODUCED.
120 IF(IPFLG.EQ.0) RETURN
CALL SBAS1T(KSTP,KPER,DELT,PERTIM,TOTIM,ITMUNI,IOUT)
WRITE(IOUT,101)
101 FORMAT(1H1)
C
C6-----RETURN
RETURN
END
SUBROUTINE BAS1RP(BOUND,HNEW,STRT,HOLD,ISTR,INBAS,
1 HEADNG,NCOL,NROW,NLAY,NODES,VBVL,IOFLG,INOC,IHEDFM,
2 IDDNFM,IHEDUN,IDDNUN,IOUT)
C-----VERSION 1628 15MAY1987 BAS1RP
C *****
C READ AND INITIALIZE BASIC MODEL ARRAYS
C *****
C
C SPECIFICATIONS:
C-----
C CHARACTER*4 HEADNG,ANAME
DOUBLE PRECISION HNEW,HNOFLO
C
C DIMENSION HNEW(NODES),IBOUND(NODES),STRT(NODES),HOLD(NODES),
1 ANAME(6,2),VBVL(4,20),IOFLG(NLAY,4),HEADNG(32)
C
DATA ANAME(1,1),ANAME(2,1),ANAME(3,1),ANAME(4,1),ANAME(5,1),
1 ANAME(6,1) / ' ',' ',' ',' ' BO','UNDA','RY A','RRAY'/
DATA ANAME(1,2),ANAME(2,2),ANAME(3,2),ANAME(4,2),ANAME(5,2),
1 ANAME(6,2) / ' ',' ',' ',' ' INIT','IAL','HEAD'/
C-----
C
C1-----PRINT SIMULATION TITLE, CALCULATE # OF CELLS IN A LAYER.
WRITE(IOUT,1) HEADNG
1 FORMAT(1H1,32A4)

```


A-10 BAS1.FOR Modifications

```

NCR=NCOL*NROW
C
C2-----READ BOUNDARY ARRAY(IBOUND) ONE LAYER AT A TIME.
      DO 100 K=1,NLAY
      KK=K
      LOC=1+(K-1)*NCR
      CALL U2DINT(IBOUND(LOC),ANAME(1,1),NROW,NCOL,KK,INBAS,IOUT)
100 CONTINUE
C
C3-----READ AND PRINT HEAD VALUE TO BE PRINTED FOR NO-FLOW CELLS.
      READ(INBAS,2) TMP
      2 FORMAT(F10.0)
      HNOFLO=TMP
      WRITE(IOUT,3) TMP
      3 FORMAT(1H0,'AQUIFER HEAD WILL BE SET TO ',1PG11.5,
      1      ' AT ALL NO-FLOW NODES (IBOUND=0).')
C
C4-----READ STARTING HEADS.
      DO 300 K=1,NLAY
      KK=K
      LOC=1+(K-1)*NCR
      CALL U2DREL(HOLD(LOC),ANAME(1,2),NROW,NCOL,KK,INBAS,IOUT)
300 CONTINUE
CZ...
C5-----SET IBOUND=0 IF HOLD IS 1.E30 OR 888.88
      DO 350 I=1,NODES
      IF (IBOUND(I).EQ.0) GOTO 350
      IF (HOLD(I).EQ.1.E30.OR.HOLD(I).EQ.888.88) IBOUND(I)=0
350 CONTINUE
CZ...
C5-----COPY INITIAL HEADS FROM HOLD TO HNEW.
      DO 400 I=1,NODES
      HNEW(I)=HOLD(I)
      IF (IBOUND(I).EQ.0) HNEW(I)=HNOFLO
400 CONTINUE
C
C6-----IF STARTING HEADS ARE TO BE SAVED THEN COPY HOLD TO STRT.
      IF (ISTRT.EQ.0) GO TO 590
      DO 500 I=1,NODES
      STRT(I)=HOLD(I)
500 CONTINUE
C
C7-----INITIALIZE VOLUMETRIC BUDGET ACCUMULATORS TO ZERO.
      590 DO 600 I=1,20
      DO 600 J=1,4
      VBVL(J,I)=0.
600 CONTINUE
C
C8-----SET UP OUTPUT CONTROL.
      CALL SBAS1I(NLAY,ISTRT,IOFLG,INOC,IOUT,IHEDFM,
      1      IDDNFM,IHEDUN,IDDNUM)
C
C9-----RETURN
1000 RETURN
      END
      SUBROUTINE BAS1ST(NSTP,DELT,TSMULT,PERTIM,KPER,INBAS,IOUT)
C
C
C-----VERSION 1614 08SEP1982 BAS1ST
C.....
C      SETUP TIME PARAMETERS FOR NEW TIME PERIOD
C.....
C
C      SPECIFICATIONS:
C-----
C
C1-----READ LENGTH OF STRESS PERIOD, NUMBER OF TIME STEPS AND.
C1-----TIME STEP MULTIPLIER.
      READ (INBAS,1) PERLEN,NSTP,TSMULT
      1 FORMAT(F10.0,I10,F10.0)
C
C2-----CALCULATE THE LENGTH OF THE FIRST TIME STEP.
C
C2A-----ASSUME TIME STEP MULTIPLIER IS EQUAL TO ONE.
      DELT=PERLEN/FLOAT(NSTP)
C
C2B-----IF TIME STEP MULTIPLIER IS NOT ONE THEN CALCULATE FIRST
C2B-----TERM OF GEOMETRIC PROGRESSION.
      IF(TSMULT.NE.1.) DELT=PERLEN*(1.-TSMULT)/(1.-TSMULT**NSTP)
C
C3-----PRINT TIMING INFORMATION.
      WRITE (IOUT,2) KPER,PERLEN,NSTP,TSMULT,DELT
      2 FORMAT(1H1,51X,'STRESS PERIOD NO.',I4,', LENGTH =',G15.7/52X
      1,46('-')//52X,'NUMBER OF TIME STEPS =',I6
      2//53X,'MULTIPLIER FOR DELT =',F10.3
      3//50X,'INITIAL TIME STEP SIZE =',G15.7)
C
C4-----INITIALIZE PERTIM (ELAPSED TIME WITHIN STRESS PERIOD).
      PERTIM=0.
C
C5-----RETURN
      RETURN
      END
      SUBROUTINE SBAS1D(HNEW,BUFF,IOFLG,KSTP,KPER,NCOL,NROW,

```

A-11
BAS1.FOR Modifications

```

1  NLAY, IOUT, IDDNFM, IDDNUN, STRT, ISTRT, IBOUND, IPFLG,
2  PERTIM, TOTIM)
C-----VERSION 1630 15MAY1987 SBAS1D
C *****
C  CALCULATE PRINT AND RECORD DRAWDOWNS
C *****
C
C  SPECIFICATIONS
C -----
C  CHARACTER*4 TEXT
C  DOUBLE PRECISION HNEW
C
C  DIMENSION HNEW(NCOL, NROW, NLAY), IOFLG(NLAY, 4), TEXT(4),
1  BUFF(NCOL, NROW, NLAY), STRT(NCOL, NROW, NLAY),
2  IBOUND(NCOL, NROW, NLAY)
C
C  DATA TEXT(1), TEXT(2), TEXT(3), TEXT(4) / ' ', ' ', ' ', 'DRAW',
1  'DOWN'/
C -----
C
C1-----FOR EACH LAYER CALCULATE DRAWDOWN IF PRINT OR RECORD
C1-----IS REQUESTED
C  DO 59 K=1, NLAY
C
C2-----IS DRAWDOWN NEEDED FRO THIS LAYER?
C  IF (IOFLG(K, 2).EQ.0 .AND. IOFLG(K, 4).EQ.0) GO TO 59
C
C3-----DRAWDOWN IS NEEDED. WERE STARTING HEADS SAVED?
C  IF (ISTRT.NE.0) GO TO 53
C
C4-----STARTING HEADS WERE NOT SAVED. PRINT MESSAGE AND STOP.
C  WRITE (IOUT, 52)
C  52 FORMAT (1H0, 'CANNOT CALCULATE DRAWDOWN BECAUSE START',
1  ' HEADS WERE NOT SAVED')
C  STOP
C
C5-----CALCULATE DRAWDOWN FOR THE LAYER.
C  53 DO 58 I=1, NROW
C  DO 58 J=1, NCOL
C  Hsing=HNEW(J, I, K)
C  BUFF(J, I, K)=Hsing
C  IF (IBOUND(J, I, K).NE.0) BUFF(J, I, K)=STRT(J, I, K)-Hsing
C  58 CONTINUE
C  59 CONTINUE
C
C6-----FOR EACH LAYER: DETERMINE IF DRAWDOWN SHOULD BE PRINTED.
C6-----IF SO THEN CALL ULAPRS OR ULAPRW TO PRINT DRAWDOWN.
C  DO 69 K=1, NLAY
C  KK=K
C  IF (IOFLG(K, 2).EQ.0) GO TO 69
C  IF (IDDNFM.LT.0) CALL ULAPRS (BUFF(1, 1, K), TEXT(1), KSTP, KPER,
1  NCOL, NROW, KK, -IDDNFM, IOUT)
C  IF (IDDNFM.GE.0) CALL ULAPRW (BUFF(1, 1, K), TEXT(1), KSTP, KPER,
1  NCOL, NROW, KK, IDDNFM, IOUT)
C  IPFLG=1
C  69 CONTINUE
C
C7-----FOR EACH LAYER: DETERMINE IF DRAWDOWN SHOULD BE RECORDED.
C7-----IF SO THEN CALL ULASAV TO RECORD DRAWDOWN.
C  IFIRST=1
C  IF (IDDNUN.LE.0) GO TO 80
C  DO 79 K=1, NLAY
C  KK=K
C  IF (IOFLG(K, 4).LE.0) GO TO 79
C  IF (IFIRST.EQ.1) WRITE (IOUT, 74) IDDNUN, KSTP, KPER
C  74 FORMAT (1H0, 'DRAWDOWN WILL BE SAVED ON UNIT', I3,
1  ' AT END OF TIME STEP', I3, ', STRESS PERIOD', I3)
C  IFIRST=0
C  CALL ULASAV (BUFF(1, 1, K), TEXT(1), KSTP, KPER, PERTIM, TOTIM, NCOL,
1  NROW, KK, IDDNUN)
C  79 CONTINUE
C
C8-----RETURN
C  80 RETURN
C  END
C  SUBROUTINE SBAS1H (HNEW, BUFF, IOFLG, KSTP, KPER, NCOL, NROW,
1  NLAY, IOUT, IHEDFM, IHEDUN, IPFLG, PERTIM, TOTIM)
C
C-----VERSION 1653 15MAY1987 SBAS1H
C *****
C  PRINT AND RECORD HEADS
C *****
C
C  SPECIFICATIONS
C -----
C  CHARACTER*4 TEXT
C  DOUBLE PRECISION HNEW
C
C  DIMENSION HNEW(NCOL, NROW, NLAY), IOFLG(NLAY, 4), TEXT(4),
1  BUFF(NCOL, NROW, NLAY)
C
C  DATA TEXT(1), TEXT(2), TEXT(3), TEXT(4) / ' ', ' ', ' ', ' ',
1  'HEAD'/
C -----
C

```

A-12
BAS1.FOR Modifications

```

C1-----FOR EACH LAYER: PRINT HEAD IF REQUESTED.
      DO 39 K=1,NLAY
      KK=K
C
C2-----TEST IOFLG TO SEE IF HEAD SHOULD BE PRINTED.
      IF (IOFLG(K,1).EQ.0) GO TO 39
      IOFLG=1
C
C3-----COPY HEADS FOR THIS LAYER INTO BUFFER.
      DO 32 I=1,NROW
      DO 32 J=1,NCOL
      BUFF(J,I,1)=HNEW(J,I,K)
      32 CONTINUE
C
C4-----CALL UTILITY MODULE TO PRINT CONTENTS OF BUFFER.
      IF (IHEDFM.LT.0) CALL ULAPRS(BUFF,TEXT(1),KSTP,KPER,NCOL,NROW,KK,
1      -IHEDFM,IOUT)
      IF (IHEDFM.GE.0) CALL ULAPRW(BUFF,TEXT(1),KSTP,KPER,NCOL,NROW,KK,
1      IHEDFM,IOUT)
      39 CONTINUE
C
C5-----IF UNIT FOR RECORDING HEADS <= 0: THEN RETURN.
      IF (IHEDUN.LE.0)GO TO 50
      IFIRST=1
C
C6-----FOR EACH LAYER: RECORD HEAD IF REQUESTED.
      DO 49 K=1,NLAY
      KK=K
C
C7-----CHECK IOFLG TO SEE IF HEAD FOR THIS LAYER SHOULD BE RECORDED.
      IF (IOFLG(K,3).LE.0) GO TO 49
      IF (IFIRST.EQ.1) WRITE(IOUT,41) IHEDUN,KSTP,KPER
      41 FORMAT(1H0,'HEAD WILL BE SAVED ON UNIT',I3,' AT END OF TIME STEP',
1      I3,', STRESS PERIOD',I3)
      IFIRST=0
C
C8-----COPY HEADS FOR THIS LAYER INTO BUFFER.
      DO 44 I=1,NROW
      DO 44 J=1,NCOL
      BUFF(J,I,1)=HNEW(J,I,K)
      44 CONTINUE
C
C9-----RECORD CONTENTS OF BUFFER ON UNIT=IHEDUN
      CALL ULASAV(BUFF,TEXT(1),KSTP,KPER,PERTIM,TOTIM,NCOL,NROW,KK,
1      IHEDUN)
      49 CONTINUE
C
C10-----RETURN
      50 RETURN
      END
      SUBROUTINE SBAS1I(NLAY,ISTR,IOFLG,INOC,IOUT,IHEDFM,
1      IDDNFM,IHEDUN,IDDNUM)
C
C-----VERSION 1531 12MAY1987 SBAS1I
C *****
C      SET UP OUTPUT CONTROL
C *****
C
C      SPECIFICATIONS:
C -----
C      DIMENSION IOFLG(NLAY,4)
C -----
C
C1-----TEST UNIT NUMBER FROM IUNIT (INOC) TO SEE IF OUTPUT
C1-----CONTROL IS ACTIVE.
      IF (INOC.LE.0) GO TO 600
C
C2-----READ AND PRINT FORMATS FOR PRINTING AND UNIT NUMBERS FOR
C2-----RECORDING HEADS AND DRAWDOWN. THEN RETURN.
      500 READ (INOC,1)IHEDFM,IDDNFM,IHEDUN,IDDNUM
      1 FORMAT (4I10)
      WRITE (IOUT,3)IHEDFM,IDDNFM
      3 FORMAT (1H0,'HEAD PRINT FORMAT IS FORMAT NUMBER',I4,
1      ' DRAWDOWN PRINT FORMAT IS FORMAT NUMBER',I4)
      WRITE (IOUT,4)IHEDUN,IDDNUM
      4 FORMAT (1H0,'HEADS WILL BE SAVED ON UNIT',I3,
1      ' DRAWDOWNS WILL BE SAVED ON UNIT',I3)
      WRITE(IOUT,561)
      561 FORMAT(1H0,'OUTPUT CONTROL IS SPECIFIED EVERY TIME STEP')
      GO TO 1000
C
C3-----OUTPUT CONTROL IS INACTIVE. PRINT A MESSAGE LISTING DEFAULTS.
      600 WRITE(IOUT,641)
      641 FORMAT(1H0,'DEFAULT OUTPUT CONTROL -- THE FOLLOWING OUTPUT',
1      ' COMES AT THE END OF EACH STRESS PERIOD:')
      WRITE(IOUT,642)
      642 FORMAT(1X,'TOTAL VOLUMETRIC BUDGET')
      WRITE(IOUT,643)
      643 FORMAT(1X,10X,'HEAD')
      IF (ISTR.NE.0)WRITE(IOUT,644)
      644 FORMAT(1X,10X,'DRAWDOWN')
C
C4-----SET THE FORMAT CODES EQUAL TO THE DEFAULT FORMAT.
      IHEDFM=0
      IDDNFM=0

```

A-13
BAS1.FOR Modifications

```

C
C5-----SET DEFAULT FLAGS IN IOFLG SO THAT HEAD (AND DRAWDOWN) IS
C5-----PRINTED FOR EVERY LAYER.
      ID=0
      IF (ISTRN.NE.0) ID=1
670 DO 680 K=1,NLAY
      IOFLG(K,1)=1
      IOFLG(K,2)=ID
      IOFLG(K,3)=0
      IOFLG(K,4)=0
680 CONTINUE
      GO TO 1000

C
C6-----RETURN
1000 RETURN
      END
      SUBROUTINE SBAS1T(KSTP,KPER,DELT,PERTIM,TOTIM,ITMUNI,IOUT)

C
C
C-----VERSION 0837 09APR1982 SBAS1T
C *****
C PRINT SIMULATION TIME
C *****
C
C SPECIFICATIONS:
C -----
C
      WRITE(IOUT,199) KSTP,KPER
199 FORMAT(1H0,///10X,'TIME SUMMARY AT END OF TIME STEP',I3,
1 ' IN STRESS PERIOD',I3)

C
C1-----USE TIME UNIT INDICATOR TO GET FACTOR TO CONVERT TO SECONDS.
      CNV=0.
      IF (ITMUNI.EQ.1) CNV=1.
      IF (ITMUNI.EQ.2) CNV=60.
      IF (ITMUNI.EQ.3) CNV=3600.
      IF (ITMUNI.EQ.4) CNV=86400.
      IF (ITMUNI.EQ.5) CNV=31557600.

C
C2-----IF FACTOR=0 THEN TIME UNITS ARE NON-STANDARD.
      IF (CNV.NE.0.) GO TO 100

C
C2A-----PRINT TIMES IN NON-STANDARD TIME UNITS.
      WRITE(IOUT,301) DELT,PERTIM,TOTIM
301 FORMAT(21X,' TIME STEP LENGTH =',G15.6/
1 21X,' STRESS PERIOD TIME =',G15.6/
2 21X,' TOTAL SIMULATION TIME =',G15.6)

C
C2B-----RETURN
      RETURN

C
C3-----CALCULATE LENGTH OF TIME STEP & ELAPSED TIMES IN SECONDS.
100 DELSEC=CNV*DELT
      TOTSEC=CNV*TOTIM
      PERSEC=CNV*PERTIM

C
C4-----CALCULATE TIMES IN MINUTES,HOURS,DAYS AND YEARS.
      DELMN=DELSEC/60.
      DELHR=DELMN/60.
      DELDY=DELHR/24.
      DELYR=DELDY/365.25
      TOTMN=TOTSEC/60.
      TOTHR=TOTMN/60.
      TOTDY=TOTHR/24.
      TOTYR=TOTDY/365.25
      PERMN=PERSEC/60.
      PERHR=PERMN/60.
      PERDY=PERHR/24.
      PERYR=PERDY/365.25

C
C5-----PRINT TIME STEP LENGTH AND ELAPSED TIMES IN ALL TIME UNITS.
      WRITE(IOUT,200)
200 FORMAT(27X,' SECONDS MINUTES HOURS',10X,
1 'DAYS YEARS'/27X,75('-'))
      WRITE(IOUT,201) DELSEC,DELMN,DELHR,DELDY,DELYR
201 FORMAT(1X,' TIME STEP LENGTH',5X,5G15.6)
      WRITE(IOUT,202) PERSEC,PERMN,PERHR,PERDY,PERYR
202 FORMAT(1X,' STRESS PERIOD TIME',5X,5G15.6)
      WRITE(IOUT,203) TOTSEC,TOTMN,TOTHR,TOTDY,TOTYR
203 FORMAT(1X,' TOTAL SIMULATION TIME',5X,5G15.6)

C
C6-----RETURN
      RETURN
      END
      SUBROUTINE SBAS1V(MSUM,VBNM,VBVL,KSTP,KPER,IOUT)

C
C
C-----VERSION 1531 12MAY1987 SBAS1V
C *****
C PRINT VOLUMETRIC BUDGET
C *****
C
C SPECIFICATIONS:
C -----
C
      CHARACTER*4 VBNM

```

A-14
BAS1.FOR Modifications

```

DIMENSION VBNM(4,20),VBVL(4,20)
-----
C
C1-----DETERMINE NUMBER OF INDIVIDUAL BUDGET ENTRIES.
      MSUM1=MSUM-1
      IF (MSUM1.LE.0) RETURN
C
C2-----CLEAR RATE AND VOLUME ACCUMULATORS.
      TOTRIN=0.
      TOTROT=0.
      TOTVIN=0.
      TOTVOT=0.
C
C3-----ADD RATES AND VOLUMES (IN AND OUT) TO ACCUMULATORS.
      DO 100 L=1,MSUM1
      TOTRIN=TOTRIN+VBVL(3,L)
      TOTROT=TOTROT+VBVL(4,L)
      TOTVIN=TOTVIN+VBVL(1,L)
      TOTVOT=TOTVOT+VBVL(2,L)
100 CONTINUE
C
C4-----PRINT TIME STEP NUMBER AND STRESS PERIOD NUMBER.
      WRITE (IOUT,260) KSTP,KPER
      WRITE (IOUT,265)
C
C5-----PRINT INDIVIDUAL INFLOW RATES AND VOLUMES AND THEIR TOTALS.
      DO 200 L=1,MSUM1
      WRITE (IOUT,275) (VBNM(I,L),I=1,4),VBVL(1,L), (VBNM(I,L),I=1,4)
      1,VBVL(3,L)
200 CONTINUE
      WRITE (IOUT,286) TOTVIN,TOTRIN
C
C6-----PRINT INDIVIDUAL OUTFLOW RATES AND VOLUMES AND THEIR TOTALS.
      WRITE (IOUT,287)
      DO 250 L=1,MSUM1
      WRITE (IOUT,275) (VBNM(I,L),I=1,4),VBVL(2,L), (VBNM(I,L),I=1,4)
      1,VBVL(4,L)
250 CONTINUE
      WRITE (IOUT,298) TOTVOT,TOTROT
C
C7-----CALCULATE THE DIFFERENCE BETWEEN INFLOW AND OUTFLOW.
C
C7A-----CALCULATE DIFFERENCE BETWEEN RATE IN AND RATE OUT.
      DIFFR=TOTRIN-TOTROT
C
C7B-----CALCULATE PERCENT DIFFERENCE BETWEEN RATE IN AND RATE OUT.
      PDIFFR=100.*DIFFR/((TOTRIN+TOTROT)/2)
C
C7C-----CALCULATE DIFFERENCE BETWEEN VOLUME IN AND VOLUME OUT.
      DIFFV=TOTVIN-TOTVOT
C
C7D-----GET PERCENT DIFFERENCE BETWEEN VOLUME IN AND VOLUME OUT.
      PDIFFV=100.*DIFFV/((TOTVIN+TOTVOT)/2)
C
C8-----PRINT DIFFERENCES AND PERCENT DIFFERENCES BETWEEN INPUT
C8-----AND OUTPUT RATES AND VOLUMES.
      WRITE (IOUT,299) DIFFV,DIFFR
      WRITE (IOUT,300) PDIFFV,PDIFFR
C
C9-----RETURN
      RETURN
C
C ---FORMATS
C
260 FORMAT(1H0,///30X,'VOLUMETRIC BUDGET FOR ENTIRE MODEL AT END OF'
1,' TIME STEP',I3,' IN STRESS PERIOD',I3/30X,77('-'))
265 FORMAT(1H0,19X,'CUMULATIVE VOLUMES',6X,'L*3',37X
1,'RATES FOR THIS TIME STEP',6X,'L*3/T'/20X,18('-'),47X,24('-')
2//26X,'IN:',68X,'IN:'/26X,'---',68X,'---')
275 FORMAT(1X,18X,4A4,' =',G14.5,39X,4A4,' =',G14.5)
286 FORMAT(1H0,26X,'TOTAL IN =',G14.5,47X,'TOTAL IN ='
1,G14.5)
287 FORMAT(1H0,24X,'OUT:',67X,'OUT:'/25X,4('-'),67X,4('-'))
298 FORMAT(1H0,25X,'TOTAL OUT =',G14.5,46X,'TOTAL OUT ='
1,G14.5)
299 FORMAT(1H0,26X,'IN - OUT =',G14.5,47X,'IN - OUT =',G14.5)
300 FORMAT(1H0,15X,'PERCENT DISCREPANCY =',F20.2
1,30X,'PERCENT DISCREPANCY =',F20.2,///)
C
      END

```

A-15
BCF1.FOR Modifications

```
C      Last change: E 20 Feb 99 12:24 pm
SUBROUTINE BCF1AL(ISUM,LENX,LCSC1,LCHY,LCBOT,
1      LCTOP,LCSC2,LCTRPY,IN,ISS,NCOL,NROW,NLAY,IOUT,IBCFCB)
C
C-----VERSION 1542 12MAY1987 BCF1AL
C
C*****
C      ALLOCATE ARRAY STORAGE FOR BLOCK-CENTERED FLOW PACKAGE
C*****
C
C      SPECIFICATIONS:
C-----
C      COMMON /FLWCOM/LAYCON(80)
C-----
C
C1-----IDENTIFY PACKAGE
      WRITE(IOUT,1)IN
      1 FORMAT(1H0,'BCF1 -- BLOCK-CENTERED FLOW PACKAGE, VERSION.1',
      1', 9/1/87', ' INPUT READ FROM UNIT',I3)
C
C2-----READ AND PRINT ISS (STEADY-STATE FLAG) AND IBCFCB (FLAG FOR
C2-----PRINTING OR UNIT# FOR RECORDING CELL-BY-CELL FLOW TERMS)
      READ(IN,2) ISS,IBCFCB
      2 FORMAT(2I10)
      IF(ISS.EQ.0) WRITE(IOUT,3)
      3 FORMAT(1X,'TRANSIENT SIMULATION')
      IF(ISS.NE.0) WRITE(IOUT,4)
      4 FORMAT(1X,'STEADY-STATE SIMULATION')
      IF(IBCFCB.GT.0) WRITE(IOUT,9) IBCFCB
      9 FORMAT(1X,'CELL-BY-CELL FLOWS WILL BE RECORDED ON UNIT',I3)
      IF(IBCFCB.LT.0) WRITE(IOUT,88)
      88 FORMAT(1X,'CONSTANT HEAD CELL-BY-CELL FLOWS WILL BE PRINTED')
C
C3-----READ TYPE CODE FOR EACH LAYER AND COUNT TOPS AND BOTTOMS
      IF(NLAY.LE.80) GO TO 50
      WRITE(IOUT,11)
      11 FORMAT(1H0,'YOU HAVE SPECIFIED MORE THAN 80 MODEL LAYERS'/1X,
      1 'SPACE IS RESERVED FOR A MAXIMUM OF 80 LAYERS IN ARRAY LAYCON')
      STOP
C
C3A-----READ LAYER TYPE CODES.
      50 READ(IN,51) (LAYCON(I),I=1,NLAY)
      51 FORMAT(40I2)
C      BOTTOM IS READ FOR TYPES 1,3 TOP IS READ FOR TYPES 2,3
      WRITE(IOUT,52)
      52 FORMAT(1X,5X,'LAYER AQUIFER TYPE',/1X,5X,19('-'))
C
C3B-----INITIALIZE TOP AND BOTTOM COUNTERS.
      NBOT=0
      NTOP=0
C
C3C-----PRINT LAYER TYPE AND COUNT TOPS AND BOTTOMS NEEDED.
      DO 100 I=1,NLAY
C
C3C1-----PRINT LAYER NUMBER AND LAYER TYPE CODE.
      L=LAYCON(I)
      WRITE(IOUT,7) I,L
      7 FORMAT(1X,I9,I10)
C
C3C2-----ONLY THE TOP LAYER CAN BE UNCONFINED(LAYCON=1).
      IF(L.NE.1 .OR. I.EQ.1) GO TO 70
      WRITE(IOUT,8)
      8 FORMAT(1H0,'AQUIFER TYPE 1 IS ONLY ALLOWED IN TOP LAYER')
      STOP
C
C3C3-----LAYER TYPES 1 AND 3 NEED A BOTTOM. ADD 1 TO KB.
      70 IF(L.EQ.1 .OR. L.EQ.3) NBOT=NBOT+1
C
C3C4-----LAYER TYPES 2 AND 3 NEED A TOP. ADD 1 TO KT.
      IF(L.EQ.2 .OR. L.EQ.3) NTOP=NTOP+1
      100 CONTINUE
C
C
C
C4-----COMPUTE DIMENSIONS FOR ARRAYS.
      NRC=NROW*NCOL
      ISIZ=NRC*NLAY
C
C5-----ALLOCATE SPACE FOR ARRAYS. IF RUN IS TRANSIENT(ISS=0)
C5-----THEN SPACE MUST BE ALLOCATED FOR STORAGE.
      ISOLD=ISUM
      LCSC1=ISUM
      IF(ISS.EQ.0) ISUM=ISUM+ISIZ
      LCSC2=ISUM
      IF(ISS.EQ.0) ISUM=ISUM+NRC*NTOP
      LCTRPY=ISUM
      ISUM=ISUM+NLAY
      LCBOT=ISUM
      ISUM=ISUM+NRC*NBOT
      LCHY=ISUM
      ISUM=ISUM+NRC*NBOT
      LCTOP=ISUM
      ISUM=ISUM+NRC*NTOP
C
C6-----PRINT THE AMOUNT OF SPACE USED BY THE BCF PACKAGE.
```

A-16
BCF1.FOR Modifications

```

ISP=ISUM-ISOLD
WRITE(IOUT,101) ISP
101 FORMAT(1X,I8,' ELEMENTS IN X ARRAY ARE USED BY BCF')
ISUM1=ISUM-1
WRITE(IOUT,102) ISUM1,LENX
102 FORMAT(1X,I8,' ELEMENTS OF X ARRAY USED OUT OF',I8)
IF (ISUM1.GT.LENX) WRITE(IOUT,103)
103 FORMAT(1X,' ***X ARRAY MUST BE DIMENSIONED LARGER****')
C
C7-----RETURN
RETURN
END
SUBROUTINE BCF1RP (IBOUND,HNEW,SC1,HY,CR,CC,CV,DELR,DELCL,
1 BOT, TOP, SC2, TRPY, IN, ISS, NCOL, NROW, NLAY, NODES, IOUT,
2 econd, theta, thetas, thetao, expn, ekmob, valance, eqcond,
3 THK, ecsoil, FY, AIS, BIS)
C
C-----VERSION 1636 15MAY1987 BCF1RP
C
C *****
C READ AND INITIALIZE DATA FOR BLOCK-CENTERED FLOW PACKAGE
C *****
C
C SPECIFICATIONS:
C -----
C CHARACTER*4 ANAME
C DOUBLE PRECISION HNEW
C REAL*4 ekmob, valance, eqcond, ecsoil, AIS, BIS
C
C DIMENSION HNEW(NODES), SC1(NODES), HY(NODES), CR(NODES), CC(NODES),
1 CV(NODES), ANAME(6,10), DELR(NCOL), DELC(NROW), BOT(NODES),
2 TOP(NODES), SC2(NODES), TRPY(NLAY), IBOUND(NODES+CV(NODES), ANAME(6,16), DELR(NCOL), DELC(NROW), BOT(NODES)),
3 TOP(NODES), SC2(NODES), TRPY(NLAY), IBOUND(NODES),
4 econd(nodes), theta(nodes), thetas(nodes), thetao(nodes),
5 expn(nodes), THK(NODES), FY(NODES)
C
C COMMON /FLWCOM/LAYCON(80)
C
C DATA ANAME(1,1), ANAME(2,1), ANAME(3,1), ANAME(4,1), ANAME(5,1),
1 ANAME(6,1) / ' ', 'PRIM', 'ARY', 'STOR', 'AGE', 'COEF'/
C DATA ANAME(1,2), ANAME(2,2), ANAME(3,2), ANAME(4,2), ANAME(5,2),
1 ANAME(6,2) / ' ', 'TRAN', 'SMIS', 'AL', 'ONG', 'ROWS'/
C DATA ANAME(1,3), ANAME(2,3), ANAME(3,3), ANAME(4,3), ANAME(5,3),
1 ANAME(6,3) / ' H', 'VD', 'COND', 'AL', 'ONG', 'ROWS'/
C DATA ANAME(1,4), ANAME(2,4), ANAME(3,4), ANAME(4,4), ANAME(5,4),
1 ANAME(6,4) / 'VERT', 'HYD', 'CON', 'D/T', 'HICK', 'NESS'/
C DATA ANAME(1,5), ANAME(2,5), ANAME(3,5), ANAME(4,5), ANAME(5,5),
1 ANAME(6,5) / ' ', ' ', ' ', ' ', 'BO', 'TTOM'/
C DATA ANAME(1,6), ANAME(2,6), ANAME(3,6), ANAME(4,6), ANAME(5,6),
1 ANAME(6,6) / ' ', ' ', ' ', ' ', 'TOP'/
C DATA ANAME(1,7), ANAME(2,7), ANAME(3,7), ANAME(4,7), ANAME(5,7),
1 ANAME(6,7) / ' SE', 'COND', 'ARY', 'STOR', 'AGE', 'COEF'/
C DATA ANAME(1,8), ANAME(2,8), ANAME(3,8), ANAME(4,8), ANAME(5,8),
1 ANAME(6,8) / 'COLU', 'MN T', 'O RO', 'W AN', 'ISOT', 'ROPY'/
C DATA ANAME(1,9), ANAME(2,9), ANAME(3,9), ANAME(4,9), ANAME(5,9),
1 ANAME(6,9) / ' ', ' ', ' ', ' ', 'DELR'/
C DATA ANAME(1,10), ANAME(2,10), ANAME(3,10), ANAME(4,10), ANAME(5,10),
1 ANAME(6,10) / ' ', ' ', ' ', ' ', 'DELC'/
C
C ** added more titles**
C DATA ANAME(1,11), ANAME(2,11), ANAME(3,11), ANAME(4,11), ANAME(5,11),
1 ANAME(6,11) / ' ', 'elec', 'cond', 'AL', 'ONG', 'ROWS'/
C DATA ANAME(1,12), ANAME(2,12), ANAME(3,12), ANAME(4,12), ANAME(5,12),
1 ANAME(6,12) / ' ', 'Mois', 'Cont', 'AL', 'ONG', 'ROWS'/
C DATA ANAME(1,13), ANAME(2,13), ANAME(3,13), ANAME(4,13), ANAME(5,13),
1 ANAME(6,13) / ' ', 'Sat', 'Mois', 'AL', 'ONG', 'ROWS'/
C DATA ANAME(1,14), ANAME(2,14), ANAME(3,14), ANAME(4,14), ANAME(5,14),
1 ANAME(6,14) / ' ', 'Res', 'Mois', 'AL', 'ONG', 'ROWS'/
C DATA ANAME(1,15), ANAME(2,15), ANAME(3,15), ANAME(4,15), ANAME(5,15),
1 ANAME(6,15) / ' ', 'Exp', 'n', 'AL', 'ONG', 'ROWS'/
C DATA ANAME(1,16), ANAME(2,16), ANAME(3,16), ANAME(4,16), ANAME(5,16),
1 ANAME(6,16) / ' ', 'F(1a', 'mda', 'AL', 'ONG', 'ROWS'/
C
C-----
C1-----CALCULATE NUMBER OF NODES IN A LAYER AND READ TRPY,DELR,DELC
NIJ=NCOL*NROW
C
C CALL UIDREL(TRPY, ANAME(1,8), NLAY, IN, IOUT)
C CALL UIDREL(DELR, ANAME(1,9), NCOL, IN, IOUT)
C CALL UIDREL(DELC, ANAME(1,10), NROW, IN, IOUT)
C
C **electrokinetic read information input here**
C READ(IN,21) ekmob, valance, eqcond, ecsoil
21 FORMAT(4F10.0)
C READ(IN,22) AIS, BIS
22 FORMAT(2F10.0)
C ekmob=ekmob*valance/ABS(valance)
C2-----READ ALL PARAMETERS FOR EACH LAYER
KT=0
KB=0
DO 200 K=1, NLAY
KK=K
C
C2A-----FIND ADDRESS OF EACH LAYER IN THREE DIMENSION ARRAYS.
IF (LAYCON(K).EQ.1 .OR. LAYCON(K).EQ.3) KB=KB+1
IF (LAYCON(K).EQ.2 .OR. LAYCON(K).EQ.3) KT=KT+1

```


A-18
BCF1.FOR Modifications

```

C1B-----HORIZONTAL CONDUCTANCES.
      CALL SBCF1H(HNEW, IBOUND, CR, CC, CV, HY, TRPY, DELR, DELC, BOT, TOP,
      1      KK, KB, KT, KITER, KSTP, KPER, NCOL, NROW, NLAY, IOUT, thk)
      100 CONTINUE
C
C2-----IF THE SIMULATION IS TRANSIENT ADD STORAGE TO HCOF AND RHS
      IF (ISS.NE.0) GO TO 201
      TLED=1./DELT
      KT=0
      DO 200 K=1, NLAY
C
C3-----SEE IF THIS LAYER IS CONVERTIBLE OR NON-CONVERTIBLE.
      IF (LAYCON(K).EQ.3 .OR. LAYCON(K).EQ.2) GO TO 150
C4-----NON-CONVERTIBLE LAYER, SO USE PRIMARY STORAGE
      DO 140 I=1, NROW
      DO 140 J=1, NCOL
      IF (IBOUND(J, I, K).LE.0) GO TO 140
      RHO=SC1(J, I, K)*TLED
      HCOF(J, I, K)=HCOF(J, I, K) - RHO
      RHS(J, I, K)=RHS(J, I, K) - RHO*HOLD(J, I, K)
      140 CONTINUE
      GO TO 200
C
C5-----A CONVERTIBLE LAYER, SO CHECK OLD AND NEW HEADS TO DETERMINE
C5-----WHEN TO USE PRIMARY AND SECONDARY STORAGE
      150 KT=KT+1
      DO 180 I=1, NROW
      DO 180 J=1, NCOL
C
C5A-----IF THE CELL IS EXTERNAL THEN SKIP IT.
      IF (IBOUND(J, I, K).LE.0) GO TO 180
      TP=TOP(J, I, KT)
      RHO2=SC2(J, I, KT)*TLED
      RHO1=SC1(J, I, K)*TLED
C
C5B-----FIND STORAGE FACTOR AT START OF TIME STEP.
      SOLD=RHO2
      IF (HOLD(J, I, K).GT.TP) SOLD=RHO1
C
C5C-----FIND STORAGE FACTOR AT END OF TIME STEP.
      HTMP=HNEW(J, I, K)
      SNEW=RHO2
      IF (HTMP.GT.TP) SNEW=RHO1
C
C5D-----ADD STORAGE TERMS TO RHS AND HCOF.
      HCOF(J, I, K)=HCOF(J, I, K) - SNEW
      RHS(J, I, K)=RHS(J, I, K) - SOLD*(HOLD(J, I, K) - TP) - SNEW*TP
C
      180 CONTINUE
C
      200 CONTINUE
C
C6-----FOR EACH LAYER DETERMINE IF CORRECTION TERMS ARE NEEDED FOR
C6-----FLOW DOWN INTO PARTIALLY SATURATED LAYERS.
      201 KT=0
      DO 300 K=1, NLAY
C
C7-----SEE IF CORRECTION IS NEEDED FOR LEAKAGE FROM ABOVE.
      IF (LAYCON(K).NE.3 .AND. LAYCON(K).NE.2) GO TO 250
      KT=KT+1
      IF (K.EQ.1) GO TO 250
C
C7A-----FOR EACH CELL MAKE THE CORRECTION IF NEEDED.
      DO 220 I=1, NROW
      DO 220 J=1, NCOL
C
C7B-----IF THE CELL IS EXTERNAL (IBOUND<=0) THEN SKIP IT.
      IF (IBOUND(J, I, K).LE.0) GO TO 220
      HTMP=HNEW(J, I, K)
C
C7C-----IF HEAD IS ABOVE TOP THEN CORRECTION NOT NEEDED
      IF (HTMP.GE.TOP(J, I, KT)) GO TO 220
C
C7D-----WITH HEAD BELOW TOP ADD CORRECTION TERMS TO RHS AND HCOF.
      RHS(J, I, K)=RHS(J, I, K) + CV(J, I, K-1)*TOP(J, I, KT)
      HCOF(J, I, K)=HCOF(J, I, K) + CV(J, I, K-1)
      220 CONTINUE
C
C8-----SEE IF THIS LAYER MAY NEED CORRECTION FOR LEAKAGE TO BELOW.
      250 IF (K.EQ.NLAY) GO TO 300
      IF (LAYCON(K+1).NE.3 .AND. LAYCON(K+1).NE.2) GO TO 300
      KTT=KT+1
C
C8A-----FOR EACH CELL MAKE THE CORRECTION IF NEEDED.
      DO 280 I=1, NROW
      DO 280 J=1, NCOL
C
C8B-----IF CELL IS EXTERNAL (IBOUND<=0) THEN SKIP IT.
      IF (IBOUND(J, I, K).LE.0) GO TO 280
C
C8C-----IF HEAD IN THE LOWER CELL IS LESS THAN TOP ADD CORRECTION
C8C-----TERM TO RHS.
      HTMP=HNEW(J, I, K+1)
      IF (HTMP.LT.TOP(J, I, KTT)) RHS(J, I, K)=RHS(J, I, K)
      1      - CV(J, I, K)*(TOP(J, I, KTT) - HTMP)

```

A-19
BCF1.FOR Modifications

```

280 CONTINUE
300 CONTINUE
C
C9-----RETURN
      RETURN
      END
      SUBROUTINE BCF1BD(VBNM,VBVL,MSUM,HNEW,IBOUND,HOLD,SC1,CR,CC,CV,
1      TOP,SC2,DELT,ISS,NCOL,NROW,NLAY,KSTP,KPER,IBCFCB,
2      ICBCFL,BUFF,IOUT)
C-----VERSION 1546 12MAY1987 BCF1BD
C
C *****
C COMPUTE BUDGET FLOW TERMS FOR BCF -- STORAGE, CONSTANT HEAD, AND
C FLOW ACROSS CELL WALLS
C *****
C
C SPECIFICATIONS:
C -----
C CHARACTER*4 VBNM,TEXT
C DOUBLE PRECISION HNEW
C
C DIMENSION HNEW(NCOL,NROW,NLAY), IBOUND(NCOL,NROW,NLAY),
1 HOLD(NCOL,NROW,NLAY), SC1(NCOL,NROW,NLAY),
2 CR(NCOL,NROW,NLAY), CC(NCOL,NROW,NLAY),
3 CV(NCOL,NROW,NLAY), VBNM(4,20), VBVL(4,20),
4 SC2(NCOL,NROW,NLAY),
5 TOP(NCOL,NROW,NLAY),BUFF(NCOL,NROW,NLAY)
C
C COMMON /FLWCOM/LAYCON(80)
C
C DIMENSION TEXT(4)
C
C DATA TEXT(1),TEXT(2),TEXT(3),TEXT(4) /' ',' ',' ' STO','RAGE'/
C -----
C1-----INITIALIZE BUDGET ACCUMULATORS
      STOIN=0.
      STOUT=0.
C
C2-----IF CELL-BY-CELL FLOWS ARE NEEDED THEN SET FLAG IBD.
      IBD=0
      IF(ICBCFL.NE.0 .AND. IBCFCB.GT.0) IBD=1
C
C3-----IF STEADY STATE THEN SKIP ALL STORAGE CALCULATIONS
      IF(ISS.NE.0) GO TO 305
C
C4-----IF CELL-BY-CELL FLOWS ARE NEEDED (IBD IS SET) CLEAR BUFFER
      IF(IBD.EQ.0) GO TO 220
      DO 210 K=1,NLAY
      DO 210 I=1,NROW
      DO 210 J=1,NCOL
      BUFF(J,I,K)=0.
210 CONTINUE
C
C5-----RUN THROUGH EVERY CELL IN THE GRID
220 KT=0
      DO 300 K=1,NLAY
      LC=LAYCON(K)
      IF(LC.EQ.3 .OR. LC.EQ.2) KT=KT+1
      DO 300 I=1,NROW
      DO 300 J=1,NCOL
C
C6-----CALCULATE FLOW FROM STORAGE (VARIABLE HEAD CELLS ONLY)
      IF(IBOUND(J,I,K).LE.0) GO TO 300
      Hsing=HNEW(J,I,K)
C
C6A----CHECK LAYER TYPE TO SEE IF ONE STORAGE CAPACITY OR TWO
      IF(LC.NE.3 .AND. LC.NE.2) GO TO 285
C
C6B----TWO STORAGE CAPACITIES
      TP=TOP(J,I,KT)
      SYA=SC2(J,I,KT)
      SCFA=SC1(J,I,K)
      SOLD=SYA
      IF(HOLD(J,I,K).GT.TP) SOLD=SCFA
      SNEW=SYA
      IF(Hsing.GT.TP) SNEW=SCFA
      STRG=SOLD*(HOLD(J,I,K)-TP) + SNEW*TP - SNEW*Hsing
      GO TO 288
C
C6C----ONE STORAGE CAPACITY
285 SC=SC1(J,I,K)
      STRG=SC*HOLD(J,I,K) - SC*Hsing
C
C7-----STORE CELL-BY-CELL FLOW IN BUFFER AND ADD TO ACCUMULATORS
288 IF(IBD.EQ.1) BUFF(J,I,K)=STRG/DELT
      IF(STRG) 292,300,294
292 STOUT=STOUT-STRG
      GO TO 300
294 STOIN=STOIN+STRG
C
C 300 CONTINUE
C
C8-----IF IBD FLAG IS SET RECORD THE CONTENTS OF THE BUFFER
      IF(IBD.EQ.1) CALL UBUDSV(KSTP,KPER,TEXT,

```

A-20
BCF1.FOR Modifications

```

1          IBCFCB,BUFF,NCOL,NROW,NLAY,IOUT)
C
C9-----ADD TOTAL RATES AND VOLUMES TO VBVL & PUT TITLES IN VBNM
305 VBVL(1,MSUM)=VBVL(1,MSUM)+STOIN
    VBVL(2,MSUM)=VBVL(2,MSUM)+STOUT
    VBVL(3,MSUM)=STOIN/DELT
    VBVL(4,MSUM)=STOUT/DELT
    VBNM(1,MSUM)=TEXT(1)
    VBNM(2,MSUM)=TEXT(2)
    VBNM(3,MSUM)=TEXT(3)
    VBNM(4,MSUM)=TEXT(4)
    MSUM=MSUM+1
C
C10-----CALCULATE FLOW FROM CONSTANT HEAD NODES
CALL SBCF1F(VBNM,VBVL,MSUM,HNEW,IBOUND,CR,CC,CV,TOP,DELT,
1        NCOL,NROW,NLAY,KSTP,KPER,IBD,IBCFCB,ICBFL,BUFF,IOUT)
C
C11-----CALCULATE AND SAVE FLOW ACROSS CELL BOUNDARIES IF C-B-C
C11-----FLOW TERMS ARE REQUESTED.
    IF (IBD.NE.0) CALL SBCF1B(HNEW,IBOUND,CR,CC,CV,TOP,NCOL,NROW,NLAY,
1        KSTP,KPER,IBCFCB,BUFF,IOUT)
C
C12-----RETURN
    RETURN
    END
    SUBROUTINE SBCF1C(CR,CC,TRPY,DELR,DELC,K,NCOL,NROW,NLAY)
C
C-----VERSION 1334 22AUG1987 SBCF1C
*****
C COMPUTE BRANCH CONDUCTANCE USING HARMONIC MEAN OF BLOCK
C CONDUCTANCES -- BLOCK TRANSMISSIVITY IS IN CC UPON ENTRY
*****
C SPECIFICATIONS:
C -----
C DIMENSION CR(NCOL,NROW,NLAY), CC(NCOL,NROW,NLAY)
C 2 , TRPY(NLAY), DELR(NCOL), DELC(NROW)
C -----
C YX=TRPY(K)*2.
C
C1-----FOR EACH CELL CALCULATE BRANCH CONDUCTANCES FROM THAT CELL
C1-----TO THE ONE ON THE RIGHT AND THE ONE IN FRONT.
    DO 40 I=1,NROW
    DO 40 J=1,NCOL
    T1=CC(J,I,K)
C
C2-----IF T=0 THEN SET CONDUCTANCE EQUAL TO 0. GO ON TO NEXT CELL.
    IF (T1.NE.0.) GO TO 10
    CR(J,I,K)=0.
    GO TO 40
C
C3-----IF THIS IS NOT THE LAST COLUMN(RIGHTMOST) THEN CALCULATE
C3-----BRANCH CONDUCTANCE IN THE ROW DIRECTION (CR) TO THE RIGHT.
    10 IF (J.EQ.NCOL) GO TO 30
    T2=CC(J+1,I,K)
    CR(J,I,K)=2.*T2*T1*DELC(I)/(T1*DELR(J+1)+T2*DELR(J))
C
C4-----IF THIS IS NOT THE LAST ROW(FRONTMOST) THEN CALCULATE
C4-----BRANCH CONDUCTANCE IN THE COLUMN DIRECTION (CC) TO THE FRONT.
    30 IF (I.EQ.NROW) GO TO 40
    T2=CC(J,I+1,K)
    CC(J,I,K)=YX*T2*T1*DELR(J)/(T1*DELC(I+1)+T2*DELC(I))
    40 CONTINUE
C
C5-----RETURN
    RETURN
    END
    SUBROUTINE SBCF1B(HNEW,IBOUND,CR,CC,CV,TOP,NCOL,NROW,NLAY,
1        KSTP,KPER,IBCFCB,BUFF,IOUT)
C
C-----VERSION 1548 12MAY1987 SBCF1B
*****
C COMPUTE FLOW ACROSS EACH CELL WALL
*****
C SPECIFICATIONS:
C -----
C CHARACTER*4 TEXT
C DOUBLE PRECISION HNEW,HD
C
C DIMENSION HNEW(NCOL,NROW,NLAY), IBOUND(NCOL,NROW,NLAY),
C 1 CR(NCOL,NROW,NLAY), CC(NCOL,NROW,NLAY),
C 2 CV(NCOL,NROW,NLAY), TOP(NCOL,NROW,NLAY),
C 3 BUFF(NCOL,NROW,NLAY)
C
C COMMON /FLWCOM/LAYCON(80)
C
C DIMENSION TEXT(12)
C
C DATA TEXT(1),TEXT(2),TEXT(3),TEXT(4),TEXT(5),TEXT(6),TEXT(7),
C 1 TEXT(8),TEXT(9),TEXT(10),TEXT(11),TEXT(12)

```

A-21
BCF1.FOR Modifications

```

2  /'FLOW', ' RIG', 'HT F', 'ACE ',
2  'FLOW', ' FRO', 'NT F', 'ACE ', 'FLOW', ' LOW', 'ER F', 'ACE ' /
C  -----
C
NCM1=NCOL-1
IF(NCM1.LT.1) GO TO 405
C
C1-----CLEAR THE BUFFER
DO 310 K=1,NLAY
DO 310 I=1,NROW
DO 310 J=1,NCOL
  BUFF(J,I,K)=0.
310 CONTINUE
C
C2-----FOR EACH CELL CALCULATE FLOW THRU RIGHT FACE & STORE IN BUFFER
DO 400 K=1,NLAY
DO 400 I=1,NROW
DO 400 J=1,NCM1
  IF((IBOUND(J,I,K).LE.0) .AND. (IBOUND(J+1,I,K).LE.0)) GO TO 400
  HDIFF=HNEW(J,I,K)-HNEW(J+1,I,K)
  BUFF(J,I,K)=HDIFF*CR(J,I,K)
400 CONTINUE
C
C3-----RECORD CONTENTS OF BUFFER
CALL UBUDSV(KSTP,KPER,TEXT(1),IBCFCB,BUFF,NCOL,NROW,NLAY,IOUT)
C
C4-----CLEAR THE BUFFER
405 NRMI=NROW-1
IF(NRMI.LT.1) GO TO 505
DO 410 K=1,NLAY
DO 410 I=1,NROW
DO 410 J=1,NCOL
  BUFF(J,I,K)=0.
410 CONTINUE
C
C5-----FOR EACH CELL CALCULATE FLOW THRU FRONT FACE & STORE IN BUFFER
DO 500 K=1,NLAY
DO 500 I=1,NRMI
DO 500 J=1,NCOL
  IF((IBOUND(J,I,K).LE.0) .AND. (IBOUND(J,I+1,K).LE.0)) GO TO 500
  HDIFF=HNEW(J,I,K)-HNEW(J,I+1,K)
  BUFF(J,I,K)=HDIFF*CC(J,I,K)
500 CONTINUE
C
C6-----RECORD CONTENTS OF BUFFER.
CALL UBUDSV(KSTP,KPER,TEXT(5),IBCFCB,BUFF,NCOL,NROW,NLAY,IOUT)
505 NLM1=NLAY-1
IF(NLM1.LT.1) GO TO 1000
C
C7-----CLEAR THE BUFFER
DO 510 K=1,NLAY
DO 510 I=1,NROW
DO 510 J=1,NCOL
  BUFF(J,I,K)=0.
510 CONTINUE
C
C8-----FOR EACH CELL CALCULATE FLOW THRU LOWER FACE & STORE IN BUFFER
KT=0
DO 600 K=1,NLM1
IF(LAYCON(K).EQ.3 .OR. LAYCON(K).EQ.2) KT=KT+1
DO 600 I=1,NROW
DO 600 J=1,NCOL
  IF((IBOUND(J,I,K).LE.0) .AND. (IBOUND(J,I,K+1).LE.0)) GO TO 600
  HD=HNEW(J,I,K+1)
  IF(LAYCON(K+1).NE.3 .AND. LAYCON(K+1).NE.2) GO TO 580
  TMP=HD
  IF(TMP.LT.TOP(J,I,KT+1)) HD=TOP(J,I,KT+1)
580 HDIFF=HNEW(J,I,K)-HD
  BUFF(J,I,K)=HDIFF*CV(J,I,K)
600 CONTINUE
C
C9-----RECORD CONTENTS OF BUFFER.
CALL UBUDSV(KSTP,KPER,TEXT(9),IBCFCB,BUFF,NCOL,NROW,NLAY,IOUT)
C
C10----RETURN
1000 RETURN
END
SUBROUTINE SBCF1F(VBNM,VBVL,MSUM,HNEW,IBOUND,CR,CC,CV,
1  TOP,DELT,NCOL,NROW,NLAY,KSTP,KPER,IBD,IBCFCB,ICBCFL,
2  BUFF,IOUT)
C-----VERSION 1549 12MAY1987 SBCF1F
C
C *****
C COMPUTE FLOW FROM CONSTANT HEAD NODES
C *****
C
C SPECIFICATIONS:
C -----
C CHARACTER*4 VBNM,TEXT
C DOUBLE PRECISION HNEW,HD
C
C DIMENSION HNEW(NCOL,NROW,NLAY), IBOUND(NCOL,NROW,NLAY),
1  CR(NCOL,NROW,NLAY), CC(NCOL,NROW,NLAY),
2  CV(NCOL,NROW,NLAY), VBNM(4,20), VBVL(4,20),
3  TOP(NCOL,NROW,NLAY),BUFF(NCOL,NROW,NLAY)

```

A-22
BCF1.FOR Modifications

```

C      COMMON /FLWCOM/LAYCON(80)
C
C      DIMENSION TEXT(4)
C
C      DATA TEXT(1),TEXT(2),TEXT(3),TEXT(4) /'  C','ONST','ANT ','HEAD'/
C      -----
C1-----CLEAR BUDGET ACCUMULATORS
      CHIN=0.
      CHOUT=0.
C
C2-----CLEAR BUFFER IF CELL-BY-CELL FLOW TERM FLAG(IBD) IS SET
      IF (IBD.EQ.0) GO TO 8
      DO 5 K=1,NLAY
      DO 5 I=1,NROW
      DO 5 J=1,NCOL
      BUFF(J,I,K)=0.
      5 CONTINUE
C
C3-----FOR EACH CELL IF IT IS CONSTANT HEAD COMPUTE FLOW ACROSS 6
C3-----FACES.
      8 KT=0
      DO 200 K=1,NLAY
      LC=LAYCON(K)
      IF (LC.EQ.3 .OR. LC.EQ.2) KT=KT+1
      DO 200 I=1,NROW
      DO 200 J=1,NCOL
C
C4-----IF CELL IS NOT CONSTANT HEAD SKIP IT & GO ON TO NEXT CELL.
      IF (IBOUND(J,I,K).GE.0)GO TO 200
C
C5-----CLEAR FIELDS FOR SIX FLOW RATES.
      X1=0.
      X2=0.
      X3=0.
      X4=0.
      X5=0.
      X6=0.
C6-----FOR EACH FACE OF THE CELL CALCULATE FLOW THROUGH THAT FACE
C6-----OUT OF THE CONSTANT HEAD CELL AND INTO THE FLOW DOMAIN.
C6-----COMMENTS 7-11 APPEAR ONLY IN THE SECTION HEADED BY COMMENT 6A
C6-----BUT THEY APPLY IN A SIMILAR MANNER TO THE SECTIONS HEADED
C6-----BY COMMENTS 6B-6F.
C
C6A----CALCULATE FLOW THROUGH THE LEFT FACE
C
C7-----IF THERE IS NOT A VARIABLE HEAD CELL ON THE OTHER SIDE OF THIS
C7-----FACE THEN GO ON TO THE NEXT FACE.
      IF (J.EQ.1) GO TO 30
      IF (IBOUND(J-1,I,K).LE.0)GO TO 30
      HDIFF=HNEW(J,I,K)-HNEW(J-1,I,K)
C
C8-----CALCULATE FLOW THROUGH THIS FACE INTO THE ADJACENT CELL.
      X1=HDIFF*CR(J-1,I,K)
C
C9-----TEST TO SEE IF FLOW IS POSITIVE OR NEGATIVE
      IF (X1) 10,30,20
C
C10----IF NEGATIVE ADD TO CHOUT(FLOW OUT OF DOMAIN TO CONSTANT HEAD).
      10 CHOUT=CHOUT-X1
      GO TO 30
C
C11----IF POSITIVE ADD TO CHIN(FLOW INTO DOMAIN FROM CONSTANT HEAD).
      20 CHIN=CHIN+X1
C
C6B----CALCULATE FLOW THROUGH THE RIGHT FACE
      30 IF (J.EQ.NCOL) GO TO 60
      IF (IBOUND(J+1,I,K).LE.0) GO TO 60
      HDIFF=HNEW(J,I,K)-HNEW(J+1,I,K)
      X2=HDIFF*CR(J,I,K)
      IF (X2)40,60,50
      40 CHOUT=CHOUT-X2
      GO TO 60
      50 CHIN=CHIN+X2
C
C6C----CALCULATE FLOW THROUGH THE BACK FACE.
      60 IF (I.EQ.1) GO TO 90
      IF (IBOUND(J,I-1,K).LE.0) GO TO 90
      HDIFF=HNEW(J,I,K)-HNEW(J,I-1,K)
      X3=HDIFF*CC(J,I-1,K)
      IF (X3) 70,90,80
      70 CHOUT=CHOUT-X3
      GO TO 90
      80 CHIN=CHIN+X3
C
C6D----CALCULATE FLOW THROUGH THE FRONT FACE.
      90 IF (I.EQ.NROW) GO TO 120
      IF (IBOUND(J,I+1,K).LE.0) GO TO 120
      HDIFF=HNEW(J,I,K)-HNEW(J,I+1,K)
      X4=HDIFF*CC(J,I,K)
      IF (X4) 100,120,110
      100 CHOUT=CHOUT-X4
      GO TO 120
      110 CHIN=CHIN+X4

```

A-23
BCF1.FOR Modifications

```

C
C6E----CALCULATE FLOW THROUGH THE UPPER FACE
120 IF (K.EQ.1) GO TO 150
    IF (IBOUND(J,I,K-1).LE.0) GO TO 150
    HD=HNEW(J,I,K)
    IF (LC.NE.3 .AND. LC.NE.2) GO TO 122
    TMP=HD
    IF (TMP.LT.TOP(J,I,KT)) HD=TOP(J,I,KT)
122 HDIFF=HD-HNEW(J,I,K-1)
    X5=HDIFF*CV(J,I,K-1)
    IF (X5) 130,150,140
130 CHOUT=CHOUT-X5
    GO TO 150
140 CHIN=CHIN+X5
C
C6F----CALCULATE FLOW THROUGH THE LOWER FACE.
150 IF (K.EQ.NLAY) GO TO 180
    IF (IBOUND(J,I,K+1).LE.0) GO TO 180
    HD=HNEW(J,I,K+1)
    IF (LAYCON(K+1).NE.3 .AND. LAYCON(K+1).NE.2) GO TO 152
    TMP=HD
    IF (TMP.LT.TOP(J,I,KT+1)) HD=TOP(J,I,KT+1)
152 HDIFF=HNEW(J,I,K)-HD
    X6=HDIFF*CV(J,I,K)
    IF (X6) 160,180,170
160 CHOUT=CHOUT-X6
    GO TO 180
170 CHIN=CHIN+X6
C
C12----SUM UP FLOWS THROUGH SIX SIDES OF CONSTANT HEAD CELL.
180 RATE=X1+X2+X3+X4+X5+X6
C
C13----PRINT THE INDIVIDUAL RATES IF REQUESTED(IBCFCB<0).
    IF (IBCFCB.LT.0.AND.ICBCFL.NE.0) WRITE(IOUT,900) (TEXT(N),N=1,4),
1     KPER,KSTP,K,I,J,RATE
900 FORMAT(1H0,4A4,' PERIOD',I3,' STEP',I3,' LAYER',I3,
1     ' ROW',I4,' COL',I4,' RATE ',G15.7)
C
C14----IF CELL-BY-CELL FLAG SET STORE SUM OF FLOWS FOR CELL IN BUFFER
    IF (IBD.EQ.1) BUFF(J,I,K)=RATE
C
200 CONTINUE
C
C15----IF CELL-BY-CELL FLAG SET THEN RECORD CONTENTS OF BUFFER
    IF (IBD.EQ.1) CALL UBUDSV(KSTP,KPER,TEXT(1),
1     IBCFCB,BUFF,NCOL,NROW,NLAY,IOUT)
C
C16----SAVE TOTAL CONSTANT HEAD FLOWS AND VOLUMES IN VBVL TABLE
C16----FOR INCLUSION IN BUDGET. PUT LABELS IN VBNM TABLE.
    VBVL(1,MSUM)=VBVL(1,MSUM)+CHIN*DELT
    VBVL(2,MSUM)=VBVL(2,MSUM)+CHOUT*DELT
    VBVL(3,MSUM)=CHIN
    VBVL(4,MSUM)=CHOUT
C
C    ---SETUP VOLUMETRIC BUDGET NAMES
    VBNM(1,MSUM)=TEXT(1)
    VBNM(2,MSUM)=TEXT(2)
    VBNM(3,MSUM)=TEXT(3)
    VBNM(4,MSUM)=TEXT(4)
C
    MSUM=MSUM+1
C
C
C17----RETURN
    RETURN
    END
    SUBROUTINE SBCF1H(HNEW,IBOUND,CR,CC,CV,HY,TRPY,DELR,DELC
1,BOT,TOP,K,KB,KT,KITER,KSTP,KPER,NCOL,NROW,NLAY,IOUT,thk)
C
C-----VERSION 1442 31DEC1986 SBCF1H
C
C *****
C COMPUTE CONDUCTANCE FROM SATURATED THICKNESS AND HYDRAULIC
C CONDUCTIVITY
C *****
C
C SPECIFICATIONS:
C -----
C DOUBLE PRECISION HNEW
C
C DIMENSION HNEW(NCOL,NROW,NLAY),IBOUND(NCOL,NROW,NLAY)
1, CR(NCOL,NROW,NLAY), CC(NCOL,NROW,NLAY), CV(NCOL,NROW,NLAY)
2, HY(NCOL,NROW,NLAY), TRPY(NLAY), DELR(NCOL), DELC(NROW)
3, BOT(NCOL,NROW,NLAY),TOP(NCOL,NROW,NLAY)
4 thk(NCOL,NROW,NLAY)
C
COMMON /FLWCOM/LAYCON(80)
C-----
C1-----CALCULATE TRANSMISSIVITY AT EACH ACTIVE CELL. TRANSMISSIVITY
C1-----WILL BE STORED TEMPORARILY IN THE CC ARRAY.
    DO 200 I=1,NROW
    DO 200 J=1,NCOL

```

A-24
BCF1.FOR Modifications

```

C2-----IF CELL IS INACTIVE THEN SET T=0 & MOVE ON TO NEXT CELL.
      IF (IBOUND(J,I,K).NE.0) GO TO 10
      CC(J,I,K)=0.
      GO TO 200
C
C3-----CALCULATE SATURATED THICKNESS.
      10 HD=HNEW(J,I,K)
      IF (LAYCON(K).EQ.1) GO TO 50
      IF (HD.GT.TOP(J,I,KT)) HD=TOP(J,I,KT)
      50 THCK=HD-BOT(J,I,KB)
C
C4-----CHECK TO SEE IF SATURATED THICKNESS IS GREATER THAN ZERO.
      IF (THCK.LE.0.) GO TO 100
C
C      **save thickness in array thk
C      thk(j,i,k)=thck
C
C5-----IF SATURATED THICKNESS>0 THEN T=K*THICKNESS.
      CC(J,I,K)=THCK*HY(J,I,KB)
      GO TO 200
C
C6-----WHEN SATURATED THICKNESS < 0, PRINT A MESSAGE AND SET
      TRANSMISSIVITY, IBOUND, AND VERTICAL CONDUCTANCE =0
      100 WRITE (IOUT,150) K,I,J,KITER,KSTP,KPER
      150 FORMAT(1H0,10(' '), 'NODE',3I4, ' (LAYER,ROW,COL) WENT DRY'
      1      , ' AT ITERATION =',I3, ' TIME STEP =',I3
      2      , ' STRESS PERIOD =',I3)
      HNEW(J,I,K)=1.E30
      CC(J,I,K)=0.
      IBOUND(J,I,K)=0
      IF (K.LT.NLAY) CV(J,I,K)=0.
      IF (K.GT.1) CV(J,I,K-1)=0.
      GO TO 200
      200 CONTINUE
C
C7-----COMPUTE HORIZONTAL BRANCH CONDUCTANCES FROM TRANSMISSIVITY
      CALL SBCF1C(CR,CC,TRPY,DELR,DELC,K,NCOL,NROW,NLAY)
C
C8-----RETURN
      RETURN
      END
      SUBROUTINE SBCF1N(HNEW,IBOUND,SC1,SC2,CR,CC,CV,HY,TRPY,DELR,DELC,
      1      ISS,NCOL,NROW,NLAY,IOUT)
C
C-----VERSION 1642 15MAY1987 SBCF1N
C
C      *****
C      INITIALIZE AND CHECK BCF DATA
C      *****
C
C      SPECIFICATIONS:
C      -----
C
C      DOUBLE PRECISION HNEW,HCNV
C
C      DIMENSION HNEW(NCOL,NROW,NLAY),IBOUND(NCOL,NROW,NLAY)
      1      ,SC1(NCOL,NROW,NLAY),CR(NCOL,NROW,NLAY)
      2      ,CC(NCOL,NROW,NLAY),CV(NCOL,NROW,NLAY)
      3      ,HY(NCOL,NROW,NLAY),TRPY(NLAY),DELR(NCOL),DELC(NROW)
      4      ,SC2(NCOL,NROW,NLAY)
C
C      COMMON /FLWCOM/LAYCON(80)
C      -----
C
C1-----IF IBOUND=0, SET CV=0., CC=0., AND HY=0.
      KB=0
      DO 30 K=1,NLAY
      IF (LAYCON(K).EQ.3 .OR. LAYCON(K).EQ.1) KB=KB+1
      DO 30 I=1,NROW
      DO 30 J=1,NCOL
      IF (IBOUND(J,I,K).NE.0) GO TO 30
      IF (K.NE.NLAY) CV(J,I,K)=0.
      IF (K.NE.1) CV(J,I,K-1)=0.
      CC(J,I,K)=0.
      IF (LAYCON(K).EQ.3 .OR. LAYCON(K).EQ.1) HY(J,I,KB)=0.
      30 CONTINUE
C
C2-----INSURE THAT EACH ACTIVE CELL HAS AT LEAST ONE NON-ZERO
      TRANSMISSIVE PARAMETER. IF NOT, CONVERT CELL TO NOFLOW.
      HCNV=888.88
      KB=0
      DO 60 K=1,NLAY
      IF (LAYCON(K).EQ.1 .OR. LAYCON(K).EQ.3) GO TO 55
C2A-----WHEN LAYER TYPE 0 OR 2, TRANSMISSIVITY OR CV MUST BE NONZERO
      DO 54 I=1,NROW
      DO 54 J=1,NCOL
      IF (IBOUND(J,I,K).EQ.0) GO TO 54
      IF (CC(J,I,K).NE.0.) GO TO 54
      IF (K.EQ.NLAY) GO TO 51
      IF (CV(J,I,K).NE.0.) GO TO 54
      51 IF (K.EQ.1) GO TO 53
      IF (CV(J,I,K-1).NE.0.) GO TO 54
      53 IBOUND(J,I,K)=0
      HNEW(J,I,K)=HCNV
      WRITE (IOUT,52) K,I,J

```

A-25
BCF1.FOR Modifications

```
52 FORMAT(1X,'NODE (LAYER,ROW,COL)',3I4,  
1 ' ELIMINATED BECAUSE ALL CONDUCTANCES TO NODE ARE 0')  
54 CONTINUE  
GO TO 60  
C  
C2B-----WHEN LAYER TYPE IS 1 OR 3, HY OR CV MUST BE NONZERO  
55 KB=KB+1  
DO 59 I=1,NROW  
DO 59 J=1,NCOL  
IF (IBOUND(J,I,K).EQ.0) GO TO 59  
IF (HY(J,I,KB).NE.0.) GO TO 59  
IF (K.EQ.NLAY) GO TO 56  
IF (CV(J,I,K).NE.0.) GO TO 59  
56 IF (K.EQ.1) GO TO 57  
IF (CV(J,I,K-1).NE.0.) GO TO 59  
57 IBOUND(J,I,K)=0  
HNEW(J,I,K)=HCNV  
CC(J,I,K)=0.  
WRITE(IOUT,52) K,I,J  
59 CONTINUE  
60 CONTINUE  
C  
C3-----CALCULATE HOR. CONDUCTANCE(CR AND CC) FOR CONSTANT T LAYERS  
DO 65 K=1,NLAY  
KK=K  
IF (LAYCON(K).EQ.3 .OR. LAYCON(K).EQ.1) GO TO 65  
CALL SBCF1C(CR,CC,TRPY,DELR,DELC,KK,NCOL,NROW,NLAY)  
65 CONTINUE  
C  
C4-----MULTIPLY VERTICAL LEAKANCE BY AREA TO MAKE CONDUCTANCE  
IF (NLAY.EQ.1) GO TO 69  
K1=NLAY-1  
DO 68 K=1,K1  
DO 68 I=1,NROW  
DO 68 J=1,NCOL  
CV(J,I,K)=CV(J,I,K)*DELR(J)*DELC(I)  
68 CONTINUE  
C  
C5-----IF TRANSIENT MULTIPLY PRIMARY STORAGE COEFFICIENT BY DELR &  
C5-----DELC TO GET PRIMARY STORAGE CAPACITY(SC1).  
69 IF (ISS.NE.0) GO TO 100  
KT=0  
DO 80 K=1,NLAY  
DO 70 I=1,NROW  
DO 70 J=1,NCOL  
SC1(J,I,K)=SC1(J,I,K)*DELR(J)*DELC(I)  
70 CONTINUE  
C  
C6-----IF LAYER IS CONF/UNCONF MULTIPLY SECONDARY STORAGE COEFFICIENT  
C6-----BY DELR AND DELC TO GET SECONDARY STORAGE CAPACITY(SC2).  
IF (LAYCON(K).NE.3 .AND. LAYCON(K).NE.2) GO TO 80  
KT=KT+1  
DO 75 I=1,NROW  
DO 75 J=1,NCOL  
SC2(J,I,KT)=SC2(J,I,KT)*DELR(J)*DELC(I)  
75 CONTINUE  
C  
80 CONTINUE  
C  
C7-----RETURN  
100 RETURN  
END
```


A-26
LKMT.FOR Modifications

```

C Last change: E 18 Mar 99 8:50 pm
C
C SUBROUTINE BAS1MT(HNEW,IBOUND,
  & NCOL,NROW,NLAY,KSTP,KPER,BUFF,IOUT)
C *****
C SAVE HEADS FOR USE IN MT3D.
C HEADS IN INACTIVE CELLS (IBOUND=0) ARE IDENTIFIED WITH 1.E30.
C *****
C Modified from McDonald & Harbaugh, 1988
C last modified: 10-Aug-1990
C
C CHARACTER*16 TEXT
C DOUBLE PRECISION HNEW
C DIMENSION HNEW(NCOL,NROW,NLAY), IBOUND(NCOL,NROW,NLAY),
  1 BUFF(NCOL,NROW,NLAY)
C TEXT='HEAD'
C
C4-----STORE HOLD OR HNEW IN BUFFER
C DO 210 K=1,NLAY
C DO 210 I=1,NROW
C DO 210 J=1,NCOL
C BUFF(J,I,K)=HNEW(J,I,K)
C 210 CONTINUE
C
C-----ENSURE HEADS IN INACTIVE CELLS ARE 1.E30
C DO 300 K=1,NLAY
C DO 300 I=1,NROW
C DO 300 J=1,NCOL
C
C IF (IBOUND(J,I,K).NE.0) GO TO 300
C IF (BUFF(J,I,K).NE.1.E30) BUFF(J,I,K)=1.E30
C
C 300 CONTINUE
C
C8-----SAVE THE CONTENTS OF THE BUFFER
C WRITE(IOUT) KPER,KSTP,NCOL,NROW,NLAY,TEXT
C WRITE(IOUT) BUFF
C
C12-----RETURN
C RETURN
C END
C
C SUBROUTINE BCF1MT(HNEW,IBOUND,CR,CC,CV,
  & TOP,NCOL,NROW,NLAY,KSTP,KPER,BUFF,IOUT),TOP,NCOL,NROW,NLAY,KSTP,KPER,BUFF,IOUT,
  2 econd,theta,thetas,thetao,expn,ekmob,valance,eqcond,
  3 delr,delc,thk,ecsoil,FY,AIS,BIS)
C *****
C SAVE FLOW ACROSS THREE CELL INTERFACES (QXX, QYY, AND QZZ)
C AND LOCATIONS AND FLOW RATES OF THE CONSTANT-HEAD CELLS
C FOR USE IN MT3D. NOTE THAT FLOW BETWEEN TWO NEIGHBORING CELLS
C IS CALCULATED AND SAVED.
C *****
C Modified from McDonald & Harbaugh, 1988
C last modified: 15-Feb-1991
C
C CHARACTER*16 TEXT
C DOUBLE PRECISION HNEW
C REAL*4 factor,ceq,A,B,XIS,SQIS,AIS,BIS,AC,TEMP
C DIMENSION HNEW(NCOL,NROW,NLAY), IBOUND(NCOL,NROW,NLAY),
  2 CR(NCOL,NROW,NLAY), CC(NCOL,NROW,NLAY),
  3 CV(NCOL,NROW,NLAY),
  4 TOP(NCOL,NROW,NLAY),BUFF(NCOL,NROW,NLAY),
  5 econd(NCOL,NROW,NLAY),theta(NCOL,NROW,NLAY),
  6 thetas(NCOL,NROW,NLAY),thetao(NCOL,NROW,NLAY),
  7 expn(NCOL,NROW,NLAY),ecwater(NCOL,NROW,NLAY),
  8 cmob(NCOL,NROW,NLAY), DELR(NCOL), DELC(NROW),
  9 thk(NCOL,NROW,NLAY),FY(NCOL,NROW,NLAY)
C
C COMMON /ELNCOM/LAYCON(80)
C
C **added electrokinetic terms calcs.**
C calculate constants for electric mobility adjustment
C for concentration effects
C A=(60.2*(ABS(valance))**2)/(2*96500)
C B=0.229*(ABS(valance))**3
C IONIC STRENGTH FROM ELECTRICAL COND CALCS. PARAMETERS
C NOW BEING READ FROM INPUT FILE
C AIS=.127
C BIS=.002
C
C WRITE(*,*) 'A,B,ECOND(1,1,1),THETA(1,1,1),THETAS(1,1,1)'
C WRITE(*,*) A,B,ECOND(1,1,1),THETA(1,1,1),THETAS(1,1,1)
C WRITE(*,*) 'THETAO(1,1,1),EXPN(1,1,1)'
C WRITE(*,*) THETAO(1,1,1),EXPN(1,1,1)
C WRITE(*,*) 'EKMOB,VALANCE,EQCOND'
C WRITE(*,*) EKMOB,VALANCE,EQCOND
C
C calc electrical conductivity of the water for each cell
C from electrical conductivity of the soil by Musalem and
C Friedman (1991) equation 27 (see pg 83 edm)
C DO 309 K=1,NLAY
C DO 309 I=1,NROW

```

A-27
LKMT.FOR Modifications

```

DO 309 J=1,NCOL
c This calcs the geometric factor My equation 26.....
      factor=(theta(J,I,K)-thetao(J,I,K))**(expn(J,I,K)+2)
      factor=factor/(thetas(J,I,K)-thetao(J,I,K))
      factor=factor*FY(J,I,K)
c Water conductivity is calc here to get ionic strength
c effects in method 2.....
      ecwater(J,I,K)=(econd(J,I,K)-ecsoil)/(factor)
c
c *****
c CONCENTRATION EFFECTS ON ION MOBILITY
c *****
c **METHOD 1 Calculate the new ionic mobility via **
c the Debye-Huckel-Onsagar Equation (See EDM pg83) **
c
c ***decided to remove this method and only activity coef.
c method to adjust for ionic strength***
c
c calc equilvent concentration in the cell (see pg 86 edm)
c ceq=1000/eqcond*ecwater(J,I,K)/100
c
c calc new ion mobility adjusted for concentration
c set ek to be in units of cm2 v-1 s-1
c ek=ABS(ekmob)*10000
c cmob(J,I,K)=(ek-((A+B*ek)*ceq**0.5))/10000
c
c
c **METHOD 2 Calc the new ionic mobility via
c the Debye-Huckel activity coefficient method using
c ionic strenght (see EDM pg 96) **
c
c first calc ionic strenght (mol/l) from electrical
c conductivity (S/m) as per Griffin and Jurinak 1973...
      XIS=AIS*ecwater(J,I,K)-BIS
      cmob(j,i,k)= ABS(ekmob)
      IF(XIS.LT.0)GOTO 308
c
c DAVIES EQUATION TO GET ACTIVITY COEFFICIENT (AC)
      SQIS=XIS**0.5
      AC=10**((-5085*VALANCE**2*(SQIS/(1+SQIS)-.3*XIS))
c
c sets temp as activity coefficient adjusted mobility
      TEMP=AC*ABS(EKMOB)
c
c IF(I.eq.1 .and. J.eq.1 .and. K.eq.1)THEN
      WRITE(*,*) "factor =" factor
      WRITE(*,*) "ecwater =" ecwater(j,i,k)
      WRITE(*,*) "ionic strength=", XIS
      WRITE(*,*) "activity coef =", ac
      END IF
c
c COMPARE THE TWO METHODS AND CHOOSE THE GREATER
c MOBILITY TERM .....no longers compares mobility...
c IF(cmob(J,I,K).LT.TEMP)THEN
      cmob(J,I,K)=TEMP
c
c ENDIF
c END CONCENTRATION EFFECTS
c *****
c *****
c adjustment of cmob for verification purposes with rekka's model
c cmob(j,i,k)=ekmob*factor
c *****
c
c mult ionmob by theta/tau**2 (ie. factor)and set correct sign
      308 cmob(J,I,K)=cmob(J,I,K)*factor*valance/ABS(valance)
c
c adjust cmob by effective area to be used in MT3D
      cmob(J,I,K)=cmob(J,I,K)*theta(J,I,K)/
      * (theta(J,I,K)-thetao(J,I,K))
      309 CONTINUE
c
c
c C11-----CALCULATE AND SAVE FLOW ACROSS RIGHT FACE
      NCM1=NCOL-1
      IF(NCM1.LT.1) GO TO 405
      TEXT='QXX'
c
c
c C1-----CLEAR THE BUFFER
      DO 310 K=1,NLAY
      DO 310 I=1,NROW
      DO 310 J=1,NCOL
      BUFF(J,I,K)=0.
c
c set thicknes to eqcond input
c must have thickness of all the layers the same
      thk(j,i,k)=eqcond
c
c end hardware
      310 CONTINUE
c
c
      WRITE(*,*) 'delr(1)',delr(1)
      WRITE(*,*) 'delc(1)',delc(1)

```

A-28
LKMT.FOR Modifications

```

WRITE(*,*) 'thk(1,1,1)',thk(1,1,1)
C WRITE(*,*) 'thk(1,1,2)',thk(2,1,1)
C2-----FOR EACH CELL
DO 400 K=1,NLAY
DO 400 I=1,NROW
DO 400 J=1,NCM1
IF ((IBOUND(J,I,K).EQ.0).AND.(IBOUND(J+1,I,K).EQ.0)) GO TO 400
HDIFF=HNEW(J,I,K)-HNEW(J+1,I,K)
C BUFF(J,I,K)=HDIFF*CR(J,I,K)

C **calculated new Q by EK**
C first set buff to the harmonic mean of cmob
C BUFF(J,I,K)=(DELR(J)+DELR(J+1))/(DELR(J)/CMOB(J,I,K)+
& DELR(J+1)/CMOB(J+1,I,K))

C now mult by voltage gradient
BUFF(J,I,K)=BUFF(J,I,K)*HDIFF/((delr(J)+delr(J+1))/2)

C mult buff by area to get equivalent to volumetric discharge
BUFF(J,I,K)=BUFF(J,I,K)*delc(I)*thk(J,I,K)
C **end buff calcs**
400 CONTINUE

C
WRITE(*,*) 'BUFF(1,1,1)',BUFF(1,1,1)
C3-----RECORD CONTENTS OF BUFFER
WRITE(IOUT) KPER,KSTP,NCOL,NROW,NLAY,TEXT
WRITE(IOUT) BUFF

C
405 CONTINUE

C
C11-----CALCULATE AND SAVE FLOW ACROSS FRONT FACE
NRM1=NROW-1
IF(NRM1.LT.1) GO TO 505
TEXT='QYY'

C
C4-----CLEAR THE BUFFER
DO 410 K=1,NLAY
DO 410 I=1,NROW
DO 410 J=1,NCOL
BUFF(J,I,K)=0.
410 CONTINUE

C
C5-----FOR EACH CELL
DO 500 K=1,NLAY
DO 500 I=1,NRM1
DO 500 J=1,NCOL
IF ((IBOUND(J,I,K).EQ.0).AND.(IBOUND(J,I+1,K).EQ.0)) GO TO 500
HDIFF=HNEW(J,I,K)-HNEW(J,I+1,K)
C BUFF(J,I,K)=HDIFF*CC(J,I,K)
C **calculated new Q by EK**
C first set buff to the harmonic mean of cmob
C BUFF(J,I,K)=(DELC(I)+DELC(I+1))/(DELC(I)/CMOB(J,I,K)+
& DELC(I+1)/CMOB(J,I+1,K))

C now mult by voltage gradient
BUFF(J,I,K)=BUFF(J,I,K)*HDIFF/((delc(I)+delc(I+1))/2)

C MULT BY AREA
BUFF(J,I,K)=BUFF(J,I,K)*delr(J)*thk(J,I,K)
500 CONTINUE

C
C6-----RECORD CONTENTS OF BUFFER.
WRITE(IOUT) KPER,KSTP,NCOL,NROW,NLAY,TEXT
WRITE(IOUT) BUFF

C
505 CONTINUE

C
C11-----CALCULATE AND SAVE FLOW ACROSS FRONT FACE
NLM1=NLAY-1
IF(NLM1.LT.1) GO TO 700
TEXT='QZZ'

C
C7-----CLEAR THE BUFFER
DO 510 K=1,NLAY
DO 510 I=1,NROW
DO 510 J=1,NCOL
BUFF(J,I,K)=0.
510 CONTINUE

C
C8-----FOR EACH CELL CALCULATE FLOW THRU LOWER FACE & STORE IN BUFFER
KT=0
DO 600 K=1,NLM1
IF(LAYCON(K).EQ.3 .OR. LAYCON(K).EQ.2) KT=KT+1
DO 600 I=1,NROW
DO 600 J=1,NCOL
IF((IBOUND(J,I,K).EQ.0).AND.(IBOUND(J,I,K+1).EQ.0)) GO TO 600
HD=HNEW(J,I,K+1)
IF(LAYCON(K+1).NE.3 .AND. LAYCON(K+1).NE.2) GO TO 580
TMP=HD
IF(TMP.LT.TOP(J,I,KT+1)) HD=TOP(J,I,KT+1)
580 HDIFF=HNEW(J,I,K)-HD
C BUFF(J,I,K)=HDIFF*CV(J,I,K)
C **calculated new Q by EK**
C first set buff to the harmonic mean of cmob
C BUFF(J,I,K)=(thk(J,I,K)+thk(J,I,K+1))/

```

A-29
LKMT.FOR Modifications

```

..... & (thk(J,I,K)/CMOB(J,I,K)+thk(J,I,K+1)/CMOB(J,I,K+1))
C      MULT BY VOLTAGE GRADIENT
      BUFF(J,I,K)=BUFF(J,I,K)*HDIFF/((thk(J,I,K)+thk(J,I,K+1))/2)
C
      MULT BY AREA
      BUFF(J,I,K)=BUFF(J,I,K)*delc(I)*delr(J)
      600 CONTINUE
C
C9-----RECORD CONTENTS OF BUFFER.
      WRITE(IOUT) KPER,KSTP,NCOL,NROW,NLAY,TEXT
      WRITE(IOUT) BUFF
C
      700 CONTINUE
C
C-----CALCULATE FLOW TERMS INTO OR OUT OF CONSTANT-HEAD CELLS
      TEXT='CNH'
      NCNH=0
C
C2-----CLEAR BUFFER
      DO 5 K=1,NLAY
      DO 5 I=1,NROW
      DO 5 J=1,NCOL
      BUFF(J,I,K)=0.
      5 CONTINUE
C
C3-----FOR EACH CELL IF IT IS CONSTANT HEAD COMPUTE FLOW ACROSS 6
C3-----FACES.
      KT=0
      DO 200 K=1,NLAY
      LC=LAYCON(K)
      IF(LC.EQ.3 .OR. LC.EQ.2) KT=KT+1
      DO 200 I=1,NROW
      DO 200 J=1,NCOL
C
C4-----IF CELL IS NOT CONSTANT HEAD SKIP IT & GO ON TO NEXT CELL.
      IF (IBOUND(J,I,K).GE.0)GO TO 200
      NCNH=NCNH+1
C
C5-----CLEAR FIELDS FOR SIX FLOW RATES.
      X1=0.
      X2=0.
      X3=0.
      X4=0.
      X5=0.
      X6=0.
C
C6A----CALCULATE FLOW THROUGH THE LEFT FACE
C
C7-----IF THERE IS AN INACTIVE CELL ON THE OTHER SIDE OF THIS
C7-----FACE THEN GO ON TO THE NEXT FACE.
      IF(J.EQ.1) GO TO 30
      IF (IBOUND(J-1,I,K).EQ.0)GO TO 30
      HDIFF=HNEW(J,I,K)-HNEW(J-1,I,K)
C
C8-----CALCULATE FLOW THROUGH THIS FACE INTO THE ADJACENT CELL.
      X1=HDIFF*CR(J-1,I,K)
C  **calculated new Q by EK**
C      first set X1 to the harmonic mean of cmob
      X1=(DELR(J)+DELR(J-1))/(DELR(J)/CMOB(J,I,K)+
      & DELR(J-1)/CMOB(J-1,I,K))
      X1=X1*HDIFF/((delr(J)+delr(J-1))/2)
      X1=X1*delc(I)*thk(J-1,I,K)
C
C6B----CALCULATE FLOW THROUGH THE RIGHT FACE
      30 IF(J.EQ.NCOL) GO TO 60
      IF (IBOUND(J+1,I,K).EQ.0) GO TO 60
      HDIFF=HNEW(J,I,K)-HNEW(J+1,I,K)
C      X2=HDIFF*CR(J,I,K)
C  **calculated new Q by EK**
C      first set buff to the harmonic mean of cmob
      X2=(DELR(J)+DELR(J+1))/(DELR(J)/CMOB(J,I,K)+
      & DELR(J+1)/CMOB(J+1,I,K))
      X2=X2*HDIFF/((delr(J)+delr(J+1))/2)
      X2=X2*delc(I)*thk(J+1,I,K)
C
C6C----CALCULATE FLOW THROUGH THE BACK FACE.
      60 IF(I.EQ.1) GO TO 90
      IF (IBOUND(J,I-1,K).EQ.0) GO TO 90
      HDIFF=HNEW(J,I,K)-HNEW(J,I-1,K)
C      X3=HDIFF*CC(J,I-1,K)
C  **calculated new Q by EK**
C      first set X3 to the harmonic mean of cmob
      X3=(DELC(I)+DELC(I-1))/(DELC(I)/CMOB(J,I,K)+
      & DELC(I-1)/CMOB(J,I-1,K))
      X3=X3*HDIFF/((delc(I)+delc(I-1))/2)
      X3=X3*delr(J)*thk(J,I-1,K)
C
C6D----CALCULATE FLOW THROUGH THE FRONT FACE.
      90 IF(I.EQ.NROW) GO TO 120
      IF (IBOUND(J,I+1,K).EQ.0) GO TO 120
      HDIFF=HNEW(J,I,K)-HNEW(J,I+1,K)

```

A-30
LKMT.FOR Modifications

```

C      X4=HDIFF*CC(J,I,K)
C      **calculated new Q by EK**
C      first set X4 to the harmonic mean of cmob
C      X4=(DELC(I)+DELC(I+1))/(DELC(I)/CMOB(J,I,K)+
C      & DELC(I+1)/CMOB(J,I+1,K))
C
C      X4=X4*HDIFF/((delC(I)+delC(I+1))/2)
C      X4=X4*delR(J)*thk(J,I+1,K)
C
C6E----CALCULATE FLOW THROUGH THE UPPER FACE
120 IF(K.EQ.1) GO TO 150
    IF (IBOUND(J,I,K-1).EQ.0) GO TO 150
    HD=HNEW(J,I,K)
    IF(LC.NE.3 .AND. LC.NE.2) GO TO 122
    TMP=HD
    IF(TMP.LT.TOP(J,I,KT)) HD=TOP(J,I,KT)
122 HDIFF=HD-HNEW(J,I,K-1)
C      X5=HDIFF*CV(J,I,K-1)
C      **calculated new Q by EK**
C      first set X5 to the harmonic mean of cmob
C      X5=(thk(J,I,K)+thk(J,I,K-1))/
C      & (thk(J,I,K)/CMOB(J,I,K)+thk(J,I,K-1)/CMOB(J,I,K-1))
C
C      X5=X5*HDIFF/((thk(J,I,K)+thk(J,I,K-1))/2)
C      X5=X5*delR(J)*delC(I)
C
C6F----CALCULATE FLOW THROUGH THE LOWER FACE.
150 IF(K.EQ.NLAY) GO TO 180
    IF (IBOUND(J,I,K+1).EQ.0) GO TO 180
    HD=HNEW(J,I,K+1)
    IF(LAYCON(K+1).NE.3 .AND. LAYCON(K+1).NE.2) GO TO 152
    TMP=HD
    IF(TMP.LT.TOP(J,I,KT+1)) HD=TOP(J,I,KT+1)
152 HDIFF=HNEW(J,I,K)-HD
C      X6=HDIFF*CV(J,I,K)
C      **calculated new Q by EK**
C      first set X6 to the harmonic mean of cmob
C      X6=(thk(J,I,K)+thk(J,I,K+1))/
C      & (thk(J,I,K)/CMOB(J,I,K)+thk(J,I,K+1)/CMOB(J,I,K+1))
C
C      X6=X6*HDIFF/((thk(J,I,K)+thk(J,I,K+1))/2)
C      X6=X6*delR(J)*delC(I)
C
C12----SUM UP FLOWS THROUGH SIX SIDES OF CONSTANT HEAD CELL.
180 BUFF(J,I,K)=X1+X2+X3+X4+X5+X6
C
C      200 CONTINUE
C
C9----RECORD CONTENTS OF BUFFER.
WRITE(IOUT) KPER,KSTP,NCOL,NROW,NLAY,TEXT,NCNH
C
C2----IF THERE ARE NO CONSTANT-HEAD CELLS THEN SKIP
IF(NCNH.LE.0) GOTO 1000
C
C--WRITE CONSTANT-HEAD CELL LOCATIONS AND RATES
DO 900 K=1,NLAY
DO 900 I=1,NROW
DO 900 J=1,NCOL
IF (IBOUND(J,I,K).LT.0) WRITE(IOUT) K,I,J,BUFF(J,I,K)
900 CONTINUE
C
C17----RETURN
1000 RETURN
END
C
SUBROUTINE WEL1MT(NWELLS,MXWELL,WELL,IBOUND,
1  NCOL,NROW,NLAY,KSTP,KPER,IOUT,
2  econd,theta,thetas,thetao,expn,ekmob,valance,eqcond,
3  ecsoil,FY,AIS,BIS)
C *****
C SAVE WELL LOCATIONS AND RATES FOR USE IN MT3D.
C *****
C Modified from McDonald & Harbaugh, 1988
C last modified: 10-Aug-1990
C
CHARACTER*16 TEXT
DIMENSION WELL(4,MXWELL),IBOUND(NCOL,NROW,NLAY)REAL*4 factor,ceq,A,B
DIMENSION WELL(4,MXWELL),IBOUND(NCOL,NROW,NLAY),
6  econd(NCOL,NROW,NLAY),theta(NCOL,NROW,NLAY),
7  thetas(NCOL,NROW,NLAY),thetao(NCOL,NROW,NLAY),
8  expn(NCOL,NROW,NLAY),ecwater(NCOL,NROW,NLAY),
9  cmob(NCOL,NROW,NLAY),fy(NCOL,NROW,NLAY)
TEXT='WEL'
C
C
C      **added electrokinetic terms calcs.**
C      calculate constants for electric mobility adjustment
C      for concentration effects
C      A=(60.2*(ABS(valance))**.2)/[2*96500]
C      B=0.229*(ABS(valance))**.3
C      IONIC STRENGTH FROM ELECTRICAL COND CALCS. PARAMETERS
C      NOW BEING READ FROM INPUT FILE
C      AIS=.127
C      BIS=.002

```


A-32
LKMT FOR Modifications

```

C4-----WRITE WELL LOCATION AND RATE ONE AT A TIME
      DO 100 L=1,NWELLS
          IL=WELL(1,L)
          IR=WELL(2,L)
          IC=WELL(3,L)
C
C6-----IF CELL IS EXTERNAL Q=0
      Q=0.
      IF (IBOUND(IC,IR,IL).LE.0) GO TO 110
      Q=WELL(4,L)
C **ADJUST Q TO BE ELECTROKINETIC Q** (SEE PG 89 EDM)
      Q=Q*CMOB(IC,IR,IL)/ECWATER(IC,IR,IL)
      110 WRITE(IOUT) IL,IR,IC,Q
      100 CONTINUE
C
C11-----RETURN
      RETURN
      END
C
C
      SUBROUTINE DRN1MT(NDRAIN,MXDRN,DRAI,HNEW,
          1 NCOL,NROW,NLAY,IBOUND,KSTP,KPER,IOUT)
C *****
C CALCULATE AND SAVE DRAIN LOCATION AND RATES FOR USE IN MT3D
C *****
C Modified from McDonald & Harbaugh, 1988
C last modified: 10-Aug-1990
C
      CHARACTER*16 TEXT
      DOUBLE PRECISION HNEW
      DIMENSION DRAI(5,MXDRN),
          1 HNEW(NCOL,NROW,NLAY),IBOUND(NCOL,NROW,NLAY)
      TEXT='DRN'
C
C-----WRITE AN IDENTIFYING HEADER
      WRITE(IOUT) KPER,KSTP,NCOL,NROW,NLAY,TEXT,NDRAIN
C
C2-----IF THERE ARE NO DRAINS THEN SKIP
      IF (NDRAIN.LE.0) RETURN
C
C4-----FOR EACH DRAIN ACCUMULATE DRAIN FLOW
      DO 100 L=1,NDRAIN
C
C5-----GET LAYER, ROW & COLUMN OF CELL CONTAINING REACH.
          IL=DRAI(1,L)
          IR=DRAI(2,L)
          IC=DRAI(3,L)
C
C6-----IF CELL IS EXTERNAL Q=0
          Q=0.
          IF (IBOUND(IC,IR,IL).LE.0) GO TO 110
C
C7-----GET DRAIN PARAMETERS FROM DRAIN LIST.
          EL=DRAI(4,L)
          C=DRAI(5,L)
          HHNEW=HNEW(IC,IR,IL)
C
C8-----IF HEAD LOWER THAN DRAIN THEN FORGET THIS CELL.
          IF (HHNEW.LE.EL) GO TO 110
C
C9-----HEAD HIGHER THAN DRAIN. CALCULATE Q=C*(EL-HHNEW).
          Q=C*(EL-HHNEW)
C9-----SUBTRACT Q FROM RATOUT.
          Q=C*(EL-HHNEW)
C
C11-----WRITE DRAIN LOCATION AND RATE
          110 WRITE(IOUT) IL,IR,IC,Q
          100 CONTINUE
C
C15-----RETURN
      RETURN
      END
C
C
      SUBROUTINE RIV1MT(NRIVER,MXRIVR,RIVR,IBOUND,HNEW,
          1 NCOL,NROW,NLAY,KSTP,KPER,IOUT)
C *****
C SAVE RIVER LOCATIONS AND RATES FOR USE IN MT3D.
C *****
C Modified from McDonald & Harbaugh, 1988
C last modified: 10-Aug-1990
C
      CHARACTER*16 TEXT
      DOUBLE PRECISION HNEW
      DIMENSION RIVR(6,MXRIVR),IBOUND(NCOL,NROW,NLAY),
          1 HNEW(NCOL,NROW,NLAY)
      TEXT='RIV'
C
C-----WRITE AN IDENTIFYING HEADER
      WRITE(IOUT) KPER,KSTP,NCOL,NROW,NLAY,TEXT,NRIVER
C
C2-----IF NO REACHES SKIP
      IF (NRIVER.LE.0) RETURN
C
C4-----FOR EACH RIVER REACH ACCUMULATE RIVER FLOW
      DO 100 L=1,NRIVER

```

A-33
LKMT.FOR Modifications

```

C
C5-----GET LAYER, ROW & COLUMN OF CELL CONTAINING REACH.
      IL=RIVR(1,L)
      IR=RIVR(2,L)
      IC=RIVR(3,L)
C
C6-----IF CELL IS EXTERNAL RATE=0
      RATE=0.
      IF(IBOUND(IC,IR,IL).LE.0) GO TO 110
C
C7-----GET RIVER PARAMETERS FROM RIVER LIST.
      HRIV=RIVR(4,L)
      CRIV=RIVR(5,L)
      RBOT=RIVR(6,L)
      HHNEW=HNEW(IC,IR,IL)
C
C8-----COMPARE HEAD IN AQUIFER TO BOTTOM OF RIVERBED.
C
C9-----AQUIFER HEAD > BOTTOM THEN RATE=CRIV*(HRIV-HNEW).
      IF(HHNEW.GT.RBOT) RATE=CRIV*(HRIV-HHNEW)
C
C10-----AQUIFER HEAD < BOTTOM THEN RATE=CRIV*(HRIV-RBOT)
      IF(HHNEW.LE.RBOT) RATE=CRIV*(HRIV-RBOT)
C
C12-----WRITE RIVER REACH LOCATION AND RATE
110  WRITE(IOUT) IL,IR,IC,RATE
C
C 100 CONTINUE
C
C19-----RETURN
      RETURN
      END
C
C
      SUBROUTINE RCH1MT(NRCHOP,IRCH,RECH,IBOUND,NROW,NCOL,NLAY,
1  KSTP,KPER,BUFF,IOUT)
C *****
C SAVE RECHARGE LAYER INDICES (IF NLAY>1) AND RATES FOR USE IN MT3D.
C *****
C Modified from McDonald & Harbaugh, 1988
C last modified: 10-Aug-1990
C
      CHARACTER*16 TEXT
      DIMENSION IRCH(NCOL,NROW),RECH(NCOL,NROW),
1  IBOUND(NCOL,NROW,NLAY),BUFF(NCOL,NROW,NLAY)
      TEXT='RCH'
C
C-----WRITE AN IDENTIFYING HEADER
      WRITE(IOUT) KPER,KSTP,NCOL,NROW,NLAY,TEXT
C
C2-----CLEAR THE BUFFER.
      DO 2 IL=1,NLAY
      DO 2 IR=1,NROW
      DO 2 IC=1,NCOL
      BUFF(IC,IR,IL)=0.
2  CONTINUE
C
C3-----IF NRCHOP=1 RECH GOES INTO LAYER 1.
5  IF(NRCHOP.NE.1) GO TO 15
C
      IL=1
      IF(NLAY.GT.1) WRITE(IOUT) ((IL,J=1,NCOL),I=1,NROW)
C
C--IF EXTERNAL CELLS RECH=0
      DO 6 I=1,NROW
      DO 6 J=1,NCOL
      IL=1
      IF(IBOUND(J,I,IL).LE.0) RECH(J,I)=0
6  CONTINUE
      WRITE(IOUT) ((RECH(J,I),J=1,NCOL),I=1,NROW)
      GO TO 100
C
C4-----IF NRCHOP=2 RECH IS IN LAYER SHOWN IN INDICATOR ARRAY(IRCH).
15 IF(NRCHOP.NE.2)GO TO 25
C
      IF(NLAY.GT.1) WRITE(IOUT) ((IRCH(J,I),J=1,NCOL),I=1,NROW)
C
C--IF EXTERNAL CELLS RECH=0
      DO 16 I=1,NROW
      DO 16 J=1,NCOL
      IL=IRCH(J,I)
      IF(IBOUND(J,I,IL).LE.0) RECH(J,I)=0
16 CONTINUE
      WRITE(IOUT) ((RECH(J,I),J=1,NCOL),I=1,NROW)
      GO TO 100
C
C5-----IF OPTION=3 RECHARGE IS INTO HIGHEST INTERNAL CELL.
C-----FIND HIGHEST INTERNAL CELL AND STORE IT IN BUFFER
25 IF(NRCHOP.NE.3)GO TO 100
C
      DO 30 IR=1,NROW
      DO 30 IC=1,NCOL
      DO 28 IL=1,NLAY
C
C5A-----IF CELL IS CONSTANT HEAD MOVE ON TO NEXT HORIZONTAL LOCATION.

```


A-34
LKMT.FOR Modifications

```

        IF (IBOUND(IC,IR,IL).LT.0) THEN
            RECH(IC,IR)=0
            GO TO 30
        ENDIF
C
C5B-----IF CELL IS INACTIVE MOVE DOWN TO NEXT CELL.
        IF (IBOUND(IC,IR,IL).EQ.0) GO TO 28
        BUFF(IC,IR,1)=IL
        GO TO 30
C
        28 CONTINUE
        30 CONTINUE
C
        IF (NLAY.GT.1) WRITE(IOUT) ((INT(BUFF(J,I,1)),J=1,NCOL),I=1,NROW)
        WRITE(IOUT) ((RECH(J,I),J=1,NCOL),I=1,NROW)
C
        100 CONTINUE
C
C11-----RETURN
        RETURN
        END
C
C
        SUBROUTINE EVT1MT(NEVTOP,IEVT,EVTR,EXDP,SURF,IBOUND,HNEW,
            1  NCOL,NROW,NLAY,KSTP,KPER,BUFF,IOUT)
C *****
C SAVE EVAPOTRANSPIRATION LAYER INDICES (IF NLAY>1) AND RATES
C FOR USE IN MT3D.
C *****
C Modified from McDonald & Harbaugh, 1988
C last modified: 10-Aug-1990
C
        CHARACTER*16 TEXT
        DOUBLE PRECISION HNEW
        DIMENSION IEVT(NCOL,NROW),EVTR(NCOL,NROW),EXDP(NCOL,NROW),
            1  SURF(NCOL,NROW),IBOUND(NCOL,NROW,NLAY),
            2  HNEW(NCOL,NROW,NLAY),BUFF(NCOL,NROW,NLAY)
        TEXT='EVT'
C
C-----WRITE AN IDENTIFYING HEADER
        WRITE(IOUT) KPER,KSTP,NCOL,NROW,NLAY,TEXT
C
C2-----CLEAR THE BUFFER.
        DO 4 IL=1,NLAY
            DO 4 IR=1,NROW
                DO 4 IC=1,NCOL
                    BUFF(IC,IR,IL)=0.
                4 CONTINUE
C
C3-----PROCESS EACH HORIZONTAL CELL LOCATION
C-----AND STORE ET RATES IN BUFFER (IC,IR,1)
        DO 10 IR=1,NROW
            DO 10 IC=1,NCOL
C
C4-----SET THE LAYER INDEX EQUAL TO 1
            IL=1
C
C5-----IF OPTION 2 IS SPECIFIED THEN GET LAYER INDEX FROM IEVT ARRAY
            IF (NEVTOP.EQ.2) IL=IEVT(IC,IR)
C
C6-----IF CELL IS EXTERNAL THEN IGNORE IT.
            IF (IBOUND(IC,IR,IL).LE.0) GO TO 10
            C=EVTR(IC,IR)
            S=SURF(IC,IR)
            H=HNEW(IC,IR,IL)
C
C7-----IF AQUIFER HEAD => SURF,SET Q=MAX ET RATE
            IF (H.LT.S) GO TO 7
            Q=-C
            GO TO 9
C
C8-----IF DEPTH=>EXTINCTION DEPTH, ET IS 0
            X=EXDP(IC,IR)
            D=S-H
            IF (D.GE.X) GO TO 10
C
C9-----LINEAR RANGE . Q=-EVTR(H-EXEL)/EXDP
            Q=C*D/X-C
C
            9 CONTINUE
C
C11-----ADD Q TO BUFFER 1
            BUFF(IC,IR,1)=Q
            10 CONTINUE
C
C12-----RECORD THEM.
            IF (NLAY.GT.1.AND.NEVTOP.EQ.1)
                & WRITE(IOUT) ((1,J=1,NCOL),I=1,NROW)
            IF (NLAY.GT.1.AND.NEVTOP.EQ.2)
                & WRITE(IOUT) ((IEVT(J,I),J=1,NCOL),I=1,NROW)
            WRITE(IOUT) ((BUFF(J,I,1),J=1,NCOL),I=1,NROW)
C
C17-----RETURN
        RETURN
        END

```

A-35
LKMT.FOR Modifications

```
C
C
C      SUBROUTINE GHB1MT(NBOUND,MXBND,BNDS,HNEW,
C      1 NCOL,NROW,NLAY,IBOUND,KSTP,KPER,IOUT)
C .....
C SAVE HEAD DEP. BOUND. CELL LOCATIONS AND RATES
C FOR USE IN MT3D.
C .....
C Modified from McDonald & Harbaugh, 1988
C last modified: 10-Aug-1990
C
C      CHARACTER*16 TEXT
C      DOUBLE PRECISION HNEW
C      DIMENSION BNDS(5,MXBND),
C      1 HNEW(NCOL,NROW,NLAY),IBOUND(NCOL,NROW,NLAY)
C      TEXT='GHB'
C
C-----WRITE AN IDENTIFYING HEADER
C      WRITE(IOUT) KPER,KSTP,NCOL,NROW,NLAY,TEXT,NBOUND
C
C2-----IF NO BOUNDARIES THEN SKIP
C      IF(NBOUND.LE.0) RETURN
C
C4-----FOR EACH GENERAL HEAD BOUND ACCUMULATE FLOW INTO AQUIFER
C      DO 100 L=1,NBOUND
C
C5-----GET LAYER, ROW AND COLUMN OF EACH GENERAL HEAD BOUNDARY.
C      IL=BNDS(1,L)
C      IR=BNDS(2,L)
C      IC=BNDS(3,L)
C
C6-----IF CELL IS EXTERNAL RATE=0
C      RATE=0.
C      IF(IBOUND(IC,IR,IL).LE.0) GO TO 110
C
C7-----GET PARAMETERS FROM BOUNDARY LIST.
C      HHNEW=HNEW(IC,IR,IL)
C      HB=BNDS(4,L)
C      C=BNDS(5,L)
C
C8-----CALCULATE THE FOW RATE INTO THE CELL
C      RATE=C*(HB-HHNEW)
C
C10-----WRITE HEAD DEP. BOUND. LOCATION AND RATE
C      110 WRITE(IOUT) IL,IR,IC,RATE
C
C      100 CONTINUE
C
C17-----RETURN
C      RETURN
C      END
```

A-36
LKMT.INC Modifications

```

IMT3D=IUNIT(22)
IF (IMT3D.EQ.0) GO TO 9999
CALL BAS1MT(X(LCHNEW),X(LCIBOU),
2  NCOL,NROW,NLAY, KKSTP, KKPER, X(LCBUFF), IMT3D)
IF (IUNIT(1).GT.0) CALL BCF1MT(X(LCHNEW),X(LCIBOU),X(LCCR),
1  X(LCCC),X(LCCV),X(LCTOP),NCOL,NROW,NLAY, KKSTP, KKPER,
3  X(LCBUFF), IMT3D, X(LECOND), X(LTHETA), X(LTHETAS),
4  X(LTHETAO), X(LEKPN), EKMOB, VALANCE, EQCOND, X(LCDELR),
5  X(LCDELC), X(LTHK), ecsoil,x(lfy),ais,bis)
IF (IUNIT(2).GT.0) CALL WEL1MT(NWELLS, MXWELL,
1  X(LCWELL), X(LCIBOU), NCOL, NROW, NLAY, KKSTP, KKPER, IMT3D,
3  X(LECOND), X(LTHETA), X(LTHETAS),
4  X(LTHETAO), X(LEKPN), EKMOB, VALANCE, EQCOND, ecsoil,x(lfy),
5  ais,bis)
IF (IUNIT(3).GT.0) CALL DRN1MT(NDRAIN, MXDRN,
1  X(LCDRAI), X(LCHNEW), NCOL, NROW, NLAY, X(LCIBOU), KKSTP,
2  KKPER, IMT3D)
IF (IUNIT(8).GT.0) CALL RCH1MT(NRCHOP, X(LCIRCH), X(LCRECH),
1  X(LCIBOU), NROW, NCOL, NLAY, KKSTP, KKPER, X(LCBUFF), IMT3D)
IF (IUNIT(5).GT.0) CALL EVT1MT(NEVTOP, X(LCIEVT), X(LCEVTR),
1  X(LCEXDP), X(LCSURF), X(LCIBOU), X(LCHNEW), NCOL, NROW, NLAY,
2  KKSTP, KKPER, X(LCBUFF), IMT3D)
IF (IUNIT(4).GT.0) CALL RIV1MT(NRIVER, MXRIVR, X(LCRIVR), X(LCIBOU),
1  X(LCHNEW), NCOL, NROW, NLAY, KKSTP, KKPER, IMT3D)
IF (IUNIT(7).GT.0) CALL GH1MT(NBOUND, MXBND,
1  X(LCBNDS), X(LCHNEW), NCOL, NROW, NLAY, X(LCIBOU), KKSTP,
2  KKPER, IMT3D)
9999 CONTINUE

```

APPENDIX B. MODFLOW Input File Example: One-Dimensional Laboratory Dye Experiment

Appendix B includes example MODFLOW input files for a one-dimensional laboratory experiment. In order to save space, these example input files describe a simulation domain that contains 210 cells (each 0.001 m long) rather than the 2100 cells (each 0.0001 m long) described in Chapter 2. The files included in this appendix use the same nomenclature and format as described in the MODFLOW User's Manual (McDonald and Harbaugh, 1988).

BAS.dat is the code control file that sets up the problem. The input shown here is identical to the format described by McDonald and Harbaugh (1988, p. 4-9 – 4-12) with the exception that voltage is used rather than hydraulic head (data entry #8, Line 12, HEAD).

BCF.dat contains most of the input modifications to implement electromigration transport. Line 6 contains the ion mobility ($\text{m}^2 \text{v}^{-1} \text{s}^{-1}$), ion valence (-), depth of each cell (m), and the soil electrical conductivity of (S m^{-1}), all assigned 4F10.0 format. On line 8 are the slope and intercept to convert EC_w to ionic strength. Beginning on Line 9 there are a series of inputs in RARRAY format that describe the EC_a (S m^{-1}), θ ($\text{m}^3 \text{m}^{-3}$), θ_s ($\text{m}^3 \text{m}^{-3}$), θ_o ($\text{m}^3 \text{m}^{-3}$), the Mualem and Friedman model parameters $F(\lambda)$ (-) and n (-). The remainder of input included in this file are unchanged from the MODFLOW User's Manual (McDonald and Harbaugh, 1988).

WEL.dat is unchanged from the MODFLOW User's Manual example except that the well pumping and extraction rates are input as electrical current from electrodes (C s^{-1}).

References:

McDonald, M. C., and A. W. Harbaugh, 1988. "A Modular Three-Dimensional Finite-Difference Ground-Water Flow Model." USGS Open-file Report 83-875.

B-2
BAS.dat

1D TEST PROBLEM

EK testing of closed cell

11 09 00 0 0 0 0 0 00 00 0 0 22 19 00 00 00 00 00 00 00 00 66 00
00

0 0 IAPART, ISTRT
101 1(15I3) 3 IBOUND-1

2
1 1 1 210 1
1 1 210 210 -1
999.99

101 1(15F3.0) 4 HEAD-1

4
1 1 1 210 30
1.1 50 210 20
1 1 150 210 10
1 1 210 210 0

18000. 1 1. PERLEN, NSTP, TSMULT

B-3
BCF.dat

| | | | | | |
|---|--------------------------------|-------|-------------|-----------|------------------------|
| 0 | 1 | 0 | ISS, IBCFBD | | |
| | 0 | 1. | | | TRPY |
| | 0 | .001 | | | DELR |
| | 0 | .0191 | | | DELC |
| | 2.7e-8 | -2. | .1524 | .0028 | |
| | ekmob, valance, eqcond, ecsoil | | | | |
| | 0.127 | .002 | | | IS slope, IS intercept |
| | 101 | 1. | (4G10.4) | | 12 econd |
| 2 | | | | | |
| 1 | 1 | 1 | 210 | 0.6284e-2 | |
| 1 | 1 | 95 | 105 | 2.514e-02 | |
| | 101 | 1. | (4G10.4) | | 12 theta |
| 1 | | | | | |
| 1 | 1 | 1 | 210 | .135 | |
| | 101 | 1. | (4G10.4) | | 12 thetas |
| 1 | | | | | |
| 1 | 1 | 1 | 210 | .375 | |
| | 101 | 1. | (4G10.4) | | 12 thetao |
| 1 | | | | | |
| 1 | 1 | 1 | 210 | .03 | |
| | 101 | 1. | (4G10.4) | | 12 F(y) |
| 1 | | | | | |
| 1 | 1 | 1 | 210 | 2.73 | |
| | 101 | 1. | (4G10.4) | | 12 expn |
| 1 | | | | | |
| 1 | 1 | 1 | 210 | .5373 | |
| | 101 | .1524 | (4G10.4) | | 12 T-1a |
| 2 | | | | | |
| 1 | 1 | 1 | 210 | 0.6284e-2 | |
| 1 | 1 | 95 | 105 | 2.514e-02 | |

B-4
WEL.dat

| | | | |
|---|---|----------------|-----------|
| 2 | 0 | MXWELL, IWELCB | |
| 2 | | ITMP | |
| 1 | 1 | 1 | 0.010187 |
| 1 | 1 | 210 | -0.010187 |

APPENDIX C. MT3D Input File Example: One-Dimensional Laboratory Dye Experiment

Appendix C includes input files required to run an example MT3D simulation for the one-dimensional laboratory dye experiment described in Chapter 2. The three files included in this appendix are unchanged from those presented by Zheng (1990). `BTN.inp` is the control file, `DSP.inp` sets the dispersion input parameters, and `SSM.inp` defines the source/sink boundary conditions. See the description of these input files in Zheng's Appendix B (1990). Note that `PRSITY` in `BTN.inp` must match the input value for θ in `BCF.dat` (see Appendix B).

References:

Zheng C., 1990. "MT3D: A Modular Three-Dimensional Transport Model for Simulation of Advection, Dispersion and Chemical Reactions of Contaminants in Groundwater Systems." Report prepared for the U.S. EPA.

C-2
BTN.inp

1D TEST PROBLEM - EK TEST
STRIP DYE EXPERIMENT

| | | | | |
|---|--------|------------|----------------------|----------------------------|
| 1 | 1 | 210 | 1 | |
| !NLAY, NROW, NCOL, NPER | | | | |
| SEC | M | MOLES | !TUNIT, LUNIT, MUNIT | |
| T | T | T | F | !FADV, FDISP, FSSM, FREACT |
| 0 | | | | !LAYCON |
| | 0 | .001 | | !DELR |
| | 0 | .0191 | | !DELC |
| | 0 | .0 | | !HTOP |
| | 0 | .1524 | | !DZ-LAYER 1 |
| | 0 | .135 | | !PRSITY-LAYER 1 |
| | 101 | 1(15I3) | 3 | !ICBUND-LAYER 1 |
| 1 | | | | |
| 1 | 1 | 1 | 210 | 1 |
| | 101 | 1.(15F3.0) | 4 | !SCONC-1 |
| 2 | | | | |
| 1 | 1 | 1 | 210 | 0. |
| 1 | 1 | 95 | 105 | 20. |
| | | -999.00 | | !CINACT |
| | 9 | 8 | 8 | 8 |
| !IFMTCN, IFMTNP, IFMTRF, IFMTDP, UCNSAV | | | | |
| | 3 | | | !NPRS |
| | 3600 | 10800 | 18000 | !TIMPRS |
| | 0 | | | !NOBS |
| | T | | | !CHKMAS |
| | 18000. | 1 | 1. | !PERLEN, NSTP, TSMULT |
| | 3. | 50000 | | !DT0, MXSTRN |

C-3
DSP.inp

| | | | |
|--------------------------|---|----------|------|
| <input type="checkbox"/> | 0 | 0 | AL |
| <input type="checkbox"/> | 0 | 0 | TRPT |
| <input type="checkbox"/> | 0 | 0 | TRPV |
| <input type="checkbox"/> | 0 | 3.65E-10 | DM |

T F F F F F
□

2

1

1

1

1

0.

2

APPENDIX D. MODFLOW Output File Example: One-Dimensional Laboratory Dye Experiment

This appendix contains a MODFLOW output file called OUTPUT.txt for the example problem described in Appendix B. The MODFLOW output echoes the MODFLOW input (see Appendix B) and lists the calculated electric potential field. The details for the output file contents can be found in McDonald and Harbaugh (1988, pp. 4-14 – 4-17).

References:

McDonald, M. C., and A. W. Harbaugh, 1988. "A Modular Three-Dimensional Finite-Difference Ground-Water Flow Model." USGS Open-file Report 83-875.

D-11
OUTPUT.txt

| | | | | | | | | | | | | | | |
|-----|-----|-----|-----|-----|-----|-----|-----|-----|-----|-----|-----|-----|-----|-----|
| 135 | 121 | 122 | 123 | 124 | 125 | 126 | 127 | 128 | 129 | 130 | 131 | 132 | 133 | 134 |
| | 136 | 137 | 138 | 139 | 140 | 141 | 142 | 143 | 144 | 145 | 146 | 147 | 148 | 149 |
| 150 | 151 | 152 | 153 | 154 | 155 | 156 | 157 | 158 | 159 | 160 | 161 | 162 | 163 | 164 |
| 165 | 166 | 167 | 168 | 169 | 170 | 171 | 172 | 173 | 174 | 175 | 176 | 177 | 178 | 179 |
| 180 | 181 | 182 | 183 | 184 | 185 | 186 | 187 | 188 | 189 | 190 | 191 | 192 | 193 | 194 |
| 195 | 196 | 197 | 198 | 199 | 200 | 201 | 202 | 203 | 204 | 205 | 206 | 207 | 208 | 209 |
| 210 | | | | | | | | | | | | | | |

| | | | | | | | | | | | | | | |
|--------|--------|--------|--------|--------|--------|--------|--------|--------|--------|--------|--------|--------|--------|--------|
| 0 | 109.75 | 109.20 | 108.66 | 108.11 | 107.56 | 107.02 | 106.47 | 105.92 | 105.38 | 104.83 | 104.28 | 103.74 | 103.19 | 102.64 |
| 102.10 | 101.55 | 101.00 | 100.46 | 99.91 | 99.36 | 98.81 | 98.27 | 97.72 | 97.17 | 96.63 | 96.08 | 95.53 | 94.99 | 94.44 |
| 93.89 | 93.35 | 92.80 | 92.25 | 91.71 | 91.16 | 90.61 | 90.07 | 89.52 | 88.97 | 88.43 | 87.88 | 87.33 | 86.79 | 86.24 |
| 85.69 | 85.15 | 84.60 | 84.05 | 83.51 | 82.96 | 82.41 | 81.87 | 81.32 | 80.77 | 80.23 | 79.68 | 79.13 | 78.59 | 78.04 |
| 77.49 | 76.95 | 76.40 | 75.85 | 75.31 | 74.76 | 74.21 | 73.67 | 73.12 | 72.57 | 72.03 | 71.48 | 70.93 | 70.39 | 69.84 |
| 69.29 | 68.75 | 68.20 | 67.65 | 67.11 | 66.56 | 66.01 | 65.47 | 64.92 | 64.37 | 63.83 | 63.28 | 62.73 | 62.19 | 61.64 |
| 61.09 | 60.55 | 60.00 | 59.45 | 58.91 | 58.36 | 57.81 | 57.27 | 56.72 | 56.17 | 55.63 | 55.08 | 54.53 | 53.99 | 53.44 |
| 57.20 | 56.66 | 56.11 | 55.56 | 55.02 | 54.47 | 53.92 | 53.38 | 52.83 | 52.28 | 51.74 | 51.19 | 50.64 | 50.10 | 49.55 |
| 49.20 | 48.66 | 48.11 | 47.56 | 47.02 | 46.47 | 45.92 | 45.38 | 44.83 | 44.28 | 43.74 | 43.19 | 42.64 | 42.10 | 41.55 |
| 41.00 | 40.46 | 39.91 | 39.36 | 38.82 | 38.27 | 37.72 | 37.18 | 36.63 | 36.08 | 35.54 | 34.99 | 34.44 | 33.90 | 33.35 |
| 32.80 | 32.26 | 31.71 | 31.16 | 30.61 | 30.07 | 29.52 | 28.97 | 28.43 | 27.88 | 27.33 | 26.79 | 26.24 | 25.69 | 25.15 |
| 24.60 | 24.05 | 23.51 | 22.96 | 22.41 | 21.87 | 21.32 | 20.77 | 20.23 | 19.68 | 19.13 | 18.59 | 18.04 | 17.49 | 16.95 |
| 16.40 | 15.85 | 15.31 | 14.76 | 14.21 | 13.67 | 13.12 | 12.57 | 12.03 | 11.48 | 10.93 | 10.39 | 9.84 | 9.29 | 8.75 |
| 8.20 | 7.65 | 7.11 | 6.56 | 6.01 | 5.47 | 4.92 | 4.37 | 3.83 | 3.28 | 2.73 | 2.19 | 1.64 | 1.09 | 0.55 |
| 0.00 | | | | | | | | | | | | | | |
| 0 | | | | | | | | | | | | | | |

VOLUMETRIC BUDGET FOR ENTIRE MODEL AT END OF TIME STEP 1 IN STRESS PERIOD 1

| 0 L**3/T | CUMULATIVE VOLUMES | L**3 | RATES FOR THIS TIME STEP |
|-------------|-----------------------|---------|--------------------------|
| | IN: | | IN: |
| | STORAGE = | 0.00000 | STORAGE = |
| | CONSTANT HEAD = | 0.00000 | CONSTANT HEAD = |
| | WELLS = | 180.00 | WELLS = |
| 0.10000E-01 | TOTAL IN = | 180.00 | TOTAL IN = |
| 0 | OUT: | | OUT: |
| | STORAGE = | 0.00000 | STORAGE = |
| | CONSTANT HEAD = | 180.00 | CONSTANT HEAD = |
| 0.10000E-01 | WELLS = | 0.00000 | WELLS = |
| 0 | TOTAL OUT = | 180.00 | TOTAL OUT = |
| 0.10000E-01 | IN - OUT = | 0.00000 | IN - OUT = |
| 0 | PERCENT DISCREPANCY = | 0.00 | PERCENT DISCREPANCY = |
| 0.00 | | | |

0

| TIME SUMMARY AT END OF TIME STEP 1 IN STRESS PERIOD 1 | SECONDS | MINUTES | HOURS | DAYS | YEARS |
|---|---------|---------|---------|----------|--------------|
| TIME STEP LENGTH | 18000.0 | 300.000 | 5.00000 | 0.208333 | 0.570386E-03 |
| STRESS PERIOD TIME | 18000.0 | 300.000 | 5.00000 | 0.208333 | 0.570386E-03 |
| TOTAL SIMULATION TIME | 18000.0 | 300.000 | 5.00000 | 0.208333 | 0.570386E-03 |

1

APPENDIX E. MT3D Output File Example: One-Dimensional Laboratory Dye Experiment

This appendix contains the file OUTPUT.ek, the output from MT3D. The output file echoes the input from MT3D (see Appendix C), and lists the concentration in each cell at user specified times. Zheng (1990, pp. 6-8 – 6-13) describe the contents of the output file in detail.

References:

Zheng C., 1990. "MT3D: A Modular Three-Dimensional Transport Model for Simulation of Advection, Dispersion and Chemical Reactions of Contaminants in Groundwater Systems." Report prepared for the U.S. EPA.
OUTPUT.ek

E-3
OUTPUT.ek

| | INITIAL CONCENTRATION | | | | | | | | | | | | | FOR LAYER | 1 READ ON UNIT | 1 USING BLOCK FORMAT | |
|-----|-----------------------|-----|-----|-----|-----|-----|-----|-----|-----|-----|-----|-----|-----|-----------|----------------|----------------------|--|
| | 1 | 2 | 3 | 4 | 5 | 6 | 7 | 8 | 9 | 10 | 11 | 12 | 13 | 14 | | | |
| 15 | | | | | | | | | | | | | | | | | |
| 30 | 16 | 17 | 18 | 19 | 20 | 21 | 22 | 23 | 24 | 25 | 26 | 27 | 28 | 29 | | | |
| 45 | 31 | 32 | 33 | 34 | 35 | 36 | 37 | 38 | 39 | 40 | 41 | 42 | 43 | 44 | | | |
| 60 | 46 | 47 | 48 | 49 | 50 | 51 | 52 | 53 | 54 | 55 | 56 | 57 | 58 | 59 | | | |
| 75 | 61 | 62 | 63 | 64 | 65 | 66 | 67 | 68 | 69 | 70 | 71 | 72 | 73 | 74 | | | |
| 90 | 76 | 77 | 78 | 79 | 80 | 81 | 82 | 83 | 84 | 85 | 86 | 87 | 88 | 89 | | | |
| 105 | 91 | 92 | 93 | 94 | 95 | 96 | 97 | 98 | 99 | 100 | 101 | 102 | 103 | 104 | | | |
| 120 | 106 | 107 | 108 | 109 | 110 | 111 | 112 | 113 | 114 | 115 | 116 | 117 | 118 | 119 | | | |
| 135 | 121 | 122 | 123 | 124 | 125 | 126 | 127 | 128 | 129 | 130 | 131 | 132 | 133 | 134 | | | |
| 150 | 136 | 137 | 138 | 139 | 140 | 141 | 142 | 143 | 144 | 145 | 146 | 147 | 148 | 149 | | | |
| 165 | 151 | 152 | 153 | 154 | 155 | 156 | 157 | 158 | 159 | 160 | 161 | 162 | 163 | 164 | | | |
| 180 | 166 | 167 | 168 | 169 | 170 | 171 | 172 | 173 | 174 | 175 | 176 | 177 | 178 | 179 | | | |
| 195 | 181 | 182 | 183 | 184 | 185 | 186 | 187 | 188 | 189 | 190 | 191 | 192 | 193 | 194 | | | |
| 210 | 196 | 197 | 198 | 199 | 200 | 201 | 202 | 203 | 204 | 205 | 206 | 207 | 208 | 209 | | | |

| | | | | | | | | | | | | | | | | | |
|-------|------|------|------|------|-------|-------|-------|-------|-------|-------|-------|-------|-------|-------|-------|-------|-------|
| 1 | 0.00 | 0.00 | 0.00 | 0.00 | 0.00 | 0.00 | 0.00 | 0.00 | 0.00 | 0.00 | 0.00 | 0.00 | 0.00 | 0.00 | 0.00 | 0.00 | 0.00 |
| 0.00 | 0.00 | 0.00 | 0.00 | 0.00 | 0.00 | 0.00 | 0.00 | 0.00 | 0.00 | 0.00 | 0.00 | 0.00 | 0.00 | 0.00 | 0.00 | 0.00 | 0.00 |
| 0.00 | 0.00 | 0.00 | 0.00 | 0.00 | 0.00 | 0.00 | 0.00 | 0.00 | 0.00 | 0.00 | 0.00 | 0.00 | 0.00 | 0.00 | 0.00 | 0.00 | 0.00 |
| 0.00 | 0.00 | 0.00 | 0.00 | 0.00 | 0.00 | 0.00 | 0.00 | 0.00 | 0.00 | 0.00 | 0.00 | 0.00 | 0.00 | 0.00 | 0.00 | 0.00 | 0.00 |
| 0.00 | 0.00 | 0.00 | 0.00 | 0.00 | 0.00 | 0.00 | 0.00 | 0.00 | 0.00 | 0.00 | 0.00 | 0.00 | 0.00 | 0.00 | 0.00 | 0.00 | 0.00 |
| 0.00 | 0.00 | 0.00 | 0.00 | 0.00 | 0.00 | 0.00 | 0.00 | 0.00 | 0.00 | 0.00 | 0.00 | 0.00 | 0.00 | 0.00 | 0.00 | 0.00 | 0.00 |
| 0.00 | 0.00 | 0.00 | 0.00 | 0.00 | 20.00 | 20.00 | 20.00 | 20.00 | 20.00 | 20.00 | 20.00 | 20.00 | 20.00 | 20.00 | 20.00 | 20.00 | 20.00 |
| 20.00 | 0.00 | 0.00 | 0.00 | 0.00 | 0.00 | 0.00 | 0.00 | 0.00 | 0.00 | 0.00 | 0.00 | 0.00 | 0.00 | 0.00 | 0.00 | 0.00 | 0.00 |
| 0.00 | 0.00 | 0.00 | 0.00 | 0.00 | 0.00 | 0.00 | 0.00 | 0.00 | 0.00 | 0.00 | 0.00 | 0.00 | 0.00 | 0.00 | 0.00 | 0.00 | 0.00 |
| 0.00 | 0.00 | 0.00 | 0.00 | 0.00 | 0.00 | 0.00 | 0.00 | 0.00 | 0.00 | 0.00 | 0.00 | 0.00 | 0.00 | 0.00 | 0.00 | 0.00 | 0.00 |
| 0.00 | 0.00 | 0.00 | 0.00 | 0.00 | 0.00 | 0.00 | 0.00 | 0.00 | 0.00 | 0.00 | 0.00 | 0.00 | 0.00 | 0.00 | 0.00 | 0.00 | 0.00 |
| 0.00 | 0.00 | 0.00 | 0.00 | 0.00 | 0.00 | 0.00 | 0.00 | 0.00 | 0.00 | 0.00 | 0.00 | 0.00 | 0.00 | 0.00 | 0.00 | 0.00 | 0.00 |
| 0.00 | 0.00 | 0.00 | 0.00 | 0.00 | 0.00 | 0.00 | 0.00 | 0.00 | 0.00 | 0.00 | 0.00 | 0.00 | 0.00 | 0.00 | 0.00 | 0.00 | 0.00 |
| 0.00 | 0.00 | 0.00 | 0.00 | 0.00 | 0.00 | 0.00 | 0.00 | 0.00 | 0.00 | 0.00 | 0.00 | 0.00 | 0.00 | 0.00 | 0.00 | 0.00 | 0.00 |
| 0.00 | 0.00 | 0.00 | 0.00 | 0.00 | 0.00 | 0.00 | 0.00 | 0.00 | 0.00 | 0.00 | 0.00 | 0.00 | 0.00 | 0.00 | 0.00 | 0.00 | 0.00 |
| 0.00 | 0.00 | 0.00 | 0.00 | 0.00 | 0.00 | 0.00 | 0.00 | 0.00 | 0.00 | 0.00 | 0.00 | 0.00 | 0.00 | 0.00 | 0.00 | 0.00 | 0.00 |

VALUE INDICATING INACTIVE CONCENTRATION CELLS = -999.0000

OUTPUT CONTROL OPTIONS

PRINT CELL CONCENTRATION USING FORMAT CODE: 9
 PRINT PARTICLE NUMBER IN EACH CELL USING FORMAT CODE: 8
 PRINT RETARDATION FACTOR USING FORMAT CODE: 8
 PRINT DISPERSION COEFFICIENT USING FORMAT CODE: 8
 SAVE CONCENTRATION IN UNFORMATTED FILE [MT3D.UCN] ON UNIT 18

NUMBER OF TIMES AT WHICH SIMULATION RESULTS ARE SAVED = 3
 TOTAL ELAPSED TIMES AT WHICH SIMULATION RESULTS ARE SAVED:
 3600.0 10800. 18000.

NUMBER OF OBSERVATION POINTS = 0

A ONE-LINE SUMMARY OF MASS BALANCE FOR EACH STEP SAVED IN FILE [MT3D.MAS] ON UNIT 19

MAXIMUM LENGTH ALONG THE X (J) AXIS = 0.2100002
 MAXIMUM LENGTH ALONG THE Y (I) AXIS = 0.1910000E-01
 MAXIMUM LENGTH ALONG THE Z (K) AXIS = 0.1524000

ADVECTION SOLUTION OPTIONS

DISPERSION PARAMETERS

E-9
OUTPUT.ek

0.00 0.00 0.00 0.00 0.00 0.00 0.00 0.00 0.00 0.00

CUMMULATIVE MASS BUDGETS AT END OF TRANSPORT STEP 6000, TIME STEP 1, STRESS PERIOD 1

| | IN | OUT |
|-------------------------|-------------------|--------------------|
| CONSTANT CONCENTRATION: | 0.0000000 | 0.0000000 |
| CONSTANT HEAD: | 0.0000000 | 0.0000000 |
| WELLS: | 0.0000000 | -0.6519727E-24 |
| MASS STORAGE (SOLUTE): | 0.6160047E-04 | -0.6160032E-04 |
| [TOTAL]: | 0.6160047E-04 MOL | -0.6160032E-04 MOL |
| NET (IN - OUT): | 0.1455192E-09 | |
| DISCREPANCY (PERCENT): | 0.2362309E-03 | |

| M T |
| 3 D | End of Model Output

APPENDIX F. Experimental Electrode Control System

The field demonstration was housed in two main buildings, the Electrokinetics (EK) Control Trailer and the Greenhouse (FIG F-1). The Control Trailer was located immediately outside the Chemical Waste Landfill boundary fence and housed the electrode operation control panels (FIG F-2), the data logging system, and other data analysis equipment. The Greenhouse was located on the Chemical Waste Landfill and protected the on-site equipment, electrodes, secondary containment, and personnel from the weather as well as provided an operational exclusion zone while the electrodes were energized. The two buildings were approximately 23 m (75 ft) apart and were connected by four, 7.6-cm (3-in) electrical conduits that provided protection for the numerous signal and control cables.

For the EK remediation system described in this appendix, a portion of the electrode casing functioned as a suction lysimeter, and an electrode was placed inside the lysimeter. A suction lysimeter is a device which uses a porous material that exhibits a high bubbling pressure (the pressure at which air will pass through a material when submersed in water) to extract pore water samples from the unsaturated zone. To collect a pore water sample, a vacuum is applied to the inside of the lysimeter. Depending on the magnitude of the applied vacuum and the tension in the unsaturated zone around the lysimeter, the direction of the pressure gradient across the porous material will either cause water to flow into or out of the lysimeter. Therefore, suction lysimeters offer a technique to control the addition and extraction of water in the unsaturated zone. By the application of a vacuum to the lysimeter, water can be added to the soil, but saturated conditions can never develop.

A 1.8-m (6-ft) portion of the electrode casing was constructed of porous ceramic that acted as the lysimeter. The upper portion of the electrode was constructed of an impermeable, non-conducting PVC material. The fluid between the electrode and the ceramic casing was continuously re-circulated to remove contaminants that entered the electrode, to clear the electrode of gas bubbles formed by water electrolysis, and to mitigate hydrolysis reactions. The solution extracted from the electrode lysimeter could be treated at the ground surface.

All electrode casings were constructed in a similar manner. The portion of the casing that allowed the transfer of current and water was constructed of porous ceramic. This porous-ceramic section of the electrode was constructed from two, 0.9-m (3-ft) tube sections. The porous ceramic was positioned between 2.4 and 4.3 m (8 and 14 ft) below land surface (BLS). The remainder of the electrode casing was made of 7.6-cm (3-in) schedule 40 PVC pipe and fittings. The ceramic was connected to the PVC fittings by grinding the interior surface of the PVC fitting with a drum sander and gluing the ceramic to the reamed PVC fitting using 3M[®] 2216 epoxy adhesive.

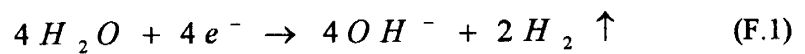
Due to the high negative zeta potential on the ceramic surface and the direction of the voltage gradient, the surfaces of the ceramic in the anodes were treated to prevent movement of water out of the anodes by electroosmosis. By treating the ceramic with a surfactant material to alter the charge on the ceramic surface, electroosmosis can be significantly decreased. The ceramic was first acid washed with a 0.1 molar HCl solution until the pH of the effluent equaled that of the influent. At this time, it was assumed that all of the surface sites were loaded with hydrogen ions. A deionized water rinse was used to remove the excess acid from the ceramic pores. Finally, a 0.01 molar hexadecyltrimethylammonium (HDTMA) hydroxide solution was purged through the ceramic. The reaction of the HDTMA-OH with the hydrogen ions on the

ceramic surface replaced the hydrogen ions with HDTMA molecules. The HDTMA likely formed a double layer on the surface of the ceramic reversing the effective charge from negative to positive on the ceramic surface. The ceramic material for the cathode electrode casings was not treated.

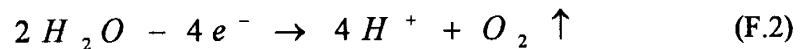
F-1.1 Vacuum Control System

To retain water in the porous-ceramic electrode casing, a vacuum was applied to the air head space within the EK electrode (FIG F-3). This vacuum system also allowed an air-purge system to be incorporated into the electrode design to prevent explosive conditions from developing in the head space. Each electrode type (anode or cathode) had a separate vacuum system to prevent mixing of the hydrogen and oxygen gases.

The transfer of current from an electrode to an electrolytic fluid involves the oxidation or reduction of the fluid or an ion within the fluid. If water is the oxidized/reduced species, then the reduction reaction at the cathode is:



Similarly, the oxidation reaction at the anode is:



An air stream was allowed to enter through the cathodes to prevent hydrogen levels from reaching explosive limits. The lower explosive limit of hydrogen gas is 4% (CRC, 1970).

Assuming that 15 amps is the maximum current each cathode could transfer (set by the power

supplies and the in-line fuse) and that all of the current transferred between the electrode and the electrolytic fluid produced hydrogen via Equation F.1, the amount of air purge needed to maintain hydrogen levels at the lower explosive limit could be calculated.

Fifteen amps will transfer 9.3 mmol of charge per min as illustrated in Equation F.3.

$$15A * 1 \frac{C}{A \cdot s} * \frac{1M_{charge}}{96500C} * \frac{60s}{min} = 9.3 \frac{mM_{charge}}{min} \quad (F.3)$$

Since each mole of charge produces 0.5 moles of hydrogen gas (Equation F.1), 4.65 mmoles of H₂ will be produced per minute.

The volume rate of hydrogen gas production can be calculated via the Ideal Gas Law. Assuming atmospheric conditions at Albuquerque (0.85 atm), 0.13 liters of hydrogen gas is produced each minute by the application of 15 amps (Equation F.4).

$$R_{H_2} = 4.65 \frac{mM_{H_2}}{min} * \frac{82.06cm^3 * atm}{mol * K} * \frac{293K}{0.85atm} = 0.13 \frac{L}{min} \quad (F.4)$$

where R_{H_2} = rate of hydrogen gas generation (L/min).

Finally, the rate of air purge need to maintain hydrogen gas at the lower explosive limit is 3.3 L/min as calculated below.

$$R_{air} = 0.13 \frac{L_{H_2}}{min} * \frac{1}{0.04} = 3.3 \frac{L_{air}}{min} \quad (F.5)$$

where R_{air} = rate of air purge required (L/min).

The purge alarm rates were set at 3.5 L/min, and the actual purge rate was maintained at approximately 8 L/min to ensure the hydrogen gas concentrations were maintained well below the explosive limit. Air was also purged through each cathode at a rate of 2 L/min to dilute the oxygen gas produced at that electrode.

A 10 HP Quincy^{®1} Model 370 air compressor provided compressed air to operate a series of PIAB^{™2} vacuum ejector pumps. The compressed air was driven through a series of venturies within the vacuum pump causing additional air to be drawn through the venturi system. This air-driven venturi system has the additional safety feature of being explosion proof.

The vacuum of the cathode system was created with a series of three parallel PIAB[®] MLD25 pumps which were able to produce 96.8 cm (27.5 in) of Hg. The anode vacuum system used four parallel PIAB[®] LX10 vacuum pumps. Each vacuum system was connected to separate manifold systems to evacuate five anodes or five cathodes. The compressed air pressure was set for each vacuum system so that each system operated at its optimal performance.

Rather than directly regulating the vacuum applied to the EK electrode, Moore^{®3} Model 44-20 vacuum regulators allowed air to enter the electrode to dilute hydrogen and oxygen gases being generated by the electrode reactions. This air flow was monitored by McMillan^{®4} flow

¹ Quincy[®] is a registered trademark of Coltec Industries, Quincy Compressor Division

² PIAB[™] is a trademark of PIAB Vacuum Technique, Sweden

³ Moore[®] is a registered trademark of Moore Products Co.

⁴ McMillan[®] is a registered trademark of McMillan Company

sensors (Model 100-8 for the anodes or Model 100-10 for the cathodes) connected to McMillan® bar graph displays. The vacuum regulators were adjusted to provide adequate flow rates through the electrodes, and generally the vacuum was maintained at 35.6 cm (14 in) of Hg for both the anodes and the cathodes.

F-1.2 Liquid Control System

The liquid control system can be divided into two separate parts, the water-circulation system (FIG F-4) and the electrode water-level control (FIG F-5).

The water-circulation system was powered by a QED®⁵ P1101S bladder pump contained in the EK drive electrode with the screen portion of the pump extending into the electrode casing sump. All parts of this pump were plastic to prevent corrosion. The pump housed a dura-flex teflon bladder which, when inflated, filled with liquid. During subsequent deflation of the bladder, the liquid contained in the bladder was driven through the circulation system and returned back to the EK electrode casing just above the drive electrode (FIG F-4).

The circulation system was employed to monitor the chemical condition of the liquid in the electrode, to cool the liquid in the electrode, and to sample and remove liquid from the electrode. A manual sampling port was located at the ground surface, just after the liquid left the EK electrode. This sampling port had a PVC ball valve which, when opened, allowed a sample to be collected while the bladder was deflating. With the sampling port in the normally closed position, the liquid then passed through a McMillan® Model 100-8T flow sensor, and the output was displayed on a McMillan® 220 flow rate/total digital display in the control rack (FIG F-2).

Due to ohmic heating of the water in the electrode and of the surrounding soil, the temperature of the recycle water was monitored by a Campbell Scientific[®] 108B temperature probe. An ITT Bell & Gossett BP Honeycomb^{™6} heat exchanger (Model 410-30 for cathodes and Model 410-40 for anodes) cooled the recycle water. Remcor^{®7} (Model CH-3002-A) chillers circulated deionized water at approximately 6 °C at a rate of 5.6 L/min (1.5 gal/min) to each heat exchanger to remove the excess heat. This cooling system maintained the water temperature in the electrodes at approximately 8 to 10 °C.

After water passed through the heat exchanger, the recycle water conductivity was measured by an inline Signet^{®8} 2820 conductivity sensor. This sensor was connected to a Signet[®] 9050 Intelek-Pro^{™9} conductivity controller in the field trailer. The conductivity controller was used only as a display to observe the electrode fluid conductivity. Each conductivity controller had two separate input channels allowing two electrodes to be monitored by one conductivity meter.

At 30-minute intervals, the effluent batch controllers (Signet[®] 9020 Intelek-Pro[®] Batch Controller) in the control trailer sent a signal to a three-way, air-operated, PVC solenoid valve (FIG F-4) to redirect the recycle water to the effluent barrels. The effluent was collected in 208-L (55-gal), closed-top, polypropylene barrels. The flow of recycle water to the effluent barrels was monitored by a McMillan[®] (Model 100-5T) flow sensor. After a set amount passed the effluent sensor (user specified at rates of 0.1 to 0.5 liters/30 minutes depending the test), the conductivity

⁵ QED[®] is a registered trademark of Q.E.D. Environmental Systems, Inc.

⁶ ITT Bell & Gossett Honeycomb[™] is a trademark of ITT Bell & Gossett

⁷ Remcor[®] is a registered trademark of Remcor Products Company

⁸ Signet[®] is a registered trademark of George Fischer Signet, Inc.

⁹ Intelek-Pro[™] is a trademark of George Fischer Signet, Inc.

controller sent a signal to de-energize the three-way valve to let the recycle water return to the electrode.

A Squire-Cogswell^{®10} M30A02 liquid ring vacuum pump was used to re-inflate the bladder in the bladder pump causing water to enter the bladder. Normally, these bladder pumps are used to sample groundwater from monitoring wells. In typical groundwater sampling situations, the static pressure of the water column allows water to fill the bladder. In our system, the water pressure at the pump in the EK electrode is sub-atmospheric due to the vacuum applied to the head space of the electrode, hence the need to re-inflate the bladder. The water was expelled by squeezing the bladder with pressurized air set at approximately 20 psi. A ChronTrol^{®11} (Model XT 4 S) timer module activated a three-way valve at three-second intervals to alternate between air pressure and vacuum to the pump bladder (FIG F-5). This system resulted in recycle flow rates of approximately 4 L/min.

The water level in the EK electrode was maintained above the ceramic/PVC interface with two sets of reed-type, water-level, float switches (Flowline^{®12} Model LV10 series). The two middle switches, spaced approximately 15.2 cm (6 in) apart, were connected to a dual-float switch controller (Levelite^{®13} Model GLL 100000) which opened and closed an influent solenoid valve (FIG F-5) to allow water to enter the electrode. The upper and lower floats acted as high and low alarm switches for water-level control failure. The water entering the electrode was monitored by a McMillan[®] (Model 100-5T) flow sensor connected to a McMillan[®] digital flow-rate/total-flow meter. Separate 946-L (250-gal) PE storage tanks (one for the anodes and one for

¹⁰ Squire-Cogswell[®] is a registered trademark of Squire-Cogswell Company

¹¹ ChronTrol[®] is a registered trademark of Linberg Enterprises

¹² Flowline[®] is a registered trademark of Flowline Inc.

¹³ Levelite[®] is a registered trademark of Levelite/Genelco, Div. Of Bindicator Co.

the cathodes) contained the influent water source; these tanks were monitored visually for water use.

F-1.3. Power Application System

The EK electrodes were energized using a series of four 10-kW power supplies (Sorensen^{®14} Model DTR-600-16T). Each power supply was capable of outputting 16 A at 600 V dc. The power supplies could either be operated in parallel mode using a parallel interface controller (PIC) (Sorensen[®] Model PICTM9A) providing up to 64 amps at 600 volts to the system (FIG F-6A) or be operated independently so that each power supply energized one set of electrodes (FIG F-6B).

In either case, the system contained a manual main disconnect to lockout power application while performing maintenance on the EK system. The amount of current to each electrode was limited by 15-amp in-line fuses and monitored by measuring the voltage drop across a 20 amp/100mV shunt with a Newport^{®15} Model 504 isolated current transmitter. This current transmitter output a 4 to 20 milliamp signal that was subsequently converted to a 1- to 5-volt signal with a precision 250-ohm resistor. The current was displayed on the control panel through a Simpson^{®16} M235 digital display.

Care was taken in choosing and installing monitoring equipment to ensure it was electrically isolated from the DC power supplies and earth ground. Anodes and cathodes can have voltage differentials as high as 600 volts between them as well as hundreds of volts between

¹⁴ Sorensen[®] is a registered trademark of Sorensen Company, A Division of ELGAR Corporation

¹⁵ Newport[®] is a registered trademark of Newport Electronics, Inc.

the electrodes and earth ground. In addition, the liquid contained in the electrodes and recirculation systems can also have sufficient voltage potentials to require monitoring equipment to be electrically isolated. Equipment that is not electrically isolated will allow some of the applied current to short circuit between the electrodes.

F-1.4. pH Control System

The pH of the electrode solutions was controlled in the range of 8.8 for the anodes and 5.5 for the cathodes. As illustrated above in Equations F.1 and F.2, hydroxyl ions are produced in the cathodes and hydrogen ions are produced in the anodes due to the electrolysis reactions at the electrodes. Researchers (Acar et al., 1989 and 1990) who have not neutralized these electrode reactions have reported pH values adjacent to anodes and cathodes of 2 and 12, respectively. These extreme pH values can have geochemical effects such as precipitation of contaminant ions and dissolution of calcium carbonate in the soil. By neutralizing the electrode reactions, the dissolution of the soil and the build up of precipitates in the pores in the of the soil, which could hinder electromigration, can be minimized.

A series of pH sensors, transmitters, controllers, and chemical feed pumps monitored and controlled the pH of the recycle water (FIG F-7). A Cole-Parmer^{®17} (Model 27001-97) pH electrode emitted a signal which was converted to a milliamp signal by a Jenco^{®18} (Model 695PH) current transmitter. A Signet[®] 9030 pH controller in the control panel subsequently converted this signal to a pH value. The pH controller emitted a pulse signal at a rate proportional to the user specified pH set point, deviation range, and maximum pulse rate. The

¹⁶ Simpson[®] is a registered trademark of Simpson Electronic Company

¹⁷ Cole-Parmer[®] is a registered trademark of Cole-Parmer Instrument Company

¹⁸ Jenco[®] is a registered trademark of Jenco Electronics, Ltd.

pulse signal controlled the pumping rate of a ProMinent^{®19} (Model G/4a) chemical feed pump located on top of a 208-L (55-gal), polypropylene drum adjacent to the EK demonstration site. This drum contained either 10 wt% NaOH to control the pH in the anodes or 20 wt% acetic acid for cathode pH control. A 30 psi stainless steel pressure relief valve provided adequate back pressure of the neutralization solution to prevent siphoning of the solution into the electrode.

F-1.5 Monitoring System

A CR7 data logger (Campbell Scientific[®], Inc.) recorded the operating parameters of the EK demonstration and automatically shut the system down and notified the operators if any parameters were out of tolerance. The data logger monitored operational parameters at one-minute intervals and stored the average of each of these parameters in a storage module each hour. If a measured parameter was out of tolerance during a one-minute reading, the data logger would store that set of parameter readings on the storage module and send a coded message, identifying the type of problem, via a cellular phone to two separate pagers held by two operators.

The data logger monitored the vacuum level and the air purge rate for the vacuum system (Section F-1.1). The system would shut down if the vacuum level was below 7.6 cm (3 in) of Hg (the required vacuum to keep the water column in the EK electrode under tension) or if the air purge rate of the cathodes was below 3.5 liters per minute (the minimum rate necessary to dilute the hydrogen gas to 4%).

The influent, effluent, and recycle rates, water temperature, conductivity, and high-low water level alarms were monitored for the liquid circulation system (Section F-1.2). The influent,

¹⁹ ProMinent[®] is a registered trademark of ProMinent Fluid Controls, Inc.

effluent, and recycle rates were qualitatively recorded by the CR7. It was originally thought that quantitative numbers could be obtained, but stray voltages produced some false readings by the CR7. To compensate for the lack of automatic recording of flow data, readings were recorded manually from the control panel meters approximately once per day. Of the three flow sensors, only the recycle rate would activate the CR7 alarm system if no recycling was detected. An electrode water temperature of over 60 °C would trigger an alarm response. The high and low water alarm floats (FIG F-5) would also activate the CR7 alarm system if either float was switched from its normal position. The current for each electrode also was recorded by the CR7 through the power system (Section F-1.3), but no alarms were necessary.

The pH of each electrode was also monitored. An alarm was activated if any cathode pH was less than 3 or greater than 11 or any anode pH was less than 5.5 or greater than 11. The lower pH level of the anodes was set higher than the cathode pH level due to the treatment of the ceramic on the anodes. At low pH levels the ceramic treatment could have desorbed from the ceramic surface.

In addition to monitoring each individual EK electrode, the CR7 also recorded some field measurements. The soil temperatures immediately outside of the active EK electrodes, as well as an additional fourteen temperature locations in the field were monitored. Temperatures over 60 °C would shut down the process and notify the operators.

A series of 27 voltage probes also was monitored by the CR7. These voltage probes consisted of stainless steel screens placed in the ground and connected to voltage divider devices so that the voltages could be recorded by the CR7. The only alarm activation would have been a measurement of a step potential over 10 volts at a location approximately 2.4 m (8 ft) west of the EK demonstration (see FIG F-1).

The CR7 data logger also monitored a number of secondary containment float detectors for leaks, full effluent barrel sensors, an alarm which indicated an open gate to the green house exclusion zone, and a "panic" button shut down of the system. If any of the above described sensors were activated, the system would be shut down and the operator notified.

An automatic shutdown controlled by the CR7 consisted of turning off the power to the EK electrodes, closing the water influent valves, de-energizing all influent and effluent solenoids, and discontinuing the pumping of neutralization solutions to the electrodes. In some cases, pumping the electrode water through the recycle board would also be terminated.

REFERENCES

- Acar, Y.B., R.J. Gale, G. Putnam, and J. Hamed, 1989. "Electrochemical Processing of Soils: Its Potential Use in Environmental Geotechnology and Significance of pH Gradients." *2nd International Symposium on Environmental Geotechnology*, Shanghai, China, May 14-17. Envo Publishing, Bethlehem, PA, Vol. 1, pp. 25-38.
- Acar, Y.B., R.J. Gale, and G. Putnam, 1990. "Electrochemical Processing of Soils: Theory of pH Gradient Development by Diffusion and Liner Convection." *Journal of Environmental Science and Health, Part (a); Environmental Science and Engineering*, Vol. 25, No. 6, pp. 687-714.
- CRC (The Chemical Rubber Company), 1971. *Handbook of Chemistry and Physics - 1970-1971*. Section 4, p. D82.

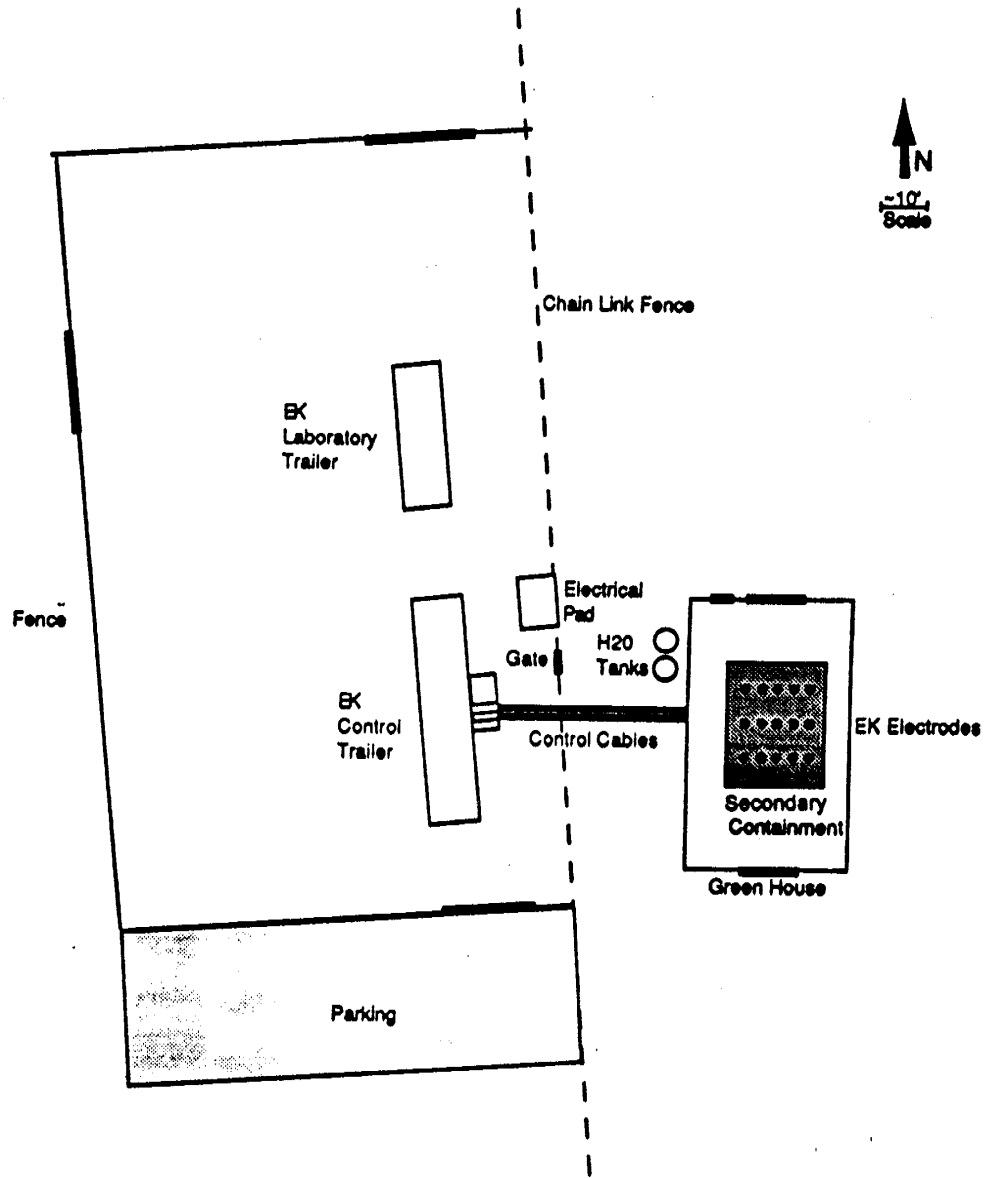


FIG. F-1. Electrokinetic demonstration plan view.

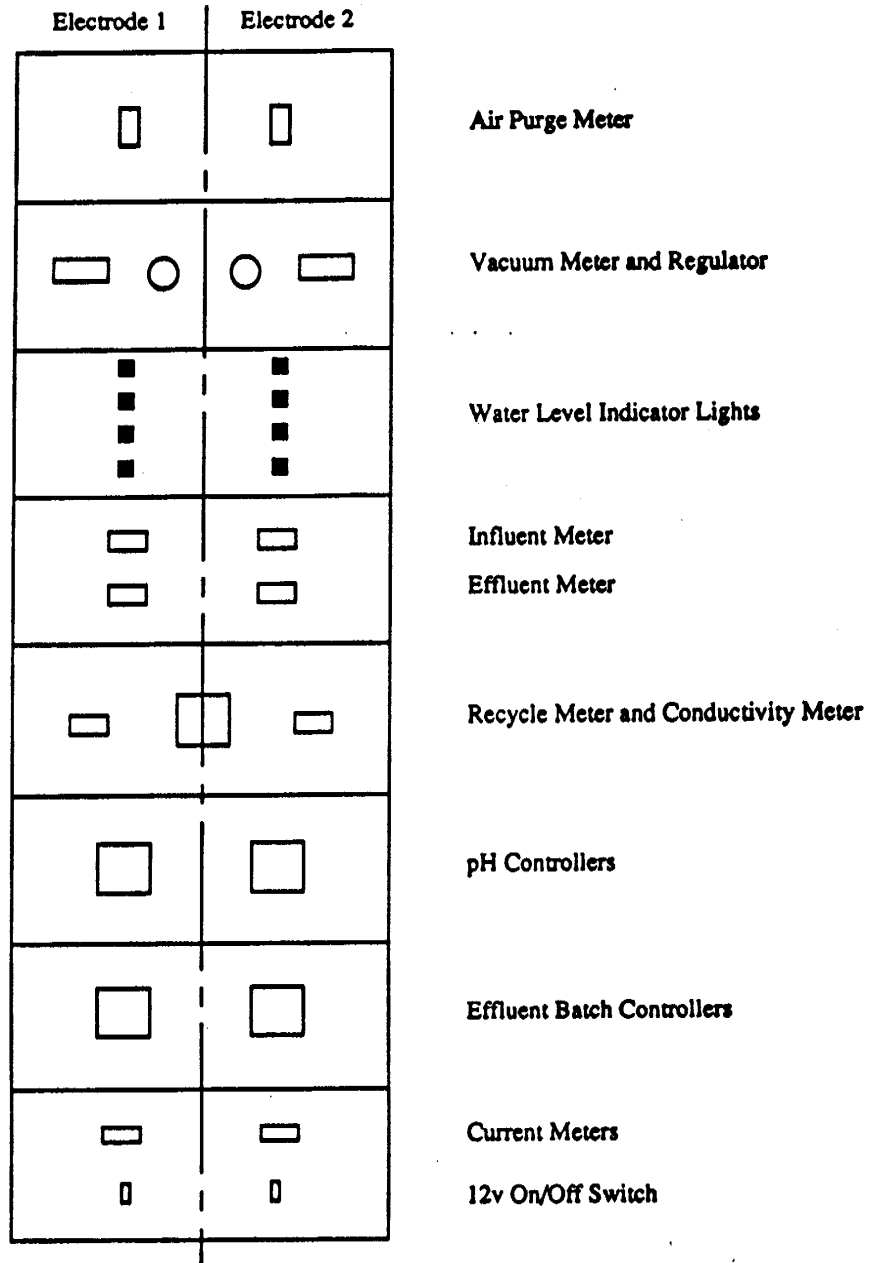


FIG. F-2. Control panel layout.

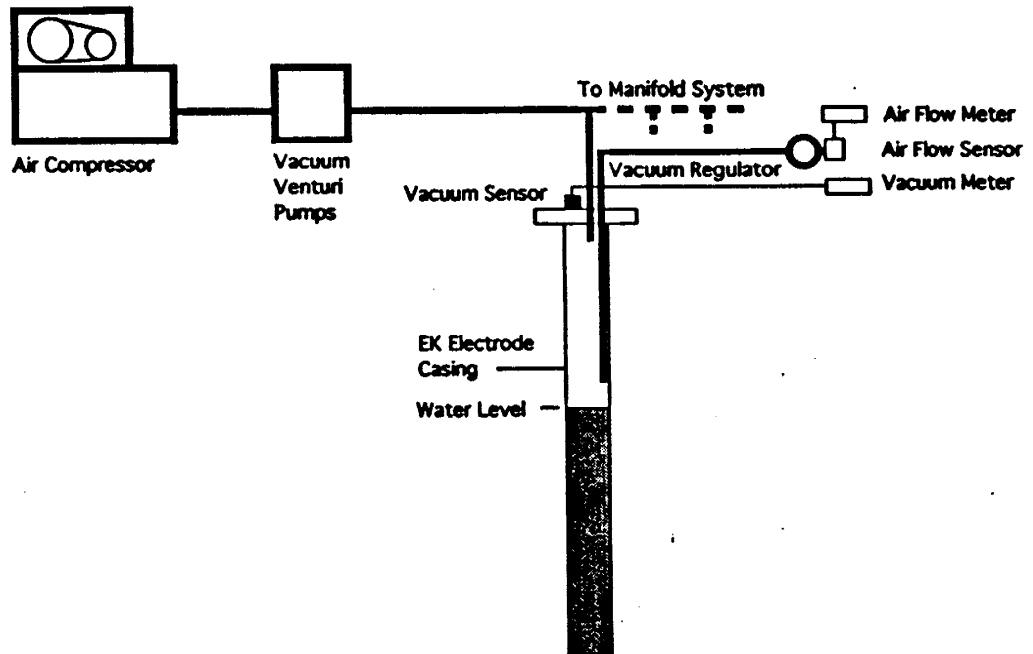


FIG. F-3. Vacuum control system.

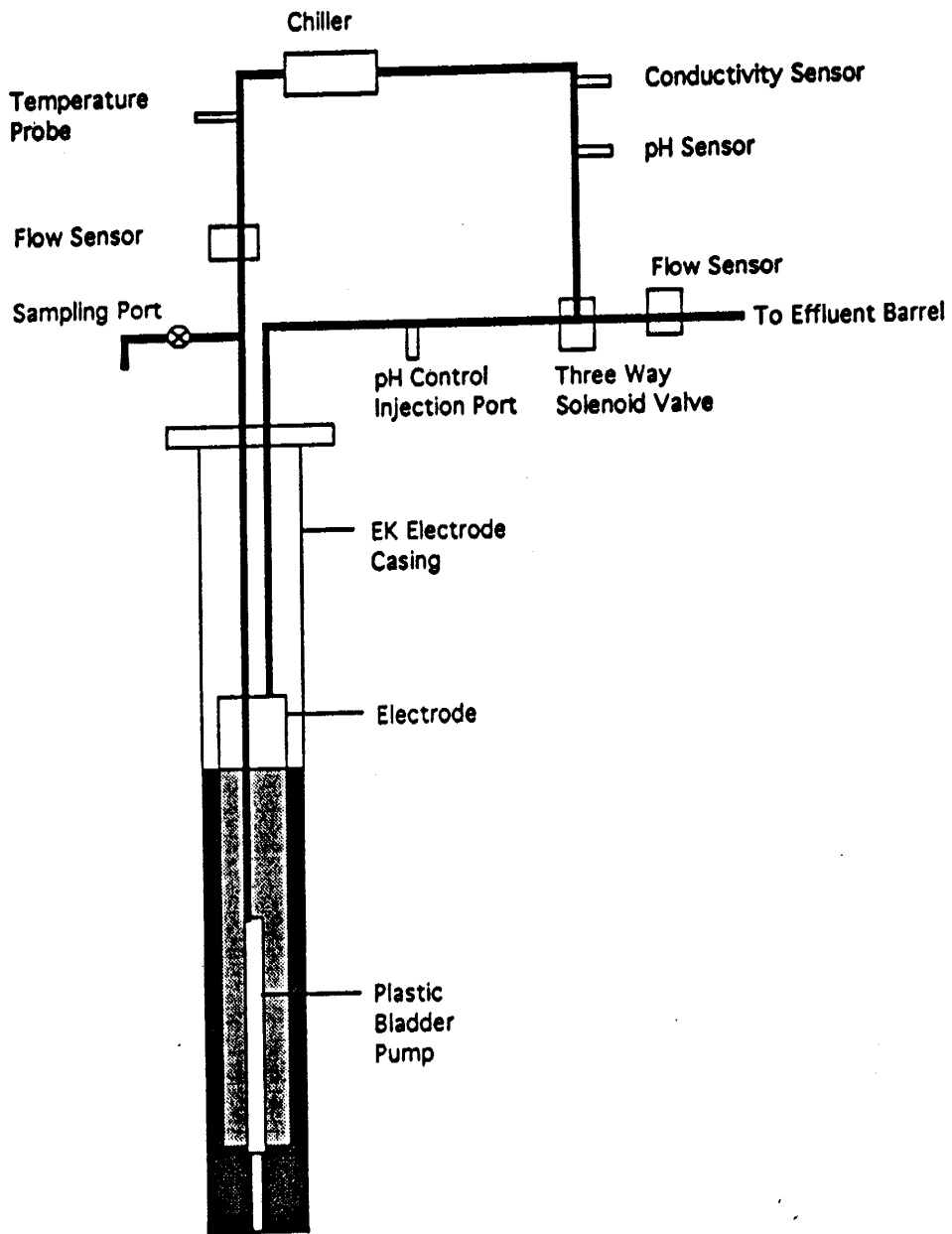


FIG. F-4. Water-circulation system.

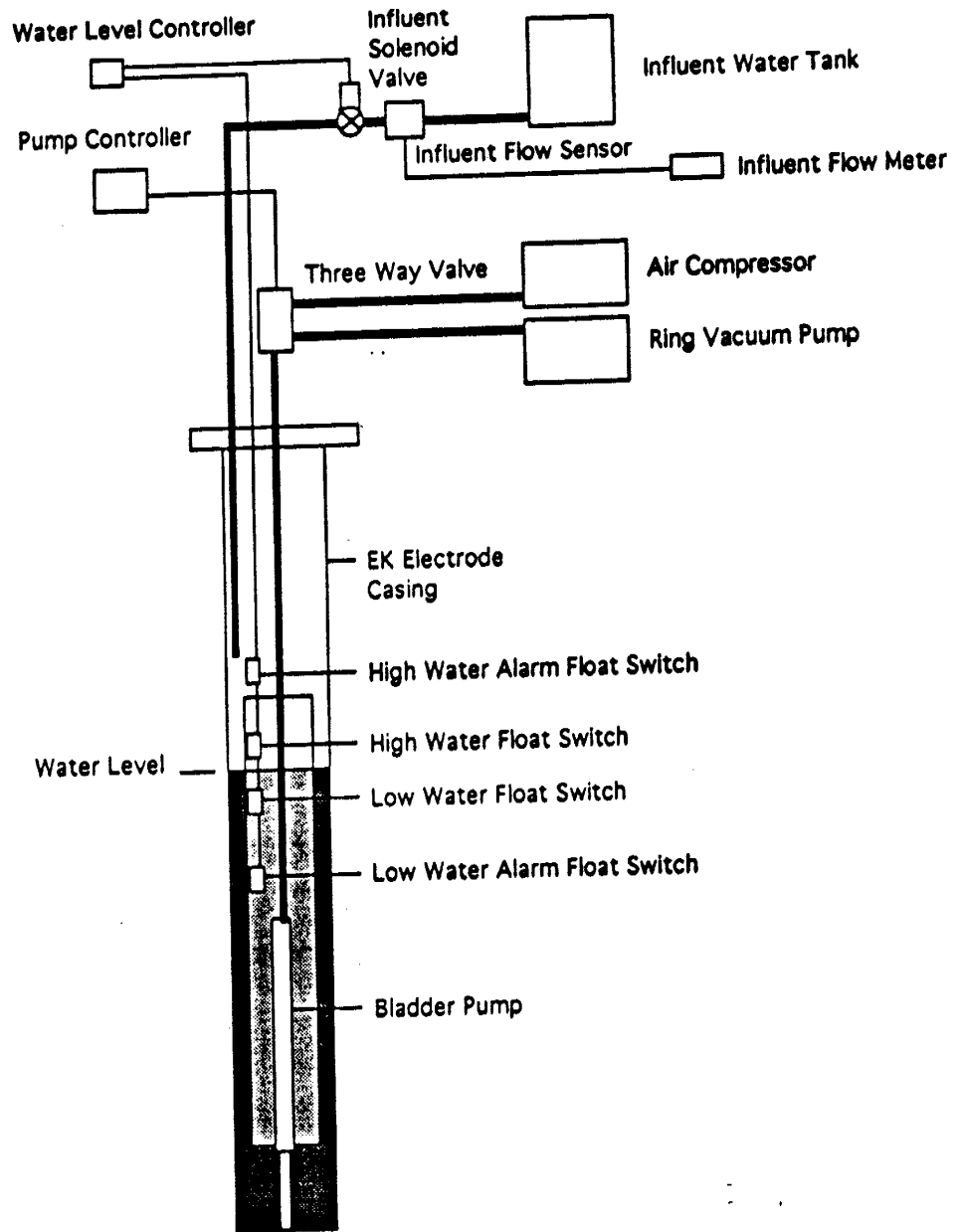
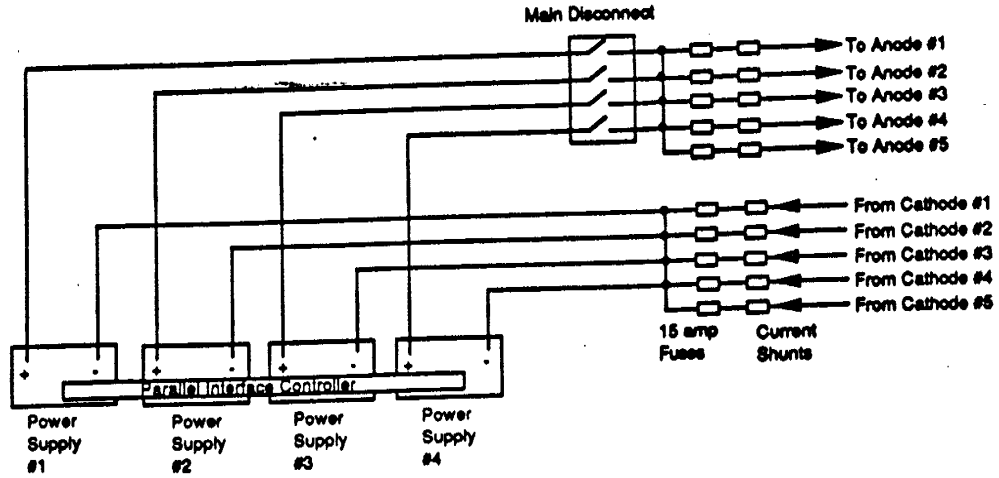
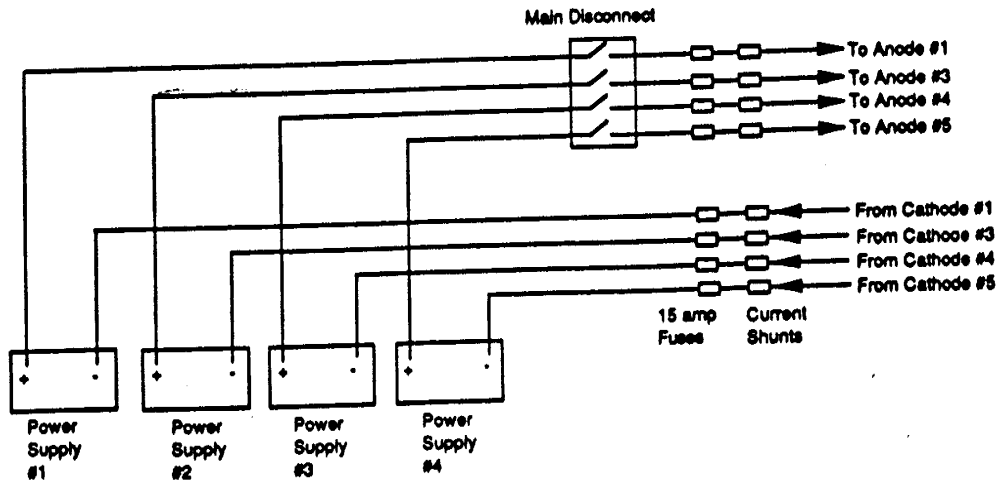


FIG. F-5. Electrode water-level control.



A) Five Anode-Cathode Pairs Operated by the Parallel Interface Controller



B) Four Anode-Cathode Pairs Controlled by Individual Power Supplies

FIG F-6. Current distribution schematic.

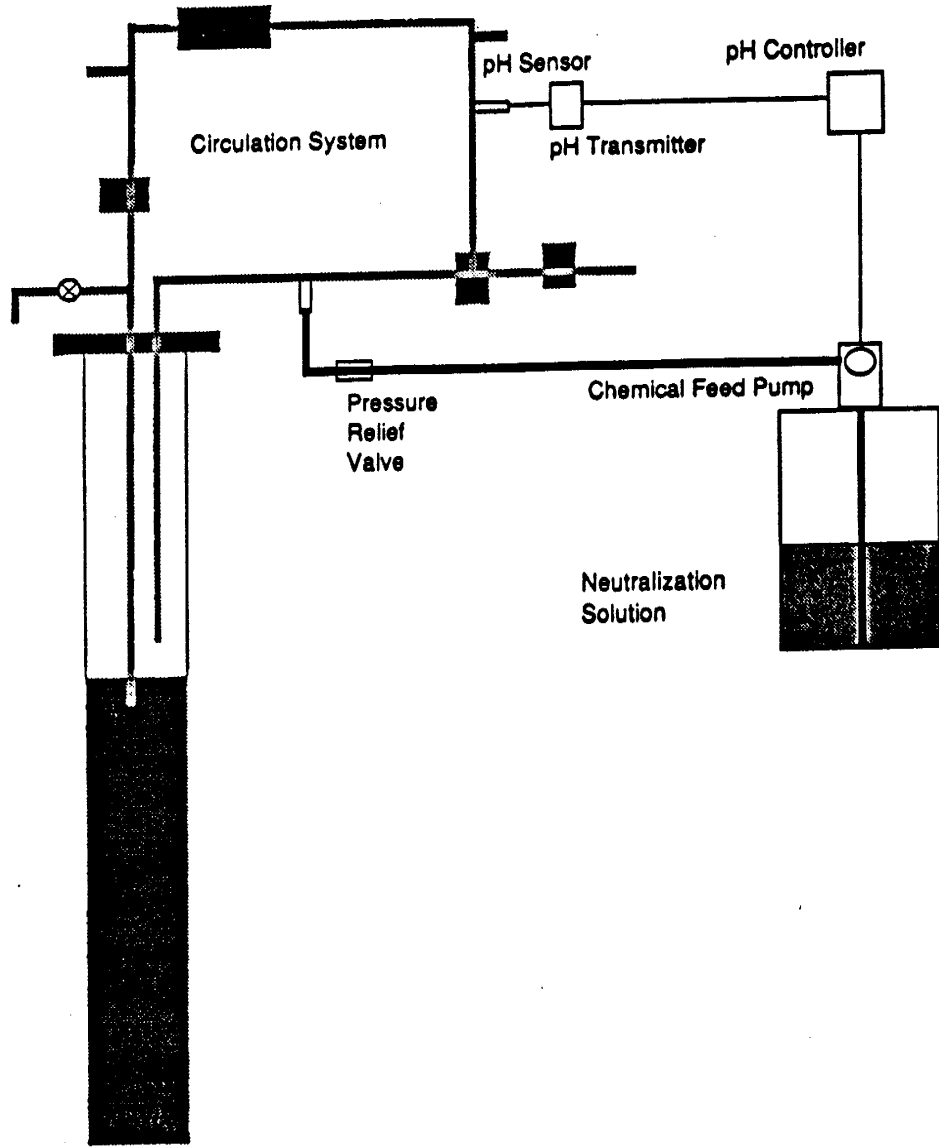


FIG. F-7. pH control system.

APPENDIX G. MODFLOW Input File Example: Three-Dimensional Field Demonstration

This appendix includes example MODFLOW input files for the three-dimensional field demonstration numerical predictions. Both Phase 1 and Phase 2 input files are presented here.

BAS-1.dat contains the code control file that sets up the problem for Phase 1 of both layered and homogeneous models.

BAS-2.dat contains the code control file that sets up the problem for Phase 2 of both the layered and homogeneous models.

For the layered model, separate input files were needed for each phase because the location of the cathode electrode and the applied electric potential were different for Phase 1 and Phase 2. BCF-L1.dat is the input for Phase 1 and BCF-L2.dat is the input for Phase 2.

Similarly, separate input files were needed for each phase of the homogeneous model predictions because the location of the cathode electrode and the applied electric potential changed between phases. BCF-H1.dat is input for Phase 1 and BCF-H2.dat is input for Phase 2.

G-2
BAS1.dat

```

3D TEST PROBLEM
EK testing of field
12 5 14 1
11 00 00 0 0 0 0 00 00 0 0 22 19 00 00 00 00 00 00 00 00 66 00 00
0 0 IAPART, ISTRT
101 1(15I3) 3 IBOUND-1
3
1 5 1 14 1
3 3 1 1 1
3 3 14 14 1
101 1(15I3) 3 IBOUND-2
3
1 5 1 14 1
3 3 1 1 1
3 3 14 14 1
101 1(15I3) 3 IBOUND-3
3
1 5 1 14 1
3 3 1 1 1
3 3 14 14 1
101 1(15I3) 3 IBOUND-4
3
1 5 1 14 1
3 3 1 1 1
3 3 14 14 1
101 1(15I3) 3 IBOUND-5
3
1 5 1 14 1
3 3 1 1 -1
3 3 14 14 -1
101 1(15I3) 3 IBOUND-6
3
1 5 1 14 1
3 3 1 1 -1
3 3 14 14 -1
101 1(15I3) 3 IBOUND-7
3
1 5 1 14 1
3 3 1 1 -1
3 3 14 14 -1
101 1(15I3) 3 IBOUND-8
3
1 5 1 14 1
3 3 1 1 -1
3 3 14 14 -1
101 1(15I3) 3 IBOUND-9
3
1 5 1 14 1
3 3 1 1 -1
3 3 14 14 -1
101 1(15I3) 3 IBOUND-10
3
1 5 1 14 1
3 3 1 1 -1
3 3 14 14 -1
101 1(15I3) 3 IBOUND-11
1
1 5 1 14 1
101 1(15I3) 3 IBOUND-12
1
1 5 1 14 1
999.99
101 1(15F3.0) 4 HEAD-1
3
1 5 1 14 109
3 3 1 1 109
3 3 14 14 109
101 1(15F3.0) 4 HEAD-2
3
1 5 1 14 109
3 3 1 1 109
3 3 14 14 109
101 1(15F3.0) 4 HEAD-3
3
1 5 1 14 109
3 3 1 1 109
3 3 14 14 109
101 1(15F3.0) 4 HEAD-4
3
1 5 1 14 109
3 3 1 1 109
3 3 14 14 109
101 1(15F3.0) 4 HEAD-5
3
1 5 1 14 109
3 3 1 1 0
3 3 14 14 109
101 1(15F3.0) 4 HEAD-6
3
1 5 1 14 109
3 3 1 1 0
3 3 14 14 109
101 1(15F3.0) 4 HEAD-7
3
1 5 1 14 109

```

G-3
BAS1.dat

| | | | |
|---------------|------------|----|--------------------|
| 3 3 1 1 0 | | | |
| 3 3 14 14 109 | | | |
| 101 | 1 (15F3.0) | 4 | HEAD-8 |
| 3 | | | |
| 1 5 1 14 109 | | | |
| 3 3 1 1 0 | | | |
| 3 3 14 14 109 | 1 (15F3.0) | 4 | HEAD-9 |
| 101 | | | |
| 3 | | | |
| 1 5 1 14 109 | | | |
| 3 3 1 1 0 | | | |
| 3 3 14 14 109 | 1 (15F3.0) | 4 | HEAD-10 |
| 101 | | | |
| 3 | | | |
| 1 5 1 14 109 | | | |
| 3 3 1 1 0 | | | |
| 3 3 14 14 109 | 1 (15F3.0) | 4 | HEAD-11 |
| 101 | | | |
| 3 | | | |
| 1 5 1 14 109 | | | |
| 3 3 1 1 109 | | | |
| 3 3 14 14 109 | 1 (15F3.0) | 4 | HEAD-12 |
| 101 | | | |
| 3 | | | |
| 1 5 1 14 109 | | | |
| 3 3 1 1 109 | | | |
| 3 3 14 14 109 | | | |
| 4485600. | 1 | 1. | PERLEN,NSTP,TSMULT |

G-4
BAS2.dat

```

3D TEST PROBLEM
EK testing of field
      12      5      14      1      1
11 00 00 0 0 0 0 00 00 0 0 22 19 00 00 00 00 00 00 00 66 00 00
      0
      101      IAPART, ISTRT      3      IBOUND-1
      3
1 5 1 14 1
3 3 1 1 1
3 3 14 14 1
      101      1(15I3)      3      IBOUND-2
      3
1 5 1 14 1
3 3 1 1 1
3 3 14 14 1
      101      1(15I3)      3      IBOUND-3
      3
1 5 1 14 1
3 3 1 1 1
3 3 14 14 1
      101      1(15I3)      3      IBOUND-4
      3
1 5 1 14 1
3 3 7 7 1
3 3 14 14 -1
      101      1(15I3)      3      IBOUND-5
      3
1 5 1 14 1
3 3 7 7 -1
3 3 14 14 -1
      101      1(15I3)      3      IBOUND-6
      3
1 5 1 14 1
3 3 7 7 -1
3 3 14 14 -1
      101      1(15I3)      3      IBOUND-7
      3
1 5 1 14 1
3 3 7 7 -1
3 3 14 14 -1
      101      1(15I3)      3      IBOUND-8
      3
1 5 1 14 1
3 3 7 7 -1
3 3 14 14 -1
      101      1(15I3)      3      IBOUND-9
      3
1 5 1 14 1
3 3 7 7 -1
3 3 14 14 -1
      101      1(15I3)      3      IBOUND-10
      3
1 5 1 14 1
3 3 7 7 -1
3 3 14 14 -1
      101      1(15I3)      3      IBOUND-11
      1
1 5 1 14 1
      101      1(15I3)      3      IBOUND-12
      1
1 5 1 14 1
      999.99      101      1(15F3.0)      4      HEAD-1
      3
1 5 1 14 68
3 3 1 1 68
3 3 14 14 68
      101      1(15F3.0)      4      HEAD-2
      3
1 5 1 14 68
3 3 1 1 68
3 3 14 14 68
      101      1(15F3.0)      4      HEAD-3
      3
1 5 1 14 68
3 3 1 1 68
3 3 14 14 68
      101      1(15F3.0)      4      HEAD-4
      3
1 5 1 14 68
3 3 7 7 0
3 3 14 14 68
      101      1(15F3.0)      4      HEAD-5
      3
1 5 1 14 68
3 3 7 7 0
3 3 14 14 68
      101      1(15F3.0)      4      HEAD-6
      3
1 5 1 14 68
3 3 7 7 0
3 3 14 14 68
      101      1(15F3.0)      4      HEAD-7
      3
1 5 1 14 68

```

G-5
BAS2.dat

| | | | | |
|--------------|-----------|----|---|--------------------|
| 3 3 7 7 0 | | | | |
| 3 3 14 14 68 | | | | |
| 101 | 1(15F3.0) | | 4 | HEAD-8 |
| 3 | | | | |
| 1 5 1 14 68 | | | | |
| 3 3 7 7 0 | | | | |
| 3 3 14 14 68 | 1(15F3.0) | | 4 | HEAD-9 |
| 101 | | | | |
| 3 | | | | |
| 1 5 1 14 68 | | | | |
| 3 3 7 7 0 | | | | |
| 3 3 14 14 68 | 1(15F3.0) | | 4 | HEAD-10 |
| 101 | | | | |
| 3 | | | | |
| 1 5 1 14 68 | | | | |
| 3 3 7 7 0 | | | | |
| 3 3 14 14 68 | 1(15F3.0) | | 4 | HEAD-11 |
| 101 | | | | |
| 3 | | | | |
| 1 5 1 14 68 | | | | |
| 3 3 1 1 68 | | | | |
| 3 3 14 14 68 | 1(15F3.0) | | 4 | HEAD-12 |
| 101 | | | | |
| 3 | | | | |
| 1 5 1 14 68 | | | | |
| 3 3 1 1 68 | | | | |
| 3 3 14 14 68 | | | | |
| 3013200. | 1 | 1. | | PERLEN,NSTP,TSMULT |

G-7
BCF-L1.dat

| | | | | |
|--------------------|-----|-------|----------|------------|
| 3 3 1 1 5.55e-2 | | | | |
| 3 3 14 14 5.55e-2 | 101 | 1. | (4G10.4) | 12 econd4 |
| 3 | | | | |
| 1 5 1 14 5.55e-2 | | | | |
| 3 3 1 1 5.55e-2 | | | | |
| 3 3 14 14 5.55e-2 | 101 | 1. | (4G10.4) | 12 theta4 |
| 1 | | | | |
| 1 5 1 14 0.198 | 101 | 1. | (4G10.4) | 12 thetas4 |
| 1 | | | | |
| 1 5 1 14 .375 | 101 | 1. | (4G10.4) | 12 thetao4 |
| 1 | | | | |
| 1 5 1 14 .045 | 101 | 1. | (4G10.4) | 12 F(y)4 |
| 1 | | | | |
| 1 5 1 14 1.394 | 101 | 1. | (4G10.4) | 12 expn4 |
| 1 | | | | |
| 1 5 1 14 0.0651 | 101 | .3048 | (4G10.4) | 12 T-4a |
| 3 | | | | |
| 1 5 1 14 5.55e-2 | | | | |
| 3 3 1 1 5.55e-2 | | | | |
| 3 3 14 14 5.55e-2 | 101 | 3.28 | (4G10.4) | 12 Vcon-4a |
| 3 | | | | |
| 1 5 1 14 5.55e-2 | | | | |
| 3 3 1 1 5.55e-2 | | | | |
| 3 3 14 14 5.55e-2 | 101 | 1. | (4G10.4) | 12 econd5 |
| 3 | | | | |
| 1 5 1 14 5.55e-2 | | | | |
| 3 3 1 1 5.55e-2 | | | | |
| 3 3 14 14 5.55e-2 | 101 | 1. | (4G10.4) | 12 theta5 |
| 3 | | | | |
| 1 5 1 14 .198 | | | | |
| 3 3 1 1 .198 | | | | |
| 3 3 14 14 .198 | 101 | 1. | (4G10.4) | 12 thetas5 |
| 1 | | | | |
| 1 5 1 14 .375 | 101 | 1. | (4G10.4) | 12 thetao5 |
| 1 | | | | |
| 1 5 1 14 .045 | 101 | 1. | (4G10.4) | 12 F(y)5 |
| 1 | | | | |
| 1 5 1 14 1.394 | 101 | 1. | (4G10.4) | 12 expn5 |
| 1 | | | | |
| 1 5 1 14 0.0651 | 101 | .3048 | (4G10.4) | 12 T-5a |
| 3 | | | | |
| 1 5 1 14 5.55e-2 | | | | |
| 3 3 1 1 5.55e-2 | | | | |
| 3 3 14 14 5.55e-2 | 101 | 3.28 | (4G10.4) | 12 Vcon-5a |
| 3 | | | | |
| 1 5 1 14 8.257e-3 | | | | |
| 3 3 1 1 8.257e-3 | | | | |
| 3 3 14 14 8.257e-3 | 101 | 1. | (4G10.4) | 12 econd6 |
| 3 | | | | |
| 1 5 1 14 4.461e-3 | | | | |
| 3 3 1 1 4.461e-3 | | | | |
| 3 3 14 14 4.461e-3 | 101 | 1. | (4G10.4) | 12 theta6 |
| 3 | | | | |
| 1 5 1 14 0.072 | | | | |
| 3 3 1 1 0.072 | | | | |
| 3 3 14 14 0.072 | 101 | 1. | (4G10.4) | 12 thetas6 |
| 1 | | | | |
| 1 5 1 14 .375 | 101 | 1. | (4G10.4) | 12 thetao6 |
| 1 | | | | |
| 1 5 1 14 .045 | 101 | 1. | (4G10.4) | 12 F(y)6 |
| 1 | | | | |
| 1 5 1 14 1.394 | 101 | 1. | (4G10.4) | 12 expn6 |
| 1 | | | | |
| 1 5 1 14 0.0651 | 101 | .3048 | (4G10.4) | 12 T-6a |
| 3 | | | | |
| 1 5 1 14 4.461e-3 | | | | |
| 3 3 1 1 4.461e-3 | | | | |
| 3 3 14 14 4.461e-3 | 101 | 3.28 | (4G10.4) | 12 Vcon-6a |
| 3 | | | | |
| 1 5 1 14 4.461e-3 | | | | |
| 3 3 1 1 4.461e-3 | | | | |

G-8
BCF-L1.dat

| | | | |
|---|----------|----|---------|
| 3 3 14 14 4.461e-3 101 1. | (4G10.4) | 12 | econd7 |
| 3 | | | |
| 1 5 1 14 4.461e-3 3 3 1 1 4.461e-3 3 3 14 14 4.461e-3 101 1. | (4G10.4) | 12 | theta7 |
| 3 | | | |
| 1 5 1 14 0.072 3 3 1 1 0.072 3 3 14 14 0.072 101 1. | (4G10.4) | 12 | thetas7 |
| 1 | | | |
| 1 5 1 14 .375 101 1. | (4G10.4) | 12 | thetao7 |
| 1 | | | |
| 1 5 1 14 .045 101 1. | (4G10.4) | 12 | F(y)7 |
| 1 | | | |
| 1 5 1 14 1.394 101 1. | (4G10.4) | 12 | expn7 |
| 1 | | | |
| 1 5 1 14 0.0651 101 .3048 | (4G10.4) | 12 | T-7a |
| 3 | | | |
| 1 5 1 14 4.461e-3 3 3 1 1 4.461e-3 3 3 14 14 4.461e-3 101 3.28 | (4G10.4) | 12 | Vcon-7a |
| 3 | | | |
| 1 5 1 14 4.461e-3 3 3 1 1 4.461e-3 3 3 14 14 4.461e-3 101 1. | (4G10.4) | 12 | econd8 |
| 3 | | | |
| 1 5 1 14 4.461e-3 3 3 1 1 4.461e-3 3 3 14 14 4.461e-3 101 1. | (4G10.4) | 12 | theta8 |
| 3 | | | |
| 1 5 1 14 0.072 3 3 1 1 0.072 3 3 14 14 0.072 101 1. | (4G10.4) | 12 | thetas8 |
| 1 | | | |
| 1 5 1 14 .375 101 1. | (4G10.4) | 12 | thetao8 |
| 1 | | | |
| 1 5 1 14 .045 101 1. | (4G10.4) | 12 | F(y)8 |
| 1 | | | |
| 1 5 1 14 1.394 101 1. | (4G10.4) | 12 | expn8 |
| 1 | | | |
| 1 5 1 14 0.0651 101 .3048 | (4G10.4) | 12 | T-8a |
| 3 | | | |
| 1 5 1 14 4.461e-3 3 3 1 1 4.461e-3 3 3 14 14 4.461e-3 101 3.28 | (4G10.4) | 12 | Vcon-8a |
| 3 | | | |
| 1 5 1 14 4.461e-3 3 3 1 1 4.461e-3 3 3 14 14 4.461e-3 101 1. | (4G10.4) | 12 | econd9 |
| 3 | | | |
| 1 5 1 14 4.461e-3 3 3 1 1 4.461e-3 3 3 14 14 4.461e-3 101 1. | (4G10.4) | 12 | theta9 |
| 3 | | | |
| 1 5 1 14 0.072 3 3 1 1 0.072 3 3 14 14 0.072 101 1. | (4G10.4) | 12 | thetas9 |
| 1 | | | |
| 1 5 1 14 .375 101 1. | (4G10.4) | 12 | thetao9 |
| 1 | | | |
| 1 5 1 14 .045 101 1. | (4G10.4) | 12 | F(y)9 |
| 1 | | | |
| 1 5 1 14 1.394 101 1. | (4G10.4) | 12 | expn9 |
| 1 | | | |
| 1 5 1 14 0.0651 101 .3048 | (4G10.4) | 12 | T-9a |
| 3 | | | |
| 1 5 1 14 4.461e-3 3 3 1 1 4.461e-3 3 3 14 14 4.461e-3 101 3.28 | (4G10.4) | 12 | Vcon-9a |
| 3 | | | |
| 1 5 1 14 4.461e-3 | | | |

G-9
BCF-L1.dat

| | | | | |
|--------------------|----------|----|--|----------|
| 3 3 1 1 4.461e-3 | | | | |
| 3 3 14 14 4.461e-3 | | | | |
| 101 1. | (4G10.4) | 12 | | econd10 |
| 3 | | | | |
| 1 5 1 14 4.461e-3 | | | | |
| 3 3 1 1 4.461e-3 | | | | |
| 3 3 14 14 4.461e-3 | | | | |
| 101 1. | (4G10.4) | 12 | | theta10 |
| 3 | | | | |
| 1 5 1 14 0.072 | | | | |
| 3 3 1 1 0.072 | | | | |
| 3 3 14 14 0.072 | | | | |
| 101 1. | (4G10.4) | 12 | | thetas10 |
| 1 | | | | |
| 1 5 1 14 .375 | | | | |
| 101 1. | (4G10.4) | 12 | | thetao10 |
| 1 | | | | |
| 1 5 1 14 .045 | | | | |
| 101 1. | (4G10.4) | 12 | | F(y)10 |
| 1 | | | | |
| 1 5 1 14 1.394 | | | | |
| 101 1. | (4G10.4) | 12 | | expn10 |
| 1 | | | | |
| 1 5 1 14 0.0651 | | | | |
| 101 .3048 | (4G10.4) | 12 | | T-10a |
| 3 | | | | |
| 1 5 1 14 4.461e-3 | | | | |
| 3 3 1 1 4.461e-3 | | | | |
| 3 3 14 14 4.461e-3 | | | | |
| 101 3.28 | (4G10.4) | 12 | | Vcon-10a |
| 3 | | | | |
| 1 5 1 14 4.461e-3 | | | | |
| 3 3 1 1 4.461e-3 | | | | |
| 3 3 14 14 4.461e-3 | | | | |
| 101 1. | (4G10.4) | 12 | | econd11 |
| 1 | | | | |
| 1 5 1 14 4.461e-3 | | | | |
| 101 1. | (4G10.4) | 12 | | theta11 |
| 1 | | | | |
| 1 5 1 14 0.072 | | | | |
| 101 1. | (4G10.4) | 12 | | thetas11 |
| 1 | | | | |
| 1 5 1 14 .375 | | | | |
| 101 1. | (4G10.4) | 12 | | thetao11 |
| 1 | | | | |
| 1 5 1 14 .045 | | | | |
| 101 1. | (4G10.4) | 12 | | F(y)11 |
| 1 | | | | |
| 1 5 1 14 1.394 | | | | |
| 101 1. | (4G10.4) | 12 | | expn11 |
| 1 | | | | |
| 1 5 1 14 0.0651 | | | | |
| 101 .3048 | (4G10.4) | 12 | | T-11a |
| 1 | | | | |
| 1 5 1 14 4.461e-3 | | | | |
| 101 3.28 | (4G10.4) | 12 | | Vcon-11a |
| 1 | | | | |
| 1 5 1 14 4.461e-3 | | | | |
| 101 1. | (4G10.4) | 12 | | econd12 |
| 1 | | | | |
| 1 5 1 14 4.461e-3 | | | | |
| 101 1. | (4G10.4) | 12 | | theta12 |
| 1 | | | | |
| 1 5 1 14 0.072 | | | | |
| 101 1. | (4G10.4) | 12 | | thetas12 |
| 1 | | | | |
| 1 5 1 14 .375 | | | | |
| 101 1. | (4G10.4) | 12 | | thetao12 |
| 1 | | | | |
| 1 5 1 14 .045 | | | | |
| 101 1. | (4G10.4) | 12 | | F(y)12 |
| 1 | | | | |
| 1 5 1 14 1.394 | | | | |
| 101 1. | (4G10.4) | 12 | | expn12 |
| 1 | | | | |
| 1 5 1 14 0.0651 | | | | |
| 101 .3048 | (4G10.4) | 12 | | T-12a |
| 1 | | | | |
| 1 5 1 14 4.461e-3 | | | | |

G-11
BCF-L2.dat

| | | | | |
|--------------------|-----|-------|----------|------------|
| 3 3 1 1 5.55e-2 | | | | |
| 3 3 14 14 5.55e-2 | 101 | 1. | (4G10.4) | 12 econd4 |
| 3 | | | | |
| 1 5 1 14 5.55e-2 | | | | |
| 3 3 1 1 5.55e-2 | | | | |
| 3 3 14 14 5.55e-2 | 101 | 1. | (4G10.4) | 12 theta4 |
| 1 | | | | |
| 1 5 1 14 0.198 | 101 | 1. | (4G10.4) | 12 thetas4 |
| 1 | | | | |
| 1 5 1 14 .375 | 101 | 1. | (4G10.4) | 12 thetao4 |
| 1 | | | | |
| 1 5 1 14 .045 | 101 | 1. | (4G10.4) | 12 F(y)4 |
| 1 | | | | |
| 1 5 1 14 1.394 | 101 | 1. | (4G10.4) | 12 expn4 |
| 1 | | | | |
| 1 5 1 14 0.0651 | 101 | .3048 | (4G10.4) | 12 T-4a |
| 3 | | | | |
| 1 5 1 14 5.55e-2 | | | | |
| 3 3 1 1 5.55e-2 | | | | |
| 3 3 14 14 5.55e-2 | 101 | 3.28 | (4G10.4) | 12 Vcon-4a |
| 3 | | | | |
| 1 5 1 14 5.55e-2 | | | | |
| 3 3 1 1 5.55e-2 | | | | |
| 3 3 14 14 5.55e-2 | 101 | 1. | (4G10.4) | 12 econd5 |
| 3 | | | | |
| 1 5 1 14 5.55e-2 | | | | |
| 3 3 1 1 5.55e-2 | | | | |
| 3 3 14 14 5.55e-2 | 101 | 1. | (4G10.4) | 12 theta5 |
| 3 | | | | |
| 1 5 1 14 .198 | | | | |
| 3 3 1 1 .198 | | | | |
| 3 3 14 14 .198 | 101 | 1. | (4G10.4) | 12 thetas5 |
| 1 | | | | |
| 1 5 1 14 .375 | 101 | 1. | (4G10.4) | 12 thetao5 |
| 1 | | | | |
| 1 5 1 14 .045 | 101 | 1. | (4G10.4) | 12 F(y)5 |
| 1 | | | | |
| 1 5 1 14 1.394 | 101 | 1. | (4G10.4) | 12 expn5 |
| 1 | | | | |
| 1 5 1 14 0.0651 | 101 | .3048 | (4G10.4) | 12 T-5a |
| 3 | | | | |
| 1 5 1 14 5.55e-2 | | | | |
| 3 3 1 1 5.55e-2 | | | | |
| 3 3 14 14 5.55e-2 | 101 | 3.28 | (4G10.4) | 12 Vcon-5a |
| 3 | | | | |
| 1 5 1 14 8.257e-3 | | | | |
| 3 3 1 1 8.257e-3 | | | | |
| 3 3 14 14 8.257e-3 | 101 | 1. | (4G10.4) | 12 econd6 |
| 3 | | | | |
| 1 5 1 14 4.461e-3 | | | | |
| 3 3 1 1 4.461e-3 | | | | |
| 3 3 14 14 4.461e-3 | 101 | 1. | (4G10.4) | 12 theta6 |
| 3 | | | | |
| 1 5 1 14 0.072 | | | | |
| 3 3 1 1 0.072 | | | | |
| 3 3 14 14 0.072 | 101 | 1. | (4G10.4) | 12 thetas6 |
| 1 | | | | |
| 1 5 1 14 .375 | 101 | 1. | (4G10.4) | 12 thetao6 |
| 1 | | | | |
| 1 5 1 14 .045 | 101 | 1. | (4G10.4) | 12 F(y)6 |
| 1 | | | | |
| 1 5 1 14 1.394 | 101 | 1. | (4G10.4) | 12 expn6 |
| 1 | | | | |
| 1 5 1 14 0.0651 | 101 | .3048 | (4G10.4) | 12 T-6a |
| 3 | | | | |
| 1 5 1 14 4.461e-3 | | | | |
| 3 3 1 1 4.461e-3 | | | | |
| 3 3 14 14 4.461e-3 | 101 | 3.28 | (4G10.4) | 12 Vcon-6a |
| 3 | | | | |
| 1 5 1 14 4.461e-3 | | | | |
| 3 3 1 1 4.461e-3 | | | | |

G-12
BCF-L2.dat

| | | | |
|---|----------|----|---------|
| 3 3 14 14 4.461e-3 101 1. | (4G10.4) | 12 | econd7 |
| 3 | | | |
| 1 5 1 14 4.461e-3 3 3 1 1 4.461e-3 3 3 14 14 4.461e-3 101 1. | (4G10.4) | 12 | theta7 |
| 3 | | | |
| 1 5 1 14 0.072 3 3 1 1 0.072 3 3 14 14 0.072 101 1. | (4G10.4) | 12 | thetas7 |
| 1 | | | |
| 1 5 1 14 .375 101 1. | (4G10.4) | 12 | thetao7 |
| 1 | | | |
| 1 5 1 14 .045 101 1. | (4G10.4) | 12 | F(y)7 |
| 1 | | | |
| 1 5 1 14 1.394 101 1. | (4G10.4) | 12 | expn7 |
| 1 | | | |
| 1 5 1 14 0.0651 101 .3048 | (4G10.4) | 12 | T-7a |
| 3 | | | |
| 1 5 1 14 4.461e-3 3 3 1 1 4.461e-3 3 3 14 14 4.461e-3 101 3.28 | (4G10.4) | 12 | Vcon-7a |
| 3 | | | |
| 1 5 1 14 4.461e-3 3 3 1 1 4.461e-3 3 3 14 14 4.461e-3 101 1. | (4G10.4) | 12 | econd8 |
| 3 | | | |
| 1 5 1 14 4.461e-3 3 3 1 1 4.461e-3 3 3 14 14 4.461e-3 101 1. | (4G10.4) | 12 | theta8 |
| 3 | | | |
| 1 5 1 14 0.072 3 3 1 1 0.072 3 3 14 14 0.072 101 1. | (4G10.4) | 12 | thetas8 |
| 1 | | | |
| 1 5 1 14 .375 101 1. | (4G10.4) | 12 | thetao8 |
| 1 | | | |
| 1 5 1 14 .045 101 1. | (4G10.4) | 12 | F(y)8 |
| 1 | | | |
| 1 5 1 14 1.394 101 1. | (4G10.4) | 12 | expn8 |
| 1 | | | |
| 1 5 1 14 0.0651 101 .3048 | (4G10.4) | 12 | T-8a |
| 3 | | | |
| 1 5 1 14 4.461e-3 3 3 1 1 4.461e-3 3 3 14 14 4.461e-3 101 3.28 | (4G10.4) | 12 | Vcon-8a |
| 3 | | | |
| 1 5 1 14 4.461e-3 3 3 1 1 4.461e-3 3 3 14 14 4.461e-3 101 1. | (4G10.4) | 12 | econd9 |
| 3 | | | |
| 1 5 1 14 4.461e-3 3 3 1 1 4.461e-3 3 3 14 14 4.461e-3 101 1. | (4G10.4) | 12 | theta9 |
| 3 | | | |
| 1 5 1 14 0.072 3 3 1 1 0.072 3 3 14 14 0.072 101 1. | (4G10.4) | 12 | thetas9 |
| 1 | | | |
| 1 5 1 14 .375 101 1. | (4G10.4) | 12 | thetao9 |
| 1 | | | |
| 1 5 1 14 .045 101 1. | (4G10.4) | 12 | F(y)9 |
| 1 | | | |
| 1 5 1 14 1.394 101 1. | (4G10.4) | 12 | expn9 |
| 1 | | | |
| 1 5 1 14 0.0651 101 .3048 | (4G10.4) | 12 | T-9a |
| 3 | | | |
| 1 5 1 14 4.461e-3 3 3 1 1 4.461e-3 3 3 14 14 4.461e-3 101 3.28 | (4G10.4) | 12 | Vcon-9a |
| 3 | | | |
| 1 5 1 14 4.461e-3 | | | |

G-13
BCF-L2.dat

| | | | | |
|--------------------|----------|----|----------|--|
| 3 3 1 1 4.461e-3 | | | | |
| 3 3 14 14 4.461e-3 | | | | |
| 101 1. | (4G10.4) | 12 | econd10 | |
| 3 | | | | |
| 1 5 1 14 4.461e-3 | | | | |
| 3 3 1 1 4.461e-3 | | | | |
| 3 3 14 14 4.461e-3 | | | | |
| 101 1. | (4G10.4) | 12 | theta10 | |
| 3 | | | | |
| 1 5 1 14 0.072 | | | | |
| 3 3 1 1 0.072 | | | | |
| 3 3 14 14 0.072 | | | | |
| 101 1. | (4G10.4) | 12 | thetas10 | |
| 1 | | | | |
| 1 5 1 14 .375 | | | | |
| 101 1. | (4G10.4) | 12 | thetao10 | |
| 1 | | | | |
| 1 5 1 14 .045 | | | | |
| 101 1. | (4G10.4) | 12 | F(y)10 | |
| 1 | | | | |
| 1 5 1 14 1.394 | | | | |
| 101 1. | (4G10.4) | 12 | expn10 | |
| 1 | | | | |
| 1 5 1 14 0.0651 | | | | |
| 101 .3048 | (4G10.4) | 12 | T-10a | |
| 3 | | | | |
| 1 5 1 14 4.461e-3 | | | | |
| 3 3 1 1 4.461e-3 | | | | |
| 3 3 14 14 4.461e-3 | | | | |
| 101 3.28 | (4G10.4) | 12 | Vcon-10a | |
| 3 | | | | |
| 1 5 1 14 4.461e-3 | | | | |
| 3 3 1 1 4.461e-3 | | | | |
| 3 3 14 14 4.461e-3 | | | | |
| 101 1. | (4G10.4) | 12 | econd11 | |
| 1 | | | | |
| 1 5 1 14 4.461e-3 | | | | |
| 101 1. | (4G10.4) | 12 | theta11 | |
| 1 | | | | |
| 1 5 1 14 0.072 | | | | |
| 101 1. | (4G10.4) | 12 | thetas11 | |
| 1 | | | | |
| 1 5 1 14 .375 | | | | |
| 101 1. | (4G10.4) | 12 | thetao11 | |
| 1 | | | | |
| 1 5 1 14 .045 | | | | |
| 101 1. | (4G10.4) | 12 | F(y)11 | |
| 1 | | | | |
| 1 5 1 14 1.394 | | | | |
| 101 1. | (4G10.4) | 12 | expn11 | |
| 1 | | | | |
| 1 5 1 14 0.0651 | | | | |
| 101 .3048 | (4G10.4) | 12 | T-11a | |
| 1 | | | | |
| 1 5 1 14 4.461e-3 | | | | |
| 101 3.28 | (4G10.4) | 12 | Vcon-11a | |
| 1 | | | | |
| 1 5 1 14 4.461e-3 | | | | |
| 101 1. | (4G10.4) | 12 | econd12 | |
| 1 | | | | |
| 1 5 1 14 4.461e-3 | | | | |
| 101 1. | (4G10.4) | 12 | theta12 | |
| 1 | | | | |
| 1 5 1 14 0.072 | | | | |
| 101 1. | (4G10.4) | 12 | thetas12 | |
| 1 | | | | |
| 1 5 1 14 .375 | | | | |
| 101 1. | (4G10.4) | 12 | thetao12 | |
| 1 | | | | |
| 1 5 1 14 .045 | | | | |
| 101 1. | (4G10.4) | 12 | F(y)12 | |
| 1 | | | | |
| 1 5 1 14 1.394 | | | | |
| 101 1. | (4G10.4) | 12 | expn12 | |
| 1 | | | | |
| 1 5 1 14 0.0651 | | | | |
| 101 .3048 | (4G10.4) | 12 | T-12a | |
| 1 | | | | |
| 1 5 1 14 4.461e-3 | | | | |

G-15
BCF-H1.dat

| | | | | |
|--------------------|----------|----|---------|--|
| 3 3 1 1 1.722e-2 | | | | |
| 3 3 14 14 1.722e-2 | | | | |
| 101 1. | (4G10.4) | 12 | econd4 | |
| 3 | | | | |
| 1 5 1 14 1.722e-2 | | | | |
| 3 3 1 1 1.722e-2 | | | | |
| 3 3 14 14 1.722e-2 | | | | |
| 101 1. | (4G10.4) | 12 | theta4 | |
| 1 | | | | |
| 1 5 1 14 0.126 | | | | |
| 101 1. | (4G10.4) | 12 | thetas4 | |
| 1 | | | | |
| 1 5 1 14 .375 | | | | |
| 101 1. | (4G10.4) | 12 | thetao4 | |
| 1 | | | | |
| 1 5 1 14 .045 | | | | |
| 101 1. | (4G10.4) | 12 | F(y)4 | |
| 1 | | | | |
| 1 5 1 14 1.394 | | | | |
| 101 1. | (4G10.4) | 12 | expn4 | |
| 1 | | | | |
| 1 5 1 14 0.0651 | | | | |
| 101 .3048 | (4G10.4) | 12 | T-4a | |
| 3 | | | | |
| 1 5 1 14 1.722e-2 | | | | |
| 3 3 1 1 1.722e-2 | | | | |
| 3 3 14 14 1.722e-2 | | | | |
| 101 3.28 | (4G10.4) | 12 | Vcon-4a | |
| 3 | | | | |
| 1 5 1 14 1.722e-2 | | | | |
| 3 3 1 1 1.722e-2 | | | | |
| 3 3 14 14 1.722e-2 | | | | |
| 101 1. | (4G10.4) | 12 | econd5 | |
| 3 | | | | |
| 1 5 1 14 1.722e-2 | | | | |
| 3 3 1 1 1.722e-2 | | | | |
| 3 3 14 14 1.722e-2 | | | | |
| 101 1. | (4G10.4) | 12 | theta5 | |
| 3 | | | | |
| 1 5 1 14 .126 | | | | |
| 3 3 1 1 .126 | | | | |
| 3 3 14 14 .126 | | | | |
| 101 1. | (4G10.4) | 12 | thetas5 | |
| 1 | | | | |
| 1 5 1 14 .375 | | | | |
| 101 1. | (4G10.4) | 12 | thetao5 | |
| 1 | | | | |
| 1 5 1 14 .045 | | | | |
| 101 1. | (4G10.4) | 12 | F(y)5 | |
| 1 | | | | |
| 1 5 1 14 1.394 | | | | |
| 101 1. | (4G10.4) | 12 | expn5 | |
| 1 | | | | |
| 1 5 1 14 0.0651 | | | | |
| 101 .3048 | (4G10.4) | 12 | T-5a | |
| 3 | | | | |
| 1 5 1 14 1.722e-2 | | | | |
| 3 3 1 1 1.722e-2 | | | | |
| 3 3 14 14 1.722e-2 | | | | |
| 101 3.28 | (4G10.4) | 12 | Vcon-5a | |
| 3 | | | | |
| 1 5 1 14 1.722e-2 | | | | |
| 3 3 1 1 1.722e-2 | | | | |
| 3 3 14 14 1.722e-2 | | | | |
| 101 1. | (4G10.4) | 12 | econd6 | |
| 3 | | | | |
| 1 5 1 14 1.722e-2 | | | | |
| 3 3 1 1 1.722e-2 | | | | |
| 3 3 14 14 1.722e-2 | | | | |
| 101 1. | (4G10.4) | 12 | theta6 | |
| 3 | | | | |
| 1 5 1 14 0.126 | | | | |
| 3 3 1 1 0.126 | | | | |
| 3 3 14 14 0.126 | | | | |
| 101 1. | (4G10.4) | 12 | thetas6 | |
| 1 | | | | |
| 1 5 1 14 .375 | | | | |
| 101 1. | (4G10.4) | 12 | thetao6 | |
| 1 | | | | |
| 1 5 1 14 .045 | | | | |
| 101 1. | (4G10.4) | 12 | F(y)6 | |
| 1 | | | | |
| 1 5 1 14 1.394 | | | | |
| 101 1. | (4G10.4) | 12 | expn6 | |
| 1 | | | | |
| 1 5 1 14 0.0651 | | | | |
| 101 .3048 | (4G10.4) | 12 | T-6a | |
| 3 | | | | |
| 1 5 1 14 1.722e-2 | | | | |
| 3 3 1 1 1.722e-2 | | | | |
| 3 3 14 14 1.722e-2 | | | | |
| 101 3.28 | (4G10.4) | 12 | Vcon-6a | |
| 3 | | | | |
| 1 5 1 14 1.722e-2 | | | | |
| 3 3 1 1 1.722e-2 | | | | |

G-16
BCF-H1.dat

| | | | |
|---|----------|----|---------|
| 3 3 14 14 1.722e-2 101 1. | (4G10.4) | 12 | econd7 |
| 3 | | | |
| 1 5 1 14 1.722e-2 3 3 1 1 1.722e-2 3 3 14 14 1.722e-2 101 1. | (4G10.4) | 12 | theta7 |
| 3 | | | |
| 1 5 1 14 0.126 3 3 1 1 0.126 3 3 14 14 0.126 101 1. | (4G10.4) | 12 | thetas7 |
| 1 | | | |
| 1 5 1 14 .375 101 1. | (4G10.4) | 12 | thetao7 |
| 1 | | | |
| 1 5 1 14 .045 101 1. | (4G10.4) | 12 | F(y)7 |
| 1 | | | |
| 1 5 1 14 1.394 101 1. | (4G10.4) | 12 | expn7 |
| 1 | | | |
| 1 5 1 14 0.0651 101 .3048 | (4G10.4) | 12 | T-7a |
| 3 | | | |
| 1 5 1 14 1.722e-2 3 3 1 1 1.722e-2 3 3 14 14 1.722e-2 101 3.28 | (4G10.4) | 12 | Vcon-7a |
| 3 | | | |
| 1 5 1 14 1.722e-2 3 3 1 1 1.722e-2 3 3 14 14 1.722e-2 101 1. | (4G10.4) | 12 | econd8 |
| 3 | | | |
| 1 5 1 14 1.722e-2 3 3 1 1 1.722e-2 3 3 14 14 1.722e-2 101 1. | (4G10.4) | 12 | theta8 |
| 3 | | | |
| 1 5 1 14 0.126 3 3 1 1 0.126 3 3 14 14 0.126 101 1. | (4G10.4) | 12 | thetas8 |
| 1 | | | |
| 1 5 1 14 .375 101 1. | (4G10.4) | 12 | thetao8 |
| 1 | | | |
| 1 5 1 14 .045 101 1. | (4G10.4) | 12 | F(y)8 |
| 1 | | | |
| 1 5 1 14 1.394 101 1. | (4G10.4) | 12 | expn8 |
| 1 | | | |
| 1 5 1 14 0.0651 101 .3048 | (4G10.4) | 12 | T-8a |
| 3 | | | |
| 1 5 1 14 1.722e-2 3 3 1 1 1.722e-2 3 3 14 14 1.722e-2 101 3.28 | (4G10.4) | 12 | Vcon-8a |
| 3 | | | |
| 1 5 1 14 1.722e-2 3 3 1 1 1.722e-2 3 3 14 14 1.722e-2 101 1. | (4G10.4) | 12 | econd9 |
| 3 | | | |
| 1 5 1 14 1.722e-2 3 3 1 1 1.722e-2 3 3 14 14 1.722e-2 101 1. | (4G10.4) | 12 | theta9 |
| 3 | | | |
| 1 5 1 14 0.126 3 3 1 1 0.126 3 3 14 14 0.126 101 1. | (4G10.4) | 12 | thetas9 |
| 1 | | | |
| 1 5 1 14 .375 101 1. | (4G10.4) | 12 | thetao9 |
| 1 | | | |
| 1 5 1 14 .045 101 1. | (4G10.4) | 12 | F(y)9 |
| 1 | | | |
| 1 5 1 14 1.394 101 1. | (4G10.4) | 12 | expn9 |
| 1 | | | |
| 1 5 1 14 0.0651 101 .3048 | (4G10.4) | 12 | T-9a |
| 3 | | | |
| 1 5 1 14 1.722e-2 3 3 1 1 1.722e-2 3 3 14 14 1.722e-2 101 3.28 | (4G10.4) | 12 | Vcon-9a |
| 3 | | | |
| 1 5 1 14 1.722e-2 | | | |

G-17
BCF-H1.dat

| | | | | |
|--------------------|-------|----------|----|----------|
| 3 3 1 1 1.722e-2 | | | | |
| 3 3 14 14 1.722e-2 | | | | |
| 101 | 1. | (4G10.4) | 12 | econd10 |
| 3 | | | | |
| 1 5 1 14 1.722e-2 | | | | |
| 3 3 1 1 1.722e-2 | | | | |
| 3 3 14 14 1.722e-2 | | | | |
| 101 | 1. | (4G10.4) | 12 | theta10 |
| 3 | | | | |
| 1 5 1 14 0.126 | | | | |
| 3 3 1 1 0.126 | | | | |
| 3 3 14 14 0.126 | | | | |
| 101 | 1. | (4G10.4) | 12 | thetas10 |
| 1 | | | | |
| 1 5 1 14 .375 | | | | |
| 101 | 1. | (4G10.4) | 12 | thetao10 |
| 1 | | | | |
| 1 5 1 14 .045 | | | | |
| 101 | 1. | (4G10.4) | 12 | F(y)10 |
| 1 | | | | |
| 1 5 1 14 1.394 | | | | |
| 101 | 1. | (4G10.4) | 12 | expn10 |
| 1 | | | | |
| 1 5 1 14 0.0651 | | | | |
| 101 | .3048 | (4G10.4) | 12 | T-10a |
| 3 | | | | |
| 1 5 1 14 1.722e-2 | | | | |
| 3 3 1 1 1.722e-2 | | | | |
| 3 3 14 14 1.722e-2 | | | | |
| 101 | 3.28 | (4G10.4) | 12 | Vcon-10a |
| 3 | | | | |
| 1 5 1 14 1.722e-2 | | | | |
| 3 3 1 1 1.722e-2 | | | | |
| 3 3 14 14 1.722e-2 | | | | |
| 101 | 1. | (4G10.4) | 12 | econd11 |
| 1 | | | | |
| 1 5 1 14 1.722e-2 | | | | |
| 101 | 1. | (4G10.4) | 12 | theta11 |
| 1 | | | | |
| 1 5 1 14 0.126 | | | | |
| 101 | 1. | (4G10.4) | 12 | thetas11 |
| 1 | | | | |
| 1 5 1 14 .375 | | | | |
| 101 | 1. | (4G10.4) | 12 | thetao11 |
| 1 | | | | |
| 1 5 1 14 .045 | | | | |
| 101 | 1. | (4G10.4) | 12 | F(y)11 |
| 1 | | | | |
| 1 5 1 14 1.394 | | | | |
| 101 | 1. | (4G10.4) | 12 | expn11 |
| 1 | | | | |
| 1 5 1 14 0.0651 | | | | |
| 101 | .3048 | (4G10.4) | 12 | T-11a |
| 1 | | | | |
| 1 5 1 14 1.722e-2 | | | | |
| 101 | 3.28 | (4G10.4) | 12 | Vcon-11a |
| 1 | | | | |
| 1 5 1 14 1.722e-2 | | | | |
| 101 | 1. | (4G10.4) | 12 | econd12 |
| 1 | | | | |
| 1 5 1 14 1.722e-2 | | | | |
| 101 | 1. | (4G10.4) | 12 | theta12 |
| 1 | | | | |
| 1 5 1 14 0.126 | | | | |
| 101 | 1. | (4G10.4) | 12 | thetas12 |
| 1 | | | | |
| 1 5 1 14 .375 | | | | |
| 101 | 1. | (4G10.4) | 12 | thetao12 |
| 1 | | | | |
| 1 5 1 14 .045 | | | | |
| 101 | 1. | (4G10.4) | 12 | F(y)12 |
| 1 | | | | |
| 1 5 1 14 1.394 | | | | |
| 101 | 1. | (4G10.4) | 12 | expn12 |
| 1 | | | | |
| 1 5 1 14 0.0651 | | | | |
| 101 | .3048 | (4G10.4) | 12 | T-12a |
| 1 | | | | |
| 1 5 1 14 1.722e-2 | | | | |

G-19
BCF-H2.dat

| | | | | |
|--------------------|----------|----|---------|--|
| 3 3 1 1 1.722e-2 | | | | |
| 3 3 14 14 1.722e-2 | | | | |
| 101 1. | (4G10.4) | 12 | econd4 | |
| 3 | | | | |
| 1 5 1 14 1.722e-2 | | | | |
| 3 3 1 1 1.722e-2 | | | | |
| 3 3 14 14 1.722e-2 | | | | |
| 101 1. | (4G10.4) | 12 | theta4 | |
| 1 | | | | |
| 1 5 1 14 0.126 | | | | |
| 101 1. | (4G10.4) | 12 | thetas4 | |
| 1 | | | | |
| 1 5 1 14 .375 | | | | |
| 101 1. | (4G10.4) | 12 | thetao4 | |
| 1 | | | | |
| 1 5 1 14 .045 | | | | |
| 101 1. | (4G10.4) | 12 | F(y)4 | |
| 1 | | | | |
| 1 5 1 14 1.394 | | | | |
| 101 1. | (4G10.4) | 12 | expn4 | |
| 1 | | | | |
| 1 5 1 14 0.0651 | | | | |
| 101 .3048 | (4G10.4) | 12 | T-4a | |
| 3 | | | | |
| 1 5 1 14 1.722e-2 | | | | |
| 3 3 1 1 1.722e-2 | | | | |
| 3 3 14 14 1.722e-2 | | | | |
| 101 3.28 | (4G10.4) | 12 | Vcon-4a | |
| 3 | | | | |
| 1 5 1 14 1.722e-2 | | | | |
| 3 3 1 1 1.722e-2 | | | | |
| 3 3 14 14 1.722e-2 | | | | |
| 101 1. | (4G10.4) | 12 | econd5 | |
| 3 | | | | |
| 1 5 1 14 1.722e-2 | | | | |
| 3 3 1 1 1.722e-2 | | | | |
| 3 3 14 14 1.722e-2 | | | | |
| 101 1. | (4G10.4) | 12 | theta5 | |
| 3 | | | | |
| 1 5 1 14 .126 | | | | |
| 3 3 1 1 .126 | | | | |
| 3 3 14 14 .126 | | | | |
| 101 1. | (4G10.4) | 12 | thetas5 | |
| 1 | | | | |
| 1 5 1 14 .375 | | | | |
| 101 1. | (4G10.4) | 12 | thetao5 | |
| 1 | | | | |
| 1 5 1 14 .045 | | | | |
| 101 1. | (4G10.4) | 12 | F(y)5 | |
| 1 | | | | |
| 1 5 1 14 1.394 | | | | |
| 101 1. | (4G10.4) | 12 | expn5 | |
| 1 | | | | |
| 1 5 1 14 0.0651 | | | | |
| 101 .3048 | (4G10.4) | 12 | T-5a | |
| 3 | | | | |
| 1 5 1 14 1.722e-2 | | | | |
| 3 3 1 1 1.722e-2 | | | | |
| 3 3 14 14 1.722e-2 | | | | |
| 101 3.28 | (4G10.4) | 12 | Vcon-5a | |
| 3 | | | | |
| 1 5 1 14 1.722e-2 | | | | |
| 3 3 1 1 1.722e-2 | | | | |
| 3 3 14 14 1.722e-2 | | | | |
| 101 1. | (4G10.4) | 12 | econd6 | |
| 3 | | | | |
| 1 5 1 14 1.722e-2 | | | | |
| 3 3 1 1 1.722e-2 | | | | |
| 3 3 14 14 1.722e-2 | | | | |
| 101 1. | (4G10.4) | 12 | theta6 | |
| 3 | | | | |
| 1 5 1 14 0.126 | | | | |
| 3 3 1 1 0.126 | | | | |
| 3 3 14 14 0.126 | | | | |
| 101 1. | (4G10.4) | 12 | thetas6 | |
| 1 | | | | |
| 1 5 1 14 .375 | | | | |
| 101 1. | (4G10.4) | 12 | thetao6 | |
| 1 | | | | |
| 1 5 1 14 .045 | | | | |
| 101 1. | (4G10.4) | 12 | F(y)6 | |
| 1 | | | | |
| 1 5 1 14 1.394 | | | | |
| 101 1. | (4G10.4) | 12 | expn6 | |
| 1 | | | | |
| 1 5 1 14 0.0651 | | | | |
| 101 .3048 | (4G10.4) | 12 | T-6a | |
| 3 | | | | |
| 1 5 1 14 1.722e-2 | | | | |
| 3 3 1 1 1.722e-2 | | | | |
| 3 3 14 14 1.722e-2 | | | | |
| 101 3.28 | (4G10.4) | 12 | Vcon-6a | |
| 3 | | | | |
| 1 5 1 14 1.722e-2 | | | | |
| 3 3 1 1 1.722e-2 | | | | |

G-20
BCF-H2.dat

| | | | |
|---|----------|----|---------|
| 3 3 14 14 1.722e-2 101 1. | (4G10.4) | 12 | econd7 |
| 3 | | | |
| 1 5 1 14 1.722e-2 3 3 1 1 1.722e-2 3 3 14 14 1.722e-2 101 1. | (4G10.4) | 12 | theta7 |
| 3 | | | |
| 1 5 1 14 0.126 3 3 1 1 0.126 3 3 14 14 0.126 101 1. | (4G10.4) | 12 | thetas7 |
| 1 | | | |
| 1 5 1 14 .375 101 1. | (4G10.4) | 12 | thetao7 |
| 1 | | | |
| 1 5 1 14 .045 101 1. | (4G10.4) | 12 | F(y)7 |
| 1 | | | |
| 1 5 1 14 1.394 101 1. | (4G10.4) | 12 | expn7 |
| 1 | | | |
| 1 5 1 14 0.0651 101 .3048 | (4G10.4) | 12 | T-7a |
| 3 | | | |
| 1 5 1 14 1.722e-2 3 3 1 1 1.722e-2 3 3 14 14 1.722e-2 101 3.28 | (4G10.4) | 12 | Vcon-7a |
| 3 | | | |
| 1 5 1 14 1.722e-2 3 3 1 1 1.722e-2 3 3 14 14 1.722e-2 101 1. | (4G10.4) | 12 | econd8 |
| 3 | | | |
| 1 5 1 14 1.722e-2 3 3 1 1 1.722e-2 3 3 14 14 1.722e-2 101 1. | (4G10.4) | 12 | theta8 |
| 3 | | | |
| 1 5 1 14 0.126 3 3 1 1 0.126 3 3 14 14 0.126 101 1. | (4G10.4) | 12 | thetas8 |
| 1 | | | |
| 1 5 1 14 .375 101 1. | (4G10.4) | 12 | thetao8 |
| 1 | | | |
| 1 5 1 14 .045 101 1. | (4G10.4) | 12 | F(y)8 |
| 1 | | | |
| 1 5 1 14 1.394 101 1. | (4G10.4) | 12 | expn8 |
| 1 | | | |
| 1 5 1 14 0.0651 101 .3048 | (4G10.4) | 12 | T-8a |
| 3 | | | |
| 1 5 1 14 1.722e-2 3 3 1 1 1.722e-2 3 3 14 14 1.722e-2 101 3.28 | (4G10.4) | 12 | Vcon-8a |
| 3 | | | |
| 1 5 1 14 1.722e-2 3 3 1 1 1.722e-2 3 3 14 14 1.722e-2 101 1. | (4G10.4) | 12 | econd9 |
| 3 | | | |
| 1 5 1 14 1.722e-2 3 3 1 1 1.722e-2 3 3 14 14 1.722e-2 101 1. | (4G10.4) | 12 | theta9 |
| 3 | | | |
| 1 5 1 14 0.126 3 3 1 1 0.126 3 3 14 14 0.126 101 1. | (4G10.4) | 12 | thetas9 |
| 1 | | | |
| 1 5 1 14 .375 101 1. | (4G10.4) | 12 | thetao9 |
| 1 | | | |
| 1 5 1 14 .045 101 1. | (4G10.4) | 12 | F(y)9 |
| 1 | | | |
| 1 5 1 14 1.394 101 1. | (4G10.4) | 12 | expn9 |
| 1 | | | |
| 1 5 1 14 0.0651 101 .3048 | (4G10.4) | 12 | T-9a |
| 3 | | | |
| 1 5 1 14 1.722e-2 3 3 1 1 1.722e-2 3 3 14 14 1.722e-2 101 3.28 | (4G10.4) | 12 | Vcon-9a |
| 3 | | | |
| 1 5 1 14 1.722e-2 | | | |

G-21
BCF-H2.dat

| | | | | |
|--------------------|-------|----------|----|----------|
| 3 3 1 1 1.722e-2 | | | | |
| 3 3 14 14 1.722e-2 | | | | |
| 101 | 1. | (4G10.4) | 12 | econd10 |
| 3 | | | | |
| 1 5 1 14 1.722e-2 | | | | |
| 3 3 1 1 1.722e-2 | | | | |
| 3 3 14 14 1.722e-2 | | | | |
| 101 | 1. | (4G10.4) | 12 | theta10 |
| 3 | | | | |
| 1 5 1 14 0.126 | | | | |
| 3 3 1 1 0.126 | | | | |
| 3 3 14 14 0.126 | | | | |
| 101 | 1. | (4G10.4) | 12 | thetas10 |
| 1 | | | | |
| 1 5 1 14 .375 | | | | |
| 101 | 1. | (4G10.4) | 12 | thetao10 |
| 1 | | | | |
| 1 5 1 14 .045 | | | | |
| 101 | 1. | (4G10.4) | 12 | F(y)10 |
| 1 | | | | |
| 1 5 1 14 1.394 | | | | |
| 101 | 1. | (4G10.4) | 12 | expn10 |
| 1 | | | | |
| 1 5 1 14 0.0651 | | | | |
| 101 | .3048 | (4G10.4) | 12 | T-10a |
| 3 | | | | |
| 1 5 1 14 1.722e-2 | | | | |
| 3 3 1 1 1.722e-2 | | | | |
| 3 3 14 14 1.722e-2 | | | | |
| 101 | 3.28 | (4G10.4) | 12 | Vcon-10a |
| 3 | | | | |
| 1 5 1 14 1.722e-2 | | | | |
| 3 3 1 1 1.722e-2 | | | | |
| 3 3 14 14 1.722e-2 | | | | |
| 101 | 1. | (4G10.4) | 12 | econd11 |
| 1 | | | | |
| 1 5 1 14 1.722e-2 | | | | |
| 101 | 1. | (4G10.4) | 12 | theta11 |
| 1 | | | | |
| 1 5 1 14 0.126 | | | | |
| 101 | 1. | (4G10.4) | 12 | thetas11 |
| 1 | | | | |
| 1 5 1 14 .375 | | | | |
| 101 | 1. | (4G10.4) | 12 | thetao11 |
| 1 | | | | |
| 1 5 1 14 .045 | | | | |
| 101 | 1. | (4G10.4) | 12 | F(y)11 |
| 1 | | | | |
| 1 5 1 14 1.394 | | | | |
| 101 | 1. | (4G10.4) | 12 | expn11 |
| 1 | | | | |
| 1 5 1 14 0.0651 | | | | |
| 101 | .3048 | (4G10.4) | 12 | T-11a |
| 1 | | | | |
| 1 5 1 14 1.722e-2 | | | | |
| 101 | 3.28 | (4G10.4) | 12 | Vcon-11a |
| 1 | | | | |
| 1 5 1 14 1.722e-2 | | | | |
| 101 | 1. | (4G10.4) | 12 | econd12 |
| 1 | | | | |
| 1 5 1 14 1.722e-2 | | | | |
| 101 | 1. | (4G10.4) | 12 | theta12 |
| 1 | | | | |
| 1 5 1 14 0.126 | | | | |
| 101 | 1. | (4G10.4) | 12 | thetas12 |
| 1 | | | | |
| 1 5 1 14 .375 | | | | |
| 101 | 1. | (4G10.4) | 12 | thetao12 |
| 1 | | | | |
| 1 5 1 14 .045 | | | | |
| 101 | 1. | (4G10.4) | 12 | F(y)12 |
| 1 | | | | |
| 1 5 1 14 1.394 | | | | |
| 101 | 1. | (4G10.4) | 12 | expn12 |
| 1 | | | | |
| 1 5 1 14 0.0651 | | | | |
| 101 | .3048 | (4G10.4) | 12 | T-12a |
| 1 | | | | |
| 1 5 1 14 1.722e-2 | | | | |

APPENDIX H. MT3D Input File Example: Three-Dimensional Field Demonstration

This appendix includes example MT3D input files for the three-dimensional field demonstration. Both Phase 1 and Phase 2 input files are included here.

For the layered model separate input files were needed for each phase because the location of the acetate constant concentration boundary condition changed between phases. BTN-L1.inp is the input file for Phase 1 where as BTN-L2.inp is the input file for Phase 2.

Similarly, separate input files were needed for each phase of the homogeneous model since the location of the cathode electrode and the applied electric potential changed between phases. BTN-H1.inp is the input file for Phase 1 and BTN-H2.inp is the input file for Phase 2.

H-3
 BTN-L1.inp

| | | | | |
|--------------|-------------|----|---|---|
| 3 | | | | |
| 1 5 1 14 0. | | | | |
| 3 3 14 14 0. | | | | |
| 3 3 1 1 0. | | | | |
| 101 | 1. (15F3.0) | | 4 | !SCONC-3 |
| 3 | | | | |
| 1 5 1 14 0. | | | | |
| 3 3 14 14 0. | | | | |
| 3 3 1 1 0. | | | | |
| 101 | 1. (15F3.0) | | 4 | !SCONC-4 |
| 3 | | | | |
| 1 5 1 14 0. | | | | |
| 3 3 14 14 0. | | | | |
| 3 3 1 1 0. | | | | |
| 101 | 1. (15F3.0) | | 4 | !SCONC-5 |
| 3 | | | | |
| 1 5 1 14 0. | | | | |
| 3 3 14 14 0. | | | | |
| 3 3 1 1 200. | | | | |
| 101 | 1. (15F3.0) | | 4 | !SCONC-6 |
| 3 | | | | |
| 1 5 1 14 0. | | | | |
| 3 3 14 14 0. | | | | |
| 3 3 1 1 200. | | | | |
| 101 | 1. (15F3.0) | | 4 | !SCONC-7 |
| 3 | | | | |
| 1 5 1 14 0. | | | | |
| 3 3 14 14 0. | | | | |
| 3 3 1 1 200. | | | | |
| 101 | 1. (15F3.0) | | 4 | !SCONC-8 |
| 3 | | | | |
| 1 5 1 14 0. | | | | |
| 3 3 14 14 0. | | | | |
| 3 3 1 1 200. | | | | |
| 101 | 1. (15F3.0) | | 4 | !SCONC-9 |
| 3 | | | | |
| 1 5 1 14 0. | | | | |
| 3 3 14 14 0. | | | | |
| 3 3 1 1 200. | | | | |
| 101 | 1. (15F3.0) | | 4 | !SCONC-10 |
| 3 | | | | |
| 1 5 1 14 0. | | | | |
| 3 3 14 14 0. | | | | |
| 3 3 1 1 200. | | | | |
| 101 | 1. (15F3.0) | | 4 | !SCONC-11 |
| 3 | | | | |
| 1 5 1 14 0. | | | | |
| 3 3 14 14 0. | | | | |
| 3 3 1 1 0. | | | | |
| 101 | 1. (15F3.0) | | 4 | !SCONC-12 |
| 3 | | | | |
| 1 5 1 14 0. | | | | |
| 3 3 14 14 0. | | | | |
| 3 3 1 1 0. | | | | |
| -999.00 | | | | |
| 3 | 3 | 3 | 3 | T |
| 1 | !NPRS | | | !CINACT |
| 4485600 | !TIMPRS | | | !IFMTCN, IFMTNP, IFMTRF, IFMTDP, UCNSAV |
| 2 | !NOBS | | | |
| 6 | 3 | 3 | | !kobs, iobs, jobs |
| 6 | 1 | 3 | | !kobs, iobs, jobs |
| T | !CHKMAS | | | |
| 4485600. | 1 | 1. | | !PERLEN, NSTP, TSMULT |
| 600. | 50000 | | | !DT0, MXSTRN |

H-5
BTN-L2.inp

```

100 0 (14F8.1) 4 !SCONC2read
78.4 70.7 59.6 46.6 33.2 20.6 9.8 3.4 1.3 0.6 0.4 0.2 0.1 0.0
96.4 87.5 74.6 59.3 43.2 27.7 13.8 5.2 2.0 1.0 0.6 0.4 0.2 0.1
108.6 98.6 84.4 67.7 49.9 32.6 16.8 6.5 2.6 1.3 0.8 0.5 0.3 0.1
96.4 87.5 74.6 59.3 43.2 27.7 13.8 5.2 2.0 1.0 0.6 0.4 0.2 0.1
78.4 70.7 59.6 46.6 33.2 20.6 9.8 3.4 1.3 0.6 0.4 0.2 0.1 0.0
100 0 (14F8.1) 4 !SCONC3read
195.9 194.1 191.3 187.3 181.7 173.9 163.2 149.1 131.7 111.4 88.6 64.2 39.1 15.8
202.3 201.7 200.6 198.7 195.8 191.3 184.4 174.0 159.7 141.0 117.8 90.1 58.7 26.1
203.3 203.3 203.0 202.3 200.7 198.0 193.4 185.8 174.2 157.9 136.2 108.4 74.5 36.1
202.3 201.7 200.6 198.7 195.8 191.3 184.4 174.0 159.7 141.0 117.8 90.1 58.7 26.1
195.9 194.1 191.3 187.3 181.7 173.9 163.2 149.1 131.7 111.4 88.6 64.2 39.1 15.8
100 0 (14F8.1) 4 !SCONC4read
198.1 197.4 196.6 195.6 194.5 193.2 191.3 187.5 179.8 166.7 146.9 119.9 85.6 44.8
199.7 199.4 199.1 198.6 198.2 197.7 197.1 195.5 191.3 182.4 166.4 141.3 105.8 59.9
200.0 199.9 199.7 199.4 199.2 198.9 198.7 197.9 195.2 188.9 176.2 154.2 120.6 74.0
199.7 199.4 199.1 198.6 198.2 197.7 197.1 195.5 191.3 182.4 166.4 141.3 105.8 59.9
198.1 197.4 196.6 195.6 194.5 193.2 191.3 187.5 179.8 166.7 146.9 119.9 85.6 44.8
100 0 (14F8.1) 4 !SCONC5read
197.4 196.1 194.1 191.8 189.4 187.5 186.3 185.4 183.9 180.5 173.2 159.4 135.6 95.6
199.5 198.9 198.0 196.7 195.0 193.5 192.5 192.0 191.3 189.4 184.0 171.7 148.7 109.6
200.0 199.7 199.1 198.3 197.2 196.0 195.2 194.9 194.6 193.5 189.5 179.1 158.0 0.0
199.5 198.9 198.0 196.7 195.0 193.5 192.5 192.0 191.3 189.4 184.0 171.7 148.7 109.6
197.4 196.1 194.1 191.8 189.4 187.5 186.3 185.4 183.9 180.5 173.2 159.4 135.6 95.6
100 0 (14F8.1) 4 !SCONC6read
176.3 156.8 124.3 84.6 48.9 24.5 11.4 9.6 16.7 26.3 34.3 38.2 36.4 26.7
199.0 196.4 184.8 154.4 108.3 63.3 31.8 19.0 21.9 31.3 40.4 45.2 43.2 32.6
200.0 199.6 197.6 185.1 150.7 101.8 57.5 32.8 28.8 35.7 44.5 49.4 46.4 0.0
199.0 196.4 184.8 154.4 108.3 63.3 31.8 19.0 21.9 31.3 40.4 45.2 43.2 32.6
176.3 156.8 124.3 84.6 48.9 24.5 11.4 9.6 16.7 26.3 34.3 38.2 36.4 26.7
100 0 (14F8.1) 4 !SCONC7read
171.6 150.7 118.6 81.0 47.5 23.9 10.5 4.2 1.9 1.7 2.3 3.0 3.1 2.3
199.3 196.2 183.5 153.2 109.1 65.6 33.6 15.1 6.5 3.7 3.5 3.8 3.7 2.7
200.0 199.9 198.0 185.6 153.2 106.9 62.9 31.8 14.7 7.4 5.2 4.7 4.0 0.0
199.3 196.2 183.5 153.2 109.1 65.6 33.6 15.1 6.5 3.7 3.5 3.8 3.7 2.7
171.6 150.7 118.6 81.0 47.5 23.9 10.5 4.2 1.9 1.7 2.3 3.0 3.1 2.3
100 0 (14F8.1) 4 !SCONC8read
169.4 148.0 115.8 79.1 46.6 23.8 10.6 4.2 1.5 0.5 0.2 0.1 0.1 0.0
199.2 195.8 182.4 151.9 108.6 66.0 34.4 15.7 6.4 2.4 0.9 0.3 0.1 0.1
200.0 199.9 197.8 185.1 153.2 107.9 64.5 33.3 15.1 6.3 2.4 1.0 0.4 0.0
199.2 195.8 182.4 151.9 108.6 66.0 34.4 15.7 6.4 2.4 0.9 0.3 0.1 0.1
169.4 148.0 115.8 79.1 46.6 23.8 10.6 4.2 1.5 0.5 0.2 0.1 0.1 0.0
100 0 (14F8.1) 4 !SCONC9read
171.9 150.6 117.8 79.9 46.5 23.4 10.2 4.0 1.4 0.5 0.1 0.0 0.0 0.0
199.3 196.3 183.3 152.4 108.1 64.8 33.2 14.8 5.9 2.1 0.7 0.2 0.1 0.0
200.0 199.9 198.0 185.2 152.3 106.0 62.4 31.5 14.0 5.6 2.1 0.8 0.3 0.0
199.3 196.3 183.3 152.4 108.1 64.8 33.2 14.8 5.9 2.1 0.7 0.2 0.1 0.0
171.9 150.6 117.8 79.9 46.5 23.4 10.2 4.0 1.4 0.5 0.1 0.0 0.0 0.0
100 0 (14F8.1) 4 !SCONC10read
175.0 152.4 116.4 75.5 41.6 19.6 8.0 2.9 0.9 0.3 0.1 0.0 0.0 0.0
199.5 196.9 183.3 149.0 101.1 57.3 27.6 11.4 4.2 1.4 0.4 0.1 0.0 0.0
200.0 199.9 197.9 183.3 145.9 96.5 53.4 25.1 10.2 3.7 1.2 0.4 0.1 0.0
199.5 196.9 183.3 149.0 101.1 57.3 27.6 11.4 4.2 1.4 0.4 0.1 0.0 0.0
175.0 152.4 116.4 75.5 41.6 19.6 8.0 2.9 0.9 0.3 0.1 0.0 0.0 0.0
100 0 (14F8.1) 4 !SCONC11read
103.6 77.0 48.5 25.9 11.8 4.6 1.5 0.4 0.1 0.0 0.0 0.0 0.0 0.0
172.3 148.6 112.0 71.3 38.0 17.1 6.5 2.1 0.6 0.2 0.0 0.0 0.0 0.0
196.0 184.9 157.9 115.6 70.7 36.0 15.4 5.6 1.8 0.5 0.1 0.0 0.0 0.0
172.3 148.6 112.0 71.3 38.0 17.1 6.5 2.1 0.6 0.2 0.0 0.0 0.0 0.0
103.6 77.0 48.5 25.9 11.8 4.6 1.5 0.4 0.1 0.0 0.0 0.0 0.0 0.0
100 0 (14F8.1) 4 !SCONC12read
23.8 15.1 8.0 3.5 1.3 0.4 0.1 0.0 0.0 0.0 0.0 0.0 0.0 0.0
62.0 43.8 26.0 13.1 5.6 2.0 0.6 0.2 0.0 0.0 0.0 0.0 0.0 0.0
102.1 77.1 50.1 27.8 13.1 5.2 1.8 0.5 0.1 0.0 0.0 0.0 0.0 0.0
62.0 43.8 26.0 13.1 5.6 2.0 0.6 0.2 0.0 0.0 0.0 0.0 0.0 0.0
23.8 15.1 8.0 3.5 1.3 0.4 0.1 0.0 0.0 0.0 0.0 0.0 0.0 0.0
-999.00 !CINACT
3 3 3 3 T !IFMTCN,IFMTNP,IFMTRF,IFMTDP,UCNSAV
1 !NPRS
3013200 !TIMPRS
2 !NOBS
6 3 3 !kobs,iobs,jobs
6 1 3 !kobs,iobs,jobs
T !CHKMAS
3013200. 1 1. !PERLEN,NSTP,TSMULT
600. 50000 !DT0,MXSTRN

```

H-6 BTN-H1.inp

```

3D field PROBLEM - ACETATE
3d field problem
      12      5      14      1
sec M MOLES      !TUNIT,LUNIT,MUNIT      !NLAY,NROW,NCOL,NPER
T t F F      !FADV,FDISP,FSSM,FREACT
0 0 0 0 0 0 0 0 0 0 0 0 0 0
      0      .1524      !LAYCON
      0      .1829      !DELR
      0      0.      !DELC
      0      .3048      !HTOP
      0      .3048      !DZ-LAYER 1
      0      .3048      !DZ-LAYER 2
      0      .3048      !DZ-LAYER 3
      0      .3048      !DZ-LAYER 4
      0      .3048      !DZ-LAYER 5
      0      .3048      !DZ-LAYER 6
      0      .3048      !DZ-LAYER 7
      0      .3048      !DZ-LAYER 8
      0      .3048      !DZ-LAYER 9
      0      .3048      !DZ-LAYER 10
      0      .3048      !DZ-LAYER 11
      0      .3048      !DZ-LAYER 12
      0      .126      !PRSITY-LAYER 1
      0      .126      !PRSITY-LAYER 2
      0      .126      !PRSITY-LAYER 3
      0      .126      !PRSITY-LAYER 4
      0      .126      !PRSITY-LAYER 5
      0      .126      !PRSITY-LAYER 6
      0      .126      !PRSITY-LAYER 7
      0      .126      !PRSITY-LAYER 8
      0      .126      !PRSITY-LAYER 9
      0      .126      !PRSITY-LAYER 10
      0      .126      !PRSITY-LAYER 11
      0      .126      !PRSITY-LAYER 12
      101      1(15I3)      3      !ICBUND-LAYER 1
3
1 5 1 14 1
3 3 1 1 1
3 3 14 14 1
      101      1(15I3)      3      !ICBUND-LAYER 2
3
1 5 1 14 1
3 3 1 1 1
3 3 14 14 1
      101      1(15I3)      3      !ICBUND-LAYER 3
3
1 5 1 14 1
3 3 1 1 1
3 3 14 14 1
      101      1(15I3)      3      !ICBUND-LAYER 4
3
1 5 1 14 1
3 3 1 1 1
3 3 14 14 1
      101      1(15I3)      3      !ICBUND-LAYER 5
3
1 5 1 14 1
3 3 1 1 -1
3 3 14 14 -1
      101      1(15I3)      3      !ICBUND-LAYER 6
3
1 5 1 14 1
3 3 1 1 -1
3 3 14 14 -1
      101      1(15I3)      3      !ICBUND-LAYER 7
3
1 5 1 14 1
3 3 1 1 -1
3 3 14 14 -1
      101      1(15I3)      3      !ICBUND-LAYER 8
3
1 5 1 14 1
3 3 1 1 -1
3 3 14 14 -1
      101      1(15I3)      3      !ICBUND-LAYER 9
3
1 5 1 14 1
3 3 1 1 -1
3 3 14 14 -1
      101      1(15I3)      3      !ICBUND-LAYER 10
3
1 5 1 14 1
3 3 1 1 -1
3 3 14 14 -1
      101      1(15I3)      3      !ICBUND-LAYER 11
1
1 5 1 14 1
      101      1(15I3)      3      !ICBUND-LAYER 12
1
1 5 1 14 1
      101      1.(15F3.0)      4      !SCONC-1
3
1 5 1 14 0.
3 3 14 14 0.
3 3 1 1 0.
      101      1.(15F3.0)      4      !SCONC-2

```

H-7
 BTN-H1.inp

| | | | | |
|--------------|-------------|----|---|---|
| 3 | | | | |
| 1 5 1 14 0. | | | | |
| 3 3 14 14 0. | | | | |
| 3 3 1 1 0. | | | | |
| 101 | 1. (15F3.0) | | 4 | !SCONC-3 |
| 3 | | | | |
| 1 5 1 14 0. | | | | |
| 3 3 14 14 0. | | | | |
| 3 3 1 1 0. | | | | |
| 101 | 1. (15F3.0) | | 4 | !SCONC-4 |
| 3 | | | | |
| 1 5 1 14 0. | | | | |
| 3 3 14 14 0. | | | | |
| 3 3 1 1 0. | | | | |
| 101 | 1. (15F3.0) | | 4 | !SCONC-5 |
| 3 | | | | |
| 1 5 1 14 0. | | | | |
| 3 3 14 14 0. | | | | |
| 3 3 1 1 200. | | | | |
| 101 | 1. (15F3.0) | | 4 | !SCONC-6 |
| 3 | | | | |
| 1 5 1 14 0. | | | | |
| 3 3 14 14 0. | | | | |
| 3 3 1 1 200. | | | | |
| 101 | 1. (15F3.0) | | 4 | !SCONC-7 |
| 3 | | | | |
| 1 5 1 14 0. | | | | |
| 3 3 14 14 0. | | | | |
| 3 3 1 1 200. | | | | |
| 101 | 1. (15F3.0) | | 4 | !SCONC-8 |
| 3 | | | | |
| 1 5 1 14 0. | | | | |
| 3 3 14 14 0. | | | | |
| 3 3 1 1 200. | | | | |
| 101 | 1. (15F3.0) | | 4 | !SCONC-9 |
| 3 | | | | |
| 1 5 1 14 0. | | | | |
| 3 3 14 14 0. | | | | |
| 3 3 1 1 200. | | | | |
| 101 | 1. (15F3.0) | | 4 | !SCONC-10 |
| 3 | | | | |
| 1 5 1 14 0. | | | | |
| 3 3 14 14 0. | | | | |
| 3 3 1 1 200. | | | | |
| 101 | 1. (15F3.0) | | 4 | !SCONC-11 |
| 3 | | | | |
| 1 5 1 14 0. | | | | |
| 3 3 14 14 0. | | | | |
| 3 3 1 1 0. | | | | |
| 101 | 1. (15F3.0) | | 4 | !SCONC-12 |
| 3 | | | | |
| 1 5 1 14 0. | | | | |
| 3 3 14 14 0. | | | | |
| 3 3 1 1 0. | | | | |
| -999.00 | | | | |
| 3 | 3 | 3 | 3 | T |
| 1 | !NPRS | | | !CINACT |
| 4485600 | !TIMPRS | | | !IFMTCN, IFMTNP, IFMTRF, IFMTDP, UCNSAV |
| 2 | !NOBS | | | |
| 6 | 3 | 3 | | !kobs,iobs,jobs |
| 6 | 1 | 3 | | !kobs,iobs,jobs |
| T | !CHKMAS | | | |
| 4485600. | 1 | 1. | | !PERLEN, NSTP, TSMULT |
| 600. | 50000 | | | !DT0, MXSTRN |

APPENDIX I. MODFLOW Output File Example: Three-Dimensional Field Demonstration

This appendix includes example MODFLOW output files for the three-dimensional field demonstration. Both Phase 1 (OUTPUT-H1.txt) and Phase 2 (OUTPUT-H2.txt) output files are listed. To save space only the homogeneous model results are shown here.

I-17
OUTPUT-H1.txt

| | 11 | 12 | 13 | 14 |
|-----|------------|------------|------------|------------|
| 0 1 | 6.5100E-02 | 6.5100E-02 | 6.5100E-02 | 6.5100E-02 |
| 0 2 | 6.5100E-02 | 6.5100E-02 | 6.5100E-02 | 6.5100E-02 |
| 0 3 | 6.5100E-02 | 6.5100E-02 | 6.5100E-02 | 6.5100E-02 |
| 0 4 | 6.5100E-02 | 6.5100E-02 | 6.5100E-02 | 6.5100E-02 |
| 0 5 | 6.5100E-02 | 6.5100E-02 | 6.5100E-02 | 6.5100E-02 |
| 0 | 6.5100E-02 | 6.5100E-02 | 6.5100E-02 | 6.5100E-02 |

TRANSIS. ALONG ROWS FOR LAYER 12 WILL BE READ ON UNIT 11 USING BLOCK FORMAT

| | 1 | 2 | 3 | 4 | 5 | 6 | 7 | 8 | 9 | 10 |
|-----|------------|------------|------------|------------|------------|------------|------------|------------|------------|------------|
| 0 1 | 5.2487E-03 | 5.2487E-03 | 5.2487E-03 | 5.2487E-03 | 5.2487E-03 | 5.2487E-03 | 5.2487E-03 | 5.2487E-03 | 5.2487E-03 | 5.2487E-03 |
| 0 2 | 5.2487E-03 | 5.2487E-03 | 5.2487E-03 | 5.2487E-03 | 5.2487E-03 | 5.2487E-03 | 5.2487E-03 | 5.2487E-03 | 5.2487E-03 | 5.2487E-03 |
| 0 3 | 5.2487E-03 | 5.2487E-03 | 5.2487E-03 | 5.2487E-03 | 5.2487E-03 | 5.2487E-03 | 5.2487E-03 | 5.2487E-03 | 5.2487E-03 | 5.2487E-03 |
| 0 4 | 5.2487E-03 | 5.2487E-03 | 5.2487E-03 | 5.2487E-03 | 5.2487E-03 | 5.2487E-03 | 5.2487E-03 | 5.2487E-03 | 5.2487E-03 | 5.2487E-03 |
| 0 5 | 5.2487E-03 | 5.2487E-03 | 5.2487E-03 | 5.2487E-03 | 5.2487E-03 | 5.2487E-03 | 5.2487E-03 | 5.2487E-03 | 5.2487E-03 | 5.2487E-03 |
| 0 | 5.2487E-03 | 5.2487E-03 | 5.2487E-03 | 5.2487E-03 | 5.2487E-03 | 5.2487E-03 | 5.2487E-03 | 5.2487E-03 | 5.2487E-03 | 5.2487E-03 |

SOLUTION BY PRECONDITIONED CONJUGATE GRADIENT

0
1
2
3
4
5
6
7
8
9
10
11
12
13
14
15
16
17
18
19
20
21
22
23
24
25
26
27
28
29
30
31
32
33
34
35
36
37
38
39
40
41
42
43
44
45
46
47
48
49
50
51
52
53
54
55
56
57
58
59
60
61
62
63
64
65
66
67
68
69
70
71
72
73
74
75
76
77
78
79
80
81
82
83
84
85
86
87
88
89
90
91
92
93
94
95
96
97
98
99
100
101
102
103
104
105
106
107
108
109
110
111
112
113
114
115
116
117
118
119
120
121
122
123
124
125
126
127
128
129
130
131
132
133
134
135
136
137
138
139
140
141
142
143
144
145
146
147
148
149
150
151
152
153
154
155
156
157
158
159
160
161
162
163
164
165
166
167
168
169
170
171
172
173
174
175
176
177
178
179
180
181
182
183
184
185
186
187
188
189
190
191
192
193
194
195
196
197
198
199
200
201
202
203
204
205
206
207
208
209
210
211
212
213
214
215
216
217
218
219
220
221
222
223
224
225
226
227
228
229
230
231
232
233
234
235
236
237
238
239
240
241
242
243
244
245
246
247
248
249
250
251
252
253
254
255
256
257
258
259
260
261
262
263
264
265
266
267
268
269
270
271
272
273
274
275
276
277
278
279
280
281
282
283
284
285
286
287
288
289
290
291
292
293
294
295
296
297
298
299
300
301
302
303
304
305
306
307
308
309
310
311
312
313
314
315
316
317
318
319
320
321
322
323
324
325
326
327
328
329
330
331
332
333
334
335
336
337
338
339
340
341
342
343
344
345
346
347
348
349
350
351
352
353
354
355
356
357
358
359
360
361
362
363
364
365
366
367
368
369
370
371
372
373
374
375
376
377
378
379
380
381
382
383
384
385
386
387
388
389
390
391
392
393
394
395
396
397
398
399
400
401
402
403
404
405
406
407
408
409
410
411
412
413
414
415
416
417
418
419
420
421
422
423
424
425
426
427
428
429
430
431
432
433
434
435
436
437
438
439
440
441
442
443
444
445
446
447
448
449
450
451
452
453
454
455
456
457
458
459
460
461
462
463
464
465
466
467
468
469
470
471
472
473
474
475
476
477
478
479
480
481
482
483
484
485
486
487
488
489
490
491
492
493
494
495
496
497
498
499
500
501
502
503
504
505
506
507
508
509
510
511
512
513
514
515
516
517
518
519
520
521
522
523
524
525
526
527
528
529
530
531
532
533
534
535
536
537
538
539
540
541
542
543
544
545
546
547
548
549
550
551
552
553
554
555
556
557
558
559
560
561
562
563
564
565
566
567
568
569
570
571
572
573
574
575
576
577
578
579
580
581
582
583
584
585
586
587
588
589
590
591
592
593
594
595
596
597
598
599
600
601
602
603
604
605
606
607
608
609
610
611
612
613
614
615
616
617
618
619
620
621
622
623
624
625
626
627
628
629
630
631
632
633
634
635
636
637
638
639
640
641
642
643
644
645
646
647
648
649
650
651
652
653
654
655
656
657
658
659
660
661
662
663
664
665
666
667
668
669
670
671
672
673
674
675
676
677
678
679
680
681
682
683
684
685
686
687
688
689
690
691
692
693
694
695
696
697
698
699
700
701
702
703
704
705
706
707
708
709
710
711
712
713
714
715
716
717
718
719
720
721
722
723
724
725
726
727
728
729
730
731
732
733
734
735
736
737
738
739
740
741
742
743
744
745
746
747
748
749
750
751
752
753
754
755
756
757
758
759
760
761
762
763
764
765
766
767
768
769
770
771
772
773
774
775
776
777
778
779
780
781
782
783
784
785
786
787
788
789
790
791
792
793
794
795
796
797
798
799
800
801
802
803
804
805
806
807
808
809
810
811
812
813
814
815
816
817
818
819
820
821
822
823
824
825
826
827
828
829
830
831
832
833
834
835
836
837
838
839
840
841
842
843
844
845
846
847
848
849
850
851
852
853
854
855
856
857
858
859
860
861
862
863
864
865
866
867
868
869
870
871
872
873
874
875
876
877
878
879
880
881
882
883
884
885
886
887
888
889
890
891
892
893
894
895
896
897
898
899
900
901
902
903
904
905
906
907
908
909
910
911
912
913
914
915
916
917
918
919
920
921
922
923
924
925
926
927
928
929
930
931
932
933
934
935
936
937
938
939
940
941
942
943
944
945
946
947
948
949
950
951
952
953
954
955
956
957
958
959
960
961
962
963
964
965
966
967
968
969
970
971
972
973
974
975
976
977
978
979
980
981
982
983
984
985
986
987
988
989
990
991
992
993
994
995
996
997
998
999
1000

NUMBER OF TIME STEPS = 1

MULTIPLIER FOR DELT = 1.000

INITIAL TIME STEP SIZE = 4485600.

0 18 ITERATIONS FOR TIME STEP 1 IN STRESS PERIOD 1

0 HEAD/DRAWDOWN PRINTOUT FLAG = 1 TOTAL BUDGET PRINTOUT FLAG = 0 CELL-BY-CELL FLOW TERM FLAG = 1

0 OUTPUT FLAGS FOR ALL LAYERS ARE THE SAME:

0 HEAD DRAWDOWN HEAD DRAWDOWN

0 PRINTOUT PRINTOUT SAVE SAVE

0 1 0 1 0

0 HEAD IN LAYER 1 AT END OF TIME STEP 1 IN STRESS PERIOD 1

| | 1 | 2 | 3 | 4 | 5 | 6 | 7 | 8 | 9 | 10 | 11 | 12 | 13 | 14 |
|-----|-------|-------|-------|-------|-------|-------|-------|-------|-------|-------|-------|-------|-------|-------|
| 0 1 | 46.46 | 46.88 | 47.69 | 48.84 | 50.26 | 51.88 | 53.61 | 55.39 | 57.12 | 58.74 | 60.16 | 61.31 | 62.12 | 62.54 |
| 0 2 | 46.46 | 46.87 | 47.69 | 48.83 | 50.26 | 51.87 | 53.61 | 55.39 | 57.13 | 58.74 | 60.17 | 61.32 | 62.13 | 62.55 |
| 0 3 | 46.45 | 46.87 | 47.69 | 48.83 | 50.26 | 51.87 | 53.61 | 55.39 | 57.12 | 58.74 | 60.16 | 61.31 | 62.13 | 62.55 |
| 0 4 | 46.45 | 46.87 | 47.69 | 48.84 | 50.26 | 51.88 | 53.61 | 55.39 | 57.12 | 58.74 | 60.16 | 61.31 | 62.12 | 62.54 |
| 0 5 | 46.46 | 46.88 | 47.69 | 48.84 | 50.26 | 51.88 | 53.61 | 55.39 | 57.12 | 58.74 | 60.16 | 61.31 | 62.12 | 62.54 |

| | 1 | 2 | 3 | 4 | 5 | 6 | 7 | 8 | 9 | 10 | 11 | 12 | 13 | 14 |
|-----|-------|-------|-------|-------|-------|-------|-------|-------|-------|-------|-------|-------|-------|-------|
| 0 1 | 44.80 | 45.33 | 46.35 | 47.76 | 49.47 | 51.40 | 53.45 | 55.55 | 57.60 | 59.53 | 61.24 | 62.65 | 63.67 | 64.20 |
| 0 2 | 44.76 | 45.30 | 46.33 | 47.75 | 49.47 | 51.40 | 53.45 | 55.55 | 57.60 | 59.53 | 61.25 | 62.67 | 63.70 | 64.24 |
| 0 3 | 44.73 | 45.28 | 46.31 | 47.74 | 49.46 | 51.40 | 53.45 | 55.55 | 57.60 | 59.53 | 61.26 | 62.69 | 63.72 | 64.27 |
| 0 4 | 44.76 | 45.30 | 46.33 | 47.75 | 49.47 | 51.40 | 53.45 | 55.55 | 57.60 | 59.53 | 61.25 | 62.67 | 63.70 | 64.24 |
| 0 5 | 44.80 | 45.33 | 46.35 | 47.76 | 49.47 | 51.40 | 53.45 | 55.55 | 57.60 | 59.53 | 61.24 | 62.65 | 63.67 | 64.20 |

| | 1 | 2 | 3 | 4 | 5 | 6 | 7 | 8 | 9 | 10 | 11 | 12 | 13 | 14 |
|-----|-------|-------|-------|-------|-------|-------|-------|-------|-------|-------|-------|-------|-------|-------|
| 0 1 | 41.11 | 41.94 | 43.47 | 45.50 | 47.96 | 50.44 | 53.13 | 55.87 | 58.57 | 61.16 | 63.56 | 65.63 | 67.22 | 68.12 |
| 0 2 | 40.88 | 41.78 | 43.31 | 45.44 | 47.84 | 50.43 | 53.13 | 55.87 | 58.57 | 61.16 | 63.56 | 65.63 | 67.22 | 68.12 |
| 0 3 | 40.67 | 41.64 | 43.30 | 45.41 | 47.82 | 50.42 | 53.13 | 55.87 | 58.58 | 61.18 | 63.59 | 65.70 | 67.36 | 68.33 |
| 0 4 | 40.88 | 41.78 | 43.37 | 45.44 | 47.84 | 50.43 | 53.13 | 55.87 | 58.57 | 61.16 | 63.56 | 65.63 | 67.22 | 68.12 |
| 0 5 | 41.11 | 41.94 | 43.47 | 45.50 | 47.96 | 50.44 | 53.13 | 55.87 | 58.56 | 61.14 | 63.50 | 65.53 | 67.06 | 67.89 |

| | 1 | 2 | 3 | 4 | 5 | 6 | 7 | 8 | 9 | 10 | 11 | 12 | 13 | 14 |
|-----|-------|-------|-------|-------|-------|-------|-------|-------|-------|-------|-------|-------|-------|-------|
| 0 1 | 34.68 | 36.25 | 38.85 | 42.02 | 45.46 | 49.04 | 52.67 | 56.33 | 59.96 | 63.54 | 66.98 | 70.14 | 72.75 | 74.32 |
| 0 2 | 33.38 | 35.43 | 38.43 | 41.82 | 45.38 | 49.00 | 52.67 | 56.33 | 60.00 | 63.62 | 67.18 | 70.57 | 73.57 | 75.62 |
| 0 3 | 31.52 | 34.52 | 38.04 | 41.66 | 45.31 | 48.98 | 52.66 | 56.34 | 60.02 | 63.69 | 67.34 | 70.96 | 74.48 | 77.48 |
| 0 4 | 33.38 | 35.43 | 38.43 | 41.82 | 45.38 | 49.00 | 52.67 | 56.33 | 60.00 | 63.62 | 67.18 | 70.57 | 73.57 | 75.62 |
| 0 5 | 34.68 | 36.25 | 38.85 | 42.02 | 45.46 | 49.04 | 52.67 | 56.33 | 59.96 | 63.54 | 66.98 | 70.14 | 72.75 | 74.32 |

| | 1 | 2 | 3 | 4 | 5 | 6 | 7 | 8 | 9 | 10 | 11 | 12 | 13 | 14 |
|-----|-------|-------|-------|-------|-------|-------|-------|-------|-------|-------|-------|-------|-------|--------|
| 0 1 | 25.57 | 28.73 | 33.19 | 37.97 | 42.77 | 47.50 | 52.17 | 56.83 | 61.50 | 66.23 | 71.03 | 75.82 | 80.27 | 83.43 |
| 0 2 | 19.23 | 25.54 | 31.82 | 37.43 | 42.56 | 47.43 | 52.16 | 56.84 | 61.57 | 66.44 | 71.57 | 77.18 | 82.46 | 89.77 |
| 0 3 | 0.00 | 20.21 | 30.24 | 36.93 | 42.39 | 47.37 | 52.14 | 56.86 | 61.63 | 66.61 | 72.07 | 78.76 | 86.79 | 109.00 |
| 0 4 | 19.23 | 25.54 | 31.82 | 37.43 | 42.56 | 47.43 | 52.16 | 56.84 | 61.57 | 66.44 | 71.57 | 77.18 | 83.46 | 89.77 |
| 0 5 | 25.57 | 28.73 | 33.19 | 37.97 | 42.77 | 47.50 | 52.17 | 56.83 | | | | | | |

I-18
OUTPUT-H1.txt

0 3 0.00 16.65 26.45 33.78 40.11 45.99 51.68 57.32 63.01 68.89 75.22 82.55 92.35 109.00
 0 4 15.19 21.26 27.93 34.28 40.28 46.05 51.70 57.30 62.95 68.72 74.72 81.07 87.74 93.81
 0 5 20.87 24.27 29.28 34.84 40.51 46.14 51.72 57.28 62.86 68.49 74.16 79.72 84.73 88.13
 1 HEAD IN LAYER 10 AT END OF TIME STEP 1 IN STRESS PERIOD 1

| | 1 | 2 | 3 | 4 | 5 | 6 | 7 | 8 | 9 | 10 | 11 | 12 | 13 | 14 |
|-----|---|-------|-------|-------|-------|-------|-------|-------|-------|-------|-------|-------|-------|--------|
| 0 1 | 24.15 | 27.29 | 31.01 | 36.78 | 41.85 | 46.92 | 51.98 | 57.02 | 62.08 | 67.15 | 72.22 | 77.19 | 81.71 | 84.85 |
| 0 2 | 18.14 | 24.27 | 30.52 | 36.26 | 41.65 | 46.85 | 51.96 | 57.04 | 62.15 | 67.35 | 72.74 | 78.48 | 84.73 | 90.86 |
| 0 3 | 0.00 | 19.23 | 29.02 | 35.79 | 41.49 | 46.79 | 51.94 | 57.06 | 62.21 | 67.51 | 73.21 | 79.98 | 89.77 | 105.00 |
| 0 4 | 18.14 | 24.27 | 30.52 | 36.26 | 41.65 | 46.85 | 51.96 | 57.04 | 62.15 | 67.35 | 72.74 | 78.48 | 84.73 | 90.86 |
| 0 5 | 24.15 | 27.29 | 31.01 | 36.78 | 41.85 | 46.92 | 51.98 | 57.02 | 62.08 | 67.15 | 72.22 | 77.19 | 81.71 | 84.85 |
| 1 | HEAD IN LAYER 11 AT END OF TIME STEP 1 IN STRESS PERIOD 1 | | | | | | | | | | | | | |

| | 1 | 2 | 3 | 4 | 5 | 6 | 7 | 8 | 9 | 10 | 11 | 12 | 13 | 14 |
|-----|---|-------|-------|-------|-------|-------|-------|-------|-------|-------|-------|-------|-------|-------|
| 0 1 | 31.52 | 33.23 | 36.13 | 39.73 | 43.74 | 47.97 | 52.31 | 56.69 | 61.03 | 65.26 | 69.27 | 72.87 | 75.77 | 77.48 |
| 0 2 | 30.28 | 32.45 | 35.72 | 39.54 | 43.66 | 47.94 | 52.30 | 56.70 | 61.06 | 65.34 | 69.46 | 73.28 | 76.55 | 78.72 |
| 0 3 | 28.92 | 31.58 | 35.35 | 39.39 | 43.60 | 47.91 | 52.30 | 56.70 | 61.09 | 65.40 | 69.61 | 73.65 | 77.42 | 80.48 |
| 0 4 | 30.28 | 32.45 | 35.72 | 39.54 | 43.66 | 47.94 | 52.30 | 56.70 | 61.06 | 65.34 | 69.46 | 73.28 | 76.55 | 78.72 |
| 0 5 | 31.52 | 33.23 | 36.13 | 39.73 | 43.74 | 47.97 | 52.31 | 56.69 | 61.03 | 65.26 | 69.27 | 72.87 | 75.77 | 77.48 |
| 1 | HEAD IN LAYER 12 AT END OF TIME STEP 1 IN STRESS PERIOD 1 | | | | | | | | | | | | | |

| | 1 | 2 | 3 | 4 | 5 | 6 | 7 | 8 | 9 | 10 | 11 | 12 | 13 | 14 |
|-----|-------|-------|-------|-------|-------|-------|-------|-------|-------|-------|-------|-------|-------|-------|
| 0 1 | 35.46 | 36.62 | 38.74 | 41.60 | 44.97 | 48.66 | 52.53 | 56.47 | 60.34 | 64.03 | 67.40 | 70.26 | 72.38 | 73.54 |
| 0 2 | 35.22 | 36.44 | 38.64 | 41.54 | 44.94 | 48.65 | 52.53 | 56.47 | 60.35 | 64.06 | 67.46 | 70.36 | 72.56 | 73.78 |
| 0 3 | 34.99 | 36.29 | 38.55 | 41.50 | 44.92 | 48.64 | 52.52 | 56.47 | 60.36 | 64.08 | 67.50 | 70.45 | 72.71 | 74.01 |
| 0 4 | 35.22 | 36.44 | 38.64 | 41.54 | 44.94 | 48.65 | 52.53 | 56.47 | 60.35 | 64.06 | 67.46 | 70.36 | 72.56 | 73.78 |
| 0 5 | 35.46 | 36.62 | 38.74 | 41.60 | 44.97 | 48.66 | 52.53 | 56.47 | 60.34 | 64.03 | 67.40 | 70.26 | 72.38 | 73.54 |
| 0 | | | | | | | | | | | | | | |

VOLUMETRIC BUDGET FOR ENTIRE MODEL AT END OF TIME STEP 1 IN STRESS PERIOD 1

| | CUMULATIVE VOLUMES | L**3 | RATES FOR THIS TIME STEP | L**3/T |
|---|-----------------------|-------------|--------------------------|--------------|
| 0 | IN: | | IN: | |
| | STORAGE = | 0.00000 | STORAGE = | 0.00000 |
| | CONSTANT HEAD = | 0.71977E+07 | CONSTANT HEAD = | 1.6046 |
| | TOTAL IN = | 0.71977E+07 | TOTAL IN = | 1.6046 |
| 0 | OUT: | | OUT: | |
| | STORAGE = | 0.00000 | STORAGE = | 0.00000 |
| | CONSTANT HEAD = | 0.71977E+07 | CONSTANT HEAD = | 1.6046 |
| | TOTAL OUT = | 0.71977E+07 | TOTAL OUT = | 1.6046 |
| 0 | IN - OUT = | -2.5000 | IN - OUT = | -0.59605E-06 |
| 0 | PERCENT DISCREPANCY = | 0.00 | PERCENT DISCREPANCY = | 0.00 |

TIME SUMMARY AT END OF TIME STEP 1 IN STRESS PERIOD 1

| | SECONDS | MINUTES | HOURS | DAYS | YEARS |
|-----------------------|--------------|---------|---------|---------|----------|
| TIME STEP LENGTH | 0.448560E+07 | 74760.0 | 1246.00 | 51.9167 | 0.142140 |
| STRESS PERIOD TIME | 0.448560E+07 | 74760.0 | 1246.00 | 51.9167 | 0.142140 |
| TOTAL SIMULATION TIME | 0.448560E+07 | 74760.0 | 1246.00 | 51.9167 | 0.142140 |

I-34
OUTPUT-H2.txt

| | 11 | 12 | 13 | 14 |
|-----|------------|------------|------------|------------|
| 0 1 | 6.5100E-02 | 6.5100E-02 | 6.5100E-02 | 6.5100E-02 |
| 0 2 | 6.5100E-02 | 6.5100E-02 | 6.5100E-02 | 6.5100E-02 |
| 0 3 | 6.5100E-02 | 6.5100E-02 | 6.5100E-02 | 6.5100E-02 |
| 0 4 | 6.5100E-02 | 6.5100E-02 | 6.5100E-02 | 6.5100E-02 |
| 0 5 | 6.5100E-02 | 6.5100E-02 | 6.5100E-02 | 6.5100E-02 |
| 0 | 6.5100E-02 | 6.5100E-02 | 6.5100E-02 | 6.5100E-02 |

TRANSMIS. ALONG ROWS FOR LAYER 12 WILL BE READ ON UNIT 11 USING BLOCK FORMAT

| | 1 | 2 | 3 | 4 | 5 | 6 | 7 | 8 | 9 | 10 |
|-----|------------|------------|------------|------------|------------|------------|------------|------------|------------|------------|
| 0 1 | 5.2487E-03 | 5.2487E-03 | 5.2487E-03 | 5.2487E-03 | 5.2487E-03 | 5.2487E-03 | 5.2487E-03 | 5.2487E-03 | 5.2487E-03 | 5.2487E-03 |
| 0 2 | 5.2487E-03 | 5.2487E-03 | 5.2487E-03 | 5.2487E-03 | 5.2487E-03 | 5.2487E-03 | 5.2487E-03 | 5.2487E-03 | 5.2487E-03 | 5.2487E-03 |
| 0 3 | 5.2487E-03 | 5.2487E-03 | 5.2487E-03 | 5.2487E-03 | 5.2487E-03 | 5.2487E-03 | 5.2487E-03 | 5.2487E-03 | 5.2487E-03 | 5.2487E-03 |
| 0 4 | 5.2487E-03 | 5.2487E-03 | 5.2487E-03 | 5.2487E-03 | 5.2487E-03 | 5.2487E-03 | 5.2487E-03 | 5.2487E-03 | 5.2487E-03 | 5.2487E-03 |
| 0 5 | 5.2487E-03 | 5.2487E-03 | 5.2487E-03 | 5.2487E-03 | 5.2487E-03 | 5.2487E-03 | 5.2487E-03 | 5.2487E-03 | 5.2487E-03 | 5.2487E-03 |
| 0 | 5.2487E-03 | 5.2487E-03 | 5.2487E-03 | 5.2487E-03 | 5.2487E-03 | 5.2487E-03 | 5.2487E-03 | 5.2487E-03 | 5.2487E-03 | 5.2487E-03 |

SOLUTION BY PRECONDITIONED CONJUGATE GRADIENT

0 MAXIMUM ITERATIONS ALLOWED FOR CLOSURE = 50
 HEAD CHANGE CRITERION FOR CLOSURE = 0.10000E-02
 1 MAXIMUM ALLOWABLE RESIDUAL ERROR FOR CLOSURE = 0.00000E+00
 STRESS PERIOD NO. 1, LENGTH = 3013200.
 NUMBER OF TIME STEPS = 1
 MULTIPLIER FOR DELT = 1.000
 INITIAL TIME STEP SIZE = 3013200.

0 18 ITERATIONS FOR TIME STEP 1 IN STRESS PERIOD 1
 HEAD/DRAWDOWN PRINTOUT FLAG = 1 TOTAL BUDGET PRINTOUT FLAG = 0 CELL-BY-CELL FLOW TERM FLAG = 1
 0 OUTPUT FLAGS FOR ALL LAYERS ARE THE SAME:
 HEAD DRAWDOWN HEAD DRAWDOWN
 PRINTOUT PRINTOUT SAVE SAVE

1 HEAD IN LAYER 1 AT END OF TIME STEP 1 IN STRESS PERIOD 1

| | 1 | 2 | 3 | 4 | 5 | 6 | 7 | 8 | 9 | 10 | 11 | 12 | 13 | 14 |
|-----|--|-------|-------|-------|-------|-------|-------|-------|-------|-------|-------|-------|-------|-------|
| 0 1 | 26.48 | 26.62 | 26.90 | 27.31 | 27.85 | 28.51 | 29.26 | 30.08 | 30.94 | 31.77 | 32.54 | 33.18 | 33.65 | 33.90 |
| 0 2 | 26.48 | 26.62 | 26.90 | 27.31 | 27.85 | 28.51 | 29.26 | 30.08 | 30.94 | 31.77 | 32.54 | 33.18 | 33.65 | 33.90 |
| 0 3 | 26.48 | 26.62 | 26.90 | 27.31 | 27.85 | 28.51 | 29.26 | 30.08 | 30.94 | 31.77 | 32.54 | 33.18 | 33.65 | 33.90 |
| 0 4 | 26.48 | 26.62 | 26.90 | 27.31 | 27.85 | 28.51 | 29.26 | 30.08 | 30.94 | 31.77 | 32.54 | 33.18 | 33.65 | 33.90 |
| 0 5 | 26.48 | 26.62 | 26.90 | 27.31 | 27.85 | 28.51 | 29.26 | 30.08 | 30.94 | 31.77 | 32.54 | 33.18 | 33.65 | 33.90 |
| 1 | HEAD IN LAYER 2 AT END OF TIME STEP 1 IN STRESS PERIOD 1 | | | | | | | | | | | | | |

1 HEAD IN LAYER 3 AT END OF TIME STEP 1 IN STRESS PERIOD 1

| | 1 | 2 | 3 | 4 | 5 | 6 | 7 | 8 | 9 | 10 | 11 | 12 | 13 | 14 |
|-----|--|-------|-------|-------|-------|-------|-------|-------|-------|-------|-------|-------|-------|-------|
| 0 1 | 25.93 | 26.07 | 26.36 | 26.80 | 27.39 | 28.12 | 28.98 | 29.96 | 31.00 | 32.05 | 33.04 | 33.89 | 34.52 | 34.86 |
| 0 2 | 25.93 | 26.07 | 26.36 | 26.80 | 27.39 | 28.12 | 28.98 | 29.96 | 31.00 | 32.05 | 33.05 | 33.90 | 34.54 | 34.89 |
| 0 3 | 25.93 | 26.07 | 26.36 | 26.80 | 27.39 | 28.11 | 28.98 | 29.96 | 31.00 | 32.05 | 33.05 | 33.91 | 34.56 | 34.91 |
| 0 4 | 25.93 | 26.07 | 26.36 | 26.80 | 27.38 | 28.12 | 28.98 | 29.96 | 31.00 | 32.05 | 33.05 | 33.90 | 34.54 | 34.89 |
| 0 5 | 25.93 | 26.07 | 26.36 | 26.80 | 27.39 | 28.12 | 28.98 | 29.96 | 31.00 | 32.05 | 33.04 | 33.89 | 34.52 | 34.86 |
| 1 | HEAD IN LAYER 3 AT END OF TIME STEP 1 IN STRESS PERIOD 1 | | | | | | | | | | | | | |

1 HEAD IN LAYER 4 AT END OF TIME STEP 1 IN STRESS PERIOD 1

| | 1 | 2 | 3 | 4 | 5 | 6 | 7 | 8 | 9 | 10 | 11 | 12 | 13 | 14 |
|-----|--|-------|-------|-------|-------|-------|-------|-------|-------|-------|-------|-------|-------|-------|
| 0 1 | 24.79 | 24.94 | 25.23 | 25.70 | 26.35 | 27.21 | 28.28 | 29.57 | 31.02 | 32.55 | 34.06 | 35.43 | 36.49 | 37.09 |
| 0 2 | 24.79 | 24.93 | 25.23 | 25.69 | 26.34 | 27.19 | 28.27 | 29.56 | 31.02 | 32.57 | 34.10 | 35.51 | 36.62 | 37.27 |
| 0 3 | 24.79 | 24.93 | 25.23 | 25.68 | 26.33 | 27.18 | 28.25 | 29.55 | 31.02 | 32.58 | 34.13 | 35.56 | 36.73 | 37.44 |
| 0 4 | 24.79 | 24.93 | 25.23 | 25.69 | 26.34 | 27.19 | 28.27 | 29.56 | 31.02 | 32.57 | 34.10 | 35.51 | 36.62 | 37.27 |
| 0 5 | 24.79 | 24.94 | 25.23 | 25.70 | 26.35 | 27.21 | 28.28 | 29.57 | 31.02 | 32.55 | 34.06 | 35.43 | 36.49 | 37.09 |
| 1 | HEAD IN LAYER 4 AT END OF TIME STEP 1 IN STRESS PERIOD 1 | | | | | | | | | | | | | |

1 HEAD IN LAYER 5 AT END OF TIME STEP 1 IN STRESS PERIOD 1

| | 1 | 2 | 3 | 4 | 5 | 6 | 7 | 8 | 9 | 10 | 11 | 12 | 13 | 14 |
|-----|--|-------|-------|-------|-------|-------|-------|-------|-------|-------|-------|-------|-------|-------|
| 0 1 | 23.08 | 23.20 | 23.45 | 23.87 | 24.51 | 25.46 | 26.80 | 28.58 | 30.72 | 33.10 | 35.58 | 37.96 | 39.97 | 41.21 |
| 0 2 | 23.08 | 23.19 | 23.43 | 23.83 | 24.45 | 25.36 | 26.68 | 28.49 | 30.69 | 33.14 | 35.72 | 38.30 | 40.64 | 42.26 |
| 0 3 | 23.08 | 23.19 | 23.42 | 23.81 | 24.40 | 25.27 | 26.56 | 28.41 | 30.66 | 33.16 | 35.84 | 38.61 | 41.38 | 43.76 |
| 0 4 | 23.08 | 23.19 | 23.43 | 23.83 | 24.45 | 25.36 | 26.68 | 28.49 | 30.69 | 33.14 | 35.72 | 38.30 | 40.64 | 42.26 |
| 0 5 | 23.08 | 23.20 | 23.45 | 23.87 | 24.51 | 25.46 | 26.80 | 28.58 | 30.72 | 33.10 | 35.58 | 37.96 | 39.97 | 41.21 |
| 1 | HEAD IN LAYER 5 AT END OF TIME STEP 1 IN STRESS PERIOD 1 | | | | | | | | | | | | | |

1 HEAD IN LAYER 6 AT END OF TIME STEP 1 IN STRESS PERIOD 1

| | 1 | 2 | 3 | 4 | 5 | 6 | 7 | 8 | 9 | 10 | 11 | 12 | 13 | 14 |
|-----|--|-------|-------|-------|-------|-------|-------|-------|-------|-------|-------|-------|-------|-------|
| 0 1 | 20.93 | 20.96 | 21.04 | 21.23 | 21.62 | 22.41 | 23.90 | 26.36 | 29.54 | 33.18 | 37.07 | 41.03 | 44.73 | 47.34 |
| 0 2 | 20.91 | 20.93 | 20.98 | 21.09 | 21.33 | 21.87 | 23.14 | 25.84 | 29.32 | 33.21 | 37.45 | 42.12 | 47.31 | 52.49 |
| 0 3 | 20.90 | 20.91 | 20.93 | 20.97 | 21.05 | 21.24 | 21.92 | 25.22 | 29.09 | 33.24 | 37.82 | 43.39 | 51.63 | 68.00 |
| 0 4 | 20.91 | 20.93 | 20.98 | 21.09 | 21.33 | 21.87 | 23.14 | 25.84 | 29.32 | 33.21 | 37.45 | 42.12 | 47.31 | 52.49 |
| 0 5 | 20.93 | 20.96 | 21.04 | 21.23 | 21.62 | 22.41 | 23.90 | 26.36 | 29.54 | 33.18 | 37.07 | 41.03 | 44.73 | 47.34 |
| 1 | HEAD IN LAYER 6 AT END OF TIME STEP 1 IN STRESS PERIOD 1 | | | | | | | | | | | | | |

1 HEAD IN LAYER 7 AT END OF TIME STEP 1 IN STRESS PERIOD 1

| | 1 | 2 | 3 | 4 | 5 | 6 | 7 | 8 | 9 | 10 | 11 | 12 | 13 | 14 |
|-----|--|-------|-------|-------|-------|-------|-------|-------|-------|-------|-------|-------|-------|-------|
| 0 1 | 18.68 | 18.59 | 18.40 | 18.15 | 17.94 | 18.05 | 19.22 | 22.66 | 27.19 | 32.14 | 37.21 | 42.17 | 46.63 | 49.65 |
| 0 2 | 18.65 | 18.52 | 18.24 | 17.75 | 16.96 | 15.82 | 15.08 | 20.45 | 26.29 | 31.94 | 37.55 | 43.30 | 49.25 | 54.63 |
| 0 3 | 18.63 | 18.48 | 18.12 | 17.37 | 15.74 | 11.60 | 0.00 | 16.32 | 25.13 | 31.71 | 37.86 | 44.55 | 53.29 | 68.00 |
| 0 4 | 18.65 | 18.52 | 18.24 | 17.75 | 16.96 | 15.82 | 15.08 | 20.45 | 26.29 | 31.94 | 37.55 | 43.30 | 49.25 | 54.63 |
| 0 5 | 18.68 | 18.59 | 18.40 | 18.15 | 17.94 | 18.05 | 19.22 | 22.66 | 27.19 | 32.14 | 37.21 | 42.17 | 46.63 | 49.65 |
| 1 | HEAD IN LAYER 7 AT END OF TIME STEP 1 IN STRESS PERIOD 1 | | | | | | | | | | | | | |

1 HEAD IN LAYER 8 AT END OF TIME STEP 1 IN STRESS PERIOD 1

| | 1 | 2 | 3 | 4 | 5 | 6 | 7 | 8 | 9 | 10 | 11 | 12 | 13 | 14 |
|-----|--|-------|-------|-------|-------|-------|-------|-------|-------|-------|-------|-------|-------|-------|
| 0 1 | 16.91 | 16.75 | 16.44 | 16.03 | 15.66 | 15.70 | 16.98 | 20.69 | 25.69 | 31.19 | 36.79 | 42.21 | 46.99 | 50.17 |
| 0 2 | 16.80 | 16.60 | 16.27 | 15.59 | 14.82 | 13.43 | 12.99 | 18.45 | 24.73 | 30.95 | 37.11 | 43.32 | 49.57 | 55.03 |
| 0 3 | 16.85 | 16.63 | 16.32 | 15.19 | 13.40 | 9.56 | 9.00 | 14.60 | 23.57 | 30.70 | 37.41 | 44.55 | 51.49 | 68.00 |
| 0 4 | 16.88 | 16.68 | 16.43 | 15.82 | 14.82 | 13.43 | 12.99 | 18.45 | 24.73 | 30.95 | 37.11 | 43.32 | 49.57 | 55.03 |
| 0 5 | 16.91 | 16.75 | 16.44 | 16.03 | 15.66 | 15.70 | 16.98 | 20.69 | 25.69 | 31.19 | 36.79 | 42.21 | 46.99 | 50.17 |
| 1 | HEAD IN LAYER 8 AT END OF TIME STEP 1 IN STRESS PERIOD 1 | | | | | | | | | | | | | |

1 HEAD IN LAYER 9 AT END OF TIME STEP 1 IN STRESS PERIOD 1

| | 1 | 2 | 3 | 4 | 5 | 6 | 7 | 8 | 9 | 10 | 11 | 12 | 13 | 14 |
|-----|--|-------|-------|-------|-------|-------|-------|-------|-------|-------|-------|-------|-------|-------|
| 0 1 | 15.89 | 15.72 | 15.40 | 14.98 | 14.62 | 14.71 | 16.06 | 19.82 | 24.89 | 30.49 | 36.21 | 41.75 | 46.62 | 49.86 |
| 0 2 | 15.85 | 15.65 | 15.22 | 14.55 | 13.61 | 12.53 | 12.26 | 17.67 | 23.96 | 30.26 | 36.54 | 42.87 | 49.24 | 54.81 |
| 0 3 | 15.83 | 15.59 | 15.08 | 14.16 | 12.44 | 8.86 | 0.00 | 14.02 | 22.05 | 30.03 | 36.84 | 44.12 | 53.23 | 68.00 |
| 0 4 | 15.85 | 15.65 | 15.22 | 14.55 | 13.61 | 12.53 | 12.26 | 17.67 | 23.96 | 30.26 | 36.54 | 42.87 | 49.24 | 54.81 |
| 0 5 | 15.89 | 15.72 | 15.40 | 14.98 | 14.62 | 14.71 | 16.06 | 19.82 | 24.89 | 30.49 | 36.21 | 41.75 | 46.62 | 49.86 |
| 1 | HEAD IN LAYER 9 AT END OF TIME STEP 1 IN STRESS PERIOD 1 | | | | | | | | | | | | | |

1 HEAD IN LAYER 10 AT END OF TIME STEP 1 IN STRESS PERIOD 1

| | 1 | 2 | 3 | 4 | 5 | 6 | 7 | 8 | 9 | 10 | 11 | 12 | 13 | 14 |
|-----|-------|-------|-------|-------|-------|-------|-------|-------|-------|-------|-------|-------|-------|-------|
| 0 1 | 15.65 | 15.54 | 15.24 | 14.89 | 14.59 | 14.72 | 16.03 | 19.68 | 24.56 | 29.93 | 35.43 | 40.78 | 45.56 | 48.77 |
| 0 2 | 15.61 | 15.44 | 15.07 | 14.47 | 13.61 | 12.57 | 12.26 | 17.56 | 23.65 | 29.72 | 35.78 | 41.96 | 48.30 | 53.99 |

I-35
OUTPUT-H2.txt

```

0 3 15.59 15.39 14.93 14.09 12.45 8.92 0.00 13.92 22.56 29.50 36.10 43.27 52.53 68.00
0 4 15.61 15.44 15.07 14.47 13.61 12.57 12.26 17.56 23.65 29.72 35.78 41.96 48.30 53.99
0 5 15.65 15.51 15.24 14.89 14.60 14.72 16.03 19.68 24.56 29.93 35.43 40.78 45.56 48.77
1

```

HEAD IN LAYER 10 AT END OF TIME STEP 1 IN STRESS PERIOD 1

```

-----
1 2 3 4 5 6 7 8 9 10 11 12 13 14
-----
0 1 16.06 16.00 15.88 15.73 15.65 15.91 17.15 20.47 24.79 29.48 34.24 38.90 43.11 46.03
0 2 16.03 15.94 15.74 15.37 14.76 13.89 13.44 18.48 23.97 29.30 34.57 40.02 45.84 51.49
0 3 16.01 15.90 15.62 15.02 13.67 10.18 0.00 14.79 22.93 29.10 34.89 41.35 50.42 68.00
0 4 16.03 15.94 15.74 15.37 14.76 13.89 13.44 18.48 23.97 29.30 34.57 40.02 45.84 51.49
0 5 16.06 16.00 15.88 15.73 15.65 15.91 17.15 20.47 24.79 29.48 34.24 38.90 43.11 46.03
1

```

HEAD IN LAYER 11 AT END OF TIME STEP 1 IN STRESS PERIOD 1

```

-----
1 2 3 4 5 6 7 8 9 10 11 12 13 14
-----
0 1 16.82 16.88 17.03 17.31 17.82 18.73 20.31 22.77 25.83 29.19 32.56 35.69 38.25 39.78
0 2 16.80 16.86 16.97 17.18 17.55 18.25 19.62 22.29 25.60 29.14 32.68 36.04 38.95 40.90
0 3 16.79 16.84 16.93 17.08 17.30 17.68 18.53 21.73 25.37 29.09 32.78 36.16 39.74 42.50
0 4 16.80 16.86 16.97 17.18 17.55 18.25 19.62 22.29 25.60 29.14 32.68 36.04 38.95 40.90
0 5 16.82 16.88 17.03 17.31 17.82 18.73 20.31 22.77 25.83 29.19 32.56 35.69 38.25 39.78
1

```

HEAD IN LAYER 12 AT END OF TIME STEP 1 IN STRESS PERIOD 1

```

-----
1 2 3 4 5 6 7 8 9 10 11 12 13 14
-----
0 1 17.36 17.50 17.80 18.31 19.10 20.25 21.85 23.93 26.37 28.97 31.54 33.82 35.56 36.53
0 2 17.35 17.49 17.78 18.27 19.03 20.15 21.73 23.83 26.31 28.96 31.57 33.91 35.72 36.75
0 3 17.35 17.48 17.77 18.25 18.98 20.06 21.60 23.74 26.27 28.96 31.60 33.98 35.86 36.96
0 4 17.35 17.49 17.78 18.27 19.03 20.15 21.73 23.83 26.31 28.96 31.57 33.91 35.72 36.75
0 5 17.36 17.50 17.80 18.31 19.10 20.25 21.85 23.93 26.37 28.97 31.54 33.82 35.56 36.53
0

```

VOLUMETRIC BUDGET FOR ENTIRE MODEL AT END OF TIME STEP 1 IN STRESS PERIOD 1

```

-----
0 CUMULATIVE VOLUMES L**3 RATES FOR THIS TIME STEP L**3/T
-----
IN: IN:
--- ---
STORAGE = 0.00000 STORAGE = 0.00000
CONSTANT HEAD = 0.42638E+07 CONSTANT HEAD = 1.4150
TOTAL IN = 0.42638E+07 TOTAL IN = 1.4150
0 OUT:
0 ---
STORAGE = 0.00000 STORAGE = 0.00000
CONSTANT HEAD = 0.42638E+07 CONSTANT HEAD = 1.4150
TOTAL OUT = 0.42638E+07 TOTAL OUT = 1.4150
0 IN - OUT = 1.0000 IN - OUT = 0.35763E-06
0 PERCENT DISCREPANCY = 0.00 PERCENT DISCREPANCY = 0.00
0

```

TIME SUMMARY AT END OF TIME STEP 1 IN STRESS PERIOD 1

```

-----
SECONDS MINUTES HOURS DAYS YEARS
-----
TIME STEP LENGTH 0.301320E+07 50220.0 837.000 34.8750 0.954826E-01
STRESS PERIOD TIME 0.301320E+07 50220.0 837.000 34.8750 0.954826E-01
TOTAL SIMULATION TIME 0.301320E+07 50220.0 837.000 34.8750 0.954826E-01
1

```

APPENDIX J. MT3D Output File Example: Three-Dimensional Field Demonstration

This appendix includes example MT3D output files for the three-dimensional field demonstration. Both Phase 1 (OUTPUT-H1.ek) and Phase 2 (OUTPUT-H2.ek) output files are included. To save space, only the homogeneous model results are included.

J-2
 OUTPUT-H1.ek

```

+-----+
+           M T 3 D
+   A Modular Three-Dimensional Transport Model
+   For Simulation of Advection, Dispersion and Chemical Reactions
+   of Contaminants in Groundwater Systems
+   (V. 1.13)
+-----+
  
```

1 M T 3 D field problem - ACETATE
 1 3 D 1 3d field problem

THE TRANSPORT MODEL CONSISTS OF 12 LAYER(S) 5 ROW(S) 14 COLUMN(S)
 NUMBER OF STRESS PERIOD(S) IN SIMULATION = 1
 UNIT FOR TIME IS sec; UNIT FOR LENGTH IS M; UNIT FOR MASS IS MOL
 MAJOR TRANSPORT COMPONENTS TO BE SIMULATED:
 1 ADVECTION
 2 DISPERSION

BTW1 -- BASIC TRANSPORT PACKAGE, VER 1.0, AUGUST 1990, INPUT READ FROM UNIT 1
 10118 ELEMENTS OF THE X ARRAY USED BY THE BTW PACKAGE
 852 ELEMENTS OF THE IX ARRAY USED BY THE BTW PACKAGE

ADV1 -- ADVECTION PACKAGE, VER 1.0, AUGUST 1990, INPUT READ FROM UNIT 2
 ADVECTION IS SOLVED WITH THE UPSTREAM FINITE DIFFERENCE SCHEME
 COURANT NUMBER ALLOWED IN SOLVING THE ADVECTION TERM = 0.250
 MAXIMUM NUMBER OF MOVING PARTICLES ALLOWED = 5100
 0 ELEMENTS OF THE X ARRAY USED BY THE ADV PACKAGE
 0 ELEMENTS OF THE IX ARRAY USED BY THE ADV PACKAGE

DSF1 -- DISPERSION PACKAGE, VER 1.0, AUGUST 1990, INPUT READ FROM UNIT 3
 8436 ELEMENTS OF THE X ARRAY USED BY THE DSF PACKAGE
 0 ELEMENTS OF THE IX ARRAY USED BY THE DSF PACKAGE

18555 ELEMENTS OF THE X ARRAY USED OUT OF 700000
 853 ELEMENTS OF THE IX ARRAY USED OUT OF 70000

LAYER NUMBER AQUIFER TYPE

| | |
|----|---|
| 1 | 0 |
| 2 | 0 |
| 3 | 0 |
| 4 | 0 |
| 5 | 0 |
| 6 | 0 |
| 7 | 0 |
| 8 | 0 |
| 9 | 0 |
| 10 | 0 |
| 11 | 0 |
| 12 | 0 |

WIDTH ALONG ROWS (DELR) = 0.1524000
 WIDTH ALONG COLS (DELC) = 0.1828000
 TOP ELEV. OF 1ST LAYER = 0.0000000
 CELL THICKNESS (DZ) = 0.3048000 FOR LAYER 1
 CELL THICKNESS (DZ) = 0.3048000 FOR LAYER 2
 CELL THICKNESS (DZ) = 0.3048000 FOR LAYER 3
 CELL THICKNESS (DZ) = 0.3048000 FOR LAYER 4
 CELL THICKNESS (DZ) = 0.3048000 FOR LAYER 5
 CELL THICKNESS (DZ) = 0.3048000 FOR LAYER 6
 CELL THICKNESS (DZ) = 0.3048000 FOR LAYER 7
 CELL THICKNESS (DZ) = 0.3048000 FOR LAYER 8
 CELL THICKNESS (DZ) = 0.3048000 FOR LAYER 9
 CELL THICKNESS (DZ) = 0.3048000 FOR LAYER 10
 CELL THICKNESS (DZ) = 0.3048000 FOR LAYER 11
 CELL THICKNESS (DZ) = 0.3048000 FOR LAYER 12
 EFFECTIVE POROSITY = 0.1260000 FOR LAYER 1
 EFFECTIVE POROSITY = 0.1260000 FOR LAYER 2
 EFFECTIVE POROSITY = 0.1260000 FOR LAYER 3
 EFFECTIVE POROSITY = 0.1260000 FOR LAYER 4
 EFFECTIVE POROSITY = 0.1260000 FOR LAYER 5
 EFFECTIVE POROSITY = 0.1260000 FOR LAYER 6
 EFFECTIVE POROSITY = 0.1260000 FOR LAYER 7
 EFFECTIVE POROSITY = 0.1260000 FOR LAYER 8
 EFFECTIVE POROSITY = 0.1260000 FOR LAYER 9
 EFFECTIVE POROSITY = 0.1260000 FOR LAYER 10
 EFFECTIVE POROSITY = 0.1260000 FOR LAYER 11
 EFFECTIVE POROSITY = 0.1260000 FOR LAYER 12

CONCN. BOUNDARY ARRAY FOR LAYER 1 READ ON UNIT 1 USING BLOCK FORMAT

| | | | | | | | | | | | | | | |
|---|---|---|---|---|---|---|---|---|---|---|---|---|---|---|
| 1 | 1 | 1 | 1 | 1 | 1 | 1 | 1 | 1 | 1 | 1 | 1 | 1 | 1 | 1 |
| 2 | 1 | 1 | 1 | 1 | 1 | 1 | 1 | 1 | 1 | 1 | 1 | 1 | 1 | 1 |
| 3 | 1 | 1 | 1 | 1 | 1 | 1 | 1 | 1 | 1 | 1 | 1 | 1 | 1 | 1 |
| 4 | 1 | 1 | 1 | 1 | 1 | 1 | 1 | 1 | 1 | 1 | 1 | 1 | 1 | 1 |
| 5 | 1 | 1 | 1 | 1 | 1 | 1 | 1 | 1 | 1 | 1 | 1 | 1 | 1 | 1 |

CONCN. BOUNDARY ARRAY FOR LAYER 2 READ ON UNIT 1 USING BLOCK FORMAT

| | | | | | | | | | | | | | | |
|---|---|---|---|---|---|---|---|---|---|---|---|---|---|---|
| 1 | 1 | 1 | 1 | 1 | 1 | 1 | 1 | 1 | 1 | 1 | 1 | 1 | 1 | 1 |
| 2 | 1 | 1 | 1 | 1 | 1 | 1 | 1 | 1 | 1 | 1 | 1 | 1 | 1 | 1 |
| 3 | 1 | 1 | 1 | 1 | 1 | 1 | 1 | 1 | 1 | 1 | 1 | 1 | 1 | 1 |
| 4 | 1 | 1 | 1 | 1 | 1 | 1 | 1 | 1 | 1 | 1 | 1 | 1 | 1 | 1 |
| 5 | 1 | 1 | 1 | 1 | 1 | 1 | 1 | 1 | 1 | 1 | 1 | 1 | 1 | 1 |

CONCN. BOUNDARY ARRAY FOR LAYER 3 READ ON UNIT 1 USING BLOCK FORMAT

| | | | | | | | | | | | | | | |
|---|---|---|---|---|---|---|---|---|---|---|---|---|---|---|
| 1 | 1 | 1 | 1 | 1 | 1 | 1 | 1 | 1 | 1 | 1 | 1 | 1 | 1 | 1 |
| 2 | 1 | 1 | 1 | 1 | 1 | 1 | 1 | 1 | 1 | 1 | 1 | 1 | 1 | 1 |
| 3 | 1 | 1 | 1 | 1 | 1 | 1 | 1 | 1 | 1 | 1 | 1 | 1 | 1 | 1 |
| 4 | 1 | 1 | 1 | 1 | 1 | 1 | 1 | 1 | 1 | 1 | 1 | 1 | 1 | 1 |
| 5 | 1 | 1 | 1 | 1 | 1 | 1 | 1 | 1 | 1 | 1 | 1 | 1 | 1 | 1 |

CONCN. BOUNDARY ARRAY FOR LAYER 4 READ ON UNIT 1 USING BLOCK FORMAT

| | | | | | | | | | | | | | | |
|---|---|---|---|---|---|---|---|---|---|---|---|---|---|---|
| 1 | 1 | 1 | 1 | 1 | 1 | 1 | 1 | 1 | 1 | 1 | 1 | 1 | 1 | 1 |
| 2 | 1 | 1 | 1 | 1 | 1 | 1 | 1 | 1 | 1 | 1 | 1 | 1 | 1 | 1 |
| 3 | 1 | 1 | 1 | 1 | 1 | 1 | 1 | 1 | 1 | 1 | 1 | 1 | 1 | 1 |
| 4 | 1 | 1 | 1 | 1 | 1 | 1 | 1 | 1 | 1 | 1 | 1 | 1 | 1 | 1 |
| 5 | 1 | 1 | 1 | 1 | 1 | 1 | 1 | 1 | 1 | 1 | 1 | 1 | 1 | 1 |

CONCN. BOUNDARY ARRAY FOR LAYER 5 READ ON UNIT 1 USING BLOCK FORMAT

| | | | | | | | | | | | | | | |
|---|----|---|---|---|---|---|---|---|---|---|---|---|---|----|
| 1 | 1 | 1 | 1 | 1 | 1 | 1 | 1 | 1 | 1 | 1 | 1 | 1 | 1 | 1 |
| 2 | 1 | 1 | 1 | 1 | 1 | 1 | 1 | 1 | 1 | 1 | 1 | 1 | 1 | 1 |
| 3 | -1 | 1 | 1 | 1 | 1 | 1 | 1 | 1 | 1 | 1 | 1 | 1 | 1 | -1 |
| 4 | 1 | 1 | 1 | 1 | 1 | 1 | 1 | 1 | 1 | 1 | 1 | 1 | 1 | 1 |
| 5 | 1 | 1 | 1 | 1 | 1 | 1 | 1 | 1 | 1 | 1 | 1 | 1 | 1 | 1 |

CONCN. BOUNDARY ARRAY FOR LAYER 6 READ ON UNIT 1 USING BLOCK FORMAT

J-4
OUTPUT-H1.ek

| | 1 | 2 | 3 | 4 | 5 | 6 | 7 | 8 | 9 | 10 | 11 | 12 | 13 | 14 |
|---|--------|------|------|------|------|------|------|------|------|------|------|------|------|------|
| 1 | 0.00 | 0.00 | 0.00 | 0.00 | 0.00 | 0.00 | 0.00 | 0.00 | 0.00 | 0.00 | 0.00 | 0.00 | 0.00 | 0.00 |
| 2 | 0.00 | 0.00 | 0.00 | 0.00 | 0.00 | 0.00 | 0.00 | 0.00 | 0.00 | 0.00 | 0.00 | 0.00 | 0.00 | 0.00 |
| 3 | 200.00 | 0.00 | 0.00 | 0.00 | 0.00 | 0.00 | 0.00 | 0.00 | 0.00 | 0.00 | 0.00 | 0.00 | 0.00 | 0.00 |
| 4 | 0.00 | 0.00 | 0.00 | 0.00 | 0.00 | 0.00 | 0.00 | 0.00 | 0.00 | 0.00 | 0.00 | 0.00 | 0.00 | 0.00 |
| 5 | 0.00 | 0.00 | 0.00 | 0.00 | 0.00 | 0.00 | 0.00 | 0.00 | 0.00 | 0.00 | 0.00 | 0.00 | 0.00 | 0.00 |

INITIAL CONCENTRATION FOR LAYER 8 READ ON UNIT 1 USING BLOCK FORMAT

| | 1 | 2 | 3 | 4 | 5 | 6 | 7 | 8 | 9 | 10 | 11 | 12 | 13 | 14 |
|---|--------|------|------|------|------|------|------|------|------|------|------|------|------|------|
| 1 | 0.00 | 0.00 | 0.00 | 0.00 | 0.00 | 0.00 | 0.00 | 0.00 | 0.00 | 0.00 | 0.00 | 0.00 | 0.00 | 0.00 |
| 2 | 0.00 | 0.00 | 0.00 | 0.00 | 0.00 | 0.00 | 0.00 | 0.00 | 0.00 | 0.00 | 0.00 | 0.00 | 0.00 | 0.00 |
| 3 | 200.00 | 0.00 | 0.00 | 0.00 | 0.00 | 0.00 | 0.00 | 0.00 | 0.00 | 0.00 | 0.00 | 0.00 | 0.00 | 0.00 |
| 4 | 0.00 | 0.00 | 0.00 | 0.00 | 0.00 | 0.00 | 0.00 | 0.00 | 0.00 | 0.00 | 0.00 | 0.00 | 0.00 | 0.00 |
| 5 | 0.00 | 0.00 | 0.00 | 0.00 | 0.00 | 0.00 | 0.00 | 0.00 | 0.00 | 0.00 | 0.00 | 0.00 | 0.00 | 0.00 |

INITIAL CONCENTRATION FOR LAYER 9 READ ON UNIT 1 USING BLOCK FORMAT

| | 1 | 2 | 3 | 4 | 5 | 6 | 7 | 8 | 9 | 10 | 11 | 12 | 13 | 14 |
|---|--------|------|------|------|------|------|------|------|------|------|------|------|------|------|
| 1 | 0.00 | 0.00 | 0.00 | 0.00 | 0.00 | 0.00 | 0.00 | 0.00 | 0.00 | 0.00 | 0.00 | 0.00 | 0.00 | 0.00 |
| 2 | 0.00 | 0.00 | 0.00 | 0.00 | 0.00 | 0.00 | 0.00 | 0.00 | 0.00 | 0.00 | 0.00 | 0.00 | 0.00 | 0.00 |
| 3 | 200.00 | 0.00 | 0.00 | 0.00 | 0.00 | 0.00 | 0.00 | 0.00 | 0.00 | 0.00 | 0.00 | 0.00 | 0.00 | 0.00 |
| 4 | 0.00 | 0.00 | 0.00 | 0.00 | 0.00 | 0.00 | 0.00 | 0.00 | 0.00 | 0.00 | 0.00 | 0.00 | 0.00 | 0.00 |
| 5 | 0.00 | 0.00 | 0.00 | 0.00 | 0.00 | 0.00 | 0.00 | 0.00 | 0.00 | 0.00 | 0.00 | 0.00 | 0.00 | 0.00 |

INITIAL CONCENTRATION FOR LAYER 10 READ ON UNIT 1 USING BLOCK FORMAT

| | 1 | 2 | 3 | 4 | 5 | 6 | 7 | 8 | 9 | 10 | 11 | 12 | 13 | 14 |
|---|--------|------|------|------|------|------|------|------|------|------|------|------|------|------|
| 1 | 0.00 | 0.00 | 0.00 | 0.00 | 0.00 | 0.00 | 0.00 | 0.00 | 0.00 | 0.00 | 0.00 | 0.00 | 0.00 | 0.00 |
| 2 | 0.00 | 0.00 | 0.00 | 0.00 | 0.00 | 0.00 | 0.00 | 0.00 | 0.00 | 0.00 | 0.00 | 0.00 | 0.00 | 0.00 |
| 3 | 200.00 | 0.00 | 0.00 | 0.00 | 0.00 | 0.00 | 0.00 | 0.00 | 0.00 | 0.00 | 0.00 | 0.00 | 0.00 | 0.00 |
| 4 | 0.00 | 0.00 | 0.00 | 0.00 | 0.00 | 0.00 | 0.00 | 0.00 | 0.00 | 0.00 | 0.00 | 0.00 | 0.00 | 0.00 |
| 5 | 0.00 | 0.00 | 0.00 | 0.00 | 0.00 | 0.00 | 0.00 | 0.00 | 0.00 | 0.00 | 0.00 | 0.00 | 0.00 | 0.00 |

INITIAL CONCENTRATION FOR LAYER 11 READ ON UNIT 1 USING BLOCK FORMAT

| | 1 | 2 | 3 | 4 | 5 | 6 | 7 | 8 | 9 | 10 | 11 | 12 | 13 | 14 |
|---|------|------|------|------|------|------|------|------|------|------|------|------|------|------|
| 1 | 0.00 | 0.00 | 0.00 | 0.00 | 0.00 | 0.00 | 0.00 | 0.00 | 0.00 | 0.00 | 0.00 | 0.00 | 0.00 | 0.00 |
| 2 | 0.00 | 0.00 | 0.00 | 0.00 | 0.00 | 0.00 | 0.00 | 0.00 | 0.00 | 0.00 | 0.00 | 0.00 | 0.00 | 0.00 |
| 3 | 0.00 | 0.00 | 0.00 | 0.00 | 0.00 | 0.00 | 0.00 | 0.00 | 0.00 | 0.00 | 0.00 | 0.00 | 0.00 | 0.00 |
| 4 | 0.00 | 0.00 | 0.00 | 0.00 | 0.00 | 0.00 | 0.00 | 0.00 | 0.00 | 0.00 | 0.00 | 0.00 | 0.00 | 0.00 |
| 5 | 0.00 | 0.00 | 0.00 | 0.00 | 0.00 | 0.00 | 0.00 | 0.00 | 0.00 | 0.00 | 0.00 | 0.00 | 0.00 | 0.00 |

INITIAL CONCENTRATION FOR LAYER 12 READ ON UNIT 1 USING BLOCK FORMAT

| | 1 | 2 | 3 | 4 | 5 | 6 | 7 | 8 | 9 | 10 | 11 | 12 | 13 | 14 |
|---|------|------|------|------|------|------|------|------|------|------|------|------|------|------|
| 1 | 0.00 | 0.00 | 0.00 | 0.00 | 0.00 | 0.00 | 0.00 | 0.00 | 0.00 | 0.00 | 0.00 | 0.00 | 0.00 | 0.00 |
| 2 | 0.00 | 0.00 | 0.00 | 0.00 | 0.00 | 0.00 | 0.00 | 0.00 | 0.00 | 0.00 | 0.00 | 0.00 | 0.00 | 0.00 |
| 3 | 0.00 | 0.00 | 0.00 | 0.00 | 0.00 | 0.00 | 0.00 | 0.00 | 0.00 | 0.00 | 0.00 | 0.00 | 0.00 | 0.00 |
| 4 | 0.00 | 0.00 | 0.00 | 0.00 | 0.00 | 0.00 | 0.00 | 0.00 | 0.00 | 0.00 | 0.00 | 0.00 | 0.00 | 0.00 |
| 5 | 0.00 | 0.00 | 0.00 | 0.00 | 0.00 | 0.00 | 0.00 | 0.00 | 0.00 | 0.00 | 0.00 | 0.00 | 0.00 | 0.00 |

VALUE INDICATING INACTIVE CONCENTRATION CELLS = -999.0000

OUTPUT CONTROL OPTIONS

PRINT CELL CONCENTRATION USING FORMAT CODE: 3
 PRINT PARTICLE NUMBER IN EACH CELL USING FORMAT CODE: 3
 PRINT RETARDATION FACTOR USING FORMAT CODE: 3
 PRINT DISPERSION COEFFICIENT USING FORMAT CODE: 3
 SAVE CONCENTRATION IN UNFORMATTED FILE (MTSD.UCH) ON UNIT 18
 NUMBER OF TIMES AT WHICH SIMULATION RESULTS ARE SAVED = 1
 TOTAL ELAPSED TIMES AT WHICH SIMULATION RESULTS ARE SAVED:
 0.44856E+07

NUMBER OF OBSERVATION POINTS = 2
 CONCENTRATION AT OBSERVATION POINTS SAVED IN FILE (MTSD.OBS) ON UNIT 17
 LOCATION OF OBSERVATION POINTS

| NUMBER | LAYER | ROW | COLUMN |
|--------|-------|-----|--------|
| 1 | 6 | 3 | 3 |
| 2 | 6 | 1 | 3 |

A ONE-LINE SUMMARY OF MASS BALANCE FOR EACH STEP SAVED IN FILE (MTSD.MAS) ON UNIT 19
 MAXIMUM LENGTH ALONG THE X (J) AXIS = 2.133600
 MAXIMUM LENGTH ALONG THE Y (I) AXIS = 0.9145000
 MAXIMUM LENGTH ALONG THE Z (K) AXIS = 3.657600

ADVECTION SOLUTION OPTIONS

DISPERSION PARAMETERS

LONG. DISPERSIVITY (AL) = 0.0000000 FOR LAYER 1
 LONG. DISPERSIVITY (AL) = 0.0000000 FOR LAYER 2
 LONG. DISPERSIVITY (AL) = 0.0000000 FOR LAYER 3
 LONG. DISPERSIVITY (AL) = 0.0000000 FOR LAYER 4
 LONG. DISPERSIVITY (AL) = 0.0000000 FOR LAYER 5
 LONG. DISPERSIVITY (AL) = 0.0000000 FOR LAYER 6
 LONG. DISPERSIVITY (AL) = 0.0000000 FOR LAYER 7
 LONG. DISPERSIVITY (AL) = 0.0000000 FOR LAYER 8
 LONG. DISPERSIVITY (AL) = 0.0000000 FOR LAYER 9
 LONG. DISPERSIVITY (AL) = 0.0000000 FOR LAYER 10
 LONG. DISPERSIVITY (AL) = 0.0000000 FOR LAYER 11
 LONG. DISPERSIVITY (AL) = 0.0000000 FOR LAYER 12
 H. TRANS./LONG. DISP. = 0.0000000
 V. TRANS./LONG. DISP. = 0.0000000
 DIFFUSION COEFFICIENT = 0.3650000E-09

 STRESS PERIOD NO. 001

LENGTH OF CURRENT STRESS PERIOD = 4485600.
 NUMBER OF TIME STEPS FOR CURRENT STRESS PERIOD = 1
 TIME STEP MULTIPLIER = 1.000000
 USER-SPECIFIED TRANSPORT STEPSIZE = 600.0000 sec
 MAXIMUM NUMBER OF TRANSPORT STEPS ALLOWED IN ONE TIME STEP = 50000

 TIME STEP NO. 001

FROM TIME = 0.00000 TO 0.44856E+07

*HEAD * FLOW TERMS FOR TIME STEP 1, STRESS PERIOD 1 READ UNFORMATTED ON UNIT 10

J-6 OUTPUT-H1.ek

79.7 84.7 88.1

LAYER 10

| | 1 | 2 | 3 | 4 | 5 | 6 | 7 | 8 | 9 | 10 | 11 |
|---|-------|------|------|------|------|------|------|------|------|------|------|
| | 12 | 13 | 14 | | | | | | | | |
| 1 | 24.1 | 27.3 | 31.8 | 36.9 | 41.8 | 46.9 | 52.0 | 57.0 | 62.1 | 67.2 | 72.2 |
| | 77.2 | 81.7 | 84.9 | | | | | | | | |
| 2 | 18.1 | 24.3 | 30.5 | 36.3 | 41.6 | 46.8 | 52.0 | 57.0 | 62.2 | 67.4 | 72.7 |
| | 78.5 | 84.7 | 90.9 | | | | | | | | |
| 3 | 0.000 | 19.2 | 29.0 | 35.0 | 41.5 | 46.8 | 51.9 | 57.1 | 62.2 | 67.5 | 73.2 |
| | 83.0 | 89.8 | 109 | | | | | | | | |
| 4 | 18.1 | 24.3 | 30.5 | 36.3 | 41.6 | 46.8 | 52.0 | 57.0 | 62.2 | 67.4 | 72.7 |
| | 78.5 | 84.7 | 90.9 | | | | | | | | |
| 5 | 24.1 | 27.3 | 31.8 | 36.8 | 41.8 | 46.9 | 52.0 | 57.0 | 62.1 | 67.2 | 72.2 |
| | 77.2 | 81.7 | 84.9 | | | | | | | | |

LAYER 11

| | 1 | 2 | 3 | 4 | 5 | 6 | 7 | 8 | 9 | 10 | 11 |
|---|------|------|------|------|------|------|------|------|------|------|------|
| | 12 | 13 | 14 | | | | | | | | |
| 1 | 31.5 | 33.2 | 36.1 | 39.7 | 43.7 | 48.0 | 52.3 | 56.7 | 61.0 | 65.3 | 69.3 |
| | 72.9 | 75.8 | 77.5 | | | | | | | | |
| 2 | 30.3 | 32.5 | 35.7 | 39.5 | 43.7 | 47.9 | 52.3 | 56.7 | 61.1 | 65.3 | 69.5 |
| | 73.3 | 76.5 | 78.7 | | | | | | | | |
| 3 | 28.5 | 31.6 | 35.4 | 39.4 | 43.6 | 47.9 | 52.3 | 56.7 | 61.1 | 65.4 | 69.6 |
| | 73.6 | 77.4 | 80.5 | | | | | | | | |
| 4 | 30.3 | 32.5 | 35.7 | 39.5 | 43.7 | 47.9 | 52.3 | 56.7 | 61.1 | 65.3 | 69.5 |
| | 73.3 | 76.5 | 78.7 | | | | | | | | |
| 5 | 31.5 | 33.2 | 36.1 | 39.7 | 43.7 | 48.0 | 52.3 | 56.7 | 61.0 | 65.3 | 69.3 |
| | 72.9 | 75.8 | 77.5 | | | | | | | | |

LAYER 12

| | 1 | 2 | 3 | 4 | 5 | 6 | 7 | 8 | 9 | 10 | 11 |
|---|------|------|------|------|------|------|------|------|------|------|------|
| | 12 | 13 | 14 | | | | | | | | |
| 1 | 35.5 | 36.6 | 38.7 | 41.6 | 45.0 | 48.7 | 52.5 | 56.5 | 60.3 | 64.0 | 67.4 |
| | 70.3 | 72.4 | 73.5 | | | | | | | | |
| 2 | 35.2 | 36.4 | 38.6 | 41.5 | 44.9 | 48.6 | 52.5 | 56.5 | 60.4 | 64.1 | 67.5 |
| | 70.4 | 72.6 | 73.8 | | | | | | | | |
| 3 | 35.0 | 36.3 | 38.6 | 41.5 | 44.9 | 48.6 | 52.5 | 56.5 | 60.4 | 64.1 | 67.5 |
| | 70.4 | 72.7 | 74.0 | | | | | | | | |
| 4 | 35.2 | 36.4 | 38.6 | 41.5 | 44.9 | 48.6 | 52.5 | 56.5 | 60.4 | 64.1 | 67.5 |
| | 70.4 | 72.6 | 73.8 | | | | | | | | |
| 5 | 35.5 | 36.6 | 38.7 | 41.6 | 45.0 | 48.7 | 52.5 | 56.5 | 60.3 | 64.0 | 67.4 |
| | 70.3 | 72.4 | 73.5 | | | | | | | | |

*GXX * FLOW TERMS FOR TIME STEP 1, STRESS PERIOD 1 READ UNFORMATTED ON UNIT 10

LAYER 1

| | 1 | 2 | 3 | 4 | 5 | 6 | 7 | 8 | 9 | 10 | 11 |
|---|-----------|-----------|-----------|-----------|-----------|-----------|-----------|-----------|-----------|-----------|-----------|
| | 12 | 13 | 14 | | | | | | | | |
| 1 | 1.975E-10 | 3.812E-10 | 5.403E-10 | 6.681E-10 | 7.608E-10 | 8.167E-10 | 8.354E-10 | 8.167E-10 | 7.608E-10 | 6.681E-10 | 5.403E-10 |
| | 3.812E-10 | 1.975E-10 | 0.000 | | | | | | | | |
| 2 | 1.980E-10 | 3.819E-10 | 5.410E-10 | 6.686E-10 | 7.611E-10 | 8.170E-10 | 8.356E-10 | 8.170E-10 | 7.611E-10 | 6.686E-10 | 5.410E-10 |
| | 3.819E-10 | 1.980E-10 | 0.000 | | | | | | | | |
| 3 | 1.984E-10 | 3.824E-10 | 5.415E-10 | 6.690E-10 | 7.614E-10 | 8.173E-10 | 8.358E-10 | 8.173E-10 | 7.614E-10 | 6.690E-10 | 5.415E-10 |
| | 3.824E-10 | 1.984E-10 | 0.000 | | | | | | | | |
| 4 | 1.980E-10 | 3.819E-10 | 5.410E-10 | 6.686E-10 | 7.611E-10 | 8.170E-10 | 8.356E-10 | 8.170E-10 | 7.611E-10 | 6.686E-10 | 5.410E-10 |
| | 3.819E-10 | 1.980E-10 | 0.000 | | | | | | | | |
| 5 | 1.975E-10 | 3.812E-10 | 5.403E-10 | 6.681E-10 | 7.608E-10 | 8.167E-10 | 8.354E-10 | 8.167E-10 | 7.608E-10 | 6.681E-10 | 5.403E-10 |
| | 3.812E-10 | 1.975E-10 | 0.000 | | | | | | | | |

LAYER 2

| | 1 | 2 | 3 | 4 | 5 | 6 | 7 | 8 | 9 | 10 | 11 |
|---|-----------|-----------|-----------|-----------|-----------|-----------|-----------|-----------|-----------|-----------|-----------|
| | 12 | 13 | 14 | | | | | | | | |
| 1 | 2.510E-10 | 4.772E-10 | 6.641E-10 | 8.070E-10 | 9.066E-10 | 9.651E-10 | 9.844E-10 | 9.651E-10 | 9.066E-10 | 8.070E-10 | 6.641E-10 |
| | 4.772E-10 | 2.510E-10 | 0.000 | | | | | | | | |
| 2 | 2.547E-10 | 4.817E-10 | 6.678E-10 | 8.095E-10 | 9.082E-10 | 9.661E-10 | 9.851E-10 | 9.661E-10 | 9.082E-10 | 8.095E-10 | 6.678E-10 |
| | 4.817E-10 | 2.547E-10 | 0.000 | | | | | | | | |
| 3 | 2.530E-10 | 4.854E-10 | 6.705E-10 | 8.112E-10 | 9.092E-10 | 9.667E-10 | 9.856E-10 | 9.667E-10 | 9.092E-10 | 8.112E-10 | 6.705E-10 |
| | 4.854E-10 | 2.530E-10 | 0.000 | | | | | | | | |
| 4 | 2.547E-10 | 4.817E-10 | 6.678E-10 | 8.095E-10 | 9.082E-10 | 9.661E-10 | 9.851E-10 | 9.661E-10 | 9.082E-10 | 8.095E-10 | 6.678E-10 |
| | 4.817E-10 | 2.547E-10 | 0.000 | | | | | | | | |
| 5 | 2.510E-10 | 4.772E-10 | 6.641E-10 | 8.070E-10 | 9.066E-10 | 9.651E-10 | 9.844E-10 | 9.651E-10 | 9.066E-10 | 8.070E-10 | 6.641E-10 |
| | 4.772E-10 | 2.510E-10 | 0.000 | | | | | | | | |

LAYER 3

| | 1 | 2 | 3 | 4 | 5 | 6 | 7 | 8 | 9 | 10 | 11 |
|---|-----------|-----------|-----------|-----------|-----------|-----------|-----------|-----------|-----------|-----------|-----------|
| | 12 | 13 | 14 | | | | | | | | |
| 1 | 3.941E-10 | 7.175E-10 | 9.532E-10 | 1.113E-09 | 1.213E-09 | 1.268E-09 | 1.285E-09 | 1.268E-09 | 1.213E-09 | 1.113E-09 | 9.532E-10 |
| | 7.175E-10 | 3.941E-10 | 0.000 | | | | | | | | |
| 2 | 4.230E-10 | 7.481E-10 | 9.745E-10 | 1.125E-09 | 1.220E-09 | 1.271E-09 | 1.288E-09 | 1.271E-09 | 1.220E-09 | 1.125E-09 | 9.745E-10 |
| | 7.481E-10 | 4.230E-10 | 0.000 | | | | | | | | |
| 3 | 4.585E-10 | 7.781E-10 | 9.924E-10 | 1.134E-09 | 1.224E-09 | 1.274E-09 | 1.290E-09 | 1.274E-09 | 1.224E-09 | 1.134E-09 | 9.924E-10 |
| | 7.781E-10 | 4.585E-10 | 0.000 | | | | | | | | |
| 4 | 4.230E-10 | 7.481E-10 | 9.745E-10 | 1.125E-09 | 1.220E-09 | 1.271E-09 | 1.288E-09 | 1.271E-09 | 1.220E-09 | 1.125E-09 | 9.745E-10 |
| | 7.481E-10 | 4.230E-10 | 0.000 | | | | | | | | |
| 5 | 3.941E-10 | 7.175E-10 | 9.532E-10 | 1.113E-09 | 1.213E-09 | 1.268E-09 | 1.285E-09 | 1.268E-09 | 1.213E-09 | 1.113E-09 | 9.532E-10 |
| | 7.175E-10 | 3.941E-10 | 0.000 | | | | | | | | |

LAYER 4

| | 1 | 2 | 3 | 4 | 5 | 6 | 7 | 8 | 9 | 10 | 11 |
|---|-----------|-----------|-----------|-----------|-----------|-----------|-----------|-----------|-----------|-----------|-----------|
| | 12 | 13 | 14 | | | | | | | | |
| 1 | 7.400E-09 | 1.224E-09 | 1.488E-09 | 1.620E-09 | 1.683E-09 | 1.710E-09 | 1.718E-09 | 1.710E-09 | 1.683E-09 | 1.620E-09 | 1.488E-09 |
| | 1.224E-09 | 7.400E-10 | 0.000 | | | | | | | | |
| 2 | 9.651E-10 | 1.411E-09 | 1.595E-09 | 1.673E-09 | 1.707E-09 | 1.722E-09 | 1.726E-09 | 1.722E-09 | 1.707E-09 | 1.673E-09 | 1.595E-09 |
| | 1.411E-09 | 9.651E-10 | 0.000 | | | | | | | | |
| 3 | 1.412E-09 | 1.658E-09 | 1.704E-09 | 1.717E-09 | 1.725E-09 | 1.730E-09 | 1.732E-09 | 1.730E-09 | 1.725E-09 | 1.717E-09 | 1.704E-09 |
| | 1.658E-09 | 1.412E-09 | 0.000 | | | | | | | | |
| 4 | 9.651E-10 | 1.411E-09 | 1.595E-09 | 1.673E-09 | 1.707E-09 | 1.722E-09 | 1.726E-09 | 1.722E-09 | 1.707E-09 | 1.673E-09 | 1.595E-09 |
| | 1.411E-09 | 9.651E-10 | 0.000 | | | | | | | | |
| 5 | 7.400E-09 | 1.224E-09 | 1.488E-09 | 1.620E-09 | 1.683E-09 | 1.710E-09 | 1.718E-09 | 1.710E-09 | 1.683E-09 | 1.620E-09 | 1.488E-09 |
| | 1.224E-09 | 7.400E-10 | 0.000 | | | | | | | | |

LAYER 5

| | 1 | 2 | 3 | 4 | 5 | 6 | 7 | 8 | 9 | 10 | 11 |
|---|-----------|-----------|-----------|-----------|-----------|-----------|-----------|-----------|-----------|-----------|-----------|
| | 12 | 13 | 14 | | | | | | | | |
| 1 | 1.484E-09 | 2.092E-09 | 2.254E-09 | 2.259E-09 | 2.226E-09 | 2.198E-09 | 2.188E-09 | 2.198E-09 | 2.226E-09 | 2.259E-09 | 2.254E-09 |
| | 2.092E-09 | 1.484E-09 | 0.000 | | | | | | | | |
| 2 | 2.970E-09 | 2.951E-09 | 2.638E-09 | 2.415E-09 | 2.288E-09 | 2.225E-09 | 2.206E-09 | 2.225E-09 | 2.288E-09 | 2.415E-09 | 2.638E-09 |
| | 2.951E-09 | 2.970E-09 | 0.000 | | | | | | | | |
| 3 | 9.508E-09 | 4.715E-09 | 3.147E-09 | 2.573E-09 | 2.340E-09 | 2.245E-09 | 2.218E-09 | 2.245E-09 | 2.340E-09 | 2.573E-09 | 3.147E-09 |
| | 4.715E-09 | 9.508E-09 | 0.000 | | | | | | | | |
| 4 | 2.970E-09 | 2.951E-09 | 2.638E-09 | 2.415E-09 | 2.288E-09 | 2.225E-09 | 2.206E-09 | 2.225E-09 | 2.288E-09 | 2.415E-09 | 2.638E-09 |
| | 2.951E-09 | 2.970E-09 | 0.000 | | | | | | | | |
| 5 | 1.484E-09 | 2.092E-09 | 2.254E-09 | 2.259E-09 | 2.226E-09 | 2.198E-09 | 2.188E-09 | 2.198E-09 | 2.226E-09 | 2.259E-09 | 2.254E-09 |
| | 2.092E-09 | 1.484E-09 | 0.000 | | | | | | | | |

LAYER 6

| | 1 | 2 | 3 | 4 | 5 |
|--|---|---|---|---|---|
|--|---|---|---|---|---|

J-7
OUTPUT-H1.ek

| | | | | | | | | | | | |
|---|-----------|-----------|-----------|-----------|-----------|-----------|-----------|-----------|-----------|-----------|-----------|
| 3 | 0.019E-09 | 4.671E-09 | 3.442E-09 | 2.932E-09 | 2.699E-09 | 2.593E-09 | 2.562E-09 | 2.593E-09 | 2.699E-09 | 2.932E-09 | 3.442E-09 |
| 4 | 2.903E-09 | 3.156E-09 | 2.968E-09 | 2.775E-09 | 2.644E-09 | 2.571E-09 | 2.548E-09 | 2.571E-09 | 2.644E-09 | 2.775E-09 | 2.968E-09 |
| 5 | 3.156E-09 | 2.903E-09 | 0.000 | 0.000 | 0.000 | 0.000 | 0.000 | 0.000 | 0.000 | 0.000 | 0.000 |
| | 1.610E-09 | 2.352E-09 | 2.586E-09 | 2.612E-09 | 2.576E-09 | 2.541E-09 | 2.527E-09 | 2.541E-09 | 2.576E-09 | 2.612E-09 | 2.586E-09 |
| | 2.352E-09 | 1.610E-09 | 0.000 | 0.000 | 0.000 | 0.000 | 0.000 | 0.000 | 0.000 | 0.000 | 0.000 |

LAYER 7

| | 1 | 2 | 3 | 4 | 5 | 6 | 7 | 8 | 9 | 10 | 11 |
|----|-----------|-----------|-----------|-----------|-----------|-----------|-----------|-----------|-----------|-----------|-----------|
| | 12 | 13 | 14 | | | | | | | | |
| 1 | 1.618E-09 | 2.409E-09 | 2.694E-09 | 2.754E-09 | 2.738E-09 | 2.711E-09 | 2.700E-09 | 2.711E-09 | 2.738E-09 | 2.754E-09 | 2.694E-09 |
| 2 | 2.409E-09 | 1.618E-09 | 0.000 | 0.000 | 0.000 | 0.000 | 0.000 | 0.000 | 0.000 | 0.000 | 0.000 |
| 3 | 2.814E-09 | 3.158E-09 | 3.053E-09 | 2.910E-09 | 2.804E-09 | 2.741E-09 | 2.720E-09 | 2.741E-09 | 2.804E-09 | 2.910E-09 | 3.053E-09 |
| 4 | 3.158E-09 | 2.814E-09 | 0.000 | 0.000 | 0.000 | 0.000 | 0.000 | 0.000 | 0.000 | 0.000 | 0.000 |
| 5 | 7.541E-09 | 4.558E-09 | 3.495E-09 | 3.058E-09 | 2.856E-09 | 2.762E-09 | 2.734E-09 | 2.762E-09 | 2.856E-09 | 3.058E-09 | 3.495E-09 |
| 6 | 4.558E-09 | 7.541E-09 | 0.000 | 0.000 | 0.000 | 0.000 | 0.000 | 0.000 | 0.000 | 0.000 | 0.000 |
| 7 | 2.814E-09 | 3.158E-09 | 3.053E-09 | 2.910E-09 | 2.804E-09 | 2.741E-09 | 2.720E-09 | 2.741E-09 | 2.804E-09 | 2.910E-09 | 3.053E-09 |
| 8 | 3.158E-09 | 2.814E-09 | 0.000 | 0.000 | 0.000 | 0.000 | 0.000 | 0.000 | 0.000 | 0.000 | 0.000 |
| 9 | 1.610E-09 | 2.409E-09 | 2.694E-09 | 2.754E-09 | 2.738E-09 | 2.711E-09 | 2.700E-09 | 2.711E-09 | 2.738E-09 | 2.754E-09 | 2.694E-09 |
| 10 | 2.409E-09 | 1.610E-09 | 0.000 | 0.000 | 0.000 | 0.000 | 0.000 | 0.000 | 0.000 | 0.000 | 0.000 |

LAYER 8

| | 1 | 2 | 3 | 4 | 5 | 6 | 7 | 8 | 9 | 10 | 11 |
|----|-----------|-----------|-----------|-----------|-----------|-----------|-----------|-----------|-----------|-----------|-----------|
| | 12 | 13 | 14 | | | | | | | | |
| 1 | 1.615E-09 | 2.409E-09 | 2.781E-09 | 2.769E-09 | 2.759E-09 | 2.736E-09 | 2.726E-09 | 2.736E-09 | 2.759E-09 | 2.769E-09 | 2.781E-09 |
| 2 | 2.409E-09 | 1.615E-09 | 0.000 | 0.000 | 0.000 | 0.000 | 0.000 | 0.000 | 0.000 | 0.000 | 0.000 |
| 3 | 2.801E-09 | 3.152E-09 | 3.057E-09 | 2.923E-09 | 2.824E-09 | 2.765E-09 | 2.746E-09 | 2.765E-09 | 2.824E-09 | 2.923E-09 | 3.057E-09 |
| 4 | 3.152E-09 | 2.801E-09 | 0.000 | 0.000 | 0.000 | 0.000 | 0.000 | 0.000 | 0.000 | 0.000 | 0.000 |
| 5 | 7.490E-09 | 4.540E-09 | 3.495E-09 | 3.070E-09 | 2.876E-09 | 2.787E-09 | 2.760E-09 | 2.787E-09 | 2.876E-09 | 3.070E-09 | 3.495E-09 |
| 6 | 4.540E-09 | 7.490E-09 | 0.000 | 0.000 | 0.000 | 0.000 | 0.000 | 0.000 | 0.000 | 0.000 | 0.000 |
| 7 | 2.801E-09 | 3.152E-09 | 3.057E-09 | 2.923E-09 | 2.824E-09 | 2.765E-09 | 2.746E-09 | 2.765E-09 | 2.824E-09 | 2.923E-09 | 3.057E-09 |
| 8 | 3.152E-09 | 2.801E-09 | 0.000 | 0.000 | 0.000 | 0.000 | 0.000 | 0.000 | 0.000 | 0.000 | 0.000 |
| 9 | 1.615E-09 | 2.409E-09 | 2.781E-09 | 2.769E-09 | 2.759E-09 | 2.736E-09 | 2.726E-09 | 2.736E-09 | 2.759E-09 | 2.769E-09 | 2.781E-09 |
| 10 | 2.409E-09 | 1.615E-09 | 0.000 | 0.000 | 0.000 | 0.000 | 0.000 | 0.000 | 0.000 | 0.000 | 0.000 |

LAYER 9

| | 1 | 2 | 3 | 4 | 5 | 6 | 7 | 8 | 9 | 10 | 11 |
|----|-----------|-----------|-----------|-----------|-----------|-----------|-----------|-----------|-----------|-----------|-----------|
| | 12 | 13 | 14 | | | | | | | | |
| 1 | 1.601E-09 | 2.357E-09 | 2.615E-09 | 2.665E-09 | 2.649E-09 | 2.626E-09 | 2.616E-09 | 2.626E-09 | 2.649E-09 | 2.665E-09 | 2.615E-09 |
| 2 | 2.357E-09 | 1.601E-09 | 0.000 | 0.000 | 0.000 | 0.000 | 0.000 | 0.000 | 0.000 | 0.000 | 0.000 |
| 3 | 2.857E-09 | 3.138E-09 | 2.986E-09 | 2.824E-09 | 2.715E-09 | 2.655E-09 | 2.636E-09 | 2.655E-09 | 2.715E-09 | 2.824E-09 | 2.986E-09 |
| 4 | 3.138E-09 | 2.857E-09 | 0.000 | 0.000 | 0.000 | 0.000 | 0.000 | 0.000 | 0.000 | 0.000 | 0.000 |
| 5 | 7.834E-09 | 4.609E-09 | 3.446E-09 | 2.977E-09 | 2.769E-09 | 2.677E-09 | 2.650E-09 | 2.677E-09 | 2.769E-09 | 2.977E-09 | 3.446E-09 |
| 6 | 4.609E-09 | 7.834E-09 | 0.000 | 0.000 | 0.000 | 0.000 | 0.000 | 0.000 | 0.000 | 0.000 | 0.000 |
| 7 | 2.857E-09 | 3.138E-09 | 2.986E-09 | 2.824E-09 | 2.715E-09 | 2.655E-09 | 2.636E-09 | 2.655E-09 | 2.715E-09 | 2.824E-09 | 2.986E-09 |
| 8 | 3.138E-09 | 2.857E-09 | 0.000 | 0.000 | 0.000 | 0.000 | 0.000 | 0.000 | 0.000 | 0.000 | 0.000 |
| 9 | 1.601E-09 | 2.357E-09 | 2.615E-09 | 2.665E-09 | 2.649E-09 | 2.626E-09 | 2.616E-09 | 2.626E-09 | 2.649E-09 | 2.665E-09 | 2.615E-09 |
| 10 | 2.357E-09 | 1.601E-09 | 0.000 | 0.000 | 0.000 | 0.000 | 0.000 | 0.000 | 0.000 | 0.000 | 0.000 |

LAYER 10

| | 1 | 2 | 3 | 4 | 5 | 6 | 7 | 8 | 9 | 10 | 11 |
|----|-----------|-----------|-----------|-----------|-----------|-----------|-----------|-----------|-----------|-----------|-----------|
| | 12 | 13 | 14 | | | | | | | | |
| 1 | 1.481E-09 | 2.125E-09 | 2.336E-09 | 2.385E-09 | 2.386E-09 | 2.378E-09 | 2.375E-09 | 2.378E-09 | 2.386E-09 | 2.385E-09 | 2.336E-09 |
| 2 | 2.125E-09 | 1.481E-09 | 0.000 | 0.000 | 0.000 | 0.000 | 0.000 | 0.000 | 0.000 | 0.000 | 0.000 |
| 3 | 2.895E-09 | 2.938E-09 | 2.700E-09 | 2.534E-09 | 2.445E-09 | 2.404E-09 | 2.392E-09 | 2.404E-09 | 2.445E-09 | 2.534E-09 | 2.700E-09 |
| 4 | 2.938E-09 | 2.895E-09 | 0.000 | 0.000 | 0.000 | 0.000 | 0.000 | 0.000 | 0.000 | 0.000 | 0.000 |
| 5 | 9.047E-09 | 4.605E-09 | 3.182E-09 | 2.683E-09 | 2.495E-09 | 2.423E-09 | 2.404E-09 | 2.423E-09 | 2.495E-09 | 2.683E-09 | 3.182E-09 |
| 6 | 4.605E-09 | 9.047E-09 | 0.000 | 0.000 | 0.000 | 0.000 | 0.000 | 0.000 | 0.000 | 0.000 | 0.000 |
| 7 | 2.895E-09 | 2.938E-09 | 2.700E-09 | 2.534E-09 | 2.445E-09 | 2.404E-09 | 2.392E-09 | 2.404E-09 | 2.445E-09 | 2.534E-09 | 2.700E-09 |
| 8 | 2.938E-09 | 2.895E-09 | 0.000 | 0.000 | 0.000 | 0.000 | 0.000 | 0.000 | 0.000 | 0.000 | 0.000 |
| 9 | 1.481E-09 | 2.125E-09 | 2.336E-09 | 2.385E-09 | 2.386E-09 | 2.378E-09 | 2.375E-09 | 2.378E-09 | 2.386E-09 | 2.385E-09 | 2.336E-09 |
| 10 | 2.125E-09 | 1.481E-09 | 0.000 | 0.000 | 0.000 | 0.000 | 0.000 | 0.000 | 0.000 | 0.000 | 0.000 |

LAYER 11

| | 1 | 2 | 3 | 4 | 5 | 6 | 7 | 8 | 9 | 10 | 11 |
|----|-----------|-----------|-----------|-----------|-----------|-----------|-----------|-----------|-----------|-----------|-----------|
| | 12 | 13 | 14 | | | | | | | | |
| 1 | 0.065E-10 | 1.362E-09 | 1.695E-09 | 1.885E-09 | 1.990E-09 | 2.043E-09 | 2.059E-09 | 2.043E-09 | 1.990E-09 | 1.885E-09 | 1.695E-09 |
| 2 | 1.362E-09 | 0.065E-10 | 0.000 | 0.000 | 0.000 | 0.000 | 0.000 | 0.000 | 0.000 | 0.000 | 0.000 |
| 3 | 1.028E-09 | 1.540E-09 | 1.797E-09 | 1.935E-09 | 2.013E-09 | 2.054E-09 | 2.067E-09 | 2.054E-09 | 2.013E-09 | 1.935E-09 | 1.797E-09 |
| 4 | 1.540E-09 | 1.028E-09 | 0.000 | 0.000 | 0.000 | 0.000 | 0.000 | 0.000 | 0.000 | 0.000 | 0.000 |
| 5 | 1.441E-09 | 1.773E-09 | 1.900E-09 | 1.978E-09 | 2.031E-09 | 2.062E-09 | 2.073E-09 | 2.062E-09 | 2.031E-09 | 1.978E-09 | 1.900E-09 |
| 6 | 1.773E-09 | 1.441E-09 | 0.000 | 0.000 | 0.000 | 0.000 | 0.000 | 0.000 | 0.000 | 0.000 | 0.000 |
| 7 | 1.028E-09 | 1.540E-09 | 1.797E-09 | 1.935E-09 | 2.013E-09 | 2.054E-09 | 2.067E-09 | 2.054E-09 | 2.013E-09 | 1.935E-09 | 1.797E-09 |
| 8 | 1.540E-09 | 1.028E-09 | 0.000 | 0.000 | 0.000 | 0.000 | 0.000 | 0.000 | 0.000 | 0.000 | 0.000 |
| 9 | 0.065E-10 | 1.362E-09 | 1.695E-09 | 1.885E-09 | 1.990E-09 | 2.043E-09 | 2.059E-09 | 2.043E-09 | 1.990E-09 | 1.885E-09 | 1.695E-09 |
| 10 | 1.362E-09 | 0.065E-10 | 0.000 | 0.000 | 0.000 | 0.000 | 0.000 | 0.000 | 0.000 | 0.000 | 0.000 |

LAYER 12

| | 1 | 2 | 3 | 4 | 5 | 6 | 7 | 8 | 9 | 10 | 11 |
|----|-----------|-----------|-----------|-----------|-----------|-----------|-----------|-----------|-----------|-----------|-----------|
| | 12 | 13 | 14 | | | | | | | | |
| 1 | 5.438E-10 | 1.001E-09 | 1.344E-09 | 1.583E-09 | 1.737E-09 | 1.822E-09 | 1.850E-09 | 1.822E-09 | 1.737E-09 | 1.583E-09 | 1.344E-09 |
| 2 | 1.001E-09 | 5.438E-10 | 0.000 | 0.000 | 0.000 | 0.000 | 0.000 | 0.000 | 0.000 | 0.000 | 0.000 |
| 3 | 5.745E-10 | 1.034E-09 | 1.368E-09 | 1.597E-09 | 1.745E-09 | 1.827E-09 | 1.853E-09 | 1.827E-09 | 1.745E-09 | 1.597E-09 | 1.368E-09 |
| 4 | 1.034E-09 | 5.745E-10 | 0.000 | 0.000 | 0.000 | 0.000 | 0.000 | 0.000 | 0.000 | 0.000 | 0.000 |
| 5 | 6.111E-10 | 1.066E-09 | 1.387E-09 | 1.608E-09 | 1.750E-09 | 1.830E-09 | 1.855E-09 | 1.830E-09 | 1.750E-09 | 1.608E-09 | 1.387E-09 |
| 6 | 1.066E-09 | 6.111E-10 | 0.000 | 0.000 | 0.000 | 0.000 | 0.000 | 0.000 | 0.000 | 0.000 | 0.000 |
| 7 | 5.745E-10 | 1.034E-09 | 1.368E-09 | 1.597E-09 | 1.745E-09 | 1.827E-09 | 1.853E-09 | 1.827E-09 | 1.745E-09 | 1.597E-09 | 1.368E-09 |
| 8 | 1.034E-09 | 5.745E-10 | 0.000 | 0.000 | 0.000 | 0.000 | 0.000 | 0.000 | 0.000 | 0.000 | 0.000 |
| 9 | 5.438E-10 | 1.001E-09 | 1.344E-09 | 1.583E-09 | 1.737E-09 | 1.822E-09 | 1.850E-09 | 1.822E-09 | 1.737E-09 | 1.583E-09 | 1.344E-09 |
| 10 | 1.001E-09 | 5.438E-10 | 0.000 | 0.000 | 0.000 | 0.000 | 0.000 | 0.000 | 0.000 | 0.000 | 0.000 |

*QTY * FLOW TERMS FOR TIME STEP 1, STRESS PERIOD 1 READ UNFORMATTED ON UNIT 10

LAYER 1

| | 1 | 2 | 3 | 4 | 5 | 6 | 7 | 8 | 9 | 10 |
|--|---|---|---|---|---|---|---|---|---|----|
|--|---|---|---|---|---|---|---|---|---|----|

J-8
OUTPUT-H1.ek

| | | | | | | | | | | | |
|---|------------|------------|------------|------------|------------|------------|------------|------------|------------|------------|------------|
| 1 | -7.208E-11 | -5.282E-11 | -3.159E-11 | -1.676E-11 | -8.142E-12 | -3.541E-12 | -9.788E-13 | 9.782E-13 | 3.540E-12 | 8.138E-12 | 1.675E-11 |
| 2 | 3.158E-11 | 5.282E-11 | 7.288E-11 | 1.203E-11 | -5.554E-12 | -2.339E-12 | -6.341E-13 | 6.393E-13 | 2.338E-12 | 5.550E-12 | 1.203E-11 |
| 3 | 2.445E-11 | 4.525E-11 | 6.986E-11 | 1.203E-11 | 5.557E-12 | 2.342E-12 | 6.365E-13 | -6.372E-13 | -2.340E-12 | -5.554E-12 | -1.203E-11 |
| 4 | 7.208E-11 | 5.282E-11 | 3.159E-11 | 1.675E-11 | 8.142E-12 | 3.540E-12 | 9.771E-13 | -9.789E-13 | -3.539E-12 | -8.136E-12 | -1.675E-11 |
| 5 | 0.000 | 0.000 | 0.000 | 0.000 | 0.000 | 0.000 | 0.000 | 0.000 | 0.000 | 0.000 | 0.000 |

LAYER 4

| | | | | | | | | | | | |
|---|-----------|------------|------------|------------|------------|------------|------------|------------|------------|------------|------------|
| 1 | 12 | 2 | 3 | 4 | 5 | 6 | 7 | 8 | 9 | 10 | 11 |
| 1 | 4.249E-10 | -2.686E-10 | -1.389E-10 | -6.459E-11 | -2.804E-11 | -1.117E-11 | -2.935E-12 | 2.930E-12 | 1.117E-11 | 2.804E-11 | 6.458E-11 |
| 2 | 1.389E-10 | 2.686E-10 | 4.249E-10 | -5.152E-11 | -2.043E-11 | -7.692E-12 | -1.964E-12 | 1.965E-12 | 7.690E-12 | 2.043E-11 | 5.152E-11 |
| 3 | 4.249E-10 | -2.686E-10 | -1.389E-10 | 5.152E-11 | 2.043E-11 | 7.694E-12 | 1.963E-12 | -1.966E-12 | -7.694E-12 | -2.043E-11 | -5.152E-11 |
| 4 | 1.270E-10 | 2.987E-10 | 6.087E-10 | 6.459E-11 | 2.804E-11 | 1.117E-11 | 2.930E-12 | -2.932E-12 | -1.117E-11 | -2.804E-11 | -6.458E-11 |
| 5 | 0.000 | 0.000 | 0.000 | 0.000 | 0.000 | 0.000 | 0.000 | 0.000 | 0.000 | 0.000 | 0.000 |

LAYER 5

| | | | | | | | | | | | |
|---|------------|------------|------------|------------|------------|------------|------------|------------|------------|------------|------------|
| 1 | 12 | 2 | 3 | 4 | 5 | 6 | 7 | 8 | 9 | 10 | 11 |
| 1 | -2.072E-09 | -1.040E-09 | -4.434E-10 | -1.771E-10 | -6.829E-11 | -2.492E-11 | -6.229E-12 | 6.227E-12 | 2.492E-11 | 6.828E-11 | 1.771E-10 |
| 2 | 4.434E-10 | 1.040E-09 | 2.072E-09 | -1.634E-10 | -5.425E-11 | -1.808E-11 | -4.322E-12 | 4.319E-12 | 1.807E-11 | 5.424E-11 | 1.634E-10 |
| 3 | 5.169E-10 | 1.742E-09 | 6.281E-09 | 1.634E-10 | 5.424E-11 | 1.807E-11 | 4.316E-12 | -4.323E-12 | -1.808E-11 | -5.424E-11 | -1.634E-10 |
| 4 | -5.169E-10 | -1.742E-09 | -6.281E-09 | 1.771E-10 | 6.829E-11 | 2.492E-11 | 6.226E-12 | -6.227E-12 | -2.492E-11 | -6.828E-11 | -1.771E-10 |
| 5 | 0.000 | 0.000 | 0.000 | 0.000 | 0.000 | 0.000 | 0.000 | 0.000 | 0.000 | 0.000 | 0.000 |

LAYER 6

| | | | | | | | | | | | |
|---|------------|------------|------------|------------|------------|------------|------------|------------|------------|------------|------------|
| 1 | 12 | 2 | 3 | 4 | 5 | 6 | 7 | 8 | 9 | 10 | 11 |
| 1 | -1.910E-09 | -1.012E-09 | -4.539E-10 | -1.891E-10 | -7.544E-11 | -2.824E-11 | -7.158E-12 | 7.156E-12 | 2.824E-11 | 7.544E-11 | 1.891E-10 |
| 2 | 4.539E-10 | 1.012E-09 | 1.910E-09 | -1.674E-10 | -5.840E-11 | -2.016E-11 | -4.915E-12 | 4.910E-12 | 2.015E-11 | 5.839E-11 | 1.674E-10 |
| 3 | 5.100E-09 | 1.548E-09 | 4.967E-10 | 1.674E-10 | 5.839E-11 | 2.016E-11 | 4.908E-12 | -4.915E-12 | -2.016E-11 | -5.839E-11 | -1.674E-10 |
| 4 | -4.967E-10 | -1.548E-09 | -5.100E-09 | 1.891E-10 | 7.544E-11 | 2.823E-11 | 7.156E-12 | -7.155E-12 | -2.823E-11 | -7.544E-11 | -1.891E-10 |
| 5 | 0.000 | 0.000 | 0.000 | 0.000 | 0.000 | 0.000 | 0.000 | 0.000 | 0.000 | 0.000 | 0.000 |

LAYER 7

| | | | | | | | | | | | |
|---|------------|------------|------------|------------|------------|------------|------------|------------|------------|------------|------------|
| 1 | 12 | 2 | 3 | 4 | 5 | 6 | 7 | 8 | 9 | 10 | 11 |
| 1 | -1.782E-09 | -9.517E-10 | -4.315E-10 | -1.821E-10 | -7.363E-11 | -2.789E-11 | -7.123E-12 | 7.123E-12 | 2.789E-11 | 7.363E-11 | 1.821E-10 |
| 2 | 4.315E-10 | 9.517E-10 | 1.782E-09 | -1.594E-10 | -5.649E-11 | -1.978E-11 | -4.867E-12 | 4.864E-12 | 1.978E-11 | 5.648E-11 | 1.594E-10 |
| 3 | 4.662E-10 | 1.438E-09 | 4.719E-09 | 1.594E-10 | 5.649E-11 | 1.978E-11 | 4.863E-12 | -4.867E-12 | -1.978E-11 | -5.649E-11 | -1.594E-10 |
| 4 | -4.662E-10 | -1.438E-09 | -4.719E-09 | 1.821E-10 | 7.363E-11 | 2.789E-11 | 7.123E-12 | -7.122E-12 | -2.789E-11 | -7.363E-11 | -1.821E-10 |
| 5 | 0.000 | 0.000 | 0.000 | 0.000 | 0.000 | 0.000 | 0.000 | 0.000 | 0.000 | 0.000 | 0.000 |

LAYER 8

| | | | | | | | | | | | |
|---|------------|------------|------------|------------|------------|------------|------------|------------|------------|------------|------------|
| 1 | 12 | 2 | 3 | 4 | 5 | 6 | 7 | 8 | 9 | 10 | 11 |
| 1 | -1.766E-09 | -9.431E-10 | -4.275E-10 | -1.804E-10 | -7.293E-11 | -2.762E-11 | -7.056E-12 | 7.056E-12 | 2.762E-11 | 7.293E-11 | 1.804E-10 |
| 2 | 4.275E-10 | 9.431E-10 | 1.766E-09 | -1.579E-10 | -5.596E-11 | -1.959E-11 | -4.820E-12 | 4.818E-12 | 1.959E-11 | 5.596E-11 | 1.579E-10 |
| 3 | 4.620E-10 | 1.426E-09 | 4.681E-09 | 1.579E-10 | 5.596E-11 | 1.960E-11 | 4.818E-12 | -4.822E-12 | -1.960E-11 | -5.596E-11 | -1.579E-10 |
| 4 | -4.620E-10 | -1.426E-09 | -4.681E-09 | 1.804E-10 | 7.293E-11 | 2.762E-11 | 7.055E-12 | -7.056E-12 | -2.762E-11 | -7.293E-11 | -1.804E-10 |
| 5 | 0.000 | 0.000 | 0.000 | 0.000 | 0.000 | 0.000 | 0.000 | 0.000 | 0.000 | 0.000 | 0.000 |

LAYER 9

| | | | | | | | | | | | |
|---|------------|------------|------------|------------|------------|------------|------------|------------|------------|------------|------------|
| 1 | 12 | 2 | 3 | 4 | 5 | 6 | 7 | 8 | 9 | 10 | 11 |
| 1 | -1.855E-09 | -9.829E-10 | -4.407E-10 | -1.836E-10 | -7.328E-11 | -2.744E-11 | -6.957E-12 | 6.957E-12 | 2.744E-11 | 7.328E-11 | 1.836E-10 |
| 2 | 4.407E-10 | 9.829E-10 | 1.855E-09 | -1.625E-10 | -5.671E-11 | -1.958E-11 | -4.776E-12 | 4.771E-12 | 1.958E-11 | 5.671E-11 | 1.625E-10 |
| 3 | 4.823E-10 | 1.504E-09 | 4.960E-09 | 1.625E-10 | 5.671E-11 | 1.958E-11 | 4.773E-12 | -4.775E-12 | -1.959E-11 | -5.671E-11 | -1.625E-10 |
| 4 | -4.823E-10 | -1.504E-09 | -4.960E-09 | 1.836E-10 | 7.328E-11 | 2.744E-11 | 6.957E-12 | -6.957E-12 | -2.744E-11 | -7.328E-11 | -1.836E-10 |
| 5 | 0.000 | 0.000 | 0.000 | 0.000 | 0.000 | 0.000 | 0.000 | 0.000 | 0.000 | 0.000 | 0.000 |

LAYER 10

| | | | | | | | | | | | |
|---|------------|------------|------------|------------|------------|------------|------------|------------|------------|------------|------------|
| 1 | 12 | 2 | 3 | 4 | 5 | 6 | 7 | 8 | 9 | 10 | 11 |
| 1 | -1.961E-09 | -9.864E-10 | -4.214E-10 | -1.686E-10 | -6.518E-11 | -2.384E-11 | -5.967E-12 | 5.963E-12 | 2.384E-11 | 6.518E-11 | 1.686E-10 |
| 2 | 4.214E-10 | 9.864E-10 | 1.961E-09 | -1.553E-10 | -5.169E-11 | -1.727E-11 | -4.138E-12 | 4.131E-12 | 1.727E-11 | 5.169E-11 | 1.553E-10 |
| 3 | 4.900E-10 | 1.647E-09 | 5.925E-09 | 1.553E-10 | 5.169E-11 | 1.727E-11 | 4.132E-12 | -4.135E-12 | -1.727E-11 | -5.169E-11 | -1.553E-10 |
| 4 | -4.900E-10 | -1.647E-09 | -5.925E-09 | 1.686E-10 | 6.518E-11 | 2.384E-11 | 5.966E-12 | -5.964E-12 | -2.384E-11 | -6.518E-11 | -1.686E-10 |
| 5 | 0.000 | 0.000 | 0.000 | 0.000 | 0.000 | 0.000 | 0.000 | 0.000 | 0.000 | 0.000 | 0.000 |

LAYER 11

| | | | | | | | | | | | |
|---|------------|------------|------------|------------|------------|------------|------------|------------|------------|------------|------------|
| 1 | 12 | 2 | 3 | 4 | 5 | 6 | 7 | 8 | 9 | 10 | 11 |
| 1 | -4.036E-10 | -2.557E-10 | -1.326E-10 | -6.194E-11 | -2.702E-11 | -1.081E-11 | -2.848E-12 | 2.846E-12 | 1.081E-11 | 2.702E-11 | 6.194E-11 |
| 2 | 1.326E-10 | 2.557E-10 | 4.036E-10 | -4.926E-11 | -1.964E-11 | -7.435E-12 | -1.906E-12 | 1.905E-12 | 7.433E-12 | 1.964E-11 | 4.926E-11 |
| 3 | 5.758E-10 | 2.833E-10 | 1.209E-10 | 4.926E-11 | 1.963E-11 | 7.429E-12 | 1.904E-12 | -1.904E-12 | -7.430E-12 | -1.964E-11 | -4.926E-11 |
| 4 | -1.209E-10 | -2.833E-10 | -5.758E-10 | 6.194E-11 | 2.702E-11 | 1.081E-11 | 2.848E-12 | -2.847E-12 | -1.081E-11 | -2.702E-11 | -6.194E-11 |
| 5 | 0.000 | 0.000 | 0.000 | 0.000 | 0.000 | 0.000 | 0.000 | 0.000 | 0.000 | 0.000 | 0.000 |

LAYER 12

J-10 OUTPUT-H1.ek

5 1.321E-10 1.287E-10 1.156E-10 9.427E-11 6.845E-11 4.113E-11 1.368E-11 -1.368E-11 -4.113E-11 -6.845E-11 -9.427E-11
-1.156E-10 -1.287E-10 -1.321E-10

LAYER 9

| | 1 | 2 | 3 | 4 | 5 | 6 | 7 | 8 | 9 | 10 | 11 |
|---|------------|------------|------------|-----------|-----------|-----------|-----------|------------|------------|------------|------------|
| | 12 | 13 | 14 | | | | | | | | |
| 1 | 3.860E-10 | 3.559E-10 | 2.978E-10 | 2.280E-10 | 1.579E-10 | 9.204E-11 | 3.017E-11 | -3.017E-11 | -9.204E-11 | -1.579E-10 | -2.280E-10 |
| 2 | -2.978E-10 | -3.559E-10 | -3.860E-10 | 2.334E-10 | 1.608E-10 | 9.334E-11 | 3.052E-11 | -3.052E-11 | -9.334E-11 | -1.608E-10 | -2.334E-10 |
| 3 | -3.048E-10 | -3.546E-10 | -3.478E-10 | 2.360E-10 | 1.626E-10 | 9.417E-11 | 3.075E-11 | -3.075E-11 | -9.417E-11 | -1.626E-10 | -2.360E-10 |
| 4 | -3.020E-10 | -3.032E-10 | 0.000 | 2.348E-10 | 1.608E-10 | 9.334E-11 | 3.052E-11 | -3.052E-11 | -9.334E-11 | -1.608E-10 | -2.348E-10 |
| 5 | -3.948E-10 | -3.546E-10 | -3.478E-10 | 2.280E-10 | 1.579E-10 | 9.204E-11 | 3.017E-11 | -3.017E-11 | -9.204E-11 | -1.579E-10 | -2.280E-10 |
| | -2.978E-10 | -3.559E-10 | -3.860E-10 | | | | | | | | |

LAYER 10

| | 1 | 2 | 3 | 4 | 5 | 6 | 7 | 8 | 9 | 10 | 11 |
|---|------------|------------|------------|-----------|-----------|-----------|-----------|------------|------------|------------|------------|
| | 12 | 13 | 14 | | | | | | | | |
| 1 | 8.668E-10 | 6.983E-10 | 5.978E-10 | 3.475E-10 | 2.224E-10 | 1.234E-10 | 3.950E-11 | -3.950E-11 | -1.234E-10 | -2.224E-10 | -3.475E-10 |
| 2 | -5.078E-10 | -6.983E-10 | -8.668E-10 | 3.860E-10 | 2.362E-10 | 1.281E-10 | 4.062E-11 | -4.062E-11 | -1.281E-10 | -2.362E-10 | -3.860E-10 |
| 3 | -6.117E-10 | -9.614E-10 | -1.428E-09 | 4.241E-10 | 2.477E-10 | 1.316E-10 | 4.143E-11 | -4.143E-11 | -1.316E-10 | -2.477E-10 | -4.241E-10 |
| 4 | -7.446E-10 | -1.452E-09 | -1.354E-09 | 3.859E-10 | 2.362E-10 | 1.281E-10 | 4.062E-11 | -4.062E-11 | -1.281E-10 | -2.362E-10 | -3.859E-10 |
| 5 | -6.117E-10 | -9.614E-10 | -1.428E-09 | 3.475E-10 | 2.224E-10 | 1.234E-10 | 3.950E-11 | -3.950E-11 | -1.234E-10 | -2.224E-10 | -3.475E-10 |
| | -5.078E-10 | -6.983E-10 | -8.668E-10 | | | | | | | | |

LAYER 11

| | 1 | 2 | 3 | 4 | 5 | 6 | 7 | 8 | 9 | 10 | 11 |
|---|------------|------------|------------|-----------|-----------|-----------|-----------|------------|------------|------------|------------|
| | 12 | 13 | 14 | | | | | | | | |
| 1 | 4.637E-10 | 3.983E-10 | 2.978E-10 | 2.198E-10 | 1.444E-10 | 8.122E-11 | 2.615E-11 | -2.615E-11 | -8.122E-11 | -1.444E-10 | -2.198E-10 |
| 2 | -3.076E-10 | -3.983E-10 | -4.637E-10 | 2.352E-10 | 1.507E-10 | 8.359E-11 | 2.675E-11 | -2.675E-11 | -8.359E-11 | -1.507E-10 | -2.352E-10 |
| 3 | -3.425E-10 | -4.689E-10 | -5.802E-10 | 2.480E-10 | 1.554E-10 | 8.527E-11 | 2.716E-11 | -2.716E-11 | -8.527E-11 | -1.554E-10 | -2.480E-10 |
| 4 | -3.762E-10 | -5.532E-10 | -7.606E-10 | 2.352E-10 | 1.507E-10 | 8.359E-11 | 2.675E-11 | -2.675E-11 | -8.359E-11 | -1.507E-10 | -2.352E-10 |
| 5 | -3.425E-10 | -4.689E-10 | -5.802E-10 | 2.198E-10 | 1.444E-10 | 8.122E-11 | 2.615E-11 | -2.615E-11 | -8.122E-11 | -1.444E-10 | -2.198E-10 |
| | -3.076E-10 | -3.983E-10 | -4.637E-10 | | | | | | | | |

LAYER 12

| | 1 | 2 | 3 | 4 | 5 | 6 | 7 | 8 | 9 | 10 | 11 |
|---|-------|-------|-------|-------|-------|-------|-------|-------|-------|-------|-------|
| | 12 | 13 | 14 | | | | | | | | |
| 1 | 0.000 | 0.000 | 0.000 | 0.000 | 0.000 | 0.000 | 0.000 | 0.000 | 0.000 | 0.000 | 0.000 |
| 2 | 0.000 | 0.000 | 0.000 | 0.000 | 0.000 | 0.000 | 0.000 | 0.000 | 0.000 | 0.000 | 0.000 |
| 3 | 0.000 | 0.000 | 0.000 | 0.000 | 0.000 | 0.000 | 0.000 | 0.000 | 0.000 | 0.000 | 0.000 |
| 4 | 0.000 | 0.000 | 0.000 | 0.000 | 0.000 | 0.000 | 0.000 | 0.000 | 0.000 | 0.000 | 0.000 |
| 5 | 0.000 | 0.000 | 0.000 | 0.000 | 0.000 | 0.000 | 0.000 | 0.000 | 0.000 | 0.000 | 0.000 |

MAXIMUM STEPSIZE DURING WHICH ANY PARTICLE CANNOT MOVE MORE THAN ONE CELL
= 0.1505E+06 (WHEN MIN. R.F.=1) AT K= 5, I= 3, J= 13

MAXIMUM STEPSIZE WHICH MEETS STABILITY CRITERION OF THE DISPERSION TERM
= 0.1636E+08 (WHEN MIN. R.F.=1) AT K= 11, I= 4, J= 13

DISP. COEFF. DXX IN LAYER 1 FOR TIME STEP 1, STRESS PERIOD 1

| | 1 | 2 | 3 | 4 | 5 | 6 | 7 | 8 | 9 | 10 | 11 | 12 | 13 | 14 |
|---|-----|-----|-----|-----|-----|-----|-----|-----|-----|-----|-----|-----|-----|-----|
| 1 | 0.0 | 0.0 | 0.0 | 0.0 | 0.0 | 0.0 | 0.0 | 0.0 | 0.0 | 0.0 | 0.0 | 0.0 | 0.0 | 0.0 |
| 2 | 0.0 | 0.0 | 0.0 | 0.0 | 0.0 | 0.0 | 0.0 | 0.0 | 0.0 | 0.0 | 0.0 | 0.0 | 0.0 | 0.0 |
| 3 | 0.0 | 0.0 | 0.0 | 0.0 | 0.0 | 0.0 | 0.0 | 0.0 | 0.0 | 0.0 | 0.0 | 0.0 | 0.0 | 0.0 |
| 4 | 0.0 | 0.0 | 0.0 | 0.0 | 0.0 | 0.0 | 0.0 | 0.0 | 0.0 | 0.0 | 0.0 | 0.0 | 0.0 | 0.0 |
| 5 | 0.0 | 0.0 | 0.0 | 0.0 | 0.0 | 0.0 | 0.0 | 0.0 | 0.0 | 0.0 | 0.0 | 0.0 | 0.0 | 0.0 |

DISP. COEFF. DXX IN LAYER 2 FOR TIME STEP 1, STRESS PERIOD 1

| | 1 | 2 | 3 | 4 | 5 | 6 | 7 | 8 | 9 | 10 | 11 | 12 | 13 | 14 |
|---|-----|-----|-----|-----|-----|-----|-----|-----|-----|-----|-----|-----|-----|-----|
| 1 | 0.0 | 0.0 | 0.0 | 0.0 | 0.0 | 0.0 | 0.0 | 0.0 | 0.0 | 0.0 | 0.0 | 0.0 | 0.0 | 0.0 |
| 2 | 0.0 | 0.0 | 0.0 | 0.0 | 0.0 | 0.0 | 0.0 | 0.0 | 0.0 | 0.0 | 0.0 | 0.0 | 0.0 | 0.0 |
| 3 | 0.0 | 0.0 | 0.0 | 0.0 | 0.0 | 0.0 | 0.0 | 0.0 | 0.0 | 0.0 | 0.0 | 0.0 | 0.0 | 0.0 |
| 4 | 0.0 | 0.0 | 0.0 | 0.0 | 0.0 | 0.0 | 0.0 | 0.0 | 0.0 | 0.0 | 0.0 | 0.0 | 0.0 | 0.0 |
| 5 | 0.0 | 0.0 | 0.0 | 0.0 | 0.0 | 0.0 | 0.0 | 0.0 | 0.0 | 0.0 | 0.0 | 0.0 | 0.0 | 0.0 |

DISP. COEFF. DXX IN LAYER 3 FOR TIME STEP 1, STRESS PERIOD 1

| | 1 | 2 | 3 | 4 | 5 | 6 | 7 | 8 | 9 | 10 | 11 | 12 | 13 | 14 |
|---|-----|-----|-----|-----|-----|-----|-----|-----|-----|-----|-----|-----|-----|-----|
| 1 | 0.0 | 0.0 | 0.0 | 0.0 | 0.0 | 0.0 | 0.0 | 0.0 | 0.0 | 0.0 | 0.0 | 0.0 | 0.0 | 0.0 |
| 2 | 0.0 | 0.0 | 0.0 | 0.0 | 0.0 | 0.0 | 0.0 | 0.0 | 0.0 | 0.0 | 0.0 | 0.0 | 0.0 | 0.0 |
| 3 | 0.0 | 0.0 | 0.0 | 0.0 | 0.0 | 0.0 | 0.0 | 0.0 | 0.0 | 0.0 | 0.0 | 0.0 | 0.0 | 0.0 |
| 4 | 0.0 | 0.0 | 0.0 | 0.0 | 0.0 | 0.0 | 0.0 | 0.0 | 0.0 | 0.0 | 0.0 | 0.0 | 0.0 | 0.0 |
| 5 | 0.0 | 0.0 | 0.0 | 0.0 | 0.0 | 0.0 | 0.0 | 0.0 | 0.0 | 0.0 | 0.0 | 0.0 | 0.0 | 0.0 |

DISP. COEFF. DXX IN LAYER 4 FOR TIME STEP 1, STRESS PERIOD 1

| | 1 | 2 | 3 | 4 | 5 | 6 | 7 | 8 | 9 | 10 | 11 | 12 | 13 | 14 |
|---|-----|-----|-----|-----|-----|-----|-----|-----|-----|-----|-----|-----|-----|-----|
| 1 | 0.0 | 0.0 | 0.0 | 0.0 | 0.0 | 0.0 | 0.0 | 0.0 | 0.0 | 0.0 | 0.0 | 0.0 | 0.0 | 0.0 |
| 2 | 0.0 | 0.0 | 0.0 | 0.0 | 0.0 | 0.0 | 0.0 | 0.0 | 0.0 | 0.0 | 0.0 | 0.0 | 0.0 | 0.0 |
| 3 | 0.0 | 0.0 | 0.0 | 0.0 | 0.0 | 0.0 | 0.0 | 0.0 | 0.0 | 0.0 | 0.0 | 0.0 | 0.0 | 0.0 |
| 4 | 0.0 | 0.0 | 0.0 | 0.0 | 0.0 | 0.0 | 0.0 | 0.0 | 0.0 | 0.0 | 0.0 | 0.0 | 0.0 | 0.0 |
| 5 | 0.0 | 0.0 | 0.0 | 0.0 | 0.0 | 0.0 | 0.0 | 0.0 | 0.0 | 0.0 | 0.0 | 0.0 | 0.0 | 0.0 |

DISP. COEFF. DXX IN LAYER 5 FOR TIME STEP 1, STRESS PERIOD 1

| | 1 | 2 | 3 | 4 | 5 | 6 | 7 | 8 | 9 | 10 | 11 | 12 | 13 | 14 |
|---|-----|-----|-----|-----|-----|-----|-----|-----|-----|-----|-----|-----|-----|-----|
| 1 | 0.0 | 0.0 | 0.0 | 0.0 | 0.0 | 0.0 | 0.0 | 0.0 | 0.0 | 0.0 | 0.0 | 0.0 | 0.0 | 0.0 |
| 2 | 0.0 | 0.0 | 0.0 | 0.0 | 0.0 | 0.0 | 0.0 | 0.0 | 0.0 | 0.0 | 0.0 | 0.0 | 0.0 | 0.0 |
| 3 | 0.0 | 0.0 | 0.0 | 0.0 | 0.0 | 0.0 | 0.0 | 0.0 | 0.0 | 0.0 | 0.0 | 0.0 | 0.0 | 0.0 |
| 4 | 0.0 | 0.0 | 0.0 | 0.0 | 0.0 | 0.0 | 0.0 | 0.0 | 0.0 | 0.0 | 0.0 | 0.0 | 0.0 | 0.0 |
| 5 | 0.0 | 0.0 | 0.0 | 0.0 | 0.0 | 0.0 | 0.0 | 0.0 | 0.0 | 0.0 | 0.0 | 0.0 | 0.0 | 0.0 |

DISP. COEFF. DXX IN LAYER 6 FOR TIME STEP 1, STRESS PERIOD 1

| | 1 | 2 | 3 | 4 | 5 | 6 | 7 | 8 | 9 | 10 | 11 | 12 | 13 | 14 |
|---|-----|-----|-----|-----|-----|-----|-----|-----|-----|-----|-----|-----|-----|-----|
| 1 | 0.0 | 0.0 | 0.0 | 0.0 | 0.0 | 0.0 | 0.0 | 0.0 | 0.0 | 0.0 | 0.0 | 0.0 | 0.0 | 0.0 |
| 2 | 0.0 | 0.0 | 0.0 | 0.0 | 0.0 | 0.0 | 0.0 | 0.0 | 0.0 | 0.0 | 0.0 | 0.0 | 0.0 | 0.0 |
| 3 | 0.0 | 0.0 | 0.0 | 0.0 | 0.0 | 0.0 | 0.0 | 0.0 | 0.0 | 0.0 | 0.0 | 0.0 | 0.0 | 0.0 |
| 4 | 0.0 | 0.0 | 0.0 | 0.0 | 0.0 | 0.0 | 0.0 | 0.0 | 0.0 | 0.0 | 0.0 | 0.0 | 0.0 | 0.0 |
| 5 | 0.0 | 0.0 | 0.0 | 0.0 | 0.0 | 0.0 | 0.0 | 0.0 | 0.0 | 0.0 | 0.0 | 0.0 | 0.0 | 0.0 |

DISP. COEFF. DXX IN LAYER 7 FOR TIME STEP 1, STRESS PERIOD 1

J-19
OUTPUT-H1.ek

5 23.2 19.1 14.1 9.3 5.3 2.6 1.0 0.3 0.1 0.0 0.0 0.0 0.0 0.0 0.0

CONCENTRATIONS IN LAYER 2 AT END OF TRANSPORT STEP 7476, TIME STEP 1, STRESS PERIOD 1

| | 1 | 2 | 3 | 4 | 5 | 6 | 7 | 8 | 9 | 10 | 11 | 12 | 13 | 14 |
|---|-------|-------|-------|------|------|------|------|------|------|-----|-----|-----|-----|-----|
| 1 | 97.8 | 87.3 | 72.6 | 55.5 | 38.1 | 22.8 | 14.8 | 9.8 | 6.2 | 4.0 | 2.5 | 1.5 | 0.9 | 0.5 |
| 2 | 127.3 | 116.8 | 101.5 | 82.1 | 60.4 | 39.1 | 21.3 | 14.6 | 9.8 | 6.3 | 4.0 | 2.5 | 1.5 | 0.9 |
| 3 | 144.9 | 134.7 | 119.6 | 99.8 | 76.5 | 52.0 | 30.0 | 18.6 | 12.3 | 8.0 | 5.0 | 3.0 | 1.8 | 1.1 |
| 4 | 127.3 | 116.8 | 101.5 | 82.1 | 60.4 | 39.1 | 21.3 | 14.6 | 9.8 | 6.3 | 4.0 | 2.5 | 1.5 | 0.9 |
| 5 | 97.8 | 87.3 | 72.6 | 55.5 | 38.1 | 22.8 | 14.8 | 9.8 | 6.2 | 4.0 | 2.5 | 1.5 | 0.9 | 0.5 |

CONCENTRATIONS IN LAYER 3 AT END OF TRANSPORT STEP 7476, TIME STEP 1, STRESS PERIOD 1

| | 1 | 2 | 3 | 4 | 5 | 6 | 7 | 8 | 9 | 10 | 11 | 12 | 13 | 14 |
|---|-------|-------|-------|-------|-------|-------|-------|------|------|------|-----|-----|-----|-----|
| 1 | 173.7 | 166.3 | 154.0 | 135.8 | 111.6 | 83.3 | 54.5 | 30.8 | 15.4 | 6.7 | 2.5 | 0.8 | 0.2 | 0.0 |
| 2 | 190.6 | 186.5 | 178.9 | 166.1 | 146.1 | 118.4 | 85.1 | 53.1 | 29.0 | 13.8 | 5.6 | 1.9 | 0.5 | 0.1 |
| 3 | 196.3 | 192.8 | 188.8 | 179.4 | 162.3 | 138.6 | 105.5 | 70.1 | 40.7 | 20.6 | 8.9 | 3.2 | 0.9 | 0.1 |
| 4 | 190.6 | 186.5 | 178.9 | 166.1 | 146.1 | 118.4 | 85.1 | 53.1 | 29.0 | 13.8 | 5.6 | 1.9 | 0.5 | 0.1 |
| 5 | 173.7 | 166.3 | 154.0 | 135.8 | 111.6 | 83.3 | 54.5 | 30.8 | 15.4 | 6.7 | 2.5 | 0.8 | 0.2 | 0.0 |

CONCENTRATIONS IN LAYER 4 AT END OF TRANSPORT STEP 7476, TIME STEP 1, STRESS PERIOD 1

| | 1 | 2 | 3 | 4 | 5 | 6 | 7 | 8 | 9 | 10 | 11 | 12 | 13 | 14 |
|---|-------|-------|-------|-------|-------|-------|-------|-------|-------|------|------|------|------|-----|
| 1 | 198.1 | 199.6 | 193.6 | 187.1 | 175.0 | 155.2 | 127.4 | 94.2 | 62.3 | 36.6 | 19.0 | 8.5 | 3.1 | 0.7 |
| 2 | 199.9 | 199.8 | 199.3 | 197.7 | 193.2 | 182.6 | 162.8 | 132.2 | 95.8 | 61.5 | 34.8 | 17.0 | 6.8 | 1.9 |
| 3 | 200.0 | 200.0 | 199.9 | 199.4 | 197.5 | 191.5 | 177.8 | 152.1 | 116.6 | 79.5 | 47.8 | 25.0 | 11.0 | 3.6 |
| 4 | 199.9 | 199.8 | 199.3 | 197.7 | 193.2 | 182.6 | 162.8 | 132.2 | 95.8 | 61.5 | 34.8 | 17.0 | 6.8 | 1.9 |
| 5 | 198.1 | 196.7 | 193.6 | 187.1 | 175.0 | 155.2 | 127.4 | 94.2 | 62.3 | 36.6 | 19.0 | 8.5 | 3.1 | 0.7 |

CONCENTRATIONS IN LAYER 5 AT END OF TRANSPORT STEP 7476, TIME STEP 1, STRESS PERIOD 1

| | 1 | 2 | 3 | 4 | 5 | 6 | 7 | 8 | 9 | 10 | 11 | 12 | 13 | 14 |
|---|-------|-------|-------|-------|-------|-------|-------|-------|-------|-------|-------|------|------|------|
| 1 | 199.9 | 199.7 | 199.3 | 197.9 | 194.5 | 187.0 | 173.4 | 151.7 | 122.7 | 91.0 | 61.5 | 37.6 | 20.0 | 8.0 |
| 2 | 200.0 | 200.0 | 200.0 | 199.9 | 199.5 | 197.7 | 192.5 | 180.1 | 157.3 | 126.0 | 91.7 | 60.0 | 34.4 | 15.9 |
| 3 | 200.0 | 200.0 | 200.0 | 200.0 | 199.9 | 199.3 | 196.9 | 189.2 | 171.9 | 144.5 | 111.0 | 77.1 | 47.6 | 0.0 |
| 4 | 200.0 | 200.0 | 200.0 | 199.9 | 199.5 | 197.7 | 192.5 | 180.1 | 157.3 | 126.0 | 91.7 | 60.0 | 34.4 | 15.9 |
| 5 | 199.9 | 199.7 | 199.3 | 197.9 | 194.5 | 187.0 | 173.4 | 151.7 | 122.7 | 91.0 | 61.5 | 37.6 | 20.0 | 8.0 |

CONCENTRATIONS IN LAYER 6 AT END OF TRANSPORT STEP 7476, TIME STEP 1, STRESS PERIOD 1

| | 1 | 2 | 3 | 4 | 5 | 6 | 7 | 8 | 9 | 10 | 11 | 12 | 13 | 14 |
|---|-------|-------|-------|-------|-------|-------|-------|-------|-------|-------|-------|-------|------|------|
| 1 | 199.9 | 199.7 | 199.3 | 198.3 | 195.9 | 190.8 | 181.5 | 166.8 | 146.3 | 121.6 | 95.1 | 69.3 | 45.6 | 23.6 |
| 2 | 200.0 | 200.0 | 200.0 | 199.9 | 199.7 | 198.8 | 196.0 | 189.4 | 176.9 | 157.3 | 131.6 | 102.4 | 72.5 | 42.8 |
| 3 | 200.0 | 200.0 | 200.0 | 199.9 | 199.9 | 199.7 | 198.6 | 195.3 | 187.5 | 172.2 | 152.1 | 125.5 | 95.4 | 0.0 |
| 4 | 200.0 | 200.0 | 200.0 | 199.9 | 199.7 | 198.8 | 196.0 | 189.4 | 176.9 | 157.3 | 131.6 | 102.4 | 72.5 | 42.8 |
| 5 | 199.9 | 199.7 | 199.3 | 198.3 | 195.9 | 190.8 | 181.5 | 166.8 | 146.3 | 121.6 | 95.1 | 69.3 | 45.6 | 23.6 |

CONCENTRATIONS IN LAYER 7 AT END OF TRANSPORT STEP 7476, TIME STEP 1, STRESS PERIOD 1

| | 1 | 2 | 3 | 4 | 5 | 6 | 7 | 8 | 9 | 10 | 11 | 12 | 13 | 14 |
|---|-------|-------|-------|-------|-------|-------|-------|-------|-------|-------|-------|-------|-------|-------|
| 1 | 199.8 | 199.6 | 199.2 | 198.1 | 195.8 | 191.1 | 182.9 | 170.2 | 152.8 | 131.8 | 108.5 | 84.5 | 60.2 | 34.3 |
| 2 | 200.0 | 200.0 | 200.0 | 199.9 | 199.7 | 199.0 | 196.7 | 191.6 | 182.1 | 167.1 | 146.6 | 121.2 | 91.8 | 58.2 |
| 3 | 200.0 | 200.0 | 200.0 | 200.0 | 200.0 | 199.9 | 199.8 | 199.0 | 196.6 | 191.3 | 181.5 | 166.3 | 144.8 | 116.2 |
| 4 | 200.0 | 200.0 | 200.0 | 199.9 | 199.7 | 199.0 | 196.7 | 191.6 | 182.1 | 167.1 | 146.6 | 121.2 | 91.8 | 58.2 |
| 5 | 199.8 | 199.6 | 199.2 | 198.1 | 195.8 | 191.1 | 182.9 | 170.2 | 152.8 | 131.8 | 108.5 | 84.5 | 60.2 | 34.3 |

CONCENTRATIONS IN LAYER 8 AT END OF TRANSPORT STEP 7476, TIME STEP 1, STRESS PERIOD 1

| | 1 | 2 | 3 | 4 | 5 | 6 | 7 | 8 | 9 | 10 | 11 | 12 | 13 | 14 |
|---|-------|-------|-------|-------|-------|-------|-------|-------|-------|-------|-------|-------|-------|------|
| 1 | 199.8 | 199.6 | 199.1 | 198.0 | 195.7 | 191.1 | 182.9 | 170.4 | 153.4 | 132.7 | 109.9 | 86.1 | 61.9 | 35.6 |
| 2 | 200.0 | 200.0 | 200.0 | 199.9 | 199.7 | 199.0 | 196.8 | 191.8 | 182.6 | 168.2 | 148.3 | 123.3 | 94.0 | 60.0 |
| 3 | 200.0 | 200.0 | 200.0 | 200.0 | 200.0 | 199.8 | 199.0 | 196.7 | 191.7 | 182.4 | 167.8 | 146.9 | 118.5 | 0.0 |
| 4 | 200.0 | 200.0 | 200.0 | 199.9 | 199.7 | 199.0 | 196.8 | 191.8 | 182.6 | 168.2 | 148.3 | 123.3 | 94.0 | 60.0 |
| 5 | 199.8 | 199.6 | 199.1 | 198.0 | 195.7 | 191.1 | 182.9 | 170.4 | 153.4 | 132.7 | 109.9 | 86.1 | 61.9 | 35.6 |

CONCENTRATIONS IN LAYER 9 AT END OF TRANSPORT STEP 7476, TIME STEP 1, STRESS PERIOD 1

| | 1 | 2 | 3 | 4 | 5 | 6 | 7 | 8 | 9 | 10 | 11 | 12 | 13 | 14 |
|---|-------|-------|-------|-------|-------|-------|-------|-------|-------|-------|-------|-------|-------|------|
| 1 | 199.8 | 199.7 | 199.2 | 198.2 | 195.8 | 190.8 | 182.0 | 168.3 | 149.4 | 126.4 | 101.3 | 76.0 | 51.5 | 27.5 |
| 2 | 200.0 | 200.0 | 200.0 | 199.9 | 199.7 | 198.8 | 196.3 | 190.5 | 179.5 | 162.3 | 139.0 | 111.1 | 80.7 | 48.8 |
| 3 | 200.0 | 200.0 | 200.0 | 200.0 | 200.0 | 199.9 | 199.8 | 199.5 | 189.5 | 177.6 | 159.4 | 134.7 | 104.5 | 0.0 |
| 4 | 200.0 | 200.0 | 200.0 | 199.9 | 199.7 | 198.8 | 196.3 | 190.5 | 179.5 | 162.3 | 139.0 | 111.1 | 80.7 | 48.8 |
| 5 | 199.8 | 199.7 | 199.2 | 198.2 | 195.8 | 190.8 | 182.0 | 168.3 | 149.4 | 126.4 | 101.3 | 76.0 | 51.5 | 27.5 |

CONCENTRATIONS IN LAYER 10 AT END OF TRANSPORT STEP 7476, TIME STEP 1, STRESS PERIOD 1

| | 1 | 2 | 3 | 4 | 5 | 6 | 7 | 8 | 9 | 10 | 11 | 12 | 13 | 14 |
|---|-------|-------|-------|-------|-------|-------|-------|-------|-------|-------|-------|------|------|------|
| 1 | 199.8 | 199.7 | 199.1 | 197.8 | 194.4 | 187.6 | 175.8 | 157.3 | 132.4 | 103.7 | 74.9 | 49.1 | 28.1 | 12.0 |
| 2 | 200.0 | 200.0 | 200.0 | 199.9 | 199.5 | 198.0 | 193.9 | 184.3 | 166.7 | 140.9 | 109.5 | 76.8 | 47.1 | 22.9 |
| 3 | 200.0 | 200.0 | 200.0 | 200.0 | 199.9 | 199.4 | 197.6 | 192.2 | 180.0 | 159.2 | 130.4 | 97.0 | 63.5 | 0.0 |
| 4 | 200.0 | 200.0 | 200.0 | 199.9 | 199.5 | 198.0 | 193.9 | 184.3 | 166.7 | 140.9 | 109.5 | 76.8 | 47.1 | 22.9 |
| 5 | 199.8 | 199.7 | 199.1 | 197.8 | 194.4 | 187.6 | 175.8 | 157.3 | 132.4 | 103.7 | 74.9 | 49.1 | 28.1 | 12.0 |

CONCENTRATIONS IN LAYER 11 AT END OF TRANSPORT STEP 7476, TIME STEP 1, STRESS PERIOD 1

| | 1 | 2 | 3 | 4 | 5 | 6 | 7 | 8 | 9 | 10 | 11 | 12 | 13 | 14 |
|---|-------|-------|-------|-------|-------|-------|-------|-------|-------|-------|------|------|------|-----|
| 1 | 196.2 | 194.0 | 189.9 | 182.5 | 170.6 | 153.0 | 129.7 | 102.5 | 74.8 | 50.0 | 30.1 | 15.8 | 6.7 | 1.8 |
| 2 | 199.8 | 199.5 | 198.8 | 196.8 | 192.1 | 182.9 | 167.1 | 143.5 | 114.2 | 83.1 | 54.4 | 31.0 | 14.5 | 4.6 |
| 3 | 200.0 | 200.0 | 199.8 | 199.2 | 197.4 | 192.5 | 182.3 | 164.1 | 137.7 | 106.1 | 73.8 | 45.1 | 23.0 | 8.5 |
| 4 | 199.8 | 199.5 | 198.8 | 196.8 | 192.1 | 182.9 | 167.1 | 143.5 | 114.2 | 83.1 | 54.4 | 31.0 | 14.5 | 4.6 |
| 5 | 196.2 | 194.0 | 189.9 | 182.5 | 170.6 | 153.0 | 129.7 | 102.5 | 74.8 | 50.0 | 30.1 | 15.8 | 6.7 | 1.8 |

CONCENTRATIONS IN LAYER 12 AT END OF TRANSPORT STEP 7476, TIME STEP 1, STRESS PERIOD 1

| | 1 | 2 | 3 | 4 | 5 | 6 | 7 | 8 | 9 | 10 | 11 | 12 | 13 | 14 |
|---|-------|-------|-------|-------|-------|-------|-------|------|------|------|------|------|-----|-----|
| 1 | 143.9 | 135.2 | 122.9 | 107.3 | 89.3 | 69.9 | 50.7 | 34.1 | 21.4 | 12.3 | 6.3 | 2.8 | 0.9 | 0.2 |
| 2 | 174.3 | 167.7 | 157.9 | 144.5 | 127.3 | 106.7 | 83.6 | 61.0 | 41.4 | 25.8 | 14.3 | 6.8 | 2.5 | 0.5 |
| 3 | 188.5 | 183.6 | 176.9 | 165.2 | 150.3 | 131.1 | 107.8 | 82.8 | 58.4 | 39.1 | 23.0 | 11.6 | 4.6 | 1.1 |
| 4 | 174.3 | 167.7 | 157.9 | 144.5 | 127.3 | 106.7 | 83.6 | 61.0 | 41.4 | 25.8 | 14.3 | 6.8 | 2.5 | 0.5 |
| 5 | 143.9 | 135.2 | 122.9 | 107.3 | 89.3 | 69.9 | 50.7 | 34.1 | 21.4 | 12.3 | 6.3 | 2.8 | 0.9 | 0.2 |

CUMULATIVE MASS BUDGETS AT END OF TRANSPORT STEP 7476, TIME STEP 1, STRESS PERIOD 1

| | IN | OUT |
|-------------------------|-----------|-----------|
| CONSTANT CONCENTRATION: | 107.5207 | -6.678828 |
| CONSTANT HEAD: | 0.0000000 | 0.0000000 |
| MASS STORAGE (SOLUTE): | 0.0000000 | -100.8338 |
| (TOTAL): | 107.5207 | -107.5126 |

NET (IN - OUT): 0.8010864E-02
DISCREPANCY (PERCENT): 0.7450813E-02

MTT
3 D End of Model Output

J-20
OUTPUT-H2.ek

```

+-----+
+               M T 3 D               +
+   A Modular Three-Dimensional Transport Model   +
+   For Simulation of Advection, Dispersion and Chemical Reactions +
+   of Contaminants in Groundwater Systems       +
+               (V. 1.11)               +
+-----+

```

1 M T 3 D field PROBLEM - EK TEST
1 3 D 1 3d field problem

THE TRANSPORT MODEL CONSISTS OF 12 LAYER(S) 5 ROW(S) 14 COLUMN(S)
NUMBER OF STRESS PERIOD(S) IN SIMULATION = 1
UNIT FOR TIME IS sec; UNIT FOR LENGTH IS M; UNIT FOR MASS IS MOL
MAJOR TRANSPORT COMPONENTS TO BE SIMULATED:
1 ADVECTION
2 DISPERSION

BTM1 -- BASIC TRANSPORT PACKAGE, VER 1.0, AUGUST 1990, INPUT READ FROM UNIT 1
10118 ELEMENTS OF THE X ARRAY USED BY THE BTM PACKAGE
852 ELEMENTS OF THE IX ARRAY USED BY THE BTM PACKAGE

ADV1 -- ADVECTION PACKAGE, VER 1.0, AUGUST 1990, INPUT READ FROM UNIT 2
ADVECTION IS SOLVED WITH THE UPSTREAM FINITE DIFFERENCE SCHEME
COORDINATE NUMBER ALLOWED IN SOLVING THE ADVECTION TERM = 0.250
MAXIMUM NUMBER OF MOVING PARTICLES ALLOWED = 5100
0 ELEMENTS OF THE X ARRAY USED BY THE ADV PACKAGE
0 ELEMENTS OF THE IX ARRAY USED BY THE ADV PACKAGE

DSP1 -- DISPERSION PACKAGE, VER 1.0, AUGUST 1990, INPUT READ FROM UNIT 3
8436 ELEMENTS OF THE X ARRAY USED BY THE DSP PACKAGE
0 ELEMENTS OF THE IX ARRAY USED BY THE DSP PACKAGE

18555 ELEMENTS OF THE X ARRAY USED OUT OF 70000
853 ELEMENTS OF THE IX ARRAY USED OUT OF 70000

| LAYER NUMBER | AQUIFER TYPE |
|--------------|--------------|
| 1 | 0 |
| 2 | 0 |
| 3 | 0 |
| 4 | 0 |
| 5 | 0 |
| 6 | 0 |
| 7 | 0 |
| 8 | 0 |
| 9 | 0 |
| 10 | 0 |
| 11 | 0 |
| 12 | 0 |

```

WIDTH ALONG ROWS (DELX) = 0.1524000
WIDTH ALONG COLS (DELY) = 0.1829000
TOP ELEV. OF 1ST LAYER = 0.0000000
CELL THICKNESS (DZ) = 0.3048000 FOR LAYER 1
CELL THICKNESS (DZ) = 0.3048000 FOR LAYER 2
CELL THICKNESS (DZ) = 0.3048000 FOR LAYER 3
CELL THICKNESS (DZ) = 0.3048000 FOR LAYER 4
CELL THICKNESS (DZ) = 0.3048000 FOR LAYER 5
CELL THICKNESS (DZ) = 0.3048000 FOR LAYER 6
CELL THICKNESS (DZ) = 0.3048000 FOR LAYER 7
CELL THICKNESS (DZ) = 0.3048000 FOR LAYER 8
CELL THICKNESS (DZ) = 0.3048000 FOR LAYER 9
CELL THICKNESS (DZ) = 0.3048000 FOR LAYER 10
CELL THICKNESS (DZ) = 0.3048000 FOR LAYER 11
CELL THICKNESS (DZ) = 0.3048000 FOR LAYER 12
EFFECTIVE POROSITY = 0.1260000 FOR LAYER 1
EFFECTIVE POROSITY = 0.1260000 FOR LAYER 2
EFFECTIVE POROSITY = 0.1260000 FOR LAYER 3
EFFECTIVE POROSITY = 0.1260000 FOR LAYER 4
EFFECTIVE POROSITY = 0.1260000 FOR LAYER 5
EFFECTIVE POROSITY = 0.1260000 FOR LAYER 6
EFFECTIVE POROSITY = 0.1260000 FOR LAYER 7
EFFECTIVE POROSITY = 0.1260000 FOR LAYER 8
EFFECTIVE POROSITY = 0.1260000 FOR LAYER 9
EFFECTIVE POROSITY = 0.1260000 FOR LAYER 10
EFFECTIVE POROSITY = 0.1260000 FOR LAYER 11
EFFECTIVE POROSITY = 0.1260000 FOR LAYER 12

```

CONCN. BOUNDARY ARRAY FOR LAYER 1 READ ON UNIT 1 USING BLOCK FORMAT

```

-----
1 2 3 4 5 6 7 8 9 10 11 12 13 14
-----
1 1 1 1 1 1 1 1 1 1 1 1 1 1
2 1 1 1 1 1 1 1 1 1 1 1 1 1
3 1 1 1 1 1 1 1 1 1 1 1 1 1
4 1 1 1 1 1 1 1 1 1 1 1 1 1
5 1 1 1 1 1 1 1 1 1 1 1 1 1

```

CONCN. BOUNDARY ARRAY FOR LAYER 2 READ ON UNIT 1 USING BLOCK FORMAT

```

-----
1 2 3 4 5 6 7 8 9 10 11 12 13 14
-----
1 1 1 1 1 1 1 1 1 1 1 1 1 1
2 1 1 1 1 1 1 1 1 1 1 1 1 1
3 1 1 1 1 1 1 1 1 1 1 1 1 1
4 1 1 1 1 1 1 1 1 1 1 1 1 1
5 1 1 1 1 1 1 1 1 1 1 1 1 1

```

CONCN. BOUNDARY ARRAY FOR LAYER 3 READ ON UNIT 1 USING BLOCK FORMAT

```

-----
1 2 3 4 5 6 7 8 9 10 11 12 13 14
-----
1 1 1 1 1 1 1 1 1 1 1 1 1 1
2 1 1 1 1 1 1 1 1 1 1 1 1 1
3 1 1 1 1 1 1 1 1 1 1 1 1 1
4 1 1 1 1 1 1 1 1 1 1 1 1 1
5 1 1 1 1 1 1 1 1 1 1 1 1 1

```

CONCN. BOUNDARY ARRAY FOR LAYER 4 READ ON UNIT 1 USING BLOCK FORMAT

```

-----
1 2 3 4 5 6 7 8 9 10 11 12 13 14
-----
1 1 1 1 1 1 1 1 1 1 1 1 1 1
2 1 1 1 1 1 1 1 1 1 1 1 1 1
3 1 1 1 1 1 1 1 1 1 1 1 1 1
4 1 1 1 1 1 1 1 1 1 1 1 1 1
5 1 1 1 1 1 1 1 1 1 1 1 1 1

```

CONCN. BOUNDARY ARRAY FOR LAYER 5 READ ON UNIT 1 USING BLOCK FORMAT

```

-----
1 2 3 4 5 6 7 8 9 10 11 12 13 14
-----
1 1 1 1 1 1 1 1 1 1 1 1 1 1
2 1 1 1 1 1 1 1 1 1 1 1 1 1
3 1 1 1 1 1 1 1 1 1 1 1 1 1
4 1 1 1 1 1 1 1 1 1 1 1 1 1
5 1 1 1 1 1 1 1 1 1 1 1 1 1

```

CONCN. BOUNDARY ARRAY FOR LAYER 6 READ ON UNIT 1 USING BLOCK FORMAT

J-21
OUTPUT-H2.ek

| | 1 | 2 | 3 | 4 | 5 | 6 | 7 | 8 | 9 | 10 | 11 | 12 | 13 | 14 |
|---|---|---|---|---|---|---|---|---|---|----|----|----|----|----|
| 1 | 1 | 1 | 1 | 1 | 1 | 1 | 1 | 1 | 1 | 1 | 1 | 1 | 1 | 1 |
| 2 | 1 | 1 | 1 | 1 | 1 | 1 | 1 | 1 | 1 | 1 | 1 | 1 | 1 | 1 |
| 3 | 1 | 1 | 1 | 1 | 1 | 1 | 1 | 1 | 1 | 1 | 1 | 1 | 1 | 1 |
| 4 | 1 | 1 | 1 | 1 | 1 | 1 | 1 | 1 | 1 | 1 | 1 | 1 | 1 | 1 |
| 5 | 1 | 1 | 1 | 1 | 1 | 1 | 1 | 1 | 1 | 1 | 1 | 1 | 1 | 1 |

CONCN. BOUNDARY ARRAY FOR LAYER 7 READ ON UNIT 1 USING BLOCK FORMAT

| | 1 | 2 | 3 | 4 | 5 | 6 | 7 | 8 | 9 | 10 | 11 | 12 | 13 | 14 |
|---|---|---|---|---|---|---|---|---|---|----|----|----|----|----|
| 1 | 1 | 1 | 1 | 1 | 1 | 1 | 1 | 1 | 1 | 1 | 1 | 1 | 1 | 1 |
| 2 | 1 | 1 | 1 | 1 | 1 | 1 | 1 | 1 | 1 | 1 | 1 | 1 | 1 | 1 |
| 3 | 1 | 1 | 1 | 1 | 1 | 1 | 1 | 1 | 1 | 1 | 1 | 1 | 1 | 1 |
| 4 | 1 | 1 | 1 | 1 | 1 | 1 | 1 | 1 | 1 | 1 | 1 | 1 | 1 | 1 |
| 5 | 1 | 1 | 1 | 1 | 1 | 1 | 1 | 1 | 1 | 1 | 1 | 1 | 1 | 1 |

CONCN. BOUNDARY ARRAY FOR LAYER 8 READ ON UNIT 1 USING BLOCK FORMAT

| | 1 | 2 | 3 | 4 | 5 | 6 | 7 | 8 | 9 | 10 | 11 | 12 | 13 | 14 |
|---|---|---|---|---|---|---|---|---|---|----|----|----|----|----|
| 1 | 1 | 1 | 1 | 1 | 1 | 1 | 1 | 1 | 1 | 1 | 1 | 1 | 1 | 1 |
| 2 | 1 | 1 | 1 | 1 | 1 | 1 | 1 | 1 | 1 | 1 | 1 | 1 | 1 | 1 |
| 3 | 1 | 1 | 1 | 1 | 1 | 1 | 1 | 1 | 1 | 1 | 1 | 1 | 1 | 1 |
| 4 | 1 | 1 | 1 | 1 | 1 | 1 | 1 | 1 | 1 | 1 | 1 | 1 | 1 | 1 |
| 5 | 1 | 1 | 1 | 1 | 1 | 1 | 1 | 1 | 1 | 1 | 1 | 1 | 1 | 1 |

CONCN. BOUNDARY ARRAY FOR LAYER 9 READ ON UNIT 1 USING BLOCK FORMAT

| | 1 | 2 | 3 | 4 | 5 | 6 | 7 | 8 | 9 | 10 | 11 | 12 | 13 | 14 |
|---|---|---|---|---|---|---|---|---|---|----|----|----|----|----|
| 1 | 1 | 1 | 1 | 1 | 1 | 1 | 1 | 1 | 1 | 1 | 1 | 1 | 1 | 1 |
| 2 | 1 | 1 | 1 | 1 | 1 | 1 | 1 | 1 | 1 | 1 | 1 | 1 | 1 | 1 |
| 3 | 1 | 1 | 1 | 1 | 1 | 1 | 1 | 1 | 1 | 1 | 1 | 1 | 1 | 1 |
| 4 | 1 | 1 | 1 | 1 | 1 | 1 | 1 | 1 | 1 | 1 | 1 | 1 | 1 | 1 |
| 5 | 1 | 1 | 1 | 1 | 1 | 1 | 1 | 1 | 1 | 1 | 1 | 1 | 1 | 1 |

CONCN. BOUNDARY ARRAY FOR LAYER 10 READ ON UNIT 1 USING BLOCK FORMAT

| | 1 | 2 | 3 | 4 | 5 | 6 | 7 | 8 | 9 | 10 | 11 | 12 | 13 | 14 |
|---|---|---|---|---|---|---|---|---|---|----|----|----|----|----|
| 1 | 1 | 1 | 1 | 1 | 1 | 1 | 1 | 1 | 1 | 1 | 1 | 1 | 1 | 1 |
| 2 | 1 | 1 | 1 | 1 | 1 | 1 | 1 | 1 | 1 | 1 | 1 | 1 | 1 | 1 |
| 3 | 1 | 1 | 1 | 1 | 1 | 1 | 1 | 1 | 1 | 1 | 1 | 1 | 1 | 1 |
| 4 | 1 | 1 | 1 | 1 | 1 | 1 | 1 | 1 | 1 | 1 | 1 | 1 | 1 | 1 |
| 5 | 1 | 1 | 1 | 1 | 1 | 1 | 1 | 1 | 1 | 1 | 1 | 1 | 1 | 1 |

CONCN. BOUNDARY ARRAY FOR LAYER 11 READ ON UNIT 1 USING BLOCK FORMAT

| | 1 | 2 | 3 | 4 | 5 | 6 | 7 | 8 | 9 | 10 | 11 | 12 | 13 | 14 |
|---|---|---|---|---|---|---|---|---|---|----|----|----|----|----|
| 1 | 1 | 1 | 1 | 1 | 1 | 1 | 1 | 1 | 1 | 1 | 1 | 1 | 1 | 1 |
| 2 | 1 | 1 | 1 | 1 | 1 | 1 | 1 | 1 | 1 | 1 | 1 | 1 | 1 | 1 |
| 3 | 1 | 1 | 1 | 1 | 1 | 1 | 1 | 1 | 1 | 1 | 1 | 1 | 1 | 1 |
| 4 | 1 | 1 | 1 | 1 | 1 | 1 | 1 | 1 | 1 | 1 | 1 | 1 | 1 | 1 |
| 5 | 1 | 1 | 1 | 1 | 1 | 1 | 1 | 1 | 1 | 1 | 1 | 1 | 1 | 1 |

CONCN. BOUNDARY ARRAY FOR LAYER 12 READ ON UNIT 1 USING BLOCK FORMAT

| | 1 | 2 | 3 | 4 | 5 | 6 | 7 | 8 | 9 | 10 | 11 | 12 | 13 | 14 |
|---|---|---|---|---|---|---|---|---|---|----|----|----|----|----|
| 1 | 1 | 1 | 1 | 1 | 1 | 1 | 1 | 1 | 1 | 1 | 1 | 1 | 1 | 1 |
| 2 | 1 | 1 | 1 | 1 | 1 | 1 | 1 | 1 | 1 | 1 | 1 | 1 | 1 | 1 |
| 3 | 1 | 1 | 1 | 1 | 1 | 1 | 1 | 1 | 1 | 1 | 1 | 1 | 1 | 1 |
| 4 | 1 | 1 | 1 | 1 | 1 | 1 | 1 | 1 | 1 | 1 | 1 | 1 | 1 | 1 |
| 5 | 1 | 1 | 1 | 1 | 1 | 1 | 1 | 1 | 1 | 1 | 1 | 1 | 1 | 1 |

INITIAL CONCENTRATION FOR LAYER 1 READ ON UNIT 1 USING FORMAT: * (14F8.1) *

| | 1 | 2 | 3 | 4 | 5 | 6 | 7 | 8 | 9 | 10 | 11 | 12 | 13 | 14 |
|---|-------|-------|-------|-------|-------|------|------|------|------|------|------|------|------|------|
| 1 | 23.20 | 19.10 | 14.10 | 9.30 | 5.30 | 2.60 | 1.00 | 0.30 | 0.10 | 0.00 | 0.00 | 0.00 | 0.00 | 0.00 |
| 2 | 36.10 | 30.50 | 23.50 | 16.30 | 9.90 | 5.20 | 2.20 | 0.80 | 0.30 | 0.10 | 0.00 | 0.00 | 0.00 | 0.00 |
| 3 | 46.30 | 39.70 | 31.20 | 22.30 | 14.10 | 7.70 | 3.40 | 1.30 | 0.40 | 0.10 | 0.00 | 0.00 | 0.00 | 0.00 |
| 4 | 36.10 | 30.50 | 23.50 | 16.30 | 9.90 | 5.20 | 2.20 | 0.80 | 0.30 | 0.10 | 0.00 | 0.00 | 0.00 | 0.00 |
| 5 | 23.20 | 19.10 | 14.10 | 9.30 | 5.30 | 2.60 | 1.00 | 0.30 | 0.10 | 0.00 | 0.00 | 0.00 | 0.00 | 0.00 |

INITIAL CONCENTRATION FOR LAYER 2 READ ON UNIT 1 USING FORMAT: * (14F8.1) *

| | 1 | 2 | 3 | 4 | 5 | 6 | 7 | 8 | 9 | 10 | 11 | 12 | 13 | 14 |
|---|--------|--------|--------|-------|-------|-------|-------|-------|------|------|------|------|------|------|
| 1 | 97.80 | 87.30 | 72.60 | 55.50 | 38.10 | 22.80 | 11.40 | 4.80 | 1.80 | 0.60 | 0.20 | 0.00 | 0.00 | 0.00 |
| 2 | 127.30 | 116.80 | 101.50 | 82.10 | 60.40 | 39.10 | 21.30 | 9.80 | 4.00 | 1.40 | 0.40 | 0.10 | 0.00 | 0.00 |
| 3 | 144.90 | 134.70 | 119.60 | 99.80 | 76.50 | 52.00 | 30.00 | 14.60 | 6.30 | 2.30 | 0.70 | 0.20 | 0.00 | 0.00 |
| 4 | 127.30 | 116.80 | 101.50 | 82.10 | 60.40 | 39.10 | 21.30 | 9.80 | 4.00 | 1.40 | 0.40 | 0.10 | 0.00 | 0.00 |
| 5 | 97.80 | 87.30 | 72.60 | 55.50 | 38.10 | 22.80 | 11.40 | 4.80 | 1.80 | 0.60 | 0.20 | 0.00 | 0.00 | 0.00 |

INITIAL CONCENTRATION FOR LAYER 3 READ ON UNIT 1 USING FORMAT: * (14F8.1) *

| | 1 | 2 | 3 | 4 | 5 | 6 | 7 | 8 | 9 | 10 | 11 | 12 | 13 | 14 |
|---|--------|--------|--------|--------|--------|--------|--------|-------|-------|-------|------|------|------|------|
| 1 | 173.70 | 166.30 | 154.00 | 135.80 | 111.60 | 83.30 | 54.50 | 30.80 | 15.40 | 6.70 | 2.50 | 0.80 | 0.20 | 0.00 |
| 2 | 190.60 | 186.50 | 178.90 | 166.10 | 146.10 | 118.40 | 85.10 | 53.10 | 29.00 | 13.80 | 5.60 | 1.90 | 0.50 | 0.10 |
| 3 | 196.30 | 193.80 | 188.80 | 179.40 | 163.30 | 138.60 | 105.50 | 70.10 | 40.70 | 20.60 | 8.90 | 3.20 | 0.90 | 0.10 |
| 4 | 190.60 | 186.50 | 178.90 | 166.10 | 146.10 | 118.40 | 85.10 | 53.10 | 29.00 | 13.80 | 5.60 | 1.90 | 0.50 | 0.10 |
| 5 | 173.70 | 166.30 | 154.00 | 135.80 | 111.60 | 83.30 | 54.50 | 30.80 | 15.40 | 6.70 | 2.50 | 0.80 | 0.20 | 0.00 |

INITIAL CONCENTRATION FOR LAYER 4 READ ON UNIT 1 USING FORMAT: * (14F8.1) *

| | 1 | 2 | 3 | 4 | 5 | 6 | 7 | 8 | 9 | 10 | 11 | 12 | 13 | 14 |
|---|--------|--------|--------|--------|--------|--------|--------|--------|--------|-------|-------|-------|-------|------|
| 1 | 198.10 | 196.70 | 193.60 | 187.10 | 175.00 | 155.20 | 127.40 | 94.20 | 62.30 | 36.60 | 19.00 | 8.50 | 3.10 | 0.70 |
| 2 | 199.90 | 199.80 | 199.30 | 197.70 | 193.20 | 182.60 | 162.80 | 132.20 | 95.80 | 61.50 | 34.80 | 17.00 | 6.80 | 1.90 |
| 3 | 200.00 | 200.00 | 199.90 | 199.80 | 197.50 | 191.50 | 177.80 | 152.10 | 116.60 | 79.50 | 47.80 | 25.00 | 11.00 | 3.60 |
| 4 | 199.90 | 199.80 | 199.30 | 197.70 | 193.20 | 182.60 | 162.80 | 132.20 | 95.80 | 61.50 | 34.80 | 17.00 | 6.80 | 1.90 |
| 5 | 198.10 | 196.70 | 193.60 | 187.10 | 175.00 | 155.20 | 127.40 | 94.20 | 62.30 | 36.60 | 19.00 | 8.50 | 3.10 | 0.70 |

INITIAL CONCENTRATION FOR LAYER 5 READ ON UNIT 1 USING FORMAT: * (14F8.1) *

| | 1 | 2 | 3 | 4 | 5 | 6 | 7 | 8 | 9 | 10 | 11 | 12 | 13 | 14 |
|---|--------|--------|--------|--------|--------|--------|--------|--------|--------|--------|--------|--------|-------|-------|
| 1 | 199.90 | 199.70 | 199.30 | 197.90 | 194.50 | 187.00 | 173.40 | 151.70 | 122.70 | 91.00 | 61.50 | 37.60 | 20.00 | 8.00 |
| 2 | 200.00 | 200.00 | 200.00 | 199.90 | 199.50 | 197.70 | 192.50 | 180.10 | 157.30 | 126.00 | 91.70 | 60.00 | 34.40 | 13.90 |
| 3 | 200.00 | 200.00 | 200.00 | 199.90 | 199.70 | 198.60 | 196.00 | 189.40 | 176.90 | 157.30 | 131.60 | 102.40 | 72.50 | 42.80 |
| 4 | 200.00 | 200.00 | 200.00 | 199.90 | 199.70 | 198.60 | 196.00 | 189.40 | 176.90 | 157.30 | 131.60 | 102.40 | 72.50 | 42.80 |
| 5 | 199.90 | 199.70 | 199.30 | 197.90 | 194.50 | 187.00 | 173.40 | 151.70 | 122.70 | 91.00 | 61.50 | 37.60 | 20.00 | 8.00 |

INITIAL CONCENTRATION FOR LAYER 6 READ ON UNIT 1 USING FORMAT: * (14F8.1) *

| | 1 | 2 | 3 | 4 | 5 | 6 | 7 | 8 | 9 | 10 | 11 | 12 | 13 | 14 |
|---|--------|--------|--------|--------|--------|--------|--------|--------|--------|--------|--------|--------|-------|-------|
| 1 | 199.90 | 199.70 | 199.30 | 197.90 | 194.50 | 187.00 | 173.40 | 151.70 | 122.70 | 91.00 | 61.50 | 37.60 | 20.00 | 8.00 |
| 2 | 200.00 | 200.00 | 200.00 | 199.90 | 199.50 | 197.70 | 192.50 | 180.10 | 157.30 | 126.00 | 91.70 | 60.00 | 34.40 | 13.90 |
| 3 | 200.00 | 200.00 | 200.00 | 199.90 | 199.70 | 198.60 | 196.00 | 189.40 | 176.90 | 157.30 | 131.60 | 102.40 | 72.50 | 42.80 |
| 4 | 200.00 | 200.00 | 200.00 | 199.90 | 199.70 | 198.60 | 196.00 | 189.40 | 176.90 | 157.30 | 131.60 | 102.40 | 72.50 | 42.80 |
| 5 | 199.90 | 199.70 | 199.30 | 197.90 | 194.50 | 187.00 | 173.40 | 151.70 | 122.70 | 91.00 | 61.50 | 37.60 | 20.00 | 8.00 |

INITIAL CONCENTRATION FOR LAYER 7 READ ON UNIT 1 USING FORMAT: * (14F8.1) *

| | 1 | 2 | 3 | 4 | 5 | 6 | 7 | 8 | 9 | 10 | 11 | 12 | 13 | 14 |
|---|--------|--------|--------|--------|--------|--------|--------|--------|--------|--------|--------|--------|-------|-------|
| 1 | 199.90 | 199.70 | 199.30 | 197.90 | 194.50 | 187.00 | 173.40 | 151.70 | 122.70 | 91.00 | 61.50 | 37.60 | 20.00 | 8.00 |
| 2 | 200.00 | 200.00 | 200.00 | 199.90 | 199.50 | 197.70 | 192.50 | 180.10 | 157.30 | 126.00 | 91.70 | 60.00 | 34.40 | 13.90 |
| 3 | 200.00 | 200.00 | 200.00 | 199.90 | 199.70 | 198.60 | 196.00 | 189.40 | 176.90 | 157.30 | 131.60 | 102.40 | 72.50 | 42.80 |
| 4 | 200.00 | 200.00 | 200.00 | 199.90 | 199.70 | 198.60 | 196.00 | 189.40 | 176.90 | 157.30 | 131.60 | 102.40 | 72.50 | 42.80 |
| 5 | 199.90 | 199.70 | 199.30 | 197.90 | 194.50 | 187.00 | 173.40 | 151.70 | 122.70 | 91.00 | 61.50 | 37.60 | 20.00 | 8.00 |

J-22
OUTPUT-H2.ek

| | 1 | 2 | 3 | 4 | 5 | 6 | 7 | 8 | 9 | 10 | 11 | 12 | 13 | 14 |
|---|--------|--------|--------|--------|--------|--------|--------|--------|--------|--------|--------|--------|--------|-------|
| 1 | 199.80 | 199.60 | 199.20 | 198.10 | 195.80 | 191.10 | 182.90 | 170.20 | 152.80 | 131.80 | 108.50 | 84.50 | 60.20 | 34.30 |
| 2 | 200.00 | 200.00 | 200.00 | 199.90 | 199.70 | 199.00 | 196.70 | 191.60 | 182.10 | 167.10 | 146.60 | 121.20 | 91.80 | 58.20 |
| 3 | 200.00 | 200.00 | 200.00 | 200.00 | 200.00 | 199.80 | 199.00 | 196.60 | 191.30 | 181.50 | 166.30 | 144.80 | 116.20 | 0.00 |
| 4 | 200.00 | 200.00 | 200.00 | 199.90 | 199.70 | 199.00 | 196.70 | 191.60 | 182.10 | 167.10 | 146.60 | 121.20 | 91.80 | 58.20 |
| 5 | 199.80 | 199.60 | 199.20 | 198.10 | 195.80 | 191.10 | 182.90 | 170.20 | 152.80 | 131.80 | 108.50 | 84.50 | 60.20 | 34.30 |

INITIAL CONCENTRATION FOR LAYER 8 READ ON UNIT 1 USING FORMAT: * (14F8.1)

| | 1 | 2 | 3 | 4 | 5 | 6 | 7 | 8 | 9 | 10 | 11 | 12 | 13 | 14 |
|---|--------|--------|--------|--------|--------|--------|--------|--------|--------|--------|--------|--------|--------|-------|
| 1 | 199.80 | 199.60 | 199.10 | 198.00 | 195.70 | 191.10 | 182.90 | 170.40 | 153.40 | 132.70 | 109.90 | 86.10 | 61.90 | 35.60 |
| 2 | 200.00 | 200.00 | 200.00 | 199.90 | 199.70 | 199.00 | 196.80 | 191.80 | 182.60 | 168.20 | 148.30 | 123.30 | 94.00 | 60.00 |
| 3 | 200.00 | 200.00 | 200.00 | 200.00 | 200.00 | 199.70 | 198.80 | 195.90 | 189.30 | 177.60 | 159.40 | 134.70 | 104.50 | 0.00 |
| 4 | 200.00 | 200.00 | 200.00 | 199.90 | 199.70 | 199.00 | 196.80 | 191.80 | 182.60 | 168.20 | 148.30 | 123.30 | 94.00 | 60.00 |
| 5 | 199.80 | 199.60 | 199.10 | 198.00 | 195.70 | 191.10 | 182.90 | 170.40 | 153.40 | 132.70 | 109.90 | 86.10 | 61.90 | 35.60 |

INITIAL CONCENTRATION FOR LAYER 9 READ ON UNIT 1 USING FORMAT: * (14F8.1)

| | 1 | 2 | 3 | 4 | 5 | 6 | 7 | 8 | 9 | 10 | 11 | 12 | 13 | 14 |
|---|--------|--------|--------|--------|--------|--------|--------|--------|--------|--------|--------|--------|--------|-------|
| 1 | 199.80 | 199.70 | 199.20 | 198.20 | 195.80 | 190.80 | 182.00 | 168.30 | 149.40 | 126.40 | 101.30 | 76.80 | 51.50 | 27.50 |
| 2 | 200.00 | 200.00 | 200.00 | 199.90 | 199.70 | 198.00 | 196.30 | 190.50 | 179.50 | 162.30 | 139.00 | 111.10 | 80.70 | 48.80 |
| 3 | 200.00 | 200.00 | 200.00 | 200.00 | 200.00 | 199.70 | 198.80 | 195.90 | 189.30 | 177.60 | 159.40 | 134.70 | 104.50 | 0.00 |
| 4 | 200.00 | 200.00 | 200.00 | 199.90 | 199.70 | 199.00 | 196.80 | 191.80 | 182.60 | 168.20 | 148.30 | 123.30 | 94.00 | 60.00 |
| 5 | 199.80 | 199.70 | 199.20 | 198.20 | 195.80 | 190.80 | 182.00 | 168.30 | 149.40 | 126.40 | 101.30 | 76.80 | 51.50 | 27.50 |

INITIAL CONCENTRATION FOR LAYER 10 READ ON UNIT 1 USING FORMAT: * (14F8.1)

| | 1 | 2 | 3 | 4 | 5 | 6 | 7 | 8 | 9 | 10 | 11 | 12 | 13 | 14 |
|---|--------|--------|--------|--------|--------|--------|--------|--------|--------|--------|--------|-------|-------|-------|
| 1 | 199.80 | 199.70 | 199.10 | 197.80 | 194.40 | 187.60 | 175.80 | 157.30 | 132.40 | 103.70 | 74.90 | 49.10 | 28.10 | 12.00 |
| 2 | 200.00 | 200.00 | 200.00 | 199.90 | 199.50 | 198.00 | 193.90 | 184.30 | 166.70 | 140.90 | 109.50 | 76.80 | 47.10 | 22.90 |
| 3 | 200.00 | 200.00 | 200.00 | 200.00 | 199.90 | 199.40 | 197.60 | 192.20 | 180.00 | 159.20 | 130.40 | 97.00 | 63.50 | 0.00 |
| 4 | 200.00 | 200.00 | 200.00 | 199.90 | 199.50 | 198.00 | 193.90 | 184.30 | 166.70 | 140.90 | 109.50 | 76.80 | 47.10 | 22.90 |
| 5 | 199.80 | 199.70 | 199.10 | 197.80 | 194.40 | 187.60 | 175.80 | 157.30 | 132.40 | 103.70 | 74.90 | 49.10 | 28.10 | 12.00 |

INITIAL CONCENTRATION FOR LAYER 11 READ ON UNIT 1 USING FORMAT: * (14F8.1)

| | 1 | 2 | 3 | 4 | 5 | 6 | 7 | 8 | 9 | 10 | 11 | 12 | 13 | 14 |
|---|--------|--------|--------|--------|--------|--------|--------|--------|--------|--------|-------|-------|-------|------|
| 1 | 196.20 | 194.00 | 189.90 | 182.50 | 170.60 | 153.00 | 129.70 | 102.50 | 74.80 | 50.00 | 30.10 | 15.80 | 6.70 | 1.80 |
| 2 | 199.80 | 199.50 | 198.80 | 196.80 | 192.10 | 182.90 | 167.10 | 143.50 | 114.20 | 83.10 | 54.40 | 31.00 | 14.50 | 4.60 |
| 3 | 200.00 | 200.00 | 199.80 | 199.20 | 197.40 | 192.50 | 182.30 | 164.10 | 137.70 | 106.10 | 73.80 | 45.10 | 23.00 | 8.50 |
| 4 | 199.80 | 199.50 | 198.80 | 196.80 | 192.10 | 182.90 | 167.10 | 143.50 | 114.20 | 83.10 | 54.40 | 31.00 | 14.50 | 4.60 |
| 5 | 196.20 | 194.00 | 189.90 | 182.50 | 170.60 | 153.00 | 129.70 | 102.50 | 74.80 | 50.00 | 30.10 | 15.80 | 6.70 | 1.80 |

INITIAL CONCENTRATION FOR LAYER 12 READ ON UNIT 1 USING FORMAT: * (14F8.1)

| | 1 | 2 | 3 | 4 | 5 | 6 | 7 | 8 | 9 | 10 | 11 | 12 | 13 | 14 |
|---|--------|--------|--------|--------|--------|--------|--------|-------|-------|-------|-------|-------|------|------|
| 1 | 143.90 | 135.20 | 122.90 | 107.30 | 89.30 | 69.90 | 50.70 | 34.10 | 21.40 | 12.30 | 6.30 | 2.80 | 0.90 | 0.20 |
| 2 | 174.30 | 167.70 | 157.90 | 144.50 | 127.30 | 106.70 | 83.60 | 61.00 | 41.40 | 25.80 | 14.30 | 6.80 | 2.50 | 0.50 |
| 3 | 188.50 | 183.60 | 176.00 | 165.20 | 150.30 | 131.10 | 107.80 | 82.80 | 59.40 | 39.10 | 23.00 | 11.60 | 4.60 | 1.10 |
| 4 | 174.30 | 167.70 | 157.90 | 144.50 | 127.30 | 106.70 | 83.60 | 61.00 | 41.40 | 25.80 | 14.30 | 6.80 | 2.50 | 0.50 |
| 5 | 143.90 | 135.20 | 122.90 | 107.30 | 89.30 | 69.90 | 50.70 | 34.10 | 21.40 | 12.30 | 6.30 | 2.80 | 0.90 | 0.20 |

VALUE INDICATING INACTIVE CONCENTRATION CELLS = -999.0000

OUTPUT CONTROL OPTIONS

PRINT CELL CONCENTRATION USING FORMAT CODE: 3
 PRINT PARTICLE NUMBER IN EACH CELL USING FORMAT CODE: 3
 PRINT RETARDATION FACTOR USING FORMAT CODE: 3
 PRINT DISPERSION COEFFICIENT USING FORMAT CODE: 3
 SAVE CONCENTRATION IN UNFORMATTED FILE (MTSD.UCN) ON UNIT 18

NUMBER OF TIMES AT WHICH SIMULATION RESULTS ARE SAVED = 1
 TOTAL ELAPSED TIMES AT WHICH SIMULATION RESULTS ARE SAVED:
 0.30132E+07

NUMBER OF OBSERVATION POINTS = 2
 CONCENTRATION AT OBSERVATION POINTS SAVED IN FILE (MTSD.OBS) ON UNIT 17

LOCATION OF OBSERVATION POINTS
 NUMBER LAYER ROW COLUMN
 1 6 3 3
 2 6 1 3

A ONE-LINE SUMMARY OF MASS BALANCE FOR EACH STEP SAVED IN FILE (MTSD.MAS) ON UNIT 19

MAXIMUM LENGTH ALONG THE X (J) AXIS = 2.133600
 MINIMUM LENGTH ALONG THE Y (I) AXIS = 0.9145000
 MAXIMUM LENGTH ALONG THE Z (K) AXIS = 3.657600

ADVECTION SOLUTION OPTIONS

DISPERSION PARAMETERS

LONG. DISPERSIVITY (AL) = 0.000000 FOR LAYER 1
 LONG. DISPERSIVITY (AL) = 0.000000 FOR LAYER 2
 LONG. DISPERSIVITY (AL) = 0.000000 FOR LAYER 3
 LONG. DISPERSIVITY (AL) = 0.000000 FOR LAYER 4
 LONG. DISPERSIVITY (AL) = 0.000000 FOR LAYER 5
 LONG. DISPERSIVITY (AL) = 0.000000 FOR LAYER 6
 LONG. DISPERSIVITY (AL) = 0.000000 FOR LAYER 7
 LONG. DISPERSIVITY (AL) = 0.000000 FOR LAYER 8
 LONG. DISPERSIVITY (AL) = 0.000000 FOR LAYER 9
 LONG. DISPERSIVITY (AL) = 0.000000 FOR LAYER 10
 LONG. DISPERSIVITY (AL) = 0.000000 FOR LAYER 11
 LONG. DISPERSIVITY (AL) = 0.000000 FOR LAYER 12
 H. TRANS./LONG. DISP. = 0.000000
 V. TRANS./LONG. DISP. = 0.000000
 DIFFUSION COEFFICIENT = 0.3650000E-09

 STRESS PERIOD NO. 001

LENGTH OF CURRENT STRESS PERIOD = 3013200.
 NUMBER OF TIME STEPS FOR CURRENT STRESS PERIOD = 1
 TIME STEP MULTIPLIER = 1.000000
 USER-SPECIFIED TRANSPORT STEPSIZE = 600.0000 sec
 MAXIMUM NUMBER OF TRANSPORT STEPS ALLOWED IN ONE TIME STEP = 50000

 TIME STEP NO. 001

FROM TIME = 0.00000 TO 0.30132E+07

*HEAD * FLOW TERMS FOR TIME STEP 1, STRESS PERIOD 1 READ UNFORMATTED ON UNIT 10

J-24
OUTPUT-H2.ek

40.8 45.6 48.8

LAYER 10

| | 1 | 2 | 3 | 4 | 5 | 6 | 7 | 8 | 9 | 10 | 11 |
|---|------|------|------|------|------|------|-------|------|------|------|------|
| | 12 | 13 | 14 | | | | | | | | |
| 1 | 16.1 | 16.0 | 15.9 | 15.7 | 15.6 | 15.9 | 17.2 | 20.5 | 24.8 | 29.5 | 34.2 |
| | 38.9 | 42.1 | 46.0 | | | | | | | | |
| 2 | 16.0 | 15.9 | 15.7 | 15.4 | 14.8 | 13.9 | 13.4 | 18.5 | 24.0 | 29.3 | 34.6 |
| | 40.0 | 45.8 | 51.5 | | | | | | | | |
| 3 | 16.0 | 15.9 | 15.6 | 15.0 | 13.7 | 10.2 | 0.000 | 14.8 | 22.9 | 29.1 | 34.9 |
| | 41.4 | 50.4 | 68.0 | | | | | | | | |
| 4 | 16.0 | 15.9 | 15.7 | 15.4 | 14.8 | 13.9 | 13.4 | 18.5 | 24.0 | 29.3 | 34.6 |
| | 40.0 | 45.8 | 51.5 | | | | | | | | |
| 5 | 16.1 | 16.0 | 15.9 | 15.7 | 15.6 | 15.9 | 17.2 | 20.5 | 24.8 | 29.5 | 34.2 |
| | 38.9 | 43.1 | 46.0 | | | | | | | | |

LAYER 11

| | 1 | 2 | 3 | 4 | 5 | 6 | 7 | 8 | 9 | 10 | 11 |
|---|------|------|------|------|------|------|------|------|------|------|------|
| | 12 | 13 | 14 | | | | | | | | |
| 1 | 16.8 | 16.9 | 17.0 | 17.3 | 17.8 | 18.7 | 20.3 | 22.8 | 25.8 | 29.2 | 32.6 |
| | 35.7 | 38.3 | 39.8 | | | | | | | | |
| 2 | 16.8 | 16.9 | 17.0 | 17.2 | 17.6 | 18.2 | 19.6 | 22.3 | 25.6 | 29.1 | 32.7 |
| | 36.0 | 39.0 | 40.9 | | | | | | | | |
| 3 | 16.8 | 16.8 | 16.9 | 17.1 | 17.3 | 17.7 | 18.5 | 21.7 | 25.4 | 29.1 | 32.8 |
| | 36.4 | 39.7 | 42.5 | | | | | | | | |
| 4 | 16.8 | 16.9 | 17.0 | 17.2 | 17.6 | 18.2 | 19.6 | 22.3 | 25.6 | 29.1 | 32.7 |
| | 36.0 | 39.0 | 40.9 | | | | | | | | |
| 5 | 16.8 | 16.9 | 17.0 | 17.3 | 17.8 | 18.7 | 20.3 | 22.8 | 25.8 | 29.2 | 32.6 |
| | 35.7 | 38.3 | 39.8 | | | | | | | | |

LAYER 12

| | 1 | 2 | 3 | 4 | 5 | 6 | 7 | 8 | 9 | 10 | 11 |
|---|------|------|------|------|------|------|------|------|------|------|------|
| | 12 | 13 | 14 | | | | | | | | |
| 1 | 17.4 | 17.5 | 17.8 | 18.3 | 19.1 | 20.2 | 21.9 | 23.9 | 26.4 | 29.0 | 31.5 |
| | 33.8 | 35.6 | 36.5 | | | | | | | | |
| 2 | 17.4 | 17.5 | 17.8 | 18.3 | 19.0 | 20.1 | 21.7 | 23.8 | 26.3 | 29.0 | 31.6 |
| | 33.9 | 35.7 | 36.8 | | | | | | | | |
| 3 | 17.4 | 17.5 | 17.8 | 18.2 | 19.0 | 20.1 | 21.6 | 23.7 | 26.3 | 29.0 | 31.6 |
| | 34.0 | 35.9 | 37.0 | | | | | | | | |
| 4 | 17.4 | 17.5 | 17.8 | 18.3 | 19.0 | 20.1 | 21.7 | 23.8 | 26.3 | 29.0 | 31.6 |
| | 33.9 | 35.7 | 36.8 | | | | | | | | |
| 5 | 17.4 | 17.5 | 17.8 | 18.3 | 19.1 | 20.2 | 21.9 | 23.9 | 26.4 | 29.0 | 31.5 |
| | 33.8 | 35.6 | 36.5 | | | | | | | | |

*GXX * FLOW TERMS FOR TIME STEP 1, STRESS PERIOD 1 READ UNFORMATTED ON UNIT 10

LAYER 1

| | 1 | 2 | 3 | 4 | 5 | 6 | 7 | 8 | 9 | 10 | 11 |
|---|-----------|-----------|-----------|-----------|-----------|-----------|-----------|-----------|-----------|-----------|-----------|
| | 12 | 13 | 14 | | | | | | | | |
| 1 | 6.549E-11 | 1.304E-10 | 1.937E-10 | 2.539E-10 | 3.086E-10 | 3.543E-10 | 3.868E-10 | 4.014E-10 | 3.940E-10 | 3.614E-10 | 3.024E-10 |
| | 2.187E-10 | 1.150E-10 | 0.000 | | | | | | | | |
| 2 | 6.548E-11 | 1.303E-10 | 1.937E-10 | 2.539E-10 | 3.086E-10 | 3.543E-10 | 3.869E-10 | 4.016E-10 | 3.943E-10 | 3.618E-10 | 3.030E-10 |
| | 2.193E-10 | 1.154E-10 | 0.000 | | | | | | | | |
| 3 | 6.547E-11 | 1.302E-10 | 1.936E-10 | 2.538E-10 | 3.086E-10 | 3.544E-10 | 3.870E-10 | 4.018E-10 | 3.945E-10 | 3.622E-10 | 3.034E-10 |
| | 2.197E-10 | 1.158E-10 | 0.000 | | | | | | | | |
| 4 | 6.548E-11 | 1.303E-10 | 1.937E-10 | 2.539E-10 | 3.086E-10 | 3.543E-10 | 3.869E-10 | 4.016E-10 | 3.943E-10 | 3.618E-10 | 3.030E-10 |
| | 2.193E-10 | 1.154E-10 | 0.000 | | | | | | | | |
| 5 | 6.549E-11 | 1.304E-10 | 1.937E-10 | 2.539E-10 | 3.086E-10 | 3.543E-10 | 3.868E-10 | 4.014E-10 | 3.940E-10 | 3.614E-10 | 3.024E-10 |
| | 2.187E-10 | 1.150E-10 | 0.000 | | | | | | | | |

LAYER 2

| | 1 | 2 | 3 | 4 | 5 | 6 | 7 | 8 | 9 | 10 | 11 |
|---|-----------|-----------|-----------|-----------|-----------|-----------|-----------|-----------|-----------|-----------|-----------|
| | 12 | 13 | 14 | | | | | | | | |
| 1 | 6.792E-11 | 1.367E-10 | 2.062E-10 | 2.762E-10 | 3.445E-10 | 4.072E-10 | 4.579E-10 | 4.892E-10 | 4.937E-10 | 4.654E-10 | 4.001E-10 |
| | 2.966E-10 | 1.590E-10 | 0.000 | | | | | | | | |
| 2 | 6.792E-11 | 1.365E-10 | 2.060E-10 | 2.759E-10 | 3.443E-10 | 4.072E-10 | 4.584E-10 | 4.902E-10 | 4.952E-10 | 4.677E-10 | 4.033E-10 |
| | 3.004E-10 | 1.620E-10 | 0.000 | | | | | | | | |
| 3 | 6.787E-11 | 1.364E-10 | 2.059E-10 | 2.757E-10 | 3.441E-10 | 4.071E-10 | 4.587E-10 | 4.908E-10 | 4.962E-10 | 4.692E-10 | 4.056E-10 |
| | 3.034E-10 | 1.647E-10 | 0.000 | | | | | | | | |
| 4 | 6.791E-11 | 1.365E-10 | 2.060E-10 | 2.759E-10 | 3.443E-10 | 4.072E-10 | 4.584E-10 | 4.902E-10 | 4.952E-10 | 4.677E-10 | 4.033E-10 |
| | 3.004E-10 | 1.620E-10 | 0.000 | | | | | | | | |
| 5 | 6.792E-11 | 1.366E-10 | 2.062E-10 | 2.762E-10 | 3.445E-10 | 4.072E-10 | 4.579E-10 | 4.892E-10 | 4.937E-10 | 4.654E-10 | 4.001E-10 |
| | 2.966E-10 | 1.590E-10 | 0.000 | | | | | | | | |

LAYER 3

| | 1 | 2 | 3 | 4 | 5 | 6 | 7 | 8 | 9 | 10 | 11 |
|---|-----------|-----------|-----------|-----------|-----------|-----------|-----------|-----------|-----------|-----------|-----------|
| | 12 | 13 | 14 | | | | | | | | |
| 1 | 6.792E-11 | 1.366E-10 | 2.062E-10 | 3.060E-10 | 4.038E-10 | 5.074E-10 | 6.057E-10 | 6.816E-10 | 7.207E-10 | 7.112E-10 | 6.417E-10 |
| | 5.003E-10 | 2.806E-10 | 0.000 | | | | | | | | |
| 2 | 6.761E-11 | 1.387E-10 | 2.166E-10 | 3.040E-10 | 4.017E-10 | 5.066E-10 | 6.081E-10 | 6.865E-10 | 7.280E-10 | 7.227E-10 | 6.599E-10 |
| | 5.255E-10 | 3.041E-10 | 0.000 | | | | | | | | |
| 3 | 6.736E-11 | 1.391E-10 | 2.156E-10 | 3.024E-10 | 3.998E-10 | 5.057E-10 | 6.102E-10 | 6.902E-10 | 7.333E-10 | 7.313E-10 | 6.750E-10 |
| | 5.500E-10 | 3.329E-10 | 0.000 | | | | | | | | |
| 4 | 6.761E-11 | 1.387E-10 | 2.166E-10 | 3.040E-10 | 4.017E-10 | 5.066E-10 | 6.081E-10 | 6.865E-10 | 7.280E-10 | 7.227E-10 | 6.599E-10 |
| | 5.255E-10 | 3.041E-10 | 0.000 | | | | | | | | |
| 5 | 6.792E-11 | 1.366E-10 | 2.062E-10 | 3.060E-10 | 4.038E-10 | 5.074E-10 | 6.057E-10 | 6.817E-10 | 7.207E-10 | 7.112E-10 | 6.417E-10 |
| | 5.003E-10 | 2.806E-10 | 0.000 | | | | | | | | |

LAYER 4

| | 1 | 2 | 3 | 4 | 5 | 6 | 7 | 8 | 9 | 10 | 11 |
|---|-----------|-----------|-----------|-----------|-----------|-----------|-----------|-----------|-----------|-----------|-----------|
| | 12 | 13 | 14 | | | | | | | | |
| 1 | 5.466E-11 | 1.171E-10 | 1.961E-10 | 3.023E-10 | 4.462E-10 | 6.308E-10 | 8.361E-10 | 1.008E-09 | 1.121E-09 | 1.165E-09 | 1.121E-09 |
| | 9.489E-10 | 5.805E-10 | 0.000 | | | | | | | | |
| 2 | 5.301E-11 | 1.130E-10 | 1.882E-10 | 2.892E-10 | 4.294E-10 | 6.206E-10 | 8.512E-10 | 1.034E-09 | 1.154E-09 | 1.216E-09 | 1.212E-09 |
| | 1.100E-09 | 7.632E-10 | 0.000 | | | | | | | | |
| 3 | 5.187E-11 | 1.101E-10 | 1.820E-10 | 2.777E-10 | 4.115E-10 | 6.044E-10 | 8.706E-10 | 1.058E-09 | 1.180E-09 | 1.258E-09 | 1.303E-09 |
| | 1.301E-09 | 1.124E-09 | 0.000 | | | | | | | | |
| 4 | 5.300E-11 | 1.130E-10 | 1.882E-10 | 2.892E-10 | 4.294E-10 | 6.206E-10 | 8.512E-10 | 1.034E-09 | 1.154E-09 | 1.216E-09 | 1.212E-09 |
| | 1.100E-09 | 7.632E-10 | 0.000 | | | | | | | | |
| 5 | 5.466E-11 | 1.171E-10 | 1.961E-10 | 3.023E-10 | 4.462E-10 | 6.308E-10 | 8.361E-10 | 1.008E-09 | 1.121E-09 | 1.165E-09 | 1.121E-09 |
| | 9.489E-10 | 5.805E-10 | 0.000 | | | | | | | | |

LAYER 5

| | 1 | 2 | 3 | 4 | 5 | 6 | 7 | 8 | 9 | 10 | 11 |
|---|-----------|-----------|-----------|-----------|-----------|-----------|-----------|-----------|-----------|-----------|-----------|
| | 12 | 13 | 14 | | | | | | | | |
| 1 | 1.502E-11 | 3.936E-11 | 8.728E-11 | 1.841E-10 | 3.718E-10 | 7.000E-10 | 1.157E-09 | 1.499E-09 | 1.710E-09 | 1.830E-09 | 1.864E-09 |
| | 1.738E-09 | 1.420E-09 | 0.000 | | | | | | | | |
| 2 | 9.045E-12 | 2.327E-11 | 5.141E-11 | 1.131E-10 | 2.567E-10 | 5.934E-10 | 1.274E-09 | 1.634E-09 | 1.832E-09 | 1.995E-09 | 2.194E-09 |
| | 2.443E-09 | 2.435E-09 | 0.000 | | | | | | | | |
| 3 | 4.703E-12 | 1.069E-11 | 1.960E-11 | 3.630E-11 | 8.687E-11 | 1.199E-10 | 1.555E-09 | 1.820E-09 | 1.951E-09 | 2.155E-09 | 2.620E-09 |
| | 3.875E-09 | 7.702E-09 | 0.000 | | | | | | | | |
| 4 | 9.041E-12 | 2.326E-11 | 5.141E-11 | 1.131E-10 | 2.567E-10 | 5.934E-10 | 1.274E-09 | 1.634E-09 | 1.832E-09 | 1.994E-09 | 2.194E-09 |
| | 2.443E-09 | 2.435E-09 | 0.000 | | | | | | | | |
| 5 | 1.501E-11 | 3.937E-11 | 8.728E-11 | 1.841E-10 | 3.718E-10 | 7.000E-10 | 1.157E-09 | 1.499E-09 | 1.710E-09 | 1.830E-09 | 1.865E-09 |
| | 1.738E-09 | 1.230E-09 | 0.000 | | | | | | | | |

LAYER 6

| | 1 | 2 | 3 | 4 | 5 | 6 | 7 | 8 | 9 | 10 | 11 |
|--|----|----|----|---|---|---|---|---|---|----|----|
| | 12 | 13 | 14 | | | | | | | | |

J-25
OUTPUT-H2.ek

3 -7.176E-11 -1.703E-10 -3.507E-10 -7.673E-10 -1.912E-09 -5.492E-09 7.678E-09 4.141E-09 3.099E-09 2.890E-09 3.151E-09
 4.110E-09 6.919E-09 0.000
 4 -6.021E-11 -1.320E-10 -2.309E-10 -3.745E-10 -5.363E-10 -3.465E-10 2.524E-09 2.748E-09 2.660E-09 2.636E-09 2.707E-09
 2.801E-09 2.531E-09 0.000
 5 -4.534E-11 -8.795E-11 -1.175E-10 -1.004E-10 5.464E-11 5.495E-10 1.616E-09 2.134E-09 2.328E-09 2.382E-09 2.336E-09
 2.096E-09 1.420E-09 0.000

LAYER 7

| | 1 | 2 | 3 | 4 | 5 | 6 | 7 | 8 | 9 | 10 | 11 |
|----|------------|------------|------------|------------|------------|------------|-----------|-----------|-----------|-----------|-----------|
| | 12 | 13 | 14 | | | | | | | | |
| 1 | -7.531E-11 | -1.453E-10 | -1.939E-10 | -1.755E-10 | 1.947E-11 | 6.006E-10 | 1.748E-09 | 2.352E-09 | 2.586E-09 | 2.634E-09 | 2.550E-09 |
| 2 | 2.248E-09 | 1.493E-09 | 0.000 | | | | | | | | |
| 3 | -9.237E-11 | -1.947E-10 | -3.166E-10 | -4.589E-10 | -5.573E-10 | -2.088E-10 | 2.570E-09 | 2.954E-09 | 2.927E-09 | 2.896E-09 | 2.921E-09 |
| 4 | 2.938E-09 | 2.572E-09 | 0.000 | | | | | | | | |
| 5 | -1.054E-10 | -2.364E-10 | -4.411E-10 | -8.423E-10 | -1.803E-09 | -4.498E-09 | 6.868E-09 | 4.217E-09 | 3.357E-09 | 3.153E-09 | 3.359E-09 |
| 6 | 4.208E-09 | 6.825E-09 | 0.000 | | | | | | | | |
| 7 | -9.238E-11 | -1.946E-10 | -3.166E-10 | -4.589E-10 | -5.573E-10 | -2.088E-10 | 2.570E-09 | 2.954E-09 | 2.927E-09 | 2.896E-09 | 2.921E-09 |
| 8 | 2.938E-09 | 2.572E-09 | 0.000 | | | | | | | | |
| 9 | -7.532E-11 | -1.453E-10 | -1.939E-10 | -1.755E-10 | 1.947E-11 | 6.006E-10 | 1.748E-09 | 2.352E-09 | 2.586E-09 | 2.634E-09 | 2.550E-09 |
| 10 | 2.248E-09 | 1.493E-09 | 0.000 | | | | | | | | |

LAYER 8

| | 1 | 2 | 3 | 4 | 5 | 6 | 7 | 8 | 9 | 10 | 11 |
|----|------------|------------|------------|------------|------------|------------|-----------|-----------|-----------|-----------|-----------|
| | 12 | 13 | 14 | | | | | | | | |
| 1 | -7.928E-11 | -1.512E-10 | -1.972E-10 | -1.693E-10 | 4.131E-11 | 6.343E-10 | 1.770E-09 | 2.386E-09 | 2.633E-09 | 2.690E-09 | 2.605E-09 |
| 2 | 2.295E-09 | 1.523E-09 | 0.000 | | | | | | | | |
| 3 | -9.616E-11 | -1.996E-10 | -3.164E-10 | -4.416E-10 | -5.073E-10 | -1.294E-10 | 2.547E-09 | 2.959E-09 | 2.965E-09 | 2.951E-09 | 2.980E-09 |
| 4 | 2.996E-09 | 2.620E-09 | 0.000 | | | | | | | | |
| 5 | -1.090E-10 | -2.403E-10 | -4.261E-10 | -8.064E-10 | -1.684E-09 | -4.169E-09 | 6.595E-09 | 4.153E-09 | 3.377E-09 | 3.205E-09 | 3.424E-09 |
| 6 | 4.287E-09 | 6.947E-09 | 0.000 | | | | | | | | |
| 7 | -9.616E-11 | -1.996E-10 | -3.164E-10 | -4.417E-10 | -5.073E-10 | -1.294E-10 | 2.547E-09 | 2.959E-09 | 2.965E-09 | 2.951E-09 | 2.980E-09 |
| 8 | 2.996E-09 | 2.620E-09 | 0.000 | | | | | | | | |
| 9 | -7.928E-11 | -1.512E-10 | -1.972E-10 | -1.693E-10 | 4.130E-11 | 6.343E-10 | 1.770E-09 | 2.386E-09 | 2.633E-09 | 2.690E-09 | 2.605E-09 |
| 10 | 2.295E-09 | 1.523E-09 | 0.000 | | | | | | | | |

LAYER 9

| | 1 | 2 | 3 | 4 | 5 | 6 | 7 | 8 | 9 | 10 | 11 |
|----|------------|------------|------------|------------|------------|------------|-----------|-----------|-----------|-----------|-----------|
| | 12 | 13 | 14 | | | | | | | | |
| 1 | -6.584E-11 | -1.260E-10 | -1.647E-10 | -1.382E-10 | 5.713E-11 | 6.188E-10 | 1.715E-09 | 2.297E-09 | 2.520E-09 | 2.585E-09 | 2.519E-09 |
| 2 | 2.245E-09 | 1.511E-09 | 0.000 | | | | | | | | |
| 3 | -9.205E-11 | -1.790E-10 | -2.809E-10 | -4.062E-10 | -4.876E-10 | -1.451E-10 | 2.492E-09 | 2.867E-09 | 2.856E-09 | 2.847E-09 | 2.908E-09 |
| 4 | 2.983E-09 | 2.676E-09 | 0.000 | | | | | | | | |
| 5 | -9.442E-11 | -1.214E-10 | -3.396E-10 | -7.563E-10 | -1.664E-09 | -4.194E-09 | 6.550E-09 | 4.061E-09 | 3.266E-09 | 3.105E-09 | 3.372E-09 |
| 6 | 4.354E-09 | 7.279E-09 | 0.000 | | | | | | | | |
| 7 | -9.205E-11 | -1.790E-10 | -2.809E-10 | -4.062E-10 | -4.876E-10 | -1.451E-10 | 2.492E-09 | 2.867E-09 | 2.856E-09 | 2.847E-09 | 2.908E-09 |
| 8 | 2.983E-09 | 2.676E-09 | 0.000 | | | | | | | | |
| 9 | -6.585E-11 | -1.260E-10 | -1.647E-10 | -1.382E-10 | 5.713E-11 | 6.188E-10 | 1.715E-09 | 2.297E-09 | 2.520E-09 | 2.585E-09 | 2.519E-09 |
| 10 | 2.245E-09 | 1.511E-09 | 0.000 | | | | | | | | |

LAYER 10

| | 1 | 2 | 3 | 4 | 5 | 6 | 7 | 8 | 9 | 10 | 11 |
|----|------------|------------|------------|------------|------------|------------|-----------|-----------|-----------|-----------|-----------|
| | 12 | 13 | 14 | | | | | | | | |
| 1 | -3.012E-11 | -5.682E-11 | -6.982E-11 | -3.813E-11 | 1.206E-10 | 5.860E-10 | 1.560E-09 | 2.033E-09 | 2.204E-09 | 2.242E-09 | 2.192E-09 |
| 2 | 1.981E-09 | 1.372E-09 | 0.000 | | | | | | | | |
| 3 | -4.369E-11 | -9.680E-11 | -1.725E-10 | -2.852E-10 | -4.098E-10 | -2.142E-10 | 2.371E-09 | 2.585E-09 | 2.505E-09 | 2.481E-09 | 2.565E-09 |
| 4 | 2.738E-09 | 2.656E-09 | 0.000 | | | | | | | | |
| 5 | -5.420E-11 | -1.316E-10 | -2.806E-10 | -6.378E-10 | -1.638E-09 | -4.791E-09 | 6.955E-09 | 3.830E-09 | 2.903E-09 | 2.725E-09 | 3.039E-09 |
| 6 | 4.268E-09 | 8.268E-09 | 0.000 | | | | | | | | |
| 7 | -4.370E-11 | -9.680E-11 | -1.725E-10 | -2.852E-10 | -4.098E-10 | -2.142E-10 | 2.371E-09 | 2.585E-09 | 2.505E-09 | 2.481E-09 | 2.565E-09 |
| 8 | 2.738E-09 | 2.656E-09 | 0.000 | | | | | | | | |
| 9 | -3.012E-11 | -5.681E-11 | -6.982E-11 | -3.813E-11 | 1.206E-10 | 5.860E-10 | 1.560E-09 | 2.033E-09 | 2.204E-09 | 2.242E-09 | 2.192E-09 |
| 10 | 1.981E-09 | 1.372E-09 | 0.000 | | | | | | | | |

LAYER 11

| | 1 | 2 | 3 | 4 | 5 | 6 | 7 | 8 | 9 | 10 | 11 |
|----|------------|-----------|-----------|-----------|-----------|-----------|-----------|-----------|-----------|-----------|-----------|
| | 12 | 13 | 14 | | | | | | | | |
| 1 | 2.961E-11 | 6.889E-11 | 1.315E-10 | 2.401E-10 | 4.302E-10 | 7.418E-10 | 1.156E-09 | 1.443E-09 | 1.579E-09 | 1.587E-09 | 1.472E-09 |
| 2 | 1.203E-09 | 7.184E-10 | 0.000 | | | | | | | | |
| 3 | 2.414E-11 | 5.421E-11 | 9.898E-11 | 1.760E-10 | 3.267E-10 | 6.455E-10 | 1.257E-09 | 1.556E-09 | 1.664E-09 | 1.665E-09 | 1.580E-09 |
| 4 | 1.371E-09 | 9.148E-10 | 0.000 | | | | | | | | |
| 5 | -2.018E-11 | 4.279E-11 | 7.025E-11 | 1.070E-10 | 1.746E-10 | 4.013E-10 | 1.505E-09 | 1.715E-09 | 1.749E-09 | 1.733E-09 | 1.686E-09 |
| 6 | 1.589E-09 | 1.300E-09 | 0.000 | | | | | | | | |
| 7 | 2.414E-11 | 5.422E-11 | 9.898E-11 | 1.760E-10 | 3.267E-10 | 6.455E-10 | 1.257E-09 | 1.556E-09 | 1.664E-09 | 1.665E-09 | 1.580E-09 |
| 8 | 1.371E-09 | 9.148E-10 | 0.000 | | | | | | | | |
| 9 | 2.960E-11 | 6.888E-11 | 1.315E-10 | 2.401E-10 | 4.302E-10 | 7.418E-10 | 1.156E-09 | 1.443E-09 | 1.579E-09 | 1.587E-09 | 1.472E-09 |
| 10 | 1.203E-09 | 7.184E-10 | 0.000 | | | | | | | | |

LAYER 12

| | 1 | 2 | 3 | 4 | 5 | 6 | 7 | 8 | 9 | 10 | 11 |
|----|-----------|-----------|-----------|-----------|-----------|-----------|-----------|-----------|-----------|-----------|-----------|
| | 12 | 13 | 14 | | | | | | | | |
| 1 | 6.582E-11 | 1.420E-10 | 2.394E-10 | 1.698E-10 | 5.421E-10 | 7.543E-10 | 9.772E-10 | 1.146E-09 | 1.227E-09 | 1.205E-09 | 1.073E-09 |
| 2 | 8.223E-10 | 4.542E-10 | 0.000 | | | | | | | | |
| 3 | 6.399E-11 | 1.375E-10 | 2.310E-10 | 3.560E-10 | 5.248E-10 | 7.435E-10 | 9.902E-10 | 1.167E-09 | 1.247E-09 | 1.226E-09 | 1.099E-09 |
| 4 | 8.547E-10 | 4.820E-10 | 0.000 | | | | | | | | |
| 5 | 6.273E-11 | 1.344E-10 | 2.245E-10 | 3.482E-10 | 5.068E-10 | 7.275E-10 | 1.008E-09 | 1.188E-09 | 1.264E-09 | 1.242E-09 | 1.120E-09 |
| 6 | 8.851E-10 | 5.169E-10 | 0.000 | | | | | | | | |
| 7 | 6.399E-11 | 1.375E-10 | 2.310E-10 | 3.560E-10 | 5.248E-10 | 7.435E-10 | 9.902E-10 | 1.167E-09 | 1.247E-09 | 1.226E-09 | 1.099E-09 |
| 8 | 8.547E-10 | 4.820E-10 | 0.000 | | | | | | | | |
| 9 | 6.581E-11 | 1.420E-10 | 2.394E-10 | 1.698E-10 | 5.421E-10 | 7.543E-10 | 9.772E-10 | 1.146E-09 | 1.227E-09 | 1.205E-09 | 1.073E-09 |
| 10 | 8.223E-10 | 4.542E-10 | 0.000 | | | | | | | | |

*QVY * FLOW TERMS FOR TIME STEP 1, STRESS PERIOD 1 READ UNFORMATTED ON UNIT 10

LAYER 1

| | 1 | 2 | 3 | 4 | 5 | 6 | 7 | 8 | 9 | 10 | 11 |
|---|------------|------------|------------|------------|------------|------------|------------|------------|------------|------------|------------|
| | 12 | 13 | 14 | | | | | | | | |
| 1 | -3.485E-14 | -4.457E-14 | -6.342E-14 | -9.235E-14 | -1.239E-13 | -1.430E-13 | -1.266E-13 | -5.152E-14 | 9.451E-14 | 3.232E-13 | 6.480E-13 |
| 2 | -1.743E-14 | -2.261E-14 | -3.640E-14 | -5.700E-14 | -8.025E-14 | -9.592E-14 | -8.768E-14 | -3.940E-14 | 5.504E-14 | 2.029E-13 | 4.159E-13 |
| 3 | 6.963E-13 | 1.007E-12 | 1.236E-12 | | | | | | | | |
| 4 | 2.739E-14 | 3.366E-14 | 4.635E-14 | 6.333E-14 | 8.153E-14 | 9.206E-14 | 8.030E-14 | 3.099E-14 | -6.282E-14 | -2.097E-13 | -4.217E-13 |
| 5 | -7.010E-13 | -1.009E-12 | -1.237E-12 | | | | | | | | |
| 6 | 3.866E-14 | 4.841E-14 | 6.770E-14 | 9.557E-14 | 1.254E-13 | 1.424E-13 | 1.241E-13 | 4.826E-14 | -9.763E-14 | -3.257E-13 | -6.495E-13 |
| 7 | -1.064E-12 | -1.502E-12 | -1.809E-12 | | | | | | | | |
| 8 | 0.000 | 0.000 | 0.000 | 0.000 | 0.000 | 0.000 | 0.000 | 0.000 | 0.000 | 0.000 | 0.000 |
| 9 | 0.000 | 0.000 | 0.000 | | | | | | | | |

LAYER 2

| | 1 | 2 | 3 | 4 | 5 | 6 | 7 | 8 | 9 | 10 | 11 |
|---|------------|------------|------------|------------|------------|------------|------------|------------|-----------|-----------|-----------|
| | 12 | 13 | 14 | | | | | | | | |
| 1 | -1.249E-13 | -1.755E-13 | -2.835E-13 | -4.530E-13 | -6.644E-13 | -8.408E-13 | -8.404E-13 | -5.189E-13 | 1.381E-13 | 1.176E-12 | 2.738E-12 |
| 2 | 4.943E-12 | 7.575E-12 | 9.658E-12 | | | | | | | | |

J-26
OUTPUT-H2.ek

| | | | | | | | | | | | |
|---|------------|------------|------------|------------|------------|------------|------------|------------|------------|-----------|-----------|
| 1 | 5.020E-13 | -7.612E-13 | -1.350E-12 | -2.365E-12 | -3.805E-12 | -5.301E-12 | -5.827E-12 | -4.143E-12 | -7.535E-13 | 4.349E-12 | 1.234E-11 |
| 2 | 2.496E-11 | 4.246E-11 | 5.801E-11 | -1.609E-12 | -2.711E-12 | -4.010E-12 | -4.678E-12 | -3.261E-12 | -7.007E-13 | 2.963E-12 | 8.924E-12 |
| 3 | 1.939E-11 | 3.640E-11 | 5.483E-11 | 3.175E-13 | 4.872E-13 | 8.843E-13 | 1.606E-12 | 2.711E-12 | 4.011E-12 | 4.690E-12 | 3.265E-12 |
| 4 | -1.938E-11 | -3.639E-11 | -5.637E-11 | 5.015E-13 | 7.595E-13 | 1.347E-12 | 2.362E-12 | 3.802E-12 | 5.297E-12 | 5.824E-12 | 4.140E-12 |
| 5 | 0.000 | 0.000 | 0.000 | -2.495E-11 | -4.712E-11 | -5.895E-11 | 0.000 | 0.000 | 0.000 | 0.000 | 0.000 |
| | 0.000 | 0.000 | 0.000 | 0.000 | 0.000 | 0.000 | 0.000 | 0.000 | 0.000 | 0.000 | 0.000 |

LAYER 4

| | | | | | | | | | | | |
|---|------------|------------|------------|------------|------------|------------|------------|------------|------------|-----------|-----------|
| | 1 | 2 | 3 | 4 | 5 | 6 | 7 | 8 | 9 | 10 | 11 |
| | 12 | 13 | 14 | | | | | | | | |
| 1 | -1.757E-12 | -2.908E-12 | -5.036E-12 | -1.123E-11 | -2.031E-11 | -3.193E-11 | -3.902E-11 | -2.854E-11 | -1.076E-11 | 1.188E-11 | 4.707E-11 |
| 2 | 1.103E-10 | 2.167E-10 | 3.436E-10 | -8.211E-12 | -1.620E-11 | -2.867E-11 | -3.991E-11 | -2.642E-11 | -9.654E-12 | 8.583E-12 | 3.807E-11 |
| 3 | 1.013E-10 | 2.409E-10 | 4.912E-10 | 1.130E-12 | 1.920E-12 | 3.948E-12 | 8.212E-12 | 1.621E-11 | 2.867E-11 | 3.991E-11 | 2.641E-11 |
| 4 | -1.013E-10 | -2.409E-10 | -4.912E-10 | -1.130E-12 | -2.908E-12 | -5.733E-12 | 1.123E-11 | 2.031E-11 | 3.193E-11 | 3.902E-11 | 2.854E-11 |
| 5 | 0.000 | 0.000 | 0.000 | -1.103E-10 | -2.167E-10 | -3.436E-10 | 0.000 | 0.000 | 0.000 | 0.000 | 0.000 |
| | 0.000 | 0.000 | 0.000 | 0.000 | 0.000 | 0.000 | 0.000 | 0.000 | 0.000 | 0.000 | 0.000 |

LAYER 5

| | | | | | | | | | | | |
|---|------------|------------|------------|------------|------------|------------|------------|------------|------------|------------|------------|
| | 1 | 2 | 3 | 4 | 5 | 6 | 7 | 8 | 9 | 10 | 11 |
| | 12 | 13 | 14 | | | | | | | | |
| 1 | -1.016E-12 | -9.216E-12 | -2.036E-11 | -4.525E-11 | -9.453E-11 | -1.744E-10 | -2.484E-10 | -1.673E-10 | -7.315E-11 | 1.139E-11 | 1.254E-10 |
| 2 | 3.541E-10 | 8.438E-10 | 1.681E-09 | -3.300E-12 | -6.315E-12 | -1.505E-11 | -3.713E-11 | -9.047E-11 | -2.084E-10 | -3.983E-10 | -2.035E-10 |
| 3 | 4.149E-10 | 1.409E-09 | 5.066E-09 | 3.306E-12 | 6.318E-12 | 1.505E-11 | 3.713E-11 | 9.047E-11 | 2.084E-10 | 3.983E-10 | 2.035E-10 |
| 4 | -4.149E-10 | -1.409E-09 | -5.066E-09 | -3.306E-12 | -6.318E-12 | -1.505E-11 | -3.713E-11 | -9.047E-11 | -2.084E-10 | -3.983E-10 | -2.035E-10 |
| 5 | 0.000 | 0.000 | 0.000 | 3.541E-10 | 8.438E-10 | 1.681E-09 | 0.000 | 0.000 | 0.000 | 0.000 | 0.000 |
| | 0.000 | 0.000 | 0.000 | 0.000 | 0.000 | 0.000 | 0.000 | 0.000 | 0.000 | 0.000 | 0.000 |

LAYER 6

| | | | | | | | | | | | |
|---|------------|------------|------------|------------|------------|------------|------------|------------|------------|------------|------------|
| | 1 | 2 | 3 | 4 | 5 | 6 | 7 | 8 | 9 | 10 | 11 |
| | 12 | 13 | 14 | | | | | | | | |
| 1 | -1.034E-11 | -2.066E-11 | -5.123E-11 | -1.300E-10 | -3.202E-10 | -7.305E-10 | -1.353E-09 | -7.220E-10 | -2.951E-10 | -6.493E-11 | 1.110E-10 |
| 2 | 3.683E-10 | 8.574E-10 | 1.629E-09 | -7.007E-12 | -1.376E-11 | -4.162E-11 | -1.248E-10 | -3.975E-10 | -1.352E-09 | -4.925E-09 | -1.347E-09 |
| 3 | 4.102E-10 | 1.319E-09 | 4.365E-09 | 7.014E-12 | 1.504E-11 | 4.163E-11 | 1.248E-10 | 3.975E-10 | 1.352E-09 | 4.925E-09 | 1.347E-09 |
| 4 | -4.102E-10 | -1.319E-09 | -4.365E-09 | -7.014E-12 | -1.504E-11 | -4.163E-11 | -1.248E-10 | -3.975E-10 | -1.352E-09 | -4.925E-09 | -1.347E-09 |
| 5 | 0.000 | 0.000 | 0.000 | 3.683E-10 | 8.574E-10 | 1.629E-09 | 0.000 | 0.000 | 0.000 | 0.000 | 0.000 |
| | 0.000 | 0.000 | 0.000 | 0.000 | 0.000 | 0.000 | 0.000 | 0.000 | 0.000 | 0.000 | 0.000 |

LAYER 7

| | | | | | | | | | | | |
|---|------------|------------|------------|------------|------------|------------|------------|------------|------------|------------|------------|
| | 1 | 2 | 3 | 4 | 5 | 6 | 7 | 8 | 9 | 10 | 11 |
| | 12 | 13 | 14 | | | | | | | | |
| 1 | -1.235E-11 | -2.420E-11 | -5.847E-11 | -1.437E-10 | -3.405E-10 | -7.410E-10 | -1.303E-09 | -7.322E-10 | -3.147E-10 | -7.770E-11 | 1.043E-10 |
| 2 | 3.618E-10 | 8.408E-10 | 1.595E-09 | -8.318E-12 | -1.736E-11 | -4.677E-11 | -1.328E-10 | -3.989E-10 | -1.264E-09 | -4.242E-09 | -1.250E-09 |
| 3 | 4.001E-10 | 1.282E-09 | 4.235E-09 | 8.318E-12 | 1.736E-11 | 4.677E-11 | 1.328E-10 | 3.989E-10 | 1.264E-09 | 4.242E-09 | 1.250E-09 |
| 4 | -4.001E-10 | -1.282E-09 | -4.235E-09 | -8.318E-12 | -1.736E-11 | -4.677E-11 | -1.328E-10 | -3.989E-10 | -1.264E-09 | -4.242E-09 | -1.250E-09 |
| 5 | 0.000 | 0.000 | 0.000 | 3.618E-10 | 8.408E-10 | 1.595E-09 | 0.000 | 0.000 | 0.000 | 0.000 | 0.000 |
| | 0.000 | 0.000 | 0.000 | 0.000 | 0.000 | 0.000 | 0.000 | 0.000 | 0.000 | 0.000 | 0.000 |

LAYER 8

| | | | | | | | | | | | |
|---|------------|------------|------------|------------|------------|------------|------------|------------|------------|------------|------------|
| | 1 | 2 | 3 | 4 | 5 | 6 | 7 | 8 | 9 | 10 | 11 |
| | 12 | 13 | 14 | | | | | | | | |
| 1 | -1.248E-11 | -2.421E-11 | -5.785E-11 | -1.406E-10 | -3.297E-10 | -7.106E-10 | -1.241E-09 | -7.016E-10 | -3.035E-10 | -7.363E-11 | 1.074E-10 |
| 2 | 3.680E-10 | 8.546E-10 | 1.616E-09 | -8.379E-12 | -1.728E-11 | -4.554E-11 | -1.287E-10 | -3.819E-10 | -1.199E-09 | -4.003E-09 | -1.193E-09 |
| 3 | 4.070E-10 | 1.303E-09 | 4.307E-09 | 8.379E-12 | 1.728E-11 | 4.555E-11 | 1.287E-10 | 3.819E-10 | 1.199E-09 | 4.003E-09 | 1.193E-09 |
| 4 | -4.070E-10 | -1.303E-09 | -4.307E-09 | -8.379E-12 | -1.728E-11 | -4.555E-11 | -1.287E-10 | -3.819E-10 | -1.199E-09 | -4.003E-09 | -1.193E-09 |
| 5 | 0.000 | 0.000 | 0.000 | 3.680E-10 | 8.546E-10 | 1.616E-09 | 0.000 | 0.000 | 0.000 | 0.000 | 0.000 |
| | 0.000 | 0.000 | 0.000 | 0.000 | 0.000 | 0.000 | 0.000 | 0.000 | 0.000 | 0.000 | 0.000 |

LAYER 9

| | | | | | | | | | | | |
|---|------------|------------|------------|------------|------------|------------|------------|------------|------------|------------|------------|
| | 1 | 2 | 3 | 4 | 5 | 6 | 7 | 8 | 9 | 10 | 11 |
| | 12 | 13 | 14 | | | | | | | | |
| 1 | -1.179E-11 | -2.304E-11 | -5.555E-11 | -1.363E-10 | -3.224E-10 | -7.006E-10 | -1.231E-09 | -6.917E-10 | -2.962E-10 | -6.850E-11 | 1.136E-10 |
| 2 | -1.930E-12 | 1.652E-11 | -4.400E-11 | -1.257E-10 | -3.771E-10 | -1.194E-09 | -4.005E-09 | -1.188E-09 | -3.585E-10 | -7.331E-11 | 1.058E-10 |
| 3 | 4.282E-10 | 1.380E-09 | 4.577E-09 | 7.933E-12 | 1.652E-11 | 4.401E-11 | 1.257E-10 | 3.771E-10 | 1.194E-09 | 4.005E-09 | 1.188E-09 |
| 4 | -4.282E-10 | -1.380E-09 | -4.577E-09 | -7.933E-12 | -1.652E-11 | -4.401E-11 | -1.257E-10 | -3.771E-10 | -1.194E-09 | -4.005E-09 | -1.188E-09 |
| 5 | 0.000 | 0.000 | 0.000 | -1.179E-11 | -2.304E-11 | -5.555E-11 | 1.363E-10 | 3.224E-10 | 7.006E-10 | 1.231E-09 | 6.917E-10 |
| | 0.000 | 0.000 | 0.000 | 0.000 | 0.000 | 0.000 | 0.000 | 0.000 | 0.000 | 0.000 | 0.000 |

LAYER 10

| | | | | | | | | | | | |
|---|------------|------------|------------|------------|------------|------------|------------|------------|------------|------------|------------|
| | 1 | 2 | 3 | 4 | 5 | 6 | 7 | 8 | 9 | 10 | 11 |
| | 12 | 13 | 14 | | | | | | | | |
| 1 | -9.547E-12 | -1.897E-11 | -4.678E-11 | -1.181E-10 | -2.897E-10 | -6.579E-10 | -1.214E-09 | -6.503E-10 | -2.670E-10 | -5.813E-11 | 1.077E-10 |
| 2 | 3.665E-10 | 8.925E-10 | 1.784E-09 | -6.462E-12 | -1.377E-11 | -3.788E-11 | -1.129E-10 | -3.577E-10 | -1.211E-09 | -4.388E-09 | -1.205E-09 |
| 3 | 4.337E-10 | 1.496E-09 | 5.392E-09 | 6.465E-12 | 1.377E-11 | 3.788E-11 | 1.129E-10 | 3.577E-10 | 1.211E-09 | 4.388E-09 | 1.205E-09 |
| 4 | -4.337E-10 | -1.496E-09 | -5.392E-09 | -6.465E-12 | -1.377E-11 | -3.788E-11 | -1.129E-10 | -3.577E-10 | -1.211E-09 | -4.388E-09 | -1.205E-09 |
| 5 | 0.000 | 0.000 | 0.000 | 3.665E-10 | 8.925E-10 | 1.784E-09 | 0.000 | 0.000 | 0.000 | 0.000 | 0.000 |
| | 0.000 | 0.000 | 0.000 | 0.000 | 0.000 | 0.000 | 0.000 | 0.000 | 0.000 | 0.000 | 0.000 |

LAYER 11

| | | | | | | | | | | | |
|---|------------|------------|------------|------------|------------|------------|------------|------------|------------|------------|------------|
| | 1 | 2 | 3 | 4 | 5 | 6 | 7 | 8 | 9 | 10 | 11 |
| | 12 | 13 | 14 | | | | | | | | |
| 1 | -4.679E-12 | -8.475E-12 | -1.866E-11 | -4.125E-11 | -8.575E-11 | -1.577E-10 | -2.245E-10 | -1.540E-10 | -7.542E-11 | -1.635E-11 | 3.809E-11 |
| 2 | 1.130E-10 | 2.295E-10 | 3.659E-10 | -3.071E-12 | -5.824E-12 | -1.375E-11 | 1.048E-10 | 2.557E-10 | 5.231E-10 | 1.847E-10 | 7.455E-11 |
| 3 | 3.081E-12 | 5.830E-12 | 1.376E-11 | 3.371E-11 | 8.163E-11 | 1.872E-10 | 3.567E-10 | 1.847E-10 | 7.455E-11 | 1.563E-11 | -3.132E-11 |
| 4 | -3.081E-12 | -5.830E-12 | -1.376E-11 | -3.371E-11 | -8.163E-11 | -1.872E-10 | -3.567E-10 | -1.847E-10 | -7.455E-11 | -1.564E-11 | 3.132E-11 |
| 5 | 0.000 | 0.000 | 0.000 | 1.130E-10 | 2.295E-10 | 3.659E-10 | 0.000 | 0.000 | 0.000 | 0.000 | 0.000 |
| | 0.000 | 0.000 | 0.000 | 0.000 | 0.000 | 0.000 | 0.000 | 0.000 | 0.000 | 0.000 | 0.000 |

LAYER 12

J-28
OUTPUT-H2.ek

5 -2.861E-11 -2.525E-11 -1.897E-11 -1.084E-11 -3.056E-12 8.992E-13 -2.894E-12 -1.673E-11 -3.883E-11 -6.529E-11 -9.153E-11
-1.130E-10 -1.257E-10 -1.287E-10

LAYER 9

| | 1 | 2 | 3 | 4 | 5 | 6 | 7 | 8 | 9 | 10 | 11 |
|---|------------|------------|------------|-----------|-----------|-----------|-----------|-----------|-----------|------------|------------|
| 1 | 4.904E-11 | 5.797E-11 | 7.527E-11 | 9.899E-11 | 1.240E-10 | 1.399E-10 | 1.317E-10 | 9.292E-11 | 2.699E-11 | -5.397E-11 | -1.397E-10 |
| 2 | -2.216E-10 | -2.876E-10 | -3.224E-10 | 4.985E-11 | 5.944E-11 | 7.843E-11 | 1.055E-10 | 1.358E-10 | 1.552E-10 | 1.380E-10 | 1.078E-10 |
| 3 | -2.276E-10 | -2.887E-10 | -2.936E-10 | 5.036E-11 | 6.043E-11 | 8.052E-11 | 1.101E-10 | 1.428E-10 | 1.492E-10 | 0.000 | 1.014E-10 |
| 4 | -2.256E-10 | -2.473E-10 | 0.000 | 4.985E-11 | 5.944E-11 | 7.842E-11 | 1.055E-10 | 1.358E-10 | 1.552E-10 | 1.380E-10 | 1.078E-10 |
| 5 | -2.276E-10 | -2.887E-10 | -2.936E-10 | 4.904E-11 | 5.797E-11 | 7.527E-11 | 9.899E-11 | 1.240E-10 | 1.399E-10 | 1.317E-10 | 9.292E-11 |

LAYER 10

| | 1 | 2 | 3 | 4 | 5 | 6 | 7 | 8 | 9 | 10 | 11 |
|---|------------|------------|------------|-----------|-----------|-----------|-----------|-----------|-----------|------------|------------|
| 1 | 8.871E-11 | 1.036E-10 | 1.351E-10 | 1.854E-10 | 2.550E-10 | 3.324E-10 | 3.713E-10 | 2.703E-10 | 1.228E-10 | -3.353E-11 | -1.973E-10 |
| 2 | -1.971E-10 | -5.714E-10 | -7.348E-10 | 9.047E-11 | 1.074E-10 | 1.452E-10 | 2.131E-10 | 3.284E-10 | 5.125E-10 | 7.274E-10 | 4.490E-10 |
| 3 | -4.684E-10 | -8.102E-10 | -1.246E-09 | 9.109E-11 | 1.103E-10 | 1.539E-10 | 2.416E-10 | 4.278E-10 | 8.810E-10 | 2.179E-09 | 8.165E-10 |
| 4 | -5.469E-10 | -1.257E-09 | -2.999E-09 | 9.047E-11 | 1.074E-10 | 1.452E-10 | 2.131E-10 | 3.284E-10 | 5.125E-10 | 7.274E-10 | 4.490E-10 |
| 5 | -4.684E-10 | -8.102E-10 | -1.246E-09 | 8.872E-11 | 1.036E-10 | 1.351E-10 | 1.854E-10 | 2.550E-10 | 3.324E-10 | 3.713E-10 | 2.703E-10 |

LAYER 11

| | 1 | 2 | 3 | 4 | 5 | 6 | 7 | 8 | 9 | 10 | 11 |
|---|------------|------------|------------|-----------|-----------|-----------|-----------|-----------|-----------|------------|------------|
| 1 | 6.378E-11 | 7.284E-11 | 9.110E-11 | 1.101E-10 | 1.505E-10 | 1.785E-10 | 1.816E-10 | 1.369E-10 | 6.269E-11 | -2.533E-11 | -1.209E-10 |
| 2 | -2.208E-10 | -3.161E-10 | -3.821E-10 | 6.473E-11 | 7.469E-11 | 9.552E-11 | 1.285E-10 | 1.735E-10 | 2.231E-10 | 2.476E-10 | 1.808E-10 |
| 3 | -2.509E-10 | -3.799E-10 | -4.879E-10 | 6.378E-11 | 7.601E-11 | 9.890E-11 | 1.375E-10 | 1.968E-10 | 2.798E-10 | 3.614E-10 | 2.370E-10 |
| 4 | -2.903E-10 | -4.562E-10 | -6.520E-10 | 6.473E-11 | 7.469E-11 | 9.552E-11 | 1.285E-10 | 1.735E-10 | 2.231E-10 | 2.476E-10 | 1.808E-10 |
| 5 | -2.509E-10 | -3.799E-10 | -4.879E-10 | 6.378E-11 | 7.284E-11 | 9.110E-11 | 1.101E-10 | 1.505E-10 | 1.785E-10 | 1.816E-10 | 1.369E-10 |

LAYER 12

| | 1 | 2 | 3 | 4 | 5 | 6 | 7 | 8 | 9 | 10 | 11 |
|---|-------|-------|-------|-------|-------|-------|-------|-------|-------|-------|-------|
| 1 | 0.000 | 0.000 | 0.000 | 0.000 | 0.000 | 0.000 | 0.000 | 0.000 | 0.000 | 0.000 | 0.000 |
| 2 | 0.000 | 0.000 | 0.000 | 0.000 | 0.000 | 0.000 | 0.000 | 0.000 | 0.000 | 0.000 | 0.000 |
| 3 | 0.000 | 0.000 | 0.000 | 0.000 | 0.000 | 0.000 | 0.000 | 0.000 | 0.000 | 0.000 | 0.000 |
| 4 | 0.000 | 0.000 | 0.000 | 0.000 | 0.000 | 0.000 | 0.000 | 0.000 | 0.000 | 0.000 | 0.000 |
| 5 | 0.000 | 0.000 | 0.000 | 0.000 | 0.000 | 0.000 | 0.000 | 0.000 | 0.000 | 0.000 | 0.000 |

MAXIMUM STEPSIZE DURING WHICH ANY PARTICLE CANNOT MOVE MORE THAN ONE CELL
= 0.1708E+06 (WHEN MIN. R.F.=1) AT K= 10, I= 3, J= 13

MAXIMUM STEPSIZE WHICH MEETS STABILITY CRITERION OF THE DISPERSION TERM
= 0.1636E+06 (WHEN MIN. R.F.=1) AT K= 11, I= 4, J= 13

DISP. COEFF. DX IN LAYER 1 FOR TIME STEP 1, STRESS PERIOD 1

| | 1 | 2 | 3 | 4 | 5 | 6 | 7 | 8 | 9 | 10 | 11 | 12 | 13 | 14 |
|---|-----|-----|-----|-----|-----|-----|-----|-----|-----|-----|-----|-----|-----|-----|
| 1 | 0.0 | 0.0 | 0.0 | 0.0 | 0.0 | 0.0 | 0.0 | 0.0 | 0.0 | 0.0 | 0.0 | 0.0 | 0.0 | 0.0 |
| 2 | 0.0 | 0.0 | 0.0 | 0.0 | 0.0 | 0.0 | 0.0 | 0.0 | 0.0 | 0.0 | 0.0 | 0.0 | 0.0 | 0.0 |
| 3 | 0.0 | 0.0 | 0.0 | 0.0 | 0.0 | 0.0 | 0.0 | 0.0 | 0.0 | 0.0 | 0.0 | 0.0 | 0.0 | 0.0 |
| 4 | 0.0 | 0.0 | 0.0 | 0.0 | 0.0 | 0.0 | 0.0 | 0.0 | 0.0 | 0.0 | 0.0 | 0.0 | 0.0 | 0.0 |
| 5 | 0.0 | 0.0 | 0.0 | 0.0 | 0.0 | 0.0 | 0.0 | 0.0 | 0.0 | 0.0 | 0.0 | 0.0 | 0.0 | 0.0 |

DISP. COEFF. DX IN LAYER 2 FOR TIME STEP 1, STRESS PERIOD 1

| | 1 | 2 | 3 | 4 | 5 | 6 | 7 | 8 | 9 | 10 | 11 | 12 | 13 | 14 |
|---|-----|-----|-----|-----|-----|-----|-----|-----|-----|-----|-----|-----|-----|-----|
| 1 | 0.0 | 0.0 | 0.0 | 0.0 | 0.0 | 0.0 | 0.0 | 0.0 | 0.0 | 0.0 | 0.0 | 0.0 | 0.0 | 0.0 |
| 2 | 0.0 | 0.0 | 0.0 | 0.0 | 0.0 | 0.0 | 0.0 | 0.0 | 0.0 | 0.0 | 0.0 | 0.0 | 0.0 | 0.0 |
| 3 | 0.0 | 0.0 | 0.0 | 0.0 | 0.0 | 0.0 | 0.0 | 0.0 | 0.0 | 0.0 | 0.0 | 0.0 | 0.0 | 0.0 |
| 4 | 0.0 | 0.0 | 0.0 | 0.0 | 0.0 | 0.0 | 0.0 | 0.0 | 0.0 | 0.0 | 0.0 | 0.0 | 0.0 | 0.0 |
| 5 | 0.0 | 0.0 | 0.0 | 0.0 | 0.0 | 0.0 | 0.0 | 0.0 | 0.0 | 0.0 | 0.0 | 0.0 | 0.0 | 0.0 |

DISP. COEFF. DX IN LAYER 3 FOR TIME STEP 1, STRESS PERIOD 1

| | 1 | 2 | 3 | 4 | 5 | 6 | 7 | 8 | 9 | 10 | 11 | 12 | 13 | 14 |
|---|-----|-----|-----|-----|-----|-----|-----|-----|-----|-----|-----|-----|-----|-----|
| 1 | 0.0 | 0.0 | 0.0 | 0.0 | 0.0 | 0.0 | 0.0 | 0.0 | 0.0 | 0.0 | 0.0 | 0.0 | 0.0 | 0.0 |
| 2 | 0.0 | 0.0 | 0.0 | 0.0 | 0.0 | 0.0 | 0.0 | 0.0 | 0.0 | 0.0 | 0.0 | 0.0 | 0.0 | 0.0 |
| 3 | 0.0 | 0.0 | 0.0 | 0.0 | 0.0 | 0.0 | 0.0 | 0.0 | 0.0 | 0.0 | 0.0 | 0.0 | 0.0 | 0.0 |
| 4 | 0.0 | 0.0 | 0.0 | 0.0 | 0.0 | 0.0 | 0.0 | 0.0 | 0.0 | 0.0 | 0.0 | 0.0 | 0.0 | 0.0 |
| 5 | 0.0 | 0.0 | 0.0 | 0.0 | 0.0 | 0.0 | 0.0 | 0.0 | 0.0 | 0.0 | 0.0 | 0.0 | 0.0 | 0.0 |

DISP. COEFF. DX IN LAYER 4 FOR TIME STEP 1, STRESS PERIOD 1

| | 1 | 2 | 3 | 4 | 5 | 6 | 7 | 8 | 9 | 10 | 11 | 12 | 13 | 14 |
|---|-----|-----|-----|-----|-----|-----|-----|-----|-----|-----|-----|-----|-----|-----|
| 1 | 0.0 | 0.0 | 0.0 | 0.0 | 0.0 | 0.0 | 0.0 | 0.0 | 0.0 | 0.0 | 0.0 | 0.0 | 0.0 | 0.0 |
| 2 | 0.0 | 0.0 | 0.0 | 0.0 | 0.0 | 0.0 | 0.0 | 0.0 | 0.0 | 0.0 | 0.0 | 0.0 | 0.0 | 0.0 |
| 3 | 0.0 | 0.0 | 0.0 | 0.0 | 0.0 | 0.0 | 0.0 | 0.0 | 0.0 | 0.0 | 0.0 | 0.0 | 0.0 | 0.0 |
| 4 | 0.0 | 0.0 | 0.0 | 0.0 | 0.0 | 0.0 | 0.0 | 0.0 | 0.0 | 0.0 | 0.0 | 0.0 | 0.0 | 0.0 |
| 5 | 0.0 | 0.0 | 0.0 | 0.0 | 0.0 | 0.0 | 0.0 | 0.0 | 0.0 | 0.0 | 0.0 | 0.0 | 0.0 | 0.0 |

DISP. COEFF. DX IN LAYER 5 FOR TIME STEP 1, STRESS PERIOD 1

| | 1 | 2 | 3 | 4 | 5 | 6 | 7 | 8 | 9 | 10 | 11 | 12 | 13 | 14 |
|---|-----|-----|-----|-----|-----|-----|-----|-----|-----|-----|-----|-----|-----|-----|
| 1 | 0.0 | 0.0 | 0.0 | 0.0 | 0.0 | 0.0 | 0.0 | 0.0 | 0.0 | 0.0 | 0.0 | 0.0 | 0.0 | 0.0 |
| 2 | 0.0 | 0.0 | 0.0 | 0.0 | 0.0 | 0.0 | 0.0 | 0.0 | 0.0 | 0.0 | 0.0 | 0.0 | 0.0 | 0.0 |
| 3 | 0.0 | 0.0 | 0.0 | 0.0 | 0.0 | 0.0 | 0.0 | 0.0 | 0.0 | 0.0 | 0.0 | 0.0 | 0.0 | 0.0 |
| 4 | 0.0 | 0.0 | 0.0 | 0.0 | 0.0 | 0.0 | 0.0 | 0.0 | 0.0 | 0.0 | 0.0 | 0.0 | 0.0 | 0.0 |
| 5 | 0.0 | 0.0 | 0.0 | 0.0 | 0.0 | 0.0 | 0.0 | 0.0 | 0.0 | 0.0 | 0.0 | 0.0 | 0.0 | 0.0 |

DISP. COEFF. DX IN LAYER 6 FOR TIME STEP 1, STRESS PERIOD 1

| | 1 | 2 | 3 | 4 | 5 | 6 | 7 | 8 | 9 | 10 | 11 | 12 | 13 | 14 |
|---|-----|-----|-----|-----|-----|-----|-----|-----|-----|-----|-----|-----|-----|-----|
| 1 | 0.0 | 0.0 | 0.0 | 0.0 | 0.0 | 0.0 | 0.0 | 0.0 | 0.0 | 0.0 | 0.0 | 0.0 | 0.0 | 0.0 |
| 2 | 0.0 | 0.0 | 0.0 | 0.0 | 0.0 | 0.0 | 0.0 | 0.0 | 0.0 | 0.0 | 0.0 | 0.0 | 0.0 | 0.0 |
| 3 | 0.0 | 0.0 | 0.0 | 0.0 | 0.0 | 0.0 | 0.0 | 0.0 | 0.0 | 0.0 | 0.0 | 0.0 | 0.0 | 0.0 |
| 4 | 0.0 | 0.0 | 0.0 | 0.0 | 0.0 | 0.0 | 0.0 | 0.0 | 0.0 | 0.0 | 0.0 | 0.0 | 0.0 | 0.0 |
| 5 | 0.0 | 0.0 | 0.0 | 0.0 | 0.0 | 0.0 | 0.0 | 0.0 | 0.0 | 0.0 | 0.0 | 0.0 | 0.0 | 0.0 |

DISP. COEFF. DX IN LAYER 7 FOR TIME STEP 1, STRESS PERIOD 1

J-37
OUTPUT-H2.ek

5 39.2 35.0 29.5 23.4 17.2 11.5 6.7 3.2 1.2 0.4 0.1 0.0 0.0 0.0

CONCENTRATIONS IN LAYER 2 AT END OF TRANSPORT STEP 5022, TIME STEP 1, STRESS PERIOD 1

| | 1 | 2 | 3 | 4 | 5 | 6 | 7 | 8 | 9 | 10 | 11 | 12 | 13 | 14 |
|---|-------|-------|-------|-------|-------|------|------|------|------|------|-----|-----|-----|-----|
| 1 | 123.7 | 116.5 | 106.4 | 93.7 | 78.9 | 62.2 | 44.7 | 27.9 | 13.8 | 6.1 | 2.4 | 0.8 | 0.2 | 0.0 |
| 2 | 146.7 | 140.2 | 130.7 | 118.3 | 102.7 | 84.0 | 63.1 | 41.7 | 22.2 | 10.6 | 4.4 | 1.5 | 0.4 | 0.1 |
| 3 | 159.5 | 153.5 | 144.5 | 132.5 | 116.8 | 97.4 | 74.9 | 51.3 | 28.5 | 14.4 | 6.3 | 2.3 | 0.6 | 0.1 |
| 4 | 146.7 | 140.2 | 130.7 | 118.3 | 102.7 | 84.0 | 63.1 | 41.7 | 22.2 | 10.6 | 4.4 | 1.5 | 0.4 | 0.1 |
| 5 | 123.7 | 116.5 | 106.4 | 93.7 | 78.9 | 62.2 | 44.7 | 27.9 | 13.8 | 6.1 | 2.4 | 0.8 | 0.2 | 0.0 |

CONCENTRATIONS IN LAYER 3 AT END OF TRANSPORT STEP 5022, TIME STEP 1, STRESS PERIOD 1

| | 1 | 2 | 3 | 4 | 5 | 6 | 7 | 8 | 9 | 10 | 11 | 12 | 13 | 14 |
|---|-------|-------|-------|-------|-------|-------|-------|-------|-------|------|------|------|-----|-----|
| 1 | 184.2 | 180.6 | 175.0 | 167.0 | 155.8 | 140.3 | 120.5 | 97.6 | 70.2 | 43.0 | 10.5 | 3.7 | 0.8 | 0.0 |
| 2 | 193.9 | 192.0 | 188.7 | 183.2 | 173.5 | 157.9 | 138.2 | 117.8 | 92.3 | 61.7 | 35.7 | 17.4 | 6.6 | 1.6 |
| 3 | 197.2 | 196.0 | 193.6 | 188.3 | 177.2 | 159.6 | 139.4 | 122.6 | 102.3 | 73.0 | 44.7 | 23.0 | 9.4 | 2.5 |
| 4 | 193.9 | 192.0 | 188.7 | 183.2 | 173.5 | 157.9 | 138.2 | 117.8 | 92.3 | 61.7 | 35.7 | 17.4 | 6.6 | 1.6 |
| 5 | 184.2 | 180.6 | 175.0 | 167.0 | 155.8 | 140.3 | 120.5 | 97.6 | 70.2 | 43.0 | 10.5 | 3.7 | 0.8 | 0.0 |

CONCENTRATIONS IN LAYER 4 AT END OF TRANSPORT STEP 5022, TIME STEP 1, STRESS PERIOD 1

| | 1 | 2 | 3 | 4 | 5 | 6 | 7 | 8 | 9 | 10 | 11 | 12 | 13 | 14 |
|---|-------|-------|-------|-------|-------|-------|-------|-------|-------|-------|-------|------|------|------|
| 1 | 198.9 | 198.2 | 197.0 | 194.3 | 187.3 | 170.6 | 152.0 | 142.2 | 135.0 | 117.6 | 89.3 | 58.6 | 31.5 | 11.6 |
| 2 | 199.8 | 199.7 | 199.0 | 194.4 | 177.2 | 147.0 | 120.8 | 115.5 | 121.2 | 122.4 | 104.0 | 74.5 | 43.6 | 18.1 |
| 3 | 199.9 | 199.7 | 197.4 | 184.8 | 153.4 | 113.3 | 82.9 | 80.9 | 93.6 | 108.7 | 102.9 | 80.5 | 51.4 | 24.3 |
| 4 | 199.6 | 199.8 | 199.0 | 194.4 | 177.2 | 147.0 | 120.7 | 115.5 | 121.2 | 122.4 | 104.0 | 74.5 | 43.6 | 18.1 |
| 5 | 198.9 | 198.2 | 197.0 | 194.3 | 187.3 | 170.6 | 152.0 | 142.2 | 135.0 | 117.6 | 89.3 | 58.6 | 31.5 | 11.6 |

CONCENTRATIONS IN LAYER 5 AT END OF TRANSPORT STEP 5022, TIME STEP 1, STRESS PERIOD 1

| | 1 | 2 | 3 | 4 | 5 | 6 | 7 | 8 | 9 | 10 | 11 | 12 | 13 | 14 |
|---|-------|-------|-------|-------|-------|-------|------|------|------|-------|-------|-------|------|------|
| 1 | 199.9 | 199.6 | 198.9 | 194.6 | 175.9 | 128.9 | 93.2 | 87.5 | 95.9 | 111.1 | 119.9 | 112.2 | 89.1 | 54.4 |
| 2 | 200.0 | 199.7 | 196.2 | 175.6 | 119.7 | 58.3 | 27.4 | 25.7 | 33.8 | 52.0 | 77.6 | 90.3 | 83.3 | 58.8 |
| 3 | 199.9 | 198.4 | 185.4 | 137.0 | 64.2 | 17.3 | 3.2 | 3.7 | 7.6 | 18.4 | 43.9 | 66.1 | 71.9 | 0.0 |
| 4 | 200.0 | 199.7 | 196.2 | 175.6 | 119.7 | 58.3 | 27.4 | 25.7 | 33.8 | 52.0 | 77.6 | 90.3 | 83.3 | 58.8 |
| 5 | 199.9 | 199.6 | 198.9 | 194.6 | 175.9 | 128.9 | 93.2 | 87.5 | 95.9 | 111.1 | 119.9 | 112.2 | 89.1 | 54.4 |

CONCENTRATIONS IN LAYER 6 AT END OF TRANSPORT STEP 5022, TIME STEP 1, STRESS PERIOD 1

| | 1 | 2 | 3 | 4 | 5 | 6 | 7 | 8 | 9 | 10 | 11 | 12 | 13 | 14 |
|---|-------|-------|-------|-------|-------|------|------|------|------|------|------|------|-------|------|
| 1 | 199.8 | 199.3 | 197.8 | 183.8 | 139.9 | 57.1 | 25.2 | 24.7 | 31.5 | 45.1 | 64.4 | 85.7 | 101.8 | 98.8 |
| 2 | 199.9 | 198.0 | 182.0 | 122.7 | 39.6 | 4.4 | 0.1 | 0.2 | 0.8 | 3.5 | 13.6 | 35.8 | 62.6 | 80.9 |
| 3 | 199.4 | 190.9 | 142.8 | 49.0 | 3.2 | 0.1 | 0.0 | 0.0 | 0.4 | 3.5 | 16.8 | 39.9 | 0.0 | 0.0 |
| 4 | 199.9 | 198.0 | 182.0 | 122.7 | 39.6 | 4.4 | 0.1 | 0.2 | 0.8 | 3.5 | 13.6 | 35.8 | 62.6 | 80.9 |
| 5 | 199.8 | 199.4 | 197.0 | 183.9 | 139.9 | 57.1 | 25.2 | 24.7 | 31.5 | 45.1 | 64.4 | 85.7 | 100.8 | 98.8 |

CONCENTRATIONS IN LAYER 7 AT END OF TRANSPORT STEP 5022, TIME STEP 1, STRESS PERIOD 1

| | 1 | 2 | 3 | 4 | 5 | 6 | 7 | 8 | 9 | 10 | 11 | 12 | 13 | 14 |
|---|-------|-------|-------|-------|-------|------|------|------|------|------|------|------|-------|-------|
| 1 | 199.7 | 199.1 | 195.7 | 180.7 | 140.1 | 58.4 | 27.9 | 26.9 | 32.6 | 44.4 | 61.4 | 81.8 | 102.9 | 117.2 |
| 2 | 199.8 | 196.8 | 177.2 | 118.1 | 42.0 | 6.3 | 0.1 | 0.7 | 2.9 | 10.9 | 29.0 | 57.3 | 88.4 | 0.0 |
| 3 | 199.0 | 187.2 | 124.7 | 46.8 | 3.7 | 0.1 | 0.0 | 0.0 | 0.3 | 2.5 | 11.7 | 33.6 | 0.0 | 0.0 |
| 4 | 199.8 | 196.8 | 177.2 | 118.1 | 42.0 | 6.3 | 0.1 | 0.2 | 0.7 | 2.9 | 10.9 | 29.0 | 57.3 | 88.4 |
| 5 | 199.7 | 199.1 | 195.7 | 180.7 | 140.1 | 58.4 | 27.9 | 26.9 | 32.6 | 44.4 | 61.4 | 81.8 | 102.9 | 117.2 |

CONCENTRATIONS IN LAYER 8 AT END OF TRANSPORT STEP 5022, TIME STEP 1, STRESS PERIOD 1

| | 1 | 2 | 3 | 4 | 5 | 6 | 7 | 8 | 9 | 10 | 11 | 12 | 13 | 14 |
|---|-------|-------|-------|-------|-------|------|------|------|------|------|------|------|-------|-------|
| 1 | 199.7 | 199.1 | 196.0 | 182.5 | 144.7 | 65.6 | 32.1 | 30.5 | 36.1 | 47.7 | 64.4 | 84.0 | 104.3 | 117.9 |
| 2 | 199.8 | 197.1 | 179.2 | 124.1 | 48.4 | 8.5 | 0.2 | 0.3 | 0.9 | 3.1 | 11.3 | 29.6 | 57.8 | 88.7 |
| 3 | 199.1 | 187.9 | 138.1 | 51.4 | 4.8 | 0.1 | 0.0 | 0.0 | 0.0 | 0.3 | 2.5 | 11.9 | 33.7 | 0.0 |
| 4 | 199.8 | 197.1 | 179.2 | 124.1 | 48.4 | 8.5 | 0.2 | 0.3 | 0.9 | 3.1 | 11.3 | 29.6 | 57.8 | 88.7 |
| 5 | 199.7 | 199.1 | 196.0 | 182.5 | 144.7 | 65.6 | 32.1 | 30.5 | 36.1 | 47.7 | 64.4 | 84.0 | 104.3 | 117.9 |

CONCENTRATIONS IN LAYER 9 AT END OF TRANSPORT STEP 5022, TIME STEP 1, STRESS PERIOD 1

| | 1 | 2 | 3 | 4 | 5 | 6 | 7 | 8 | 9 | 10 | 11 | 12 | 13 | 14 |
|---|-------|-------|-------|-------|-------|------|------|------|------|------|------|------|-------|-------|
| 1 | 199.8 | 199.3 | 196.8 | 184.5 | 146.2 | 67.1 | 32.4 | 30.8 | 36.8 | 49.4 | 66.9 | 85.9 | 101.2 | 103.0 |
| 2 | 199.9 | 197.8 | 182.1 | 128.4 | 49.9 | 8.3 | 0.2 | 0.3 | 0.9 | 3.6 | 13.2 | 33.0 | 59.4 | 81.1 |
| 3 | 199.3 | 190.1 | 143.4 | 54.6 | 4.9 | 0.1 | 0.0 | 0.0 | 0.3 | 3.3 | 14.4 | 36.4 | 0.0 | 0.0 |
| 4 | 199.9 | 197.8 | 182.1 | 128.4 | 49.9 | 8.3 | 0.2 | 0.3 | 0.9 | 3.6 | 13.2 | 33.0 | 59.4 | 81.1 |
| 5 | 199.8 | 199.3 | 196.8 | 184.5 | 146.2 | 67.1 | 32.4 | 30.8 | 36.8 | 49.4 | 66.9 | 85.9 | 101.2 | 103.0 |

CONCENTRATIONS IN LAYER 10 AT END OF TRANSPORT STEP 5022, TIME STEP 1, STRESS PERIOD 1

| | 1 | 2 | 3 | 4 | 5 | 6 | 7 | 8 | 9 | 10 | 11 | 12 | 13 | 14 |
|---|-------|-------|-------|-------|-------|------|------|------|------|------|------|------|------|------|
| 1 | 199.7 | 199.5 | 198.1 | 189.9 | 150.4 | 71.9 | 33.0 | 31.5 | 38.8 | 54.2 | 74.0 | 87.6 | 86.6 | 65.2 |
| 2 | 200.0 | 199.1 | 189.6 | 142.0 | 54.3 | 7.3 | 0.2 | 0.4 | 1.3 | 5.7 | 22.8 | 47.0 | 63.9 | 59.9 |
| 3 | 199.8 | 195.0 | 158.7 | 64.8 | 5.3 | 0.1 | 0.0 | 0.0 | 0.1 | 0.7 | 9.6 | 29.1 | 49.3 | 0.0 |
| 4 | 200.0 | 199.1 | 189.7 | 142.0 | 54.3 | 7.3 | 0.2 | 0.4 | 1.3 | 5.7 | 22.8 | 47.0 | 63.9 | 59.9 |
| 5 | 199.7 | 199.5 | 198.1 | 189.9 | 150.4 | 71.9 | 33.0 | 31.5 | 38.8 | 54.2 | 74.0 | 87.6 | 86.6 | 65.2 |

CONCENTRATIONS IN LAYER 11 AT END OF TRANSPORT STEP 5022, TIME STEP 1, STRESS PERIOD 1

| | 1 | 2 | 3 | 4 | 5 | 6 | 7 | 8 | 9 | 10 | 11 | 12 | 13 | 14 |
|---|-------|-------|-------|-------|-------|-------|-------|-------|-------|-------|-------|------|------|------|
| 1 | 196.6 | 195.2 | 193.1 | 189.4 | 177.3 | 143.6 | 110.5 | 103.1 | 107.5 | 113.0 | 106.9 | 88.6 | 61.2 | 29.4 |
| 2 | 199.5 | 199.2 | 197.7 | 187.4 | 147.5 | 85.5 | 44.4 | 41.2 | 51.3 | 71.6 | 87.1 | 88.1 | 71.1 | 40.0 |
| 3 | 199.8 | 199.4 | 194.3 | 165.1 | 97.9 | 34.8 | 7.8 | 8.2 | 14.6 | 31.7 | 54.8 | 70.8 | 68.5 | 45.8 |
| 4 | 199.5 | 199.2 | 197.7 | 187.4 | 147.5 | 85.5 | 44.4 | 41.2 | 51.3 | 71.6 | 87.1 | 88.1 | 71.1 | 40.0 |
| 5 | 196.6 | 195.2 | 193.1 | 189.4 | 177.3 | 143.6 | 110.5 | 103.1 | 107.5 | 113.0 | 106.9 | 88.6 | 61.2 | 29.4 |

CONCENTRATIONS IN LAYER 12 AT END OF TRANSPORT STEP 5022, TIME STEP 1, STRESS PERIOD 1

| | 1 | 2 | 3 | 4 | 5 | 6 | 7 | 8 | 9 | 10 | 11 | 12 | 13 | 14 |
|---|-------|-------|-------|-------|-------|-------|-------|-------|------|------|------|------|------|------|
| 1 | 153.7 | 148.9 | 143.4 | 137.8 | 131.9 | 122.7 | 110.2 | 98.7 | 86.0 | 69.6 | 52.2 | 35.1 | 19.5 | 7.1 |
| 2 | 176.2 | 174.4 | 169.8 | 164.4 | 154.9 | 136.5 | 115.3 | 104.7 | 98.5 | 89.3 | 74.1 | 54.7 | 33.3 | 13.5 |
| 3 | 189.6 | 186.6 | 182.5 | 175.4 | 157.8 | 127.3 | 96.9 | 88.3 | 89.0 | 89.8 | 82.3 | 66.5 | 44.3 | 19.9 |
| 4 | 176.2 | 174.4 | 169.8 | 164.4 | 154.9 | 136.5 | 115.3 | 104.7 | 98.5 | 89.3 | 74.1 | 54.7 | 33.3 | 13.5 |
| 5 | 153.7 | 148.9 | 143.4 | 137.8 | 131.9 | 122.7 | 110.2 | 98.7 | 86.0 | 69.6 | 52.2 | 35.1 | 19.5 | 7.1 |

CUMULATIVE MASS BUDGETS AT END OF TRANSPORT STEP 5022, TIME STEP 1, STRESS PERIOD 1

| | IN | OUT |
|-------------------------|----------------|---------------|
| CONSTANT CONCENTRATION: | 0.0000000 | -24.87505 |
| CONSTANT HEAD: | 0.0000000 | 0.0000000 |
| MASS STORAGE (SOLUTE): | 42.05531 | -17.18066 |
| [TOTAL]: | 42.05531 MOL | -42.05572 MOL |
| NET (IN - OUT): | -0.404379E-03 | |
| DISCREPANCY (PERCENT): | -0.9614860E-03 | |

M T
I D End of Model Output

This dissertation is accepted on behalf of the faculty
of the Institute by the following committee

Robert A. Bowman 30 August 1999
Adviser Date

Eric R. Lindgren 8/30/99

Hendricks 9/2/99

Lee Buckley 9/2/99

M. Phillips 9 Sept 99

I release this document to New Mexico Institute of Mining and Technology.

Earl D. [Signature] 8/31/99
Student's Signature Date